National Energy Symposium 2015

20th November 2015

BMICH, Colombo 07, Sri Lanka

Organized by

Sri Lanka Sustainable Energy Authority
Ministry of Power and Renewable energy

CONTENTS

Pages

Message from the Minister of Power & Renewable Energy

Energy is one of the major aspects in the widespread social, economic and climatic concerns in the world. In this context, there is no doubt that renewable energy sources constitute a key element of a sustainable future. Renewable energy development is viewed as a means of democratizing energy supply industry in the world, considering the vast geographical spread of the resource, compared to fossil fuel resources concentrated only in a few countries.

Under the development programmes that have been envisaged by the Government, the importance of establishing energy sustainability in the country is vividly recognized. In this context the Government has geared to build up an energy self-sufficient nation by developing renewable energy to the fullest possible extent while improving energy efficiency. Especially relieving the economy of the burden of meeting energy with huge foreign exchange expenditure needs to be curtailed to the fullest possible content amidst giving the due place to the development of environmentally benign technologies. It will also be very important to take possible initiatives in energy management and conservation as well.

I do expect that the deliberations in the Vidulka National Energy Symposium will lay a sound platform to discuss technological and all other related aspects in sustainable energy development and provide extensively important inputs to anticipated developments in the sector.

Hon. Ranjith Siyambalapitiya
Minister of Power and Renewable Energy

Message from the Deputy Minister of Power & Renewable Energy

Renewable energy is one of the key solutions to the current energy challenges. Many countries already foster the production and use of renewable energy through different approaches on a political and economic level as they recognize the urgent need to change the current energy path. Developing renewable energy resources immensely contribute towards energy security, environmental sustainability and economic development of the country in the long run.

Enhancing research and development related to the thematic areas of sustainable energy is one of the focused areas as adopting new technologies, improving the existing technologies, survey-type researches for updating energy information, etc. will extensively support the sustainable energy development agenda of the country. Vidulka National Energy Symposium will provide fruitful additions in these lines.

I assure the energy professionals, researchers, academia and other experts will successfully exploit the opportunity to achieve valuable outcomes.

Hon. Ajith P Perera
Deputy Minister of Power and Renewable Energy

Message from the Secretary of Power & Renewable Energy

The Government has declared its vision for energy sector of Sri Lanka to become self-sufficient in energy by 2030 through hundred percent renewable energy sources. This vision has already drawn national and global attention. Through this vision Sri Lanka sets a good example for most of the developed and developing countries who only speak about reduction of carbon emission, climate changes and global warming without doing substantial contribution to mitigate theses grave consequences. In contrast, our effort is to reduce the carbon footprint of energy sector as low as possible, if not make it zero. This is particularly to support the global efforts of combating global warming.

Being a country blessed with an enormous amount of natural resources such as wind, solar, hydro power, bio-mass and also potential of finding commercially viable deposits of natural gas, achieving the energy self-sufficiency should not be a challenge when the country has the required knowledge and the commitment. Fortunately we have the political commitment and the leadership to achieve the hundred percent renewable energy target. What is lacking is the technology and knowledge. Even though we have a good human resource base with international level technical expertise, the application of such knowledge and experience for policy development of this sector is far from satisfactory.

I hope Vidulka National Energy Symposium will provide a good platform to energy conservation programmes in Sri Lanka which will help to pave the way for Sri Lanka to embark on a new journey towards self-sufficiency in energy.

Dr. Suren Batagoda
Secretary
Ministry of Power and Renewable Energy

Message from the Chairman of Sri Lanka Sustainable Energy Authority

Sri Lanka Sustainable Energy Authority holds the Vidulka National Energy Symposium for the sixth consecutive year. I gratefully acknowledge the keen interest among universities, research institutes and also in the industry to continue with their research & developments giving a special focus towards the subject of sustainable energy.

As the focal national institution in the field we have to lead the country in the journey towards long-term energy sustainability in the country, with the vision "Towards an Energy Secure Sri Lanka".

In developing sustainable energy in the country, there is a national target of achieving 20% of the national electricity generation from new renewable energy and also realizing a 10% energy saving by 2020. Through these the country can achieve an annual foreign expenditure reduction of Rs. 100 billion, contributing to the journey towards an Energy Secure Sri Lanka. There is also a further dimension of creating an energy conscious nation, under which all the socio-economic parameters will play pivotal roles. In leading the sustainable agenda in the country the inputs that can be obtained from different strata of the society will be immense and the research community will be at healm.

I sincerely expect that Vidulka will make a platform for sustainable energy researchers to come out with pragmatic solutions to the real practical issues in the field.

Keerthie Wickramaratne
Chairman
Sri Lanka Sustainable Energy Authority

Integration of Non-Conventional Renewable Energy Based Generation into Sri Lankan Grid

Samarasekara, M.B.S. Chief Engineer (Generation Planning), De Silva, M.T.K. Chief Engineer (Generation Development Studies), Attanayaka, T.L.B. Electrical Engineer (Generation Planning), Wijekoon, R.B. (Electrical Engineer (Generation Planning)
Ceylon Electricity Board

Abstract:

Importance of Non-Conventional Renewable Energy (NCRE) technologies is rising with the technological advances and global climatic concerns. In such a context challenges in integrating naturally replenishing energy sources such as Hydro, Wind, Solar, Geothermal and Biofuel to the power system has gained much attention in worldwide. Sri Lanka being a country with rich potential of NCRE sources currently produces 10% of its electricity generation from NCRE sources and exploring means to increase its contribution is important.

Increased penetration levels of NCRE based generation sources leads to various technical challenges depending on the system characteristics. Nature of seasonality and intermittency of sources, daily electricity demand pattern with a notable off peak period, power system stability concerns are among the main system specific limitations in the country.

Impact of two NCRE development scenarios has been studied and this paper presents the energy and economic analysis of implementing NCRE Development. Firstly the development of Wind, Solar, Mini-hydro and Biomass considering resource availability and project implementation was projected for the two scenarios. Secondly the expansion of the generation system was optimized in each scenario using a system planning model. Thereafter, using results of a short term operation simulation for two scenarios system constraints and impacts on NCRE development were analyzed. including necessary curtailments subjected to the system constraints. Further, it highlights the key observation of the results and prospective mitigation measures to facilitate the integration of more NCRE sources without violating the network restriction.

Keywords: Non Conventional Renewable Energy (NCRE), Integration, Intermittency, Curtailments, Dispatch, Network Restrictions

Introduction

Background

The existing generating system in the country is mainly owned by Ceylon Electricity Board (CEB) with a considerable share owned by the private sector. Until 1996, the total electricity system was owned by CEB. Since 1996, private sector has also participated in power generation.

Sri Lanka electricity requirement was growing at an average annual rate of around 6% during the past 20 years, and this trend is expected to continue in the foreseeable future. The total installed capacity including NCRE and peak demand over the last twenty years is shown in Figure 1.

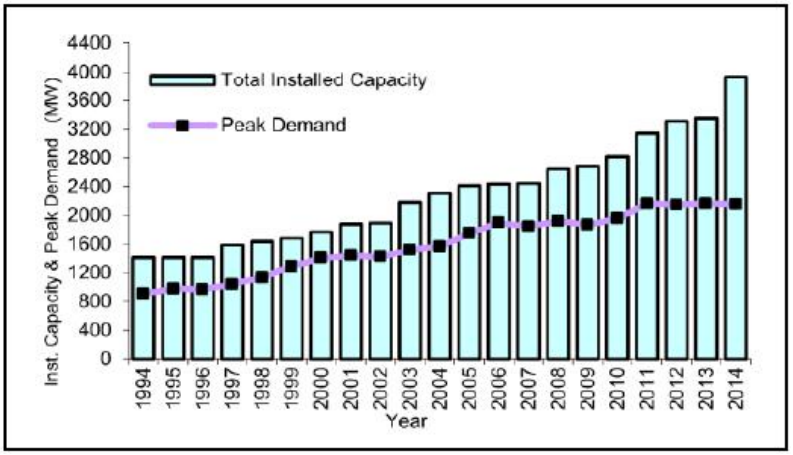

Figure 1: Total Installed Capacity and Peak Demand

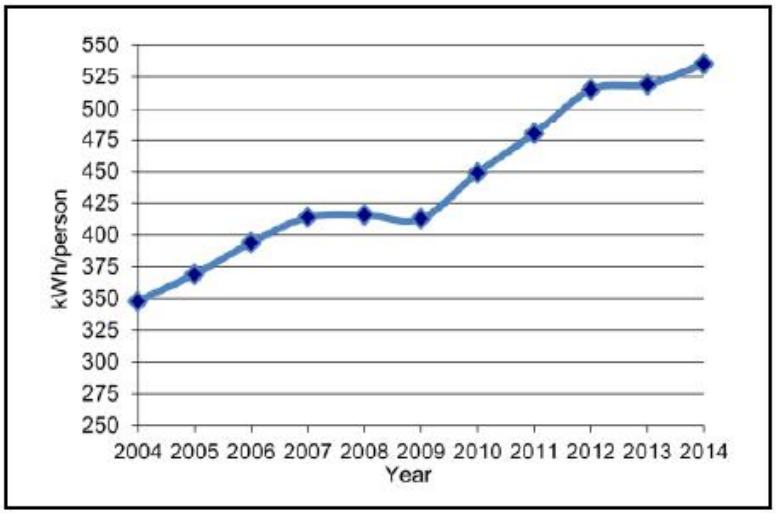

Figure 2: Per Capita Electricity Consumption

The average per capita electricity consumption in 2013 and 2014 were 519kWh per person and 535 kWh per person respectively. Generally it has been rising steadily. Figure 2, illustrates the trend of per capita electricity consumption from 2004 to 2014.

Present System

The existing generating system in the country has approximately 3932MW of installed capacity by end of 2014 including non-dispatchable plants of capacity 437MW owned by private sector developers. The majority of dispatchable capacity is owned by CEB (i.e. about 80% of the total dispatchable capacity), which includes 1356.5MW of hydro and 1444MW of thermal generation capacity. Balance dispatchable capacity, which is totally thermal plants, is owned by Independent Power Producers (IPPs).

Future System

The Ceylon Electricity Board (CEB) is under a statutory duty to develop and maintain an efficient, coordinated and economical system of Electricity Supply for the whole of Sri Lanka. Therefore, CEB is required to generate or acquire sufficient amount of electricity to satisfy the demand. CEB methodically plans its development activities in order to provide reliable, quality electricity to the entire nation at affordable prices.

CEB considers the project options from all possible sources including CEB owned generation developments, large thermal plants from the independent power producers and supply of non-conventional renewable energy sources in order to meet the system demand. Several factors are taken in to account in this process of selecting the appropriate power development project. Commercially exploitable potential, technical feasibility studies, environment impact assessment and economic feasibility are the main factors of this selection process.

The methodology adopted in the studies optimally selects plant additions from given thermal as well as hydropower generation expansion candidates, which will, together with existing and committed power plants meet the forecast electricity demand with a given level of reliability complying with National Energy Policy & Strategies (2008).

Importance of the Study

With the increase of renewable energy share, it creates several issues such as power quality, power system stability, economic operation due to intermittency, contribution to system inertia, cost of NCRE generation etc. Special consideration should be needed when integration of wind and solar to the national grid due to the rapid variation of the power from these sources. Therefore, a proper study has to

be carried out in order to identify amount of NCRE share that could be connected to system in terms of system operation and planning.

The high reliability of the electric power system is required on having adequate supply resources to meet demand at any moment. In longer term planning, system reliability is often assessed in terms of the probability that the planned generation capacity will be sufficient to meet the projected system demand. The capacity value of NCRE plants for long term planning analyses is currently a topic of significant discussion in the electric power industries. Characterizing the NCRE generation to appropriately reflect the historical statistical nature of the plant output on hourly, daily, and seasonal bases is one of the major challenges.

Main objective of the study is to address following two major concerns of NCRE integration into national grid:

- To what extent would NCRE generation contribute in Capacity and Energy to the System?
- What are the costs associated with scheduling and operating conventional generating resources to accommodate the variability and uncertainty of NCRE based generation?

Methodology

Study Approach

In planning, system reliability is often evaluated in terms of the probability that the planned generation capacity will be sufficient to meet the projected system demand. Relation between expansion planning and operation planning with the time scale is shown in Figure 3.

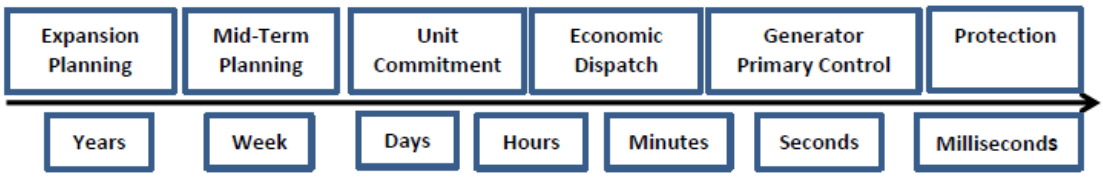

Figure 3: Transmission Planning and Operation Functions by Timescale [4]

Following steps illustrate the NCRE Integration Study Approach:

- Modeling and Assessment of NCRE resource potential of Wind, Solar, Mini-hydro and Biomass.
- Projection of NCRE Development considering, Resource availability and Grid Infrastructure.
- Optimization of Long Term Generation Expansion Plan of

the whole system including the projected NCRE Development.

- System Dispatch Simulation with imposed operational constraints to identify restrictions for NCRE integration
- Refine economic potential by combining with a transmission impact analysis.
- Evaluate and prioritize resource areas for the most significant impact on alleviating congestion on the electrical grid within a certain timeframe (i.e. to meet 2020 goals)

Data Sources

- Data files used for Generation Planning
- Half hourly historical demand data, projected system demand and losses for the period
- Existing NCRE generation
- Hydro generation constraints
- 10 mins wind data for three regions (Puttlam, Northern and Central)
- 10 mins solar radiation data for Southern and Northern
- Standard Power Purchase Agreements (SPPA), Letter of Intents (LOI) signed for Mini Hydro, Wind, Solar, Bio Mass power plants
- Details on existing conventional power plants (capacity, reactive power capability, efficiency, ramp rate etc.)
- Merit order dispatch
- Transmission Network data (Steady state and dynamic data)
- Operation restrictions such as minimum operation of base load plants, water release, plant outputs
- Pump storage data
- Other data such as hydrology, inflows etc.

Generation Planning Approach

Long Term Generation Expansion Planning with a projected NCRE development was optimized using the WASP IV (Wien Automatic System Planning) software. Wind, Solar and Mini-hydro were modeled with the negative load approach, in which, the system load data were adjusted for each year with NCRE Generation data. This method required developing half hourly Load profile data for 25 years and developing Wind, Solar and Mini-Hydro generation profiles for considered capacities. The study approach and the analyses covered in the paper are shown in the Figure 4.

Two Generation Expansion Scenarios were developed to analyze the economic impact of developing NCRE based Generation.

(i) Reference Scenario is the expansion plan that includes only the NCRE capacities as at 31 December 2014 with no further NCRE development.

(ii) 20% Energy by 2020 Scenario includes projected NCRE Development to cater 20% energy contribution from NCRE.

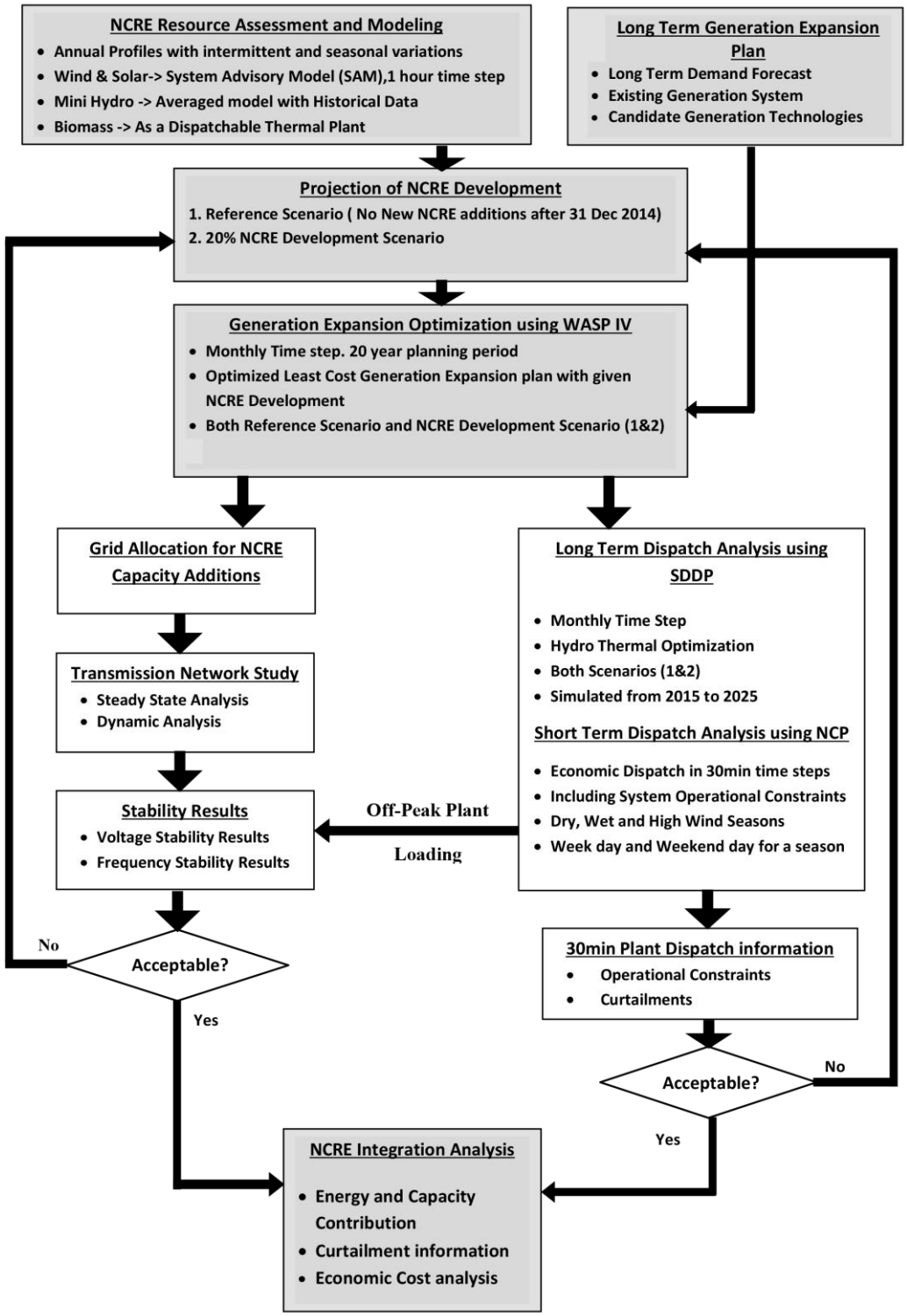

Figure 4: The study approach and the analyses covered in the paper

Load Data Preparation

30 mins Load data were prepared for 2015-2025 period using 30min load data logged at the System Control Centre for the year 2013 and the long-term demand forecast prepared by the Generation Planning Section. It is assumed that base year (2013) load variation will persist in the future and the off-peak load will grow proportionately to the growth of night peak for this study.

Modeling of NCRE Resource

The Wind, Solar and Mini-hydro potential was estimated using available site measurement data and other recorded information. Resource estimation was conducted for the study and the modeling requirements.

Wind

Areas with significant wind potential in the country were classified into three main categories, namely, Mannar, Puttalam, Northern and Hill Country for evaluation purpose. The best available wind measurement data were used to assess the resource potential. The Table 1 shows the modeling information in each location.

Table 1: Locations and Modeling Information

Location	Mannar	Puttalam	Hill Country	Northern*
Block Capacity	25MW	20MW	10MW	20MW
Wind Data	Nadukuda 2012-2013 60m Elevation	Udappuwa 2009-2010 50m Elevation	Seethaeliya 2011-2012 50m Elevation	Nadukuda 2012-2013 60m Elevation
Turbine Capacity	2.5MW	2MW	0.6MW	2MW

*Recorded data at Nadukuda was taken as the most representative wind data for the Northern category considering the limited availability of measurement data for Northern Area.

The measured monthly average wind speed in m/s and occurrence in % are shown in Figure 5 and Figure 6.

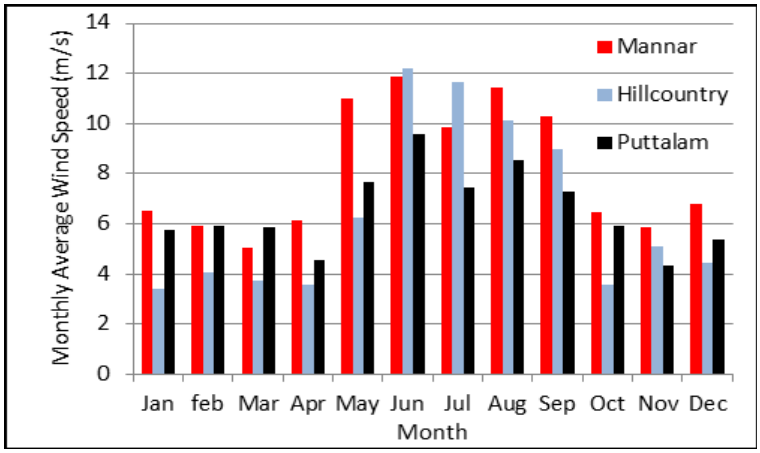

Figure 5: Monthly Average Wind Speed

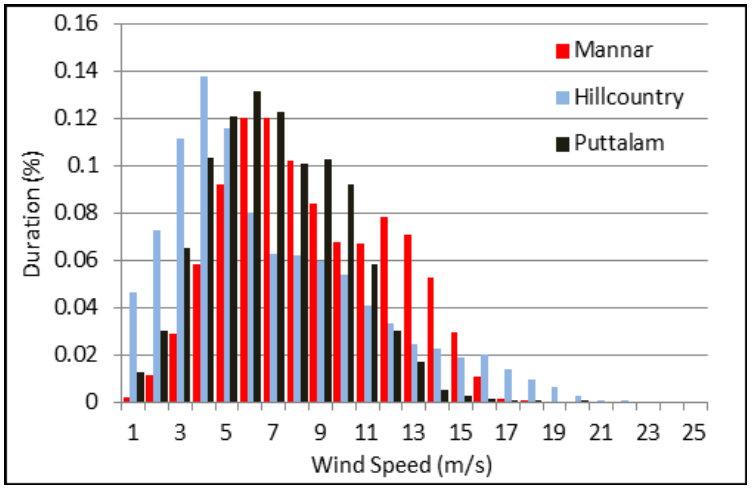

Figure 6: Monthly Average Wind Speed Duration (%)

Wind power plant modeling to estimate annual energy production and hourly capacity variation were carried out using the software named System Advisory Model (SAM) provided by National Renewable Energy Laboratory (NREL), USA.

Hourly wind speed data prepared for each site location is given as an input to the SAM software. Wind power plant capacity and energy contribution for above wind profiles were obtained from the simulation output and shown in Table 2. Commercially available wind turbine models were used for the wind power plant modeling and simulation purpose.

Table 2: Simulation Output for Wind Power Plants

Location	Mannar	Puttalam	Hill Country	Northern
Block Capacity	25MW	20MW	10MW	20MW
Annual Plant Factor	42.3%	31.4%	25.9%	42.2%
Annual Energy	93GWh	55GWh	23GWh	74GWh

Solar

Ten minute data measurements of Global Horizontal Irradiance (GHI) and Diffuse Horizontal Irradiance (DHI) at two locations, Hambantota and Kilinochchi were used in the study. Hambantota, one year (2012) data were available and in Kilinochchi, year 2014 complete data and several months from 2013 and 2015 were available. The data of a complete year was used as input to the System Advisor Model (SAM). From the available data, hourly inputs were constructed as Watts per square meter (W/m2). Latitude, Longitude, Elevation and hourly temperature were given as location inputs. GHI measurements for the two sites are given in the Figure 7. Hambantota annual average solar irradiance was 5.53 kWh/m2/day whereas 5.01 kWh/m2/day was observed in Kilinochchi.

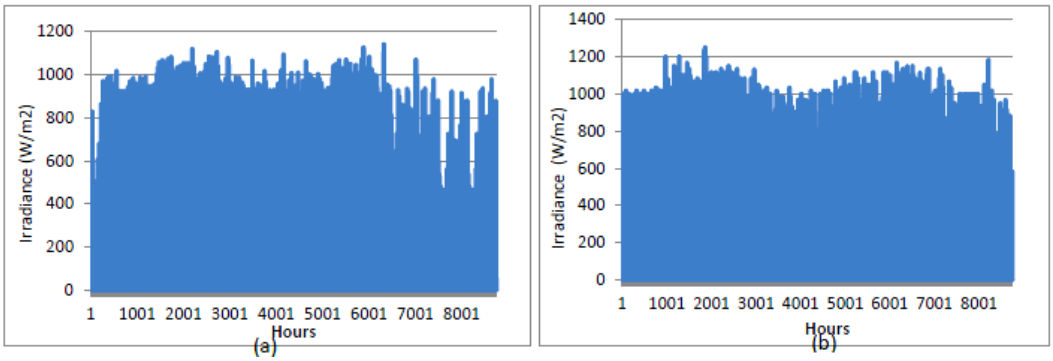

Figure 7: Global Horizontal Irradiance at Kilinochchi (a) and Hambantota (b) for one year period

Several assumptions were made during the solar energy estimation. The availability of the plants was taken as 90%. In these two sites, only GHI and DHI were available. Direct Normal Irradiance (DNI) was calculated with available GHI and DHI. The typical commercial PV module and inverter characteristics in built in SAM were used to obtain the preliminary output predictions. Plant factors of the two sites are given in the Table 3 and monthly energy output curves are given in the Figure 8.

Table 3: Solar Power Plant output plant factor

Location	Plant Factor
Kilinochchi	14.5%
Hambantota	16.3%

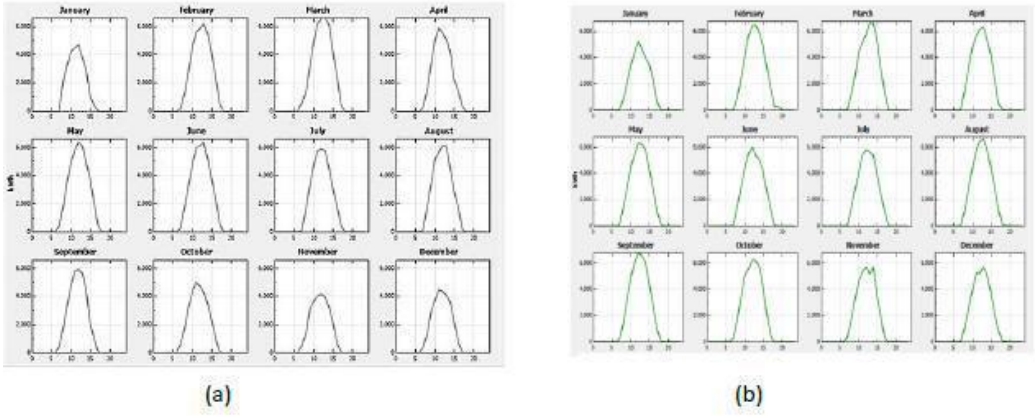

Figure 8: Monthly Solar Energy Variation at Kilinochchi (a) and Hambantota (b) for 10 MW Plant

Mini-Hydro

The Model for Mini-hydro power plant was prepared using historical data from 1998 to 2009 to reflect the seasonal energy contribution. The 2013 actual data was used to derive the monthly average capacities to be used with the corresponding load data for preparing the inputs for the negative load approach. Future additions were modeled in each year as additional capacities to represent future additions. The annual plant factor is 37.4 % under the average Hydro Condition. Figure 9 show the Monthly Energy and Capacity Variation.

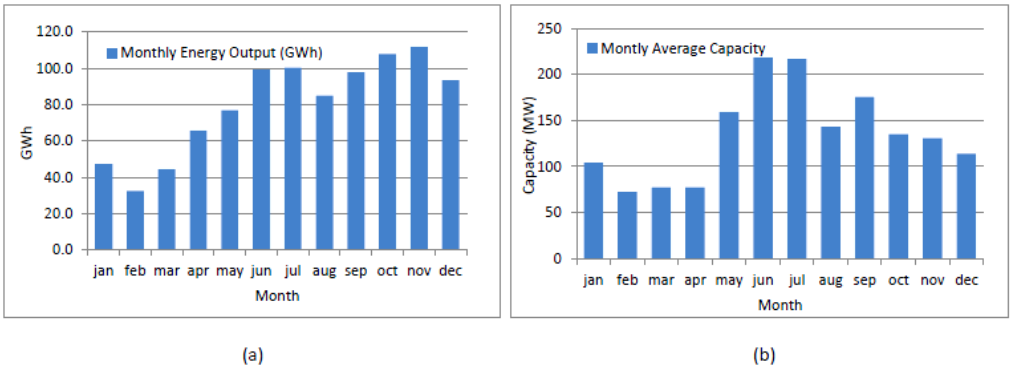

Figure 9: Monthly Energy (a) and Capacity (b) Variation of Existing Mini-hydro Capacity of 293.3MW

Non-Conventional Renewable Energy Development Scenarios

Reference Scenario

In this scenario, all the NCRE power plants in operation as at 31st December 2014 were considered without future NCRE additions. The results of the Reference Scenario were used as the baseline for comparison with future NCRE Development Scenarios.

NCRE Development Scenario to achieve 20% Energy by 2020

Future additions of NCRE were estimated considering the plants which are in the pipeline either having signed SPPAs or issued LOIs. The grid connection availability of these plants was also examined by the Transmission Planning Section. Considering all these facts, plant addition schedule was prepared by targeting to achieve 20% energy share from NCRE plants by 2020 and to continue energy share in to the future.

Planning Criteria

All the alternative generation options with various capital investments, operating costs, maintenance & repair costs and lifetimes were analyzed using screening curve method. Specific generation costs expressed in US Cents/kWh were calculated at different plant factors for all available thermal plants and were employed primarily in order to select the appropriate options among all the available thermal options.

State of the art optimization and simulation models were used in the detailed generation planning exercise. Internationally accepted planning methodologies were adopted to prepare the plant schedule for the planning horizon.

The following criterions were applied during the study.

Reserve Margin

Reserve margin is a deterministic reliability index which is the measure of the generation capacity available over and above the amount required to meet the system load requirements. Minimum of 2.5% and Maximum of 20% was applied for the studies.

Loss of Load Probability (LOLP)

LOLP indicates the percentage of time during which the System Load exceeds the available Generation capacity in the System. According to the Draft Grid Code, LOLP maximum value is given as 1.5%. This corresponds to cumulative failure duration of 5.5 days/year for the generating system.

Spinning Reserve

Spinning reserve is unloaded generating capacity, which is synchronized to the system and is ready to provide increased generation at short notice pursuant to Dispatch Instruction or instantaneously in response to a Frequency drop.

Spinning reserve is equal to the largest unit of available generation in the system in generation planning process.

Additional Spinning Reserve

Increased penetration of NCRE generation leads to higher uncertainty and increased spinning reserve requirement. Therefore additional 10% share from NCRE capacity was added to the normal spinning reserve requirement in this study.

Generation Planning Results

The optimum power plant additions for the period 2015 – 2025 for the Reference Scenario are given in the Table 3 and for the 20% NCRE Development Scenario, capacity additions are given in the Table 4. The present value of costs up to year 2025 is calculated using discount rate 10%.

Table 3: Plant Additions by type for Reference Scenario for the period 2015-2025

Plant Type	No of plants/units	Capacity (MW)
Major hydro	6	241
Coal	7	2,000
Gas Turbine	5	315
Pumped Hydro	1	200
Total		2,546

Table 4: Plant Additions by type for the 20% NCRE Development Scenario for the period 2015-2025

Plant Type	No of plants/units	Capacity (MW)
Major hydro	6	241
Coal	6	1,700
Gas Turbine	4	210
Pumped Hydro	1	200
NCRE plants		930
Total		3,281

Medium and Short Term Simulation

Plant schedule output from the generation expansion planning is taken for the dispatch model. Dispatch analysis was carried out on yearly basis over the study period from 2015 to 2025 to analyze the hydro thermal generation mix with NCRE addition. NCRE generation is considered as a negative energy demand. Further, cost function for hydro reservoirs was derived on monthly basis under three conditions, Dry, Wet and High Wind for the two scenarios, Reference Scenario and NCRE Development Scenario. Then, the short term dispatch model (NCP) used to obtain half hourly economic plant dispatch for the three conditions. With the NCRE addition to the power system, optimum energy utilization of hydro thermal generation mix was obtained under average hydrological condition. Time step considered in this economic dispatch analysis in SDDP and NCP

models are 'month' and 'Half-hour' respectively.

The above two simulations were done by the System Control Center to determine the operational restrictions of the integration of NCRE in the system. The output of hourly capacities were used as the input for curtailment and cost analysis.

Determination of Curtailments & Costs of NCRE

Economic Cost and Levelized Tariff

Economic unit cost calculation considered the capital cost, operation and maintenance and fuel costs used by the Public Utilities Commission of Sri Lanka(PUCSL) for the determination of 2012 NCRE tariff setting and escalated to the base year. For Solar technology, cost data were not published by PUCSL. Therefore, required data were taken from previous studies done by CEB. Life time of plants is assumed to be 20 years and 10% discount rate which was used in long term generation planning is applied for discounting.

Present three-tier tariff structure for Minihydro, Wind and Biomass and flat tariff for Solar was considered for the comparison. Levelized tariff rate was calculated from the 20 year tariff structure and given in the Table 5 together with economic unit cost of electricity generation from NCRE sources for comparison corresponding to the plant factors.

Table 5: Unit Cost and Plant Factors

Type	Economic Unit Cost (LKR/kWh)	Levelized tariff rate from three tier tariff (LKR/kWh	Plant Factor (%)
Biomass	18.58	24.87	80%
Solar	15.24	23.10	17%
Wind	9.73	18.37	38%
Mini-hydro	9.56	14.21	39%

Levelized tariff rate was calculated using the latest tariff announcement in 2014 and latest available escalation rates used for O&M escalation. The economic cost does not include the operation and maintenance cost escalation, return on equity etc. However, it seems that the differences between two costs were comparable and the present tariff is well above the economic value.

Curtailment

Curtailments were observed in the short-term dispatch analysis done by System Control Center from the years 2023 to 2025 in the 20% of NCRE development scenario when applying the operational limitations such as minimum operation of base load plants, maintenance

schedules etc. Study was done by dividing a year into three season's namely Dry, Wet and High wind. Days were categorized into a weekday and a weekend day during the simulation to study the basic different short term operational patterns.

Following procedure was followed in assessing future NCRE curtailment:

- Using the NCP simulation results, NCRE curtailment requirement was analyzed for 2 days in each season of the year for 10 years.
- Identifying possible curtailable NCRE capacities.
- Existing NCRE capacities and SPPA signed NCRE capacities as at January 2015 are considered as contractually Non curtailable.

- Wind Plants and biomass plants are taken as curtailable.
- Solar plants are practically not available for curtailment during the required time of the day.

The Generation Planning Section calculated the curtailment capacities based on the Short Term Dispatch model outcome. For year 2024, curtailment requirement is shown in Figure 10 (a) and 10 (b) for weekday and weekend during high wind season. This exercise was carried out for every year for 10 years.

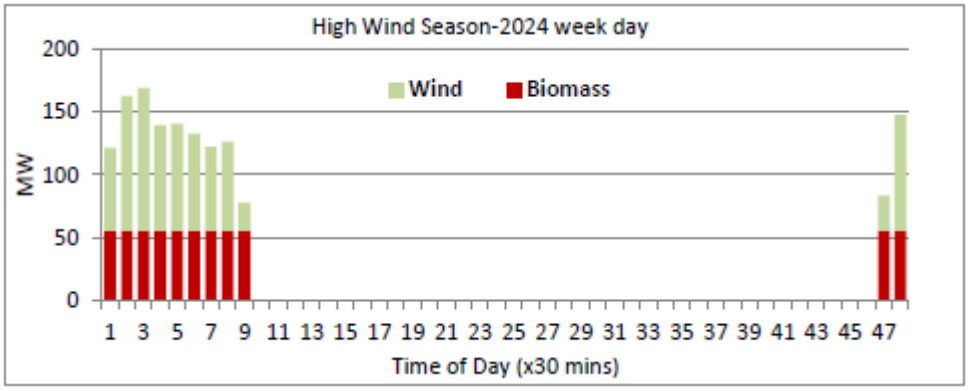

Figure 10(a): Curtailment of Capacity on a Weekday in 2024

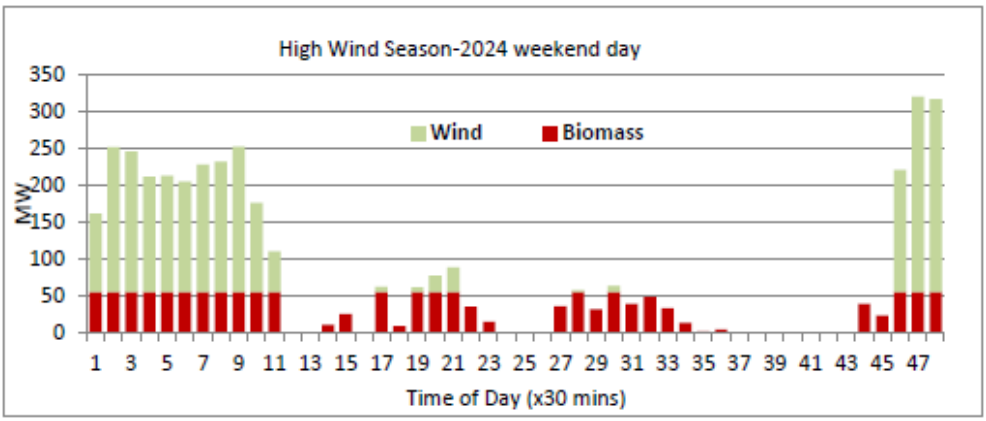

Figure 10(b): Curtailment Capacity on a Weekend day in 2024

The Table 6 shows the summary of the curtailment of NCRE capacities based on the above criterion.

Table 6: Summary of Curtailment of NCRE Energy

Year	Total NCRE Capacity (MW)	Annual NCRE Energy (GWh)	Share of NCRE from Total Generation %	NCRE curtailment (GWh)
2015	442	1,518	11.8%	No Curtailment
2016	487	1,677	12.5%	No Curtailment
2017	562	1,945	13.5%	No Curtailment
2018	727	2,561	16.7%	No Curtailment
2019	802	2,872	17.5%	No Curtailment
2020	972	3,496	20.0%	2.59
2021	1,062	3,797	20.7%	2.43
2022	1,147	4,082	21.2%	3.75
2023	1,222	4,323	21.4%	7.95
2024	1,302	4,588	21.6%	133.9
2025	1,372	4,812	21.6%	No Curtailment

Introduction of PSPP

The study was carried out with the introduction of the 200MW Pump Storage (PSPP) Unit into the system by year 2025. According to the short term dispatch model, it was observed that Pump Storage unit will operate during off peak and peak time in High wind situation in weekday as shown in Figure 11 (a). Figure 11(b) shows the very wet condition and pump storage unit will operate off peak, day and night periods. Therefore, requirement of curtailment of NCRE would not be foreseen after the

introduction of the 200MW Pump Storage Power Plant in to the system.

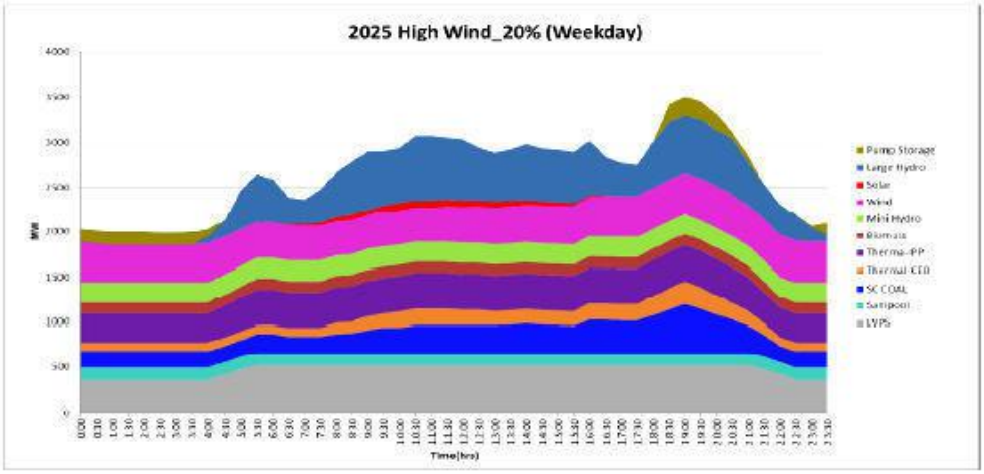

Figure 11(a): Effect on PSPP by 2025 in High Wind Condition

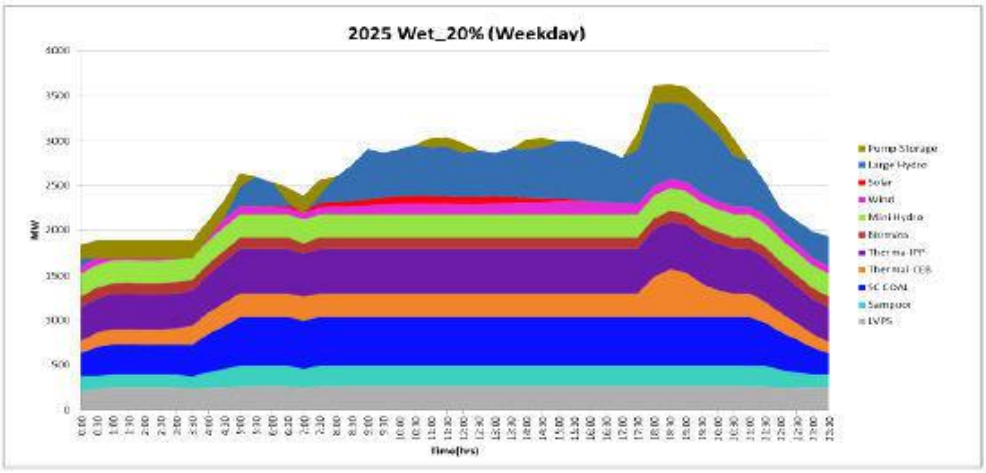

Figure 11(b): Effect on PSPP by 2025 Wet Condition

Cost Comparison

Present value cost of the total system up to year 2025 in million US dollars were calculated for scenarios, Reference Scenario and 20% NCRE Development Scenario using economic cost of a unit and available NCRE tariff levelized cost. These costs are given in following tables. For Practical and 20% NCRE cases, another scenario was studied with additional spinning reserve component to reflect the operational impact due to intermittent NCRE generation.

Table 7: Cost based on the Economic Cost

Summary of Costs	Reference Case	20% NCRE Case
Total System Cost (with normal Spinning Reserve) (mUSD)	8,918.31	8,861.83
Total System Cost (with additional Spinning Reserve) (mUSD)		9,058.42
Unit Cost (US cts/kWh)	8.32	8.45
Cost of NCRE Addition[1](mUSD)	94.2	922.1
Incremental Cost of NCRE Addition(mUSD)		140.1

Table 8: Cost based on the Present Levelized NCRE Tariff

Summary of Costs	Reference Case	20% NCRE Case
Total System Cost (with normal Spinning Reserve) (mUSD)	9,645.7	10,605.6
Total System Cost (with additional Spinning Reserve) (mUSD)		10,802.2
Unit Cost (US cts/kWh)	9.00	10.08
Cost of NCRE Addition[1](mUSD)	821.5	2,665.9
Incremental Cost of NCRE Addition(mUSD)		1,156.6

It was observed that incremental cost of the NCRE were 140mUSD based on economic cost and 1157mUS$ based on the present levelized tariff in the 20% energy share scenario.

Conclusion

Detail technical study has been carried out on the integration of NCRE into the power system by dividing into Generation Planning, Power System Analysis and Operational Study. 20% NCRE Development Scenario was compared with the Reference Scenario during the study.

Following conclusions relevant to Generation Planning were made as the outcome of the study assuming that proposed transmission and generation projects would be implemented as planned:

(1) During Initial years NCRE will replace oil power generation which has a higher cost. However, towards the end of study period, NCRE generation will replace by coal power plants due to the availability of low cost power generation.

(2) The study results show that there were significant curtailments due to operational restrictions.

(3) To achieve 20% energy by 2020 and maintain that energy share throughout the planning horizon, more biomass plants

need to be developed. If these plants are not commissioned on time, that will lead to a serious capacity shortage in the system and also lead to an unstable system due to unavailability of major thermal plants.

(4) In all the studies coal plants were kept at its minimum operation levels in order to absorb more NCRE into the system. The cost of running coal plants at their minimum levels were not taken into the consideration.

(5) Future coal plants should be developed based with higher efficiency and could be able to deload the plant up to 35% in order keep the NCRE curtailment at a minimum level.

(6) All future NCRE plant tariff should be below the economic costs derived in the Table 5. If the tariff of NCRE is higher than that it will lead to more curtailment of NCRE while running coal plants more efficiently.

(7) However after introducing PSPP into the system, overall absorption of NCRE will be smoother and also the coal plants will be able to operate more economically.

(8) Study should be periodically updated to review the NCRE integration.

References

[1] Generation Planning Section, Ceylon Electricity Board. Long Term Generation Expansion Plan 2013-2032.

[2] Generation Planning Section, Ceylon Electricity Board. Draft Long Term Generation Expansion Plan 2015-2034.

[3] Sustainable Energy Authority. Sri Lanka Energy Balance; 2013.

[4] I.J Perez-Arriaga, H. Rudnic, and M. Rivier, “Electric Energy Systems: An Overview”, Boca Raton, FL:
CRC Press, 2008.

[5] Transmission Planning Section, Ceylon Electricity Board. Long Term Transmission Development Plan 2013-2022.

[6] Jushua Earnest, Tore Wizelius. Wind Power Plants and Project Development; 2011

[7] National Renewable Energy Laboratory. Wind Resource Assessment Handbook, National Renewable Energy Laboratory; 1997.

[8] Vladimir Koritarov, Guenter Conzelmann, and Tom Veselka of Argonne National Laboratory methodology, Bruce Hamilton of ADICA Consulting, for the evaluation of wind power using the wasp-iv computer model;2005

Effective Demand Side Management for an Isolated Island Power System in Sri Lanka with Renewable Energy Sources

Ratneswaran, K.[1], Samarakoon, K.[2], Drysdale, B.[3], Prof. Ekanayake, J.[2]

[1] *Ceylon Electricity Board*

[2] *Faculty of Engineering, University of Peradeniya*

[3] *Institute of Energy, School of Engineering, Cardiff University, UK*

Abstract:

Demand side management for an isolated island power system of a small island in Sri Lanka is discussed. Electricity for this island was originally supplied by a diesel generator only for 2 hours in the morning and 4 ½ hours in the night. The cost of electricity generation in the island is five times higher than that in the mainland and hence a hybrid solution was investigated. A new hybrid solution that use wind plant, battery storage and hybrid control system was designed. Four industrial loads; two water desalination plants to produce drinking water and two ice making plants to make ice for preserving fish catch were added to the system. By controlling industrial loads at the morning and evening peaks periods a flat load profile was obtained thus optimizing the use of all generators, loads and storage. A demonstration rig for hybrid control system was developed using commercially available smart meter and smart sockets to test the operation of the control system.

Keywords: Demand side management, Renewable energy, Power distribution, Load control

Introduction

The provision of electrical and thermal energy services can play a major role in poverty alleviation for isolated populations who currently lack access to electricity. Consumers connected to grid electricity enjoy a reliable electricity supply that supports their socio economic development while marginalized communities, such as those living in rural areas and islands, strive for sufficient electrical energy to meet their basic needs [1]. In order to improve their socio economic status, the provision of basic services, such as electricity, is important without primarily considering the return on investment.

According to the Alliance for Rural Electrification (ARE) a large percentage of rural communities do not have access to electricity. This number is as small as 11% for some sub-Saharan countries and 22% for Africa as a whole (2008)[1]. As it is not economical to extend the main grid to rural areas, a majority of rural communities use diesel power plants as an isolated power supply. Some of these plants operate throughout the day while others operate for only a few hours a day. Due to rising fuel costs, increasing energy security concerns and consequences of global warming, renewable energy sources are now developing as a rival technology to diesel generators for isolated power systems. Although electricity generation using renewable energy sources can bring many benefits, its intermittent nature of production creates problems in isolated grids, thus requiring hybrid operation with diesel generators or other energy sources. A number of studies have been conducted to investigate the technical feasibility of integrating intermittent renewable energy sources with diesel power plants. Reference [1] reported a study investigating the technical and economic feasibility of diesel power generation alone as well as five different hybrid systems, at French Island, Western Port Bay in Victoria, Australia. The island has 90 full-time residents and an equal number of part-time residents occupying 86 dwellings. The different systems were examined and compared on economic and environmental grounds using a spreadsheet model and the HOMER optimization software. The wind-diesel-battery hybrid power system was selected as the most economically feasible option.

The use of renewable energy to extend the period of electricity supply to Lencois Island in Brazil is proposed in [2]. The island has 90 houses and approximately 393 inhabitants. Power supply is given by a 30 kVA diesel generator for 4 hours a day. A wind-solar-diesel-battery hybrid power system was proposed to give a reliable, high quality and continuous supply to the island.

There is increasing interest in demand side management (DSM) especially with the introduction of smart meters. DSM is defined as “systematic utility and government activities designed to

[1] http://www.ruralelec.org/9.0.html

change the amount and/or timing of the customer's use of electricity for the collective benefit of the society, the utility and its customers" [3]. DSM has the potential to vary the power system's load shape through these changes in consumption, to the benefit of the overall system. Electricity supply to isolated locations using diesel or hybrid solutions is normally very expensive. The introduction of appropriate DSM can lead to a more cost-effective operation of the system while maintaining security of supply.

In reference [4], a wind-solar-diesel-battery hybrid power system, along with a novel energy management system (EMS), was proposed to give reliable 24 hours supply to the small, isolated village of Huataconda in the Atacama Desert of Chile. Electricity supply is given by diesel generators for 10 hours a day. The EMS considers two days ahead forecast of renewable sources, a two days ahead prediction of electric consumption based on neural networks, and a new demand side management scheme that provides signals for consumers.

The costs and savings that may be attained through the implementation of various demand and supply side measures, based on a particular micro grid, is proposed in [5] for Orinoco and Marshall Point villages in Nicaragua. Orinoco and Marshall Point are two neighbouring villages located on the Atlantic coast of Nicaragua with populations of approximately 850 and 300 respectively. There are 186 clients supplied by a 110 kW diesel generator for 12 hours a day. The demand side measures presented in the paper includes the installation of meters, and low energy domestic and public lighting. Proposed supply side measures include a reduction of the size of diesel plant and the integration of renewable electricity generation based on wind, solar and biomass-based fuels. An energy supply curve has been proposed that highlights significant opportunities for reducing the costs of delivering energy services.

Reference [6] analyses the impact of demand side management options such as energy efficiency measures, eliminating standby power and dynamic demand response in the evolution of the energy mix in Flores Island in Portugal. Electricity is supplied to 4117 inhabitants by a hydro-wind-diesel hybrid power system with flywheel storage, delivering 54% of the energy from renewable sources in 2009. Dynamic demand response concentrates on domestic appliances, such as washer/driers and dish washers, to control consumption during peak hours with minimal impact on customers' lifestyles.

Many of the DSM initiatives proposed in the literature requires an advanced communication infrastructure with two way communication and flexible domestic loads. However, as many of the low income groups studied have only essential loads, such as heating and lighting, the availability of flexible loads is minimal thus reducing the impact of DSM measures [7].

Given the limitations of domestic DSM,

this paper considers a sustainable electricity supply for a Sri Lankan island incorporating a hybrid power system and industrial DSM. The industrial load improves the income generating opportunities of the island (ice making plants) as well as providing enhanced facilities for its population (water desalination plants). It also allows for more effective load management to improve the utilization of the generating plant.

Eluvaitivu Island Case Study

Eluvaitivu Island is situated in the north of Sri Lanka (9° 41' 22" N, 79° 48' 41" E) and covers an area of 1.4 km^2 (see Fig. 1). The climate is tropical monsoonal with temperatures ranging from 19°C to 31°C. Annual average rainfall is 735mm and the rainy season is from October to December. There are two windy seasons from December to February (moderate wind-average 5 m/s) and from May to September (strong wind-average 10 m/s) [8].

Figure 1: Eluvaitivu Island in Sri Lanka

There are 185 families living in 110 houses with a total population of 787. The majority of the populations are fishermen which accounts for the island's main income generating activity. Water for domestic and agricultural purposes is extracted from open dug wells the quality of which varies depending on location and season. During the dry season (April - September) the salinity levels of the dug well water increases, rendering it non potable. Drinking water supplies during these times are imported by boat from the mainland of Sri Lanka.

At present electricity for the island is provided using a 100 kVA diesel generator. It is operated from 4.30am to 6.30am and 6.00pm to 10.30pm, approximately 6½hours per day. 73 houses are connected to the electricity system and the average monthly consumption of the Island is around 3,450 kWh. The cost of electricity

generation (operational cost) is approximately 0.5 US$/kWh while the average tariff charged in the mainland Sri Lanka is approximately 0.1 US$/kWh. Given the high cost of electricity and the restricted availability of electricity supply, a hybrid solution was investigated which could deliver a reliable, cost effective supply to the community.

Methodology

The following research methodology was adopted to consider appropriate renewable based hybrid power systems for the selected location. This methodology can be applied to other communities to design a power system based on their own environmental, social and economic conditions.

A. Site selection

The first stage of the study involved the selection of a rural community for the analysis. Eluvaitivu Island in Sri Lanka was selected based on three criteria, namely:- the selected community does not have access to electricity and grid extension is not feasible; access to electricity is a high priority in order to facilitate socio-economic development of the community; and the selected community has access to renewable resources such as wind and solar.

B. Data collection

The second stage of the study involved the collection of data such as basic data about the community, socio-economic activities, potential existing and future developments and current electricity supply and its cost. In addition, availability of renewable energy sources such as hydro, wind, solar and biomass and its seasonal characteristics were established.

a) Solar resource in the island

As there is no meteorological station recording solar radiation data in the northern region of Sri Lanka, daily average solar radiation data sourced from NASA (www.eosweb.larc.nasa.gov) was used for the analysis. Solar radiation levels are fairly uniform over this region and vary from 4.3 kWh/m^2/day to 5.9 kWh/m^2/day, as shown in Fig. 2.

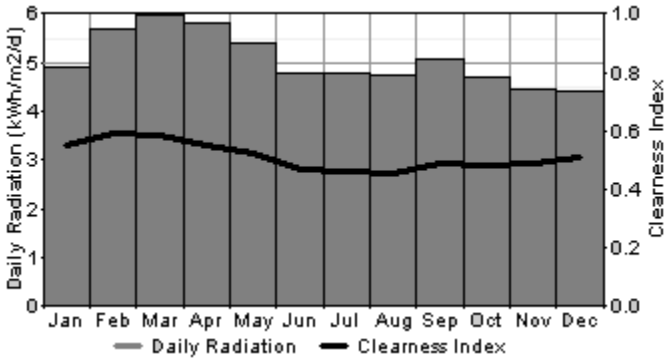

Figure 2: Monthly average solar radiation in the island

b) Wind resources in the island

The coastal areas of Sri Lanka, particularly the north-western region, experience strong winds during the period of the south-west monsoon (May to September), and moderate winds during the north-east monsoon (December to February). There is no meteorological station recording hourly wind data in the northern region of Sri Lanka. Data from a wind measurement mast installed at Mannar, 85 km south of Eluvaitivu, was used for this case study. North-western coastal areas are almost in the same wind regime as given by the wind resources potential map of Sri Lanka [8]. The annual average wind speed is 7.14 m/s at 40 m height and monthly average wind variation is shown in Fig. 3.

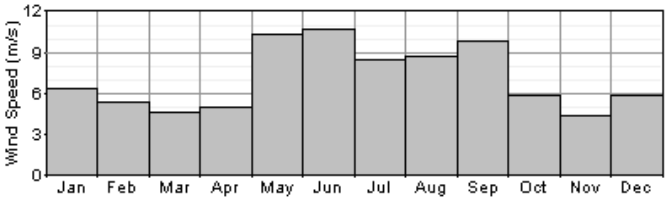

Figure 3: Monthly average wind speed at 40m in Mannar

c) Other resources in the island

There are other resources such as biomass, wave energy, and tidal energy available in this island. Biomass was not considered as it needs a large area to store the feed stock. Even though wave and tidal were ideally suited for the island, they were not considered in this study due to the absence of data and immaturity of technologies.

C. Load estimation

The third stage of this study involved the estimation of community loads including domestic, commercial, industrial and public lighting loads. The load profile of the existing system is given in Fig. 4. As the usage pattern of the present

curtailed power supply does not reflect a natural utilization pattern where continuous grid electricity is available, simply extending the existing system data on a pro rata basis is not appropriate. Therefore a survey was conducted among the island community to collect the present and the future domestic and industrial demand. Using the survey data, and an excel model was developed to forecast a future load profile by considering the island's domestic, commercial and industrial loads.

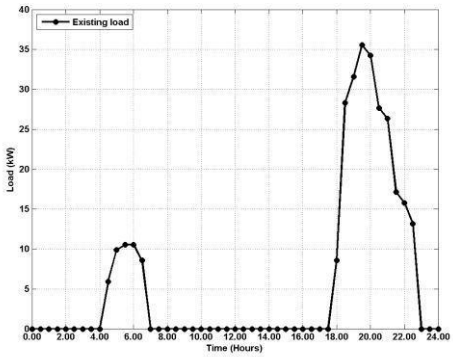

Figure 4: Load profile of the existing power system

Out of the 110 households on the island 10 can be categorized as large, 40 medium, and 60 small, based on their load consumption pattern. In addition there are schools, small medical centre, community buildings and religious institutions that use electricity. The major loads are lighting loads, electric irons and water heaters. The replacement of filament lamps (at present majority of houses use filament lamps), with compact fluorescent lamps (CFL), was the DSM measure considered for reducing peak of domestic loads. Domestic and commercial load profiles with and without CFL is given in Fig. 5.

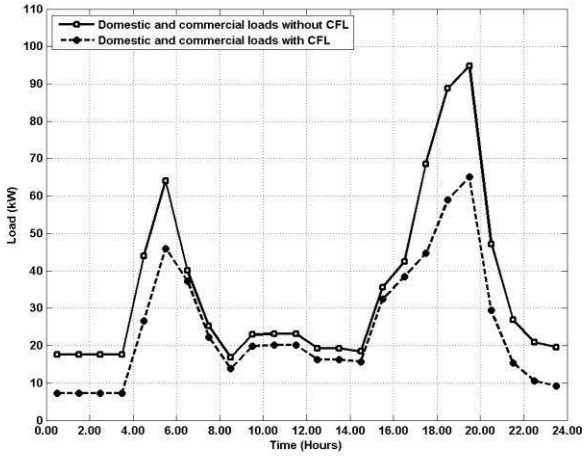

Figure 5: Load profile of the proposed domestic and commercial load with and without CFL

From the survey and other collected data the importance of adding some industrial loads was recognized. The two main industrial loads considered were water desalination plants (to produce potable drinking water) and ice making plants (to make ice to preserve the fish catch). These plants have some storage capacity thus providing a degree of flexibility over when the supply is taken. Two 5 kW water desalination plants and two 10 kW flake ice making plants were initially considered in order to construct an industrial load profile, as shown on Fig. 6 "Industrial load without DSM".

The projected industrial loads, detailed above, are significant in relation to the domestic loads and are nearly 30% of the total peak demand. In order to improve the overall load profile, the industrial loads were redesigned to incorporate two 11.5 kW ice plants and two 6 kW desalination plants, as shown on Fig. 6 "Industrial load with DSM". The industrial load was then added to the domestic load to construct a total load profile. The Curve marked 'Total load without DSM' in Fig. 7 shows the addition of domestic load with CFL and the considered industrial load without DSM. The curve marked 'Total load with DSM' shows the total load curve of domestic and commercial loads after introducing CFL and industrial loads after introducing DSM. The introduction of domestic DSM measures, noted above, and industrial load shifting, results in a significantly flatter profile. Overall peak load has been reduced from a morning peak of 75 kW to 60 kW, and an evening peak of 95 kW reduced to75 kW. This reduces the total capacity required by 21%.

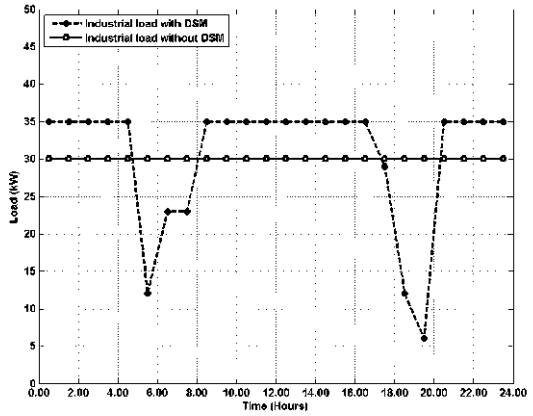

Figure 6: Industrial load profile with and without DSM

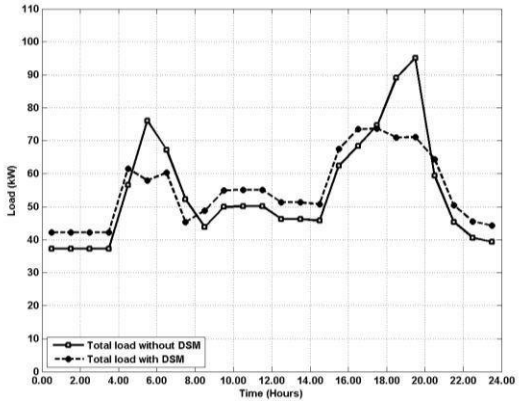

Figure 7: Total load profile with and without DSM

D. Optimization of supply side

The fourth stage of this study uses data given in sections 3.2 and 3.3 to analyze the optimal power system for the isolated island community. Wind speed, solar radiation and the power requirement of the community were determined on an hourly basis. The "HOMER" optimization tool, developed by National Renewable Energy Laboratory (NREL, USA), was used to establish the optimal power system configuration for the isolated community. In this study, the optimization was calculated to minimize the net present value (NPV) of the system over 20 years while delivering the required electricity supply to satisfy the projected demand profiles. Various system specifications and costs were analyzed for various wind turbines, solar panels, energy storages and diesel generators. A sensitivity analysis was carried out to determine different system configurations with varying wind speeds and diesel prices. The final system was selected by considering NPV of energy, renewable fraction, reliability and to accommodate the future loads

growths. Table 1 shows the equipment rating and the cost used in the HOMER software analysis.

Table 1: Rating of the Power System Equipments and Cost

Description	Life time	Rating	Capital Cost (US$)
Wind turbine Generator including installation	20 years	80kW	400,000
		10kW	80,000
Solar PV with installation	20 years	10kW	50,000
Diesel Generator including installation	16,000 running hours	60kW	19,750
		30kW	16,000
Battery	10 years	2kWh (6V, 360Ah)	300
Converter	10 years	16kW	16,000
		30kW	30,000
Hybrid controller panel		Sum	30,000

In addition to the data provided in Table 1, the following assumptions were also considered in the HOMER software analysis;

a. Project life time is 20 years.
b. Discount rate is 10% per annum.
c. Diesel Generator major overhaul is after 8,000 running hours.
d. Operators' wages is US$2500 per annum.
e. System fixed capital cost is US$50,000 (for power house and associated infrastructure).
f. Diesel Price (at site) is US$0.9/litre (for evaluation this was assumed to be constant throughout the project life).
g. No Carbon/GHG emission credits are available.
h. Diesel Generator dispatch strategy is cyclic charging

Fig. 8 shows the power system configuration considered for the analysis. Based on the analysis a comparison was made to determine the advantage of demand side management and renewable based hybrid power system with the conventional approach (diesel generator without DSM).

Results and Discussion

In the HOMER analysis two different cases were considered. Whilst industrial loads, such as ice making plant and water desalination plant, will support the socio-economic development of the island community, the basic needs of the islanders can be met by a supply which satisfies the domestic demand of the island alone. Two cases were, therefore, considered in the analysis based on the island load conditions.

They are;

Case 1: System configuration considering domestic load profile shown in Fig 5 with CFL.

Case 2: System configuration considering domestic and industrial loads with DSM as shown in Fig 7.

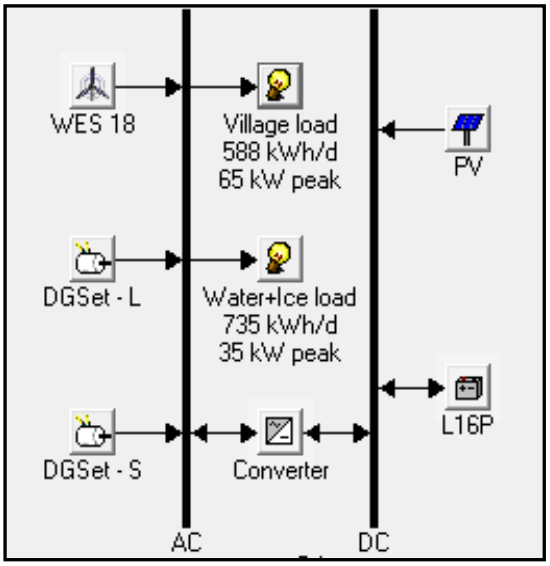

Figure 8: Power system configuration

Case 1: System configuration considering domestic loads

Analysis shows that the least cost power system configuration is a wind-diesel-battery based hybrid power system. Solar PV based hybrid power system was not selected due to the higher investment cost and lower performance factors. Out of several feasible options, two different solutions, shown in Table 2, were selected for comparison purposes. Option 1.1 uses a single 80 kW diesel generator to satisfy the continuous domestic loads. Option 1.2 is the least cost configuration in the HOMER analysis having one wind turbine (80 kW), two diesel generators (45 kW and 15 kW), a converter (16 kW) and a battery (40 kWh).

The selected wind-diesel-battery hybrid power system has the lowest lifecycle cost (i.e. lowest net present value (NPV)), cost of energy (COE), operational cost and diesel fuel consumption. Approximately 68% of the annual energy is from renewable sources i.e. wind. It is an environmental friendly system with high renewable penetration. The emissions from the proposed solution

and those from a diesel only solution are given in Table 3, indicating significant emissions reductions. Savings from the cost of diesel fuel will cover the capital cost within 6½ years, using a simple payback calculation.

Table 2: Supply options to satisfy domestic load

Option	Description	Capital Cost (US$)	Net Present Value (NPV) (US$)	Cost of Energy (US$/kWh)	Operational Cost (US$/kWh)	Renewable Fraction (%)	Fuel Consumption (Lit./Year)	Fuel Cost (US$/Year)
1.1	Single diesel generator system	71,000	1,267,516	0.700	0.656	0	122,759	110,483
1.2	Two diesel generator sets & one wind turbine generator, converter, battery and hybrid controller system	503,000	913,436	0.501	0.222	68	36,989	33,290

Table 3: Emission comparison

Option	Description	Emissions (kg/Year)			
		CO_2	CO	SO_2	NO_X
1.1	Single diesel generator system	323,265	798	649	7,120
1.2	Two diesel generator sets & one wind turbine generator, converter, battery and hybrid controller system	96,050	237	193	2,116

Case 2:System configuration considering domestic and industrial loads with DSM

Analysis shows that the least cost optimal power system configuration is a wind-diesel-battery based hybrid power system. Out of several feasible options, two different solutions, shown in Table 4, were selected for comparison purposes. Option 2.1 uses a single 80 kW diesel generator. Option 2.2 has one wind turbine (80 kW), two diesel generators (50 kW and 25 kW), a converter (30 kW) and a battery (120 kWh). The selected wind-diesel-battery hybrid power system has the lowest lifecycle cost, cost of energy (COE), operational cost and diesel fuel consumption. Approximately 42% of the annual energy is from renewable sources i.e. wind. In this case the energy utilization factor (plant factor) is high due to the industrial loads and appropriate DSM. Therefore diesel generation is slightly more competitive with the renewable based hybrid power system than in the domestic only case. Savings from the cost of diesel fuel will cover the capital cost within 7 years, using a simple payback calculation. Emission comparison is given in Table 5.

Table 4: Supply options to satisfy domestic & industrial loads

Option	Description	Capital Cost (US$)	Net Present Value (NPV) (US$)	Cost of Energy (US$/kWh)	Operational Cost (US$/kWh)	Renewable Fraction (%)	Fuel Consumption (Lit./Year)	Fuel Cost (US$/Year)
2.1	Single diesel generator system	72,250	1,812,213	0.441	0.424	0	190,706	171,635
2.2	Two diesel generator sets & one wind turbine generator, converter, battery and hybrid controller system	525,875	1,523,619	0.371	0.243	42	102,314	92,083

Table 5: Emission comparison

Option	Description	Emissions (kg/Year)			
		CO_2	CO	SO_2	NO_X
2.1	Single diesel generator system	502,191	1,240	1,008	11,061
2.2	Two diesel generator sets & one wind turbine generator, converter, battery and hybrid controller system	269,426	655	541	5,934

A Demonstration of the DSM Scheme

DSM measures are often implemented using time-varying prices or direct load control (DLC) [9]. DLC is a demand-response activity which remotely shuts down or change thermostat setting of customer's electrical equipment (e.g. air conditioner, water heater) on short notice. In this case DLC was proposed to control the industrial load as described in section 3.3.

A demonstration of the DSM scheme was implemented in the laboratory using commercially available components. A layout of the components of the scheme is shown in Fig. 9. This scheme comprises a smart meter, a load controller implemented in a PC and remote controllable sockets. Loads were represented by lamp loads having 1/100 of the actual load. Only one smart meter was used in the scheme as a metering device. It mimics the measurement of the domestic and commercial loads in the island. The industrial loads were switched off one by one when domestic and commercial demand was increasing

in the morning and afternoon and switched on when domestic and commercial demand was decreasing. Since the maximum loads of water desalination plants and ice making plants are known (assumed to be constant as they run continuously), the loads at which the plants were switched on and off were calculated in terms of village load (given in Fig. 5). This calculation was done to reduce the industrial load so that the total load profile follows the profile shown in Fig. 7 “Total load with DSM”.

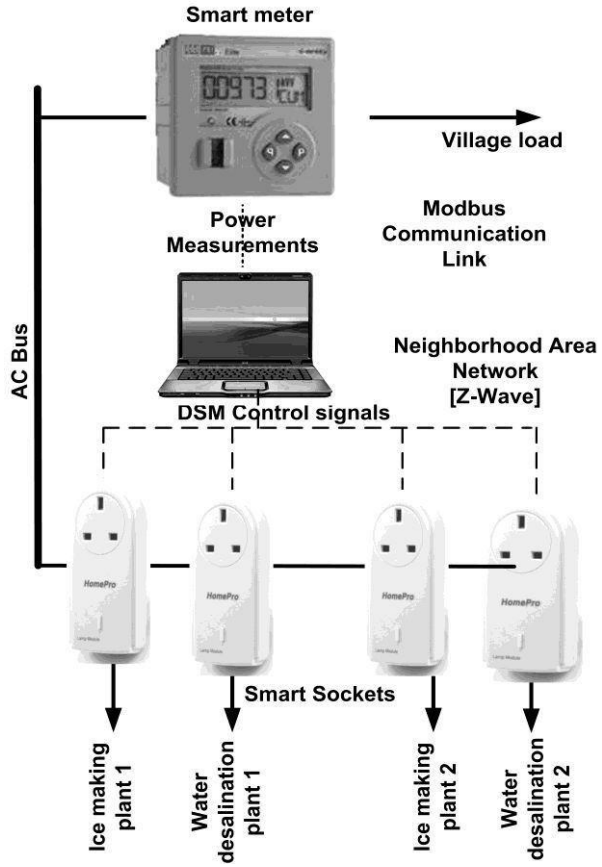

Figure 9: Layout of the components of the DSM scheme

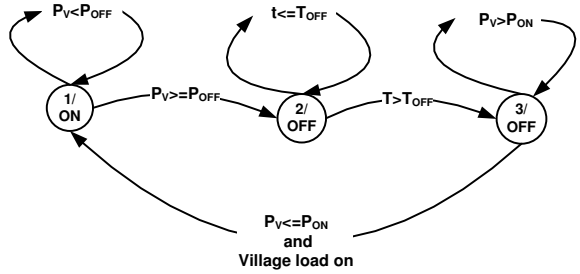

Figure 10: The state diagram of a plant

The switching operations of plants were controlled by algorithm runs in the controller. The algorithm is explained using the state diagram given in Fig. 10. In the algorithm, each plant had similar independent state transitions. Each plant was allowed to operate as long as the village load (P_V) was less than switching off load (P_{OFF}) (the plant was on in state 1). As soon as P_V exceeded P_{OFF}, the plant was switched off (moved to state 2). Then the plant stayed off for a period (T_{OFF}). This T_{OFF} period prevented switching on the plant immediately after it was switched off due to a load fluctuation. Then it started checking whether the village load is reduced (in state 3). When the village load was reduced below P_{ON} the plant was switched on (moved back to state 1). The set value of P_{ON} is less than P_{OFF} so that it introduces a hysteresis to avoid switching off the plant immediately after switching on. The set values of P_{ON}, P_{OFF}, T_{ON} and T_{OFF} are given in Table 6.

Table 6: Power and time periods of the DSM scheme

Plant	Maximum Load (kW)	Morning			Evening		
		P_{OFF} (kW)	T_{OFF} (min)	P_{ON} (kW)	P_{OFF} (kW)	T_{OFF} (min)	P_{ON} (kW)
Ice making plant 1	11.5	30	5	25	35	5	30
Water desalination plant 1	6	35	5	30	45	5	40
Ice making plant 2	11.5	40	5	35	55	5	50
Water desalination plant 2	6	45	5	40	65	5	60

The smart meter communicated with the controller through a serial port using the Modbus protocol. The controller sent load control commands to controllable sockets through a Neighborhood Area Network (NAN) using the ZWave protocol. It was assumed that the smart meter and the controller will be installed in the village feeder closer to each other. Plants will be installed in a single building located

closer to the village feeder so that the controller can send load control commands to the controllable sockets.

The Graphical User Interface (GUI) of the controller is shown in Fig. 11. The graphs shows, village load (blue) measured by the smart meter and the total load of industrial loads (black), the total load with DSM (red) and without DSM (green) that were calculated using the smart meter measurement and the maximum demand of industrial loads. From the GUI it can be seen that the control scheme was functioned according to the design requirements giving profiles similar to Fig. 5, Fig. 6 and Fig. 7.

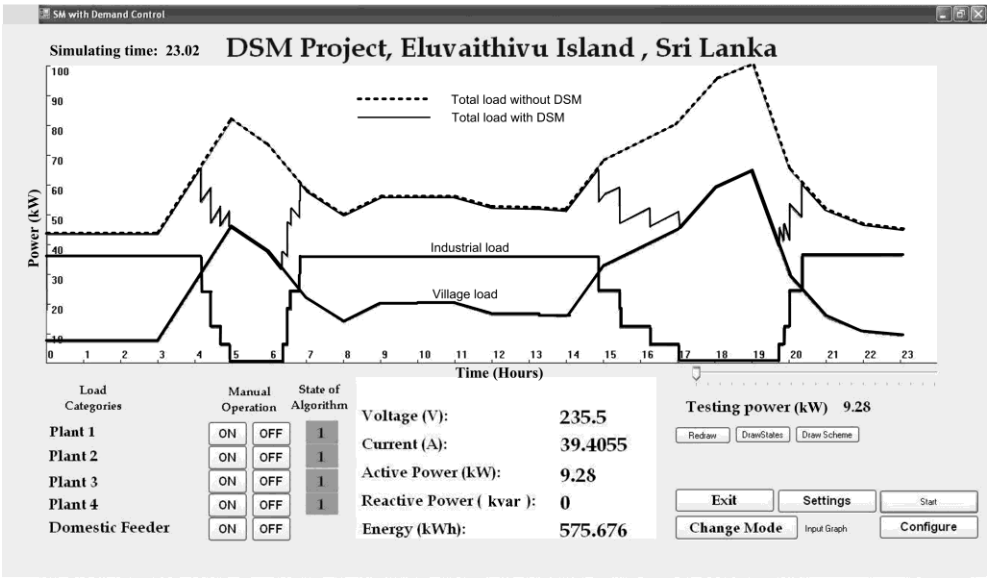

Figure 11: Graphical user interface of the controller

Conclusions

The provision of a reliable electricity system for isolated communities can deliver significant social benefits for their inhabitants. Opportunities for introducing domestic DSM are limited due to the lack of a significant flexible load. The introduction of an industrial load, with a greater degree of flexibility, can allow a hybrid power system, such as a wind-diesel-battery combination, to deliver both an electricity supply to meet the community's basic needs and provide opportunities for socio-economic development. The modeling of different supply and demand combinations can be carried out using the HOMER optimization tool, which can calculate a lowest lifecycle

cost solution from the available feasible options. The load control arrangement described in this paper was tested in the laboratory, but could easily be deployed in the field by connecting a Z-wave operated relay to MCCB/contactor of the industrial load.

References

[1] Hessami, M.-A., Campbell, H., Sanguinetti, C., A feasibility study of hybrid wind power systems for remote communities. Energy Policy 2010; 39, 877–886. doi:10.1016/j.enpol.2010.11.011

[2] De Souza Ribeiro, L.A., Saavedra, O.R., de Lima, S.L., Gomes de Matos, J., Isolated ;-Grids With Renewable Hybrid Generation: The Case of Lençóis Island. IEEE Transactions on Sustainable Energy 2011; 2, 1–11. doi:10.1109/TSTE.2010.2073723

[3] Charles River Associates, Primer on Demand-Side Management, 2005; [Online]. Available: http://siteresources.worldbank.org/INTENERGY/Resources/PrimeronDemand-SideManagement.pdf

[4] Palma-Behnke, R., Benavides, C., Aranda, E., Llanos, J., Saez, D., Energy management system for a renewable based microgrid with a demand side management mechanism, in: 2011 IEEE Symposium on Computational Intelligence Applications In Smart Grid (CIASG). pp. 1–8. doi:10.1109/CIASG.2011.5953338

[5] Casillas, C.E., Kammen, D.M., The delivery of low-cost, low-carbon rural energy services. Energy Policy 2011; 39, 4520–4528. doi:10.1016/j.enpol.2011.04.018

[6] Pina, A., Silva, C., Ferrão, P., The impact of demand side management strategies in the penetration of renewable electricity. Energy, 2012, 41, 128–137. doi:10.1016/j.energy.2011.06.013

[7] G. Owen, J. Ward, Smart Tariffs and Household Demand Response for Great Britain [Online]. Available: http://www.sustainabilityfirst.org.uk/docs/2010/Sustainability%20First%20-%20Smart%20Tariffs%20and%20Household%20Demand%20Response%20for%20Great%20Britain%20-%20Final%20-%20March%202010.pdf

[8] M. Young and R. Vilhauer, Sri Lanka Wind Farm Analysis and Site Selection Assistance, 2003; [Online]. Available: URL http://www.nrel.gov/docs/fy03osti/34646.pdf.

[9] Office of Gas and Electricity Markets, UK, Smart Metering Implementation Programme: Statement of Design Requirements,2010, [Online]. Available: URL HTTP://WWW.DECC.GOV.UK/ASSETS/DECC/Consultations/smart-meter-imp-prospectus/225-smart-metering-imp-programme-design.pdf.

Design a Contingency Electricity Feeding Plan

Kumara, G.K.A.[1], Hemapala, K.Y.M.U.[2]
[1]*Kukule Ganga Power Station, Ceylon Electricity Board*
[2]*Department of Electrical Engineering, University of Moratuwa*
[1]athula.kumara@ceb.lk, [2]udayanga@elect.mrt.ac.lk

Abstract

Ceylon Electricity Board (CEB) is mainly Electricity Generating, Distributing and solely Electricity Transmitting organization in Sri Lanka. Few years back, main target of CEB was to achieve 100% electrification level and was not greatly concerned about the reliability of electricity supply. Presently Sri Lanka has achieved 98% electrification level. It is expected to reach 100% within next few years. Presently CEB is providing electricity supply to 90% consumers and Lanka Electricity Company (LECO) is providing electricity to the remaining 10% consumers in Sri Lanka. Once electricity is there the consumers will be more concerned about supply reliability. Nowadays most human activities depend with availability of electricity supply. Electricity supply reliability can be improved providing N-1, N-2, and N-3 electricity feeding plans. At least CEB need to provide N-1 electricity feeding arrangement to their consumers. In this regard the authors have selected Dehiwala area for case study to observe the availability of N-1 feeding arrangement and find new proposals if it is not available. This study is done only for medium voltage (MV) lines. All peak load details of transformers were collected and modeled the MV network for year 2014 through Synergee software. Then acceptable growth rates for loads were applied and forecasted the model up to year 2020 and N-1 contingency electricity feeding arrangement was examined. New suggestions have been proposed considering availability, construction ability and cost where the N-1 feeding arrangement is not available. System Average Interruption Duration Index (SAIDI) value has been calculated before and after implementing the proposals. It is clearly noted that SAIDI is improved considerably after implementing the new proposals. Three common models are developed to extend this study for other Distribution areas.

Keywords: Electricity, Contingency, Primary Substation, Feeding plan, Medium Voltage

Introduction

Electricity is one of the most important factors for day to day life. Ceylon Electricity Board (CEB) is the organization, which mainly Generates, Distributes and solely Transmits Electricity in the Sri Lanka. Presently CEB has 5,210,000 consumers [01] and they use around 40 GWh per day with a peak demand of around 2100 MW [10]. Lanka Electricity Company (Pvt) Ltd (LECO) is the only other company who has license to distribute Electricity in Sri Lanka with around 500,000 consumers [02] which is 10% of the total consumers. CEB has a 3362 MW installed power capacity including Private Power Purchases. Power Consumption of Sri Lanka is 10,650 GWh per year and total revenue of CEB is around 190,488 million rupees per year. Transmission and Distribution losses are around 11% of net generation.

Generating Voltage of Power Plants is less than 20 kV. CEB uses two Transmitting Voltages, which are 220 kV & 132 kV. These are called High Voltage lines. Also CEB uses two types of MV lines as 33 kV & 11 kV. CEB owns and operates 500 km of 220 kV lines, 1900 km of 132 kV lines, 28700 km of 33 kV lines and 2400 km of 11 kV lines [01]. Sri Lanka uses 400 V for low Voltage. There are approximately 121500 km low voltage lines available all over the country. Low Voltage lines can be overhead or underground. But most of the Voltage lines are overhead lines. Underground lines are available at Colombo city and some other major cities.

Present Electrification level of Sri Lanka is 98 % [01]. Sri Lankan Government has planned to achieve 100% Electrification level by year 2012. But due to several unfavorable circumstances it was delayed. Sri Lanka is expected to achieve 100% Electrification level within next few years. Interruption of Electricity Supply is common incident in Sri Lanka and it was not highlighted at few years back. Still it remains the same for rural areas. Urban population has a very complex life style and their life style depends largely on the availability of Electricity supply. Once people have the electricity, then they think about the reliability of the supply.

Working hours of most offices in Sri Lanka including Government and Private Sector depends on the availability of electricity. Backup power is found very rarely at Offices in Sri Lanka. Once an interruption occurs, almost all work will stuck till power comes back. If the electricity supply is not reliable, it is difficult to plan any work in the office including meeting, function etc. It can lead to a huge loss of productivity in the company or organization. Industries largely depend on the reliability of Electricity supply. Most of the industries are having back up power supply. Unit cost of backup power supplies is really high compared to unit cost of CEB supply. Sri Lankan Government needs to encourage investors to start industries here. Establish the Free Trade Zones are

one encouraging point and availability of reliable electricity supply without daily power outage with reasonable unit cost will be highly attractive.

Breakdown of power distribution lines are very common. Breakdown and maintenance need to be done affecting least number of consumers. Most of the planned interruptions are done during the weekends. It is really uncomfortable to the domestic consumers which they have planned all their house works during that time. There are two common methods to calculate the reliability of electricity supply. It is System Average Interruption Duration Index (SAIDI) and System Average Interruption Frequency Index (SAIFI). SAIFI is directly affected by the number of interruption times and SAIDI is directly affected by the duration of supply interruption.

Problem Statement

At the early stage, main target of the CEB is to provide electricity for all people. Reliability is not much considered during that time. Most of the Electricity distribution lines (Feeders) are radial types. Once breakdown, all consumers at the feeder will be affected. Only few urban areas have ring type distribution system. Fault can be isolated and unaffected consumers can be fed using 2^{nd} circuit in those areas. Numbers of interrupted consumer are less in these areas.

Provide N – 1 electricity feeding arrangement to all consumers is essential once Grid Substation or Primary Substation or Feeder is out. Alternate Medium Voltage (MV) feeding arrangement should be provided for all consumers. MV feeders include 11 kV lines and 33 kV lines. MV lines are selected to reduce the considerable amount of interrupted consumers once it is failed.

100% Electrification level and availability of contingency electricity feeding plan is very common for Developed countries. Power interruptions are rarely found with them. It is totally different at developing countries. Less Electrification level and daily schedule power cuts exists. Most of the South Asian countries are having daily power outages as their installed capacity is not enough to serve the total power requirement. Sometimes power outages extends 12 – 16 hours per days. Though Electricity is available in those countries, reliability is not assured. People who are living in those countries are lucky if electricity supply is available even though it is not reliable.

At the starting stage the main target was to provide electricity. Once electricity becomes an integral part of people's lives they demand supply reliability. There are several types of contingency electricity feeding plans. Some can be represented as N-X, where X is 1, 2 or 3. X describes number of alternate electricity feeding arrangement. There should be at least one alternate feeding

arrangement to satisfy the consumers. It can be indicated N-1 and it is widely accepted in the planning and operation of the distribution systems. If more alternate electricity feeding arrangements are available it will help to provide better service to the customer.

There are several literature available for Contingency electricity feeding plan including books [09] and some were presented as papers [03], [04], [05], [06], [07], [08]. Reliability of Electricity supply is very critical point to discuss. Many studies have been done regarding the Electricity supply reliability. Measurement of supply reliability is not easy. Even though it is measured, accuracy cannot be guaranteed. It is noted that controlling the numbers of interrupted times is not easy. But duration of interrupted time can be reduced with the alternate feeding arrangement.

As it was described above, contingency electricity feeding arrangement is widely discussed in the world and really necessary for consumers. At least all Electricity service providers need to satisfied N-1 feeding arrangement for their customers satisfaction. If there are competitive electricity suppliers, consumers will more likely selected reliable service provider even though their unit cost is comparatively high.

Sri Lanka has a different situation. CEB has the monopoly to provide electricity to all over the country. CEB is not a profit making organization. CEB is providing service to consumers. Government is deciding the electricity tariff and CEB provide the service with the support of Government. Domestic consumers are receiving more concession compare to other consumers. [01] Presently CEB has no proper contingency electricity feeding plan. Consumers are suffering and complaining about that. As CEB will reach the Electrification level up to 100% within next one or two years, CEB needs to make a proper plan to provide alternate feeding arrangement to their consumers. Once reach the 100% Electrification level, CEB can mainly focus on reliability of electricity supply. This is really critical issue for CEB as they are the only electricity provider in Sri Lanka.

As Sri Lanka is developing country, there are many limitations to be considered while implementing new proposal. Even though it is really required, implementation may not occur due to various reasons. Therefore analyzing the new proposals should be done very carefully and suggestions need to be presented within the limitations. Cost, Construction ability, conflicts with other organizations, political interference and clearance & safety issues need to be analyzed properly before it is finalized.

Methodology

As it is discussed above, alternate feeding arrangement for Electricity distribution system is very important. At least alternate arrangement need to

satisfy N – 1 feeding plan which is not available in the most of the CEB electricity supply. Set of rules for switching operations to match the N-1 feeding plan need to be developed with the support of past experience.

It is required to use proper growth rate of electricity to be considered for load forecast. Main points to consider in the contingency feeding plan are Reliability, Availability, Construction Ability and Cost. Constructions of new lines need to be minimized as much as possible to avoid the conflicts during the implementation.

Dehiwala distribution area is selected for case study. This study is done only for MV lines (33 kV & 11 kV) and four possible cases have been selected for the study as it is mentioned below.

a) Primary Substation Incoming fails
b) Primary Substation fails
c) 11 kV Feeder fails
d) 33 kV Feeder fails

There are one Grid Substation (GS) and three Primary Substations (PS) in Dehiwala area. Dehiwala GS capacity is 63 MVA and Kalubowila, Attidiya, Dehiwala PSs are having capacity of 20 MVA each. There are 45,000 CEB Consumer in this area.

Table 1: Statistic of Dehiwala Area (Source: Account Branch, Western Province South 01, CEB)

Month (2014)	Consumption (kWh)	Sales (Rs)	Average Unit Sales Price (Rs/Unit)
October	12,594,860.00	306,990,877.00	24.37
November	12,488,970.00	293,954,705.11	23.54
December	11,792,985.00	257,164,047.08	21.81

Load readings of Distribution Substations have been collected. All loads reading were taken at night peak durations which is 7.00 pm to 9.00 pm. Synergee software is used to create MV network. Collected load details have been used to create a Synergee model for year 2014. Bulk loads and distribution loads were entered separately. Also MV line type, capacity, PS type, Substation type were selected correctly using the available database of Synergee software.

Decision was made to check the N-1 criteria for the MV model of year 2020. Time of implementation for new proposals can be justified at the year of 2020. Once entered the load details, load allocation need to be made. Date for feeder loads has been taken at 14th July 2014 to make the load allocation. After load allocation is made rate of load growth is added. Load growth rate is mentioned in Table 2. This rate of load

growth was calculated using the power consumption of last 10 years.

Table 2: Load Growth Rate for Dehiwala Area (Source: Planning & Development Branch, Western Province South 01, CEB)

	Domestic	Bulk
Growth Rate per year	2.0	5.0

Validation is required for create models. It is done using present values with the model of year 2015. Those readings are mentioned at Table 3.

Table 3: Comparison of Load Values (Actual and Model of Year 2015)

GS/PS Feeder	Location	Measured Value			Output from Synergee Model 2015 (A)	Error %
		Current (A)	Date	Time		
Dehi F03 (Kalu PS F06)	Peter's lane	49	13/02/2015	19.30	45	8.1
Dehi F03 (Kalu PS F06)	Kohuwala Gantry	50	13/02/2015	20.00	45	10
Dehi F03 (Kalu PS F04)	Kohuwala Gantry	59	13/02/2015	19.45	54	8.4
Dehi F08 (Atti PS F05)	Saranankara Road	50	07/03/2015	20.00	47	6.0
Dehi F08 (Atti PS F05)	Lake Road	133	09/03/2015	19.50	148	11.2
Dehi F08 (Atti PS F03)	Kaudana Road	134	09/03/2015	20.00	128	4.5
Dehi F08 (Atti PS F03)	Alubogahawatta	43	13/02/2015	20.15	44	2.3

Once receive the acceptable validation values, Synergee models were created for year 2015 to 2020. Different Synergee models with the acceptable load growth rate were created for each year. Growth rates were applied separately for bulk loads and distribution loads.

Finding and Results

All four cases have been studied separately using Synergee model for year 2020. Some feeders satisfied the N-1 feeding plan. But most cases failed to satisfy the N-1 requirement. New MV lines, Primary Substations are difficult to construct as Dehiwala is a highly urbanize area. Free locations are rarely found as per the requirement. Considering the necessity of alternate feeding plan, new proposals have been made. Cost and construction ability are mainly considered while preparing the new proposals. When run the load flow of Synergee model, overload lines can be seen highlighted at result window.

Feeder of Kalubowila Primary Substation Fails

There are six 11 kV out going feeders connected to the Kalubowila PS. Almost all feeders are loaded with considerable amount. Synergee model of year 2020 is run while open the feeder switches at PS and extending the interconnected feeder. Then check the overload feeders. This process has been repeated for all feeders of the PS.

It is noted that there are several feeders connected to the one feeder of Kalu PS. Each and every feeder was carefully checked and proposed the best solution to match the N-1 feeding plan. There are four feeders of Kalu PS which cannot be directly extended. Once make the partially load transfer and it is possible to extend the feeder as it is mentioned in the Table 5. It is noted that one MV line need to be strengthened to make the partial load transfer to avoid overloading the line. Feeder details of the Kalubowila PS at SynerGEE model 2020 is mentioned in the Table 4.

Table 4: Feeder details of Kalubowila PS at Synergee model 2020

Feeder	End Point	Peak Current (A)	Interconnect PS Feeders	Peak Current of Interconnect Feeder	Extension is possible
F1	Nadimala Gantry	11	Att. F6	101	Yes
F2	Council Lane	74	Dehi F1	100	Yes
			Att. F5	211	No
F3	Williams, AGA Office, LBS Pamankada	164	Dehi F5	55	No
			Kalu F4	150	No
F4	Pamankada LBS, Mudali Mawatha, Council Lane, Bathiya Mawatha	150	Kalu F6	129	No
			Kalu F3	164	No
			Kalu F2	74	No
F5	Peters Lane (Sakya), Nugegoda	77	Kalu F6	129	No
F6	Mudali Mawata, Alubogahawatta, Sakya Highlevel	129	Kalu F5	77	No

Table 5: Alternate proposals for Kalubowila PS to match N-1 Criteria

Feeder	Interconnect PS Feeder	Alternate Proposals
F3	Dehi F5	Convert Kalu PS F6 to Lynx Circuit upto Kohuwala, Then connect Kalu PS F6 to Saranankara Bo Tree Branch Current (229 & 66+38+63). Dehi PS F5 extend up to Saranankara Bo Tree including Kalu F3(164+55-63)
F4	Kalu F2	Open De Silva Road and Closing Mudali mawatha connect Kalu PS F6 to Pamankada LBS (129+38). Then extend Kalu PS F2 to Pamankada LBS (74+150-38)
F5	Kalu F6	Kalu. F2 Kohuwala (74+64), Then Connect Kalu F6 (129-64+77)
F6	Kalu F5	Kalu. F2 Kohuwala (74+64), Then Connect Kalu F5 (77+129-64)

Feeder of Grid Substation Fails

There are six 33 kV outgoing feeders connected to the Dehiwala GS. Capacities of the all feeders are 400A (Lynx Line). Synergee model of year 2020 is run while the feeder switches are open at GS and extending the interconnected feeder. Then check the overload feeders. This process has been repeated for all feeders of the GS. Alternate proposals have been made to provide N-1 feeding plan which is not available at Synergee model year 2020. Interconnection feeders are not available for two GS feeders. New proposals are made for those two feeders and it is mentioned in the Table 7. Feeder details of the Dehiwala GS at SynerGEE model 2020 is mentioned in the Table 6

Table 6: Feeder details of Dehiwala GS at SynerGEE model 2020

Feeder	End Point	Peak Current (A)	Interconnect PS Feeders	Peak Current of Interconnect Feeder	Extension is possible
F1	Kalubowila	11	N/A	-	N/A
F3	Kalubowila	206	N/A	-	N/A
F5	Pannipitiya	0	Panni F5	36	Yes
F7	Pannipitiya	169	Panni F3	56	Yes
F6	Ratmalana	112	Rat F7	173	Yes
F8	Ratmalana	185	Rat F6	44	Yes

Table 7: Alternate proposals for Dehiwala GS to match N-1 Criteria

Feeder	Interconnect PS Feeder	Alternate Proposals
F1	N/A	New line to Connect to Kirulapana GS
F3	N/A	New line to Connect to Kirulapana GS

Dehiwala Primary Substation Fails

There is one feeder which cannot be extended directly at Dehiwala PS. It can be extend using partial load transfer, observations of the load flow analysis of Dehiwala PS are mentioned in the Table 8 and Table 9.

Table 8: Feeder details of Dehiwala Primary at SynerGEE model 2020

Feeder	End Point	Peak Current (A)	Interconnect PS Feeders	Peak Current of Interconnect Feeder	Extension is possible
F1	Galle Road 2nd Lane	100	Kalu F2	74	Yes
F2	RMU1 Mt. Lavinia Hotel	131	Att F3	117	No
			Att F2	97	No
F3/F5	Urban Site/AGA Office	55	Kalu F3	164	No
F4	Kawdana Board way	45	Att F2	94	Yes

Table 9: Alternate proposals for Dehiwala PS to match N-1 Criteria

Feeder	Interconnect PS Feeder	Alternate Proposals
F2	Att F2	Att F3 extend Palm Beach Hotel Sw 1 (117+53). Then Att F2 extend Palm Beach hotel Sw 1 (117+131-53)
F3/F5	Kalu F3	Kalu F6 Lynx Circuit to Kohuwala, Then Connect Kalu F6 to Saranankara Bo Tree Branch Current (66+38+63). Kalu F3 Extend Up to Dehi F5 (164+55-63). Closed LBS at Urban Site to connect Dehi F3

SAIDI [11] and SAIFI [12] are the well-known index for analyzing reliability of the power supply. SAIDI is directly related to the project. SAIDI can be calculated using equation (01)

$$\text{SAIDI} = \frac{Sum\ of\ all\ consumer\ interruption\ durations}{Total\ number\ of\ consumers\ served} = \frac{\sum U_i N_i}{N_T} \quad \text{Eq.1}$$

Where N_i - Number of Consumers,
U_i - Outage time for location *i*
N_T - Total number of consumer served

SAIDI value is calculated before and after the new proposals for 3 months. It is clearly visible that SAIDI has improved considerably with the new proposals. Details of the interruptions and breakdowns for SAIDI calculation were obtained from Call Centre, Western Province South 01, CEB. Summary of the SAIDI values are mentioned at the Table 10.

Table 10: Summary of SAIDI

Month		**November 2014**	**December 2014**	**January 2015**
SAIDI Value (Mins/Consumer)	Present	394	61	218
	After Alternate Feeding plan	341	54	129
	Percentage of improvement	13.45%	11.48%	40.83%

Basically less than 10 mins interruptions are not considered for improvement of SAIDI as it will take similar time for switch operations. Also reduction of consumer interruption mins were calculated for 10 mins less than the total interrupted time. It is reserved for line preparation work and switching operations.

Common Models for N-1 Feeding plan

Case study has been conducted to initiate and analyze the result of the project proposal. Considering findings and results of the case study common models have been developed to match

the N-1 feeding plan, which can be applied to any of distribution region. Three separate models have been developed for three different cases. Those are mentioned below as Figure 2, Figure 3 & Figure 4.

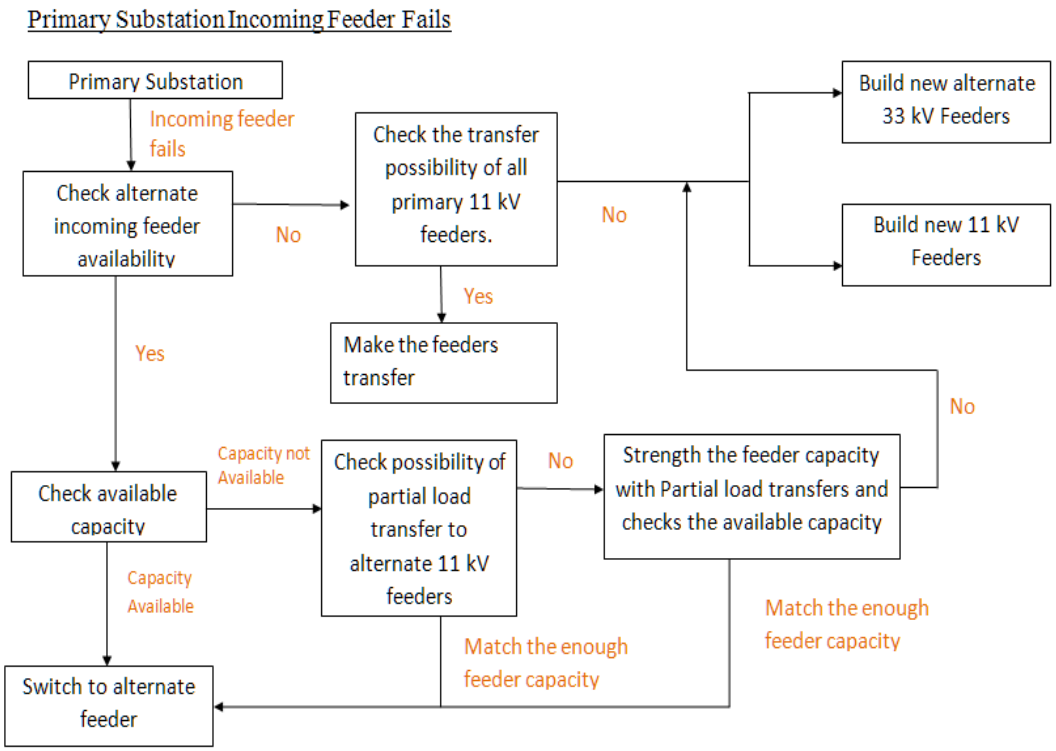

Figure 2: Develop Model for PS Incoming Feeder Fails

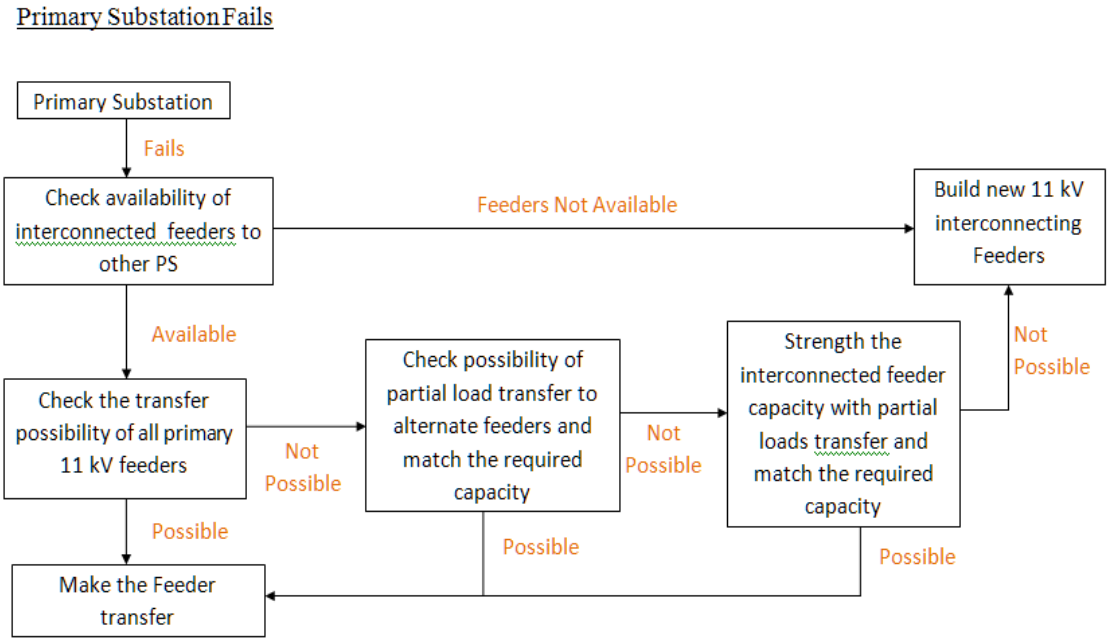

Figure 3: Develop Model for Primary Substation Fails

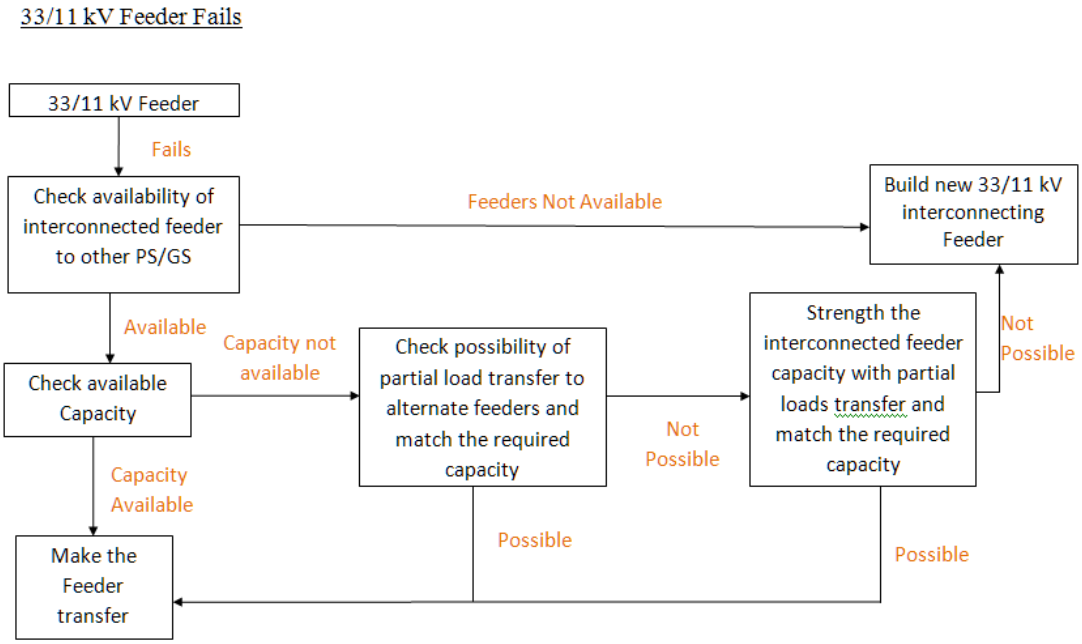

Figure 4: Develop Model for MV Feeder Fails

Conclusion

The objective of this study is to increase the reliability of CEB power supply providing N-1 Electricity feeding plan. Few years back, target of the CEB was to achieve the 100% electrification level and reliability of the electricity supply was not much of a concern. Reliability of electricity supply can be increased using N-1, N-2, N-3 electricity feeding plan. Aim of this study is to initiate N-1 electricity feeding plan for distribution area of the CEB. Case study is done to observe the present system and check the possibility of improvement. Reliability of the electricity supply can be analyzed using SAIDI and SAIFI. SAIDI is directly related to this project. Summary of calculated SAIDI values for three months are mentioned in the Table 11. When comparing the SAIDI values with the present system and proposed system, it is clearly shown that considerable amount of improvement of the SAIDI at proposed system as it is shown in the Table 11. Therefore CEB need to provide at least N-1 electricity feeding arrangement to all consumers to help to achieve their quality of life. This will help to enhance the CEB reputation within their consumers.

Three common models have been prepared to provide N-1 feeding arrangement to any distribution area using the results of case study. Three models are mentioned in Figure 2, Figure 3 and Figure 4

References

[1] Statistical Digest 2013, Ceylon Electricity Board

[2] Annual Report 2013 – LECO

[3] Jun Xiao, Xin Li, Wenzhuo Gu, Fangxing Li, Chengshan Wanga, *"Model of distribution system total supply capability considering feeder and substation transformer contingencies",* Electrical Power and Energy Systems 65 (2015) 419–424

[4] Luo Fengzhang, Wang Chengshan, Xiao Jun, Ge Shaoyun, *"Rapid evaluation method for power supply capability of urban distribution system based on N-1 contingency analysis of main-transformers",* Electrical Power and Energy Systems 32 (2010) 1063–1068

[5] J.S. Wu, T.E. Lee, Y.M. Tzeng, C.S. Chen, *"Enhancement of an object-oriented expert system for contingency load transfer of distribution systems",* Electric Power Systems Research 42 (1997) 87-94

[6] Jaeseok Choi, Timothy Mount and Robert Thomas "*Transmission System Expansion Plans in View Point of Deterministic, Probabilistic and Security Reliability Criteria*", Proceedings of the 39th Hawaii International Conference on System Sciences – 2006

[7] Mendes A., Boland N., Guiney P., Riveros C., "*(N-1) contingency planning in radial distribution networks using genetic algorithms*" Transmission and Distribution Conference and Exposition: Latin America (T&D-LA), 2010 IEEE/PES 290-297

[8] Jun Xiao, Guo-qiang Zu, Xiao-xu Gong, and Cheng-shan Wang "*Model and Topological Characteristics of Power Distribution System Security Region*" Hindawi Publishing Corporation Journal of Applied Mathematics (2014) Article ID 327078

[9] H. Lee Willis, "*Power Distribution Planning Reference Book, Second Edition, Revised and Expanded*" 499-502

[10] www.ceb.lk (Accessed: 18th March 2015)

[11] http://en.wikipedia.org/wiki/SAIDI (Accessed: 18th March 2015)

[12] http://en.wikipedia.org/wiki/SAIFI (Accessed: 18th March 2015)

Evaluation of Gliricidia Resources in Kandy District for Dendro Thermal Power Generation (DTPG)

Hitinayake, H.M.G.S.B., Gunathunga, K.M.H.
Department of Crop Science, Faculty of Agriculture, University of Peradeniya, Peradeniya

Abstract

The objective of this study was to estimate the Gliricidia wood resources available in the Kandy district for dendro thermal power generation. Hence study was focused on estimating Gliricidia woody biomass produced in the Kandy district under different cropping systems, lopping frequencies and agro ecological zones. Destructive sampling was done to evaluate the biomass production. Results of the study showed that mean differences of Gliricidia biomass produced under different agro ecological regions are not significant (p=0.05) except in the case of pepper–Gliricidia system with 12 month lopping interval. This shows that soil related factors such as soil type, soil depth, graveliness, pH and soil moisture have a bigger impact on Gliricidia yield than the agro climatic differences in the Kandy district. The amount of Gliricidia wood produced under pepper, coconut, tea and live fence systems are 114,085 tones, 7,297 tones, 111,644 tones and 18,720 tones, respectively. Under these four systems 251,746 tons of Gliricidia wood (at 20% moisture content) is produced annually and this is equivalent to 126 GW electricity.

Key words: Cropping systems with Gliricidia, Gliricidia biomass, Dendro Thermal Power

Introduction

Gliricidia (*Gliricidia sepium)* is used as a multipurpose leguminous tree crop in range of farming systems in Sri Lanka. The advantage of Gliricidia as a multipurpose species is its fast growth, wide adaptability, easy establishment and tolerance to frequent lopping or high coppicing ability [1, 2 and 3]. Dendro thermal power refers to the generation of electricity from sustainably grown biomass [4].

This typical multipurpose tree species has been introduced to Sri Lanka in 1700s for boundary planting [5]. According to past records [6], this introduction has been from the seeds of one tree from Trinidad. Gliricidia has been introduced to Trinidad and other Caribbean islands as a shade tree for coffee by the the Spanish [7]. This versatile tree is native to Mexico and Central America [8]. *Gliricidia sepium* belongs to family Fabaceae and sub family Papilionaceae. In Sri Lanka it is grown in all major ecological zones except elevations above 1200m. It thrives well with an annual rainfall of 900-1500mm. Leaf shedding and profuse flowering occurs during dry weather periods. The best temperature for Gliricidia is 22-30^{0}C. Gliricidia can be grown in a wide variety of soils and hence is used to improve degraded soil. Growth of Gliricidia is poor when pH of soil is low as 3.75 [2]. *Gliricidia sepium* has hermaphrodite flowers and they are self-incompatible (obligate outcrosser) [9].

Globally, only 8 % of electricity is generated using fossil fuel whereas 70% of electricity requirement of Sri Lanka is generated using fossil fuel. This is a huge problem for Sri Lanka when consider its cost [4]. Petroleum fuels could be replaced with relatively cheap Gliricidia wood to generate the required heat energy [10]. Every liter of fuel oil can be replaced by 5-10kg of fuelwood while minimizing the burden on national economy and foreign exchange. Every liter replaced will provide 5-10 man minutes of opportunity for rural labor to participate in a mainstream economic activity. Normally, 1KW electricity can be generated using 1.5-2.5 kg of wood under dendro thermal power generation [11].

The objective of this study was to estimate the Gliricidia wood resources available in the Kandy district for dendro thermal power generation. Hence study was focused on estimating Gliricidia woody biomass produced in the Kandy district under different cropping systems, lopping frequencies of Gliricidia commonly practiced by the farmers in them and agro ecological zones that traverse through the Kandy district.

Materials and Methods

This study was conducted in the Kandy District. The main agro ecological zones traverse through the Kandy District are mid country wet zone (WM), mid

country intermediate zone (IM), upcountry wet zone (WU) and upcountry intermediate zone (IU) (Annexure 1). The two upcountry regions were considered as one region during sampling due to their smaller coverage in the district and provision of largely similar growing conditions when consider Gliricidia. Sites in the range of 900-1200m were selected to represent up country regions (WU and IU) as growth of Gliricidia is low beyond 1200m elevation. The cropping systems which produce Gliricidia include pepper grown on Gliricidia, Gliricidia grown under coconut, Gliricidia in live fences and Gliricidia as a shade tree in tea.

Sampling sites were selected to represent different cropping systems, agro ecological zones and Gliricidia lopping frequencies commonly practiced by the farmers to evaluate Gliricidia biomass production (Table 1). Four localities were selected to represent each site. Destructive sampling (lopping of trees) was done to estimate the biomass. At each site forty trees of Gliricidia from pepper system, 20 trees of Gliricidia from coconut system, 20 trees of Gliricidia from tea system and 30m length from live fence system were selected as samples.

Table 1: Sampling sites to evaluate Gliricidia biomass production under different cropping systems, agro ecological zones and lopping intervals.

Climatic Zone	Lopping interval							
	Pepper			Coconut		Tea	Live fence	
	4 months	6 months	12 months	6 months	9 months	6 months	6 months	12 months
Mid country Intermediate Zone (IM)	Digana, Haragama, Kundasale, Teldeniya,					-	Digana, Haragama, Kundasale, Teldeniya	
Mid Country Wet Zone (WM)	Galagedara, Gampola, Peradeniya, Pilimatalawa							
Upcountry (UW/IU)	Delpitiya, Deltota, Nawalapitiya, Pupuressa			-	-	Delpitiya, Deltota, Nawalapitiya, Pupuressa		

Gliricidia wood and leaf production by different cropping systems across the agro-ecological regions and commonly practiced lopping frequencies was compared. Both fresh weight and dry weights were taken. The data presented are for 20% moisture content as it is the standard moisture content of wood used in dendro thermal power generation. Data analysis was done using the

General Liner Model (GLM) and Mean Separation was done using Duncan's Multiple Range Test.

Results and Discussion

Woody biomass production

Woody biomass production by Gliricidia under different cropping systems, lopping frequencies and agroecological zones are given in the Table 2. Woody biomass production under the four cropping systems ranged from 5.6-13.9 kg per tree per year at 20% moisture content. Mean differences of woody biomass production across different agro ecological zones under a given lopping frequency was not significant (P=0.05) except in the case of pepper–Gliricidia system under 12 month lopping interval. Similarly mean differences of woody biomass production under different lopping frequencies under a given climatic zone is not significant (P=0.05). This is due to high variation observed in the wood production.

Table 2: Woody biomass production of Gliricidia under different cropping systems, agro ecological zones and lopping intervals (kg per tree per year at 20% moisture content)

Climatic Zone	Lopping interval							
	Pepper			Coconut		Tea	Live fence	
	4 months	6 months	12 months	6 months	9 months	6 months	6 months	12 months
Mid country Intermediate Zone	13.1±0.7 (4.36)	13.7±2.6 (6.86)	10.4±0.9 (10.44)	8.5±0.9 (4.23)	8.2±0.8 (6.16)	-	6.3±0.9 (3.15)	5.6±0.6 (5.60)
Mid Country Wet Zone	13.9±0.8 (4.65)	9.7±1.6 (4.87)	8.5±0.9 (8.57)	10.3±1.3 (5.17)	7.2±0.4 (5.44)	9.5±0.9 (4.77)	6.6±0.8 (3.33)	7.1±0.9 (7.11)
Up country (WU/IU)	12.8±0.7 (4.27)	9.8±1.5 (4.92)	9.6±1.3 (9.65)	-	-	8.8±0.7 (4.42)	8.5±1.4 (4.25)	6.8±0.9 (6.86)
DNMRT (P=0.05)	P=0.05	P=0.05	P<0.05	P=0.05	P=0.05	P=0.05	P=0.05	P=0.05

Key: Per season woody biomass yield kg per tree at 20% moisture content is given in the parenthesis; DNMRT-Duncan's Multiple Range Test

Green manure production

Green manure production by Gliricidia under different cropping systems, lopping frequencies and different agroecological zones is given in the Table 3. Green biomass production of Gliricidia under four cropping systems ranged from 0.88-3.58 kg per tree per year (dry weight). Mean differences of green biomass production by cropping systems

across different agro ecological zones under a given lopping frequency was not significant (P=0.05). Also mean differences of green biomass production under different lopping frequencies under a given climatic zone was not significant (P=0.05). This is largely due to very high variation observed in the green biomass production across different sites. This can be attributed to that biomass production is more sensitive to

Table 3: Green biomass production of Gliricidia under different cropping systems, agro ecological zones and lopping frequencies (kg per tree per year)

Climatic Zone	Lopping interval							
	Pepper			Coconut		Tea	Live fence	
	4 Months	6 Months	12 Months	6 Months	9 Months	6 Months	6 Months	12 Months
Mid country Intermediate Zone	3.58 (1.19)	4.45 (2.22)	1.86 (1.86)	2.35 (1.17)	1.90 (1.42)	-	2.05 (1.04)	0.88 (0.88)
Mid Country Wet Zone	3.38 (1.12)	2.53 (1.26)	2.36 (2.36)	2.50 (1.25)	1.77 (1.32)	1.85 (0.92)	2.35 (1.17)	2.05 (2.05)
Up country (WU/IU)	3.23 (1.07)	2.63 (1.31)	2.06 (2.06)	-	-	2.05 (1.02)	1.65 (0.82)	1.45 (1.45)
Duncan MRT (P=0.05)	P=0.05	P=0.05	P=0.05	P=0.05	P=0.05	P=0.05	P=0.05	P=0.05

Key: Per season green biomass yield kg per tree at 20% moisture content is given in the parenthesis

Leaf : Stem Ratio of Gliricidia

Leaf : stem ratio of Gliricidia biomass produced under different cropping systems, lopping frequencies and agroecological zones are given in the Table 4. Leaf : stem ratio of Gliricidia produced under the four cropping systems range from 0.18-0.35. Mean differences of Leaf : stem ratio recorded for different agro ecological zones for a given lopping frequency were not significant (P=0.05). Similarly mean differences of Leaf : stem ratio recorded for different lopping frequencies under a given climatic zone were not significant (P=0.05). This is largely due to high variation observed in the biomass data collected across different sites.

Table 4: Leaf: stem ratio of Gliricidia under different cropping systems in different agro ecological zones (kg per tree per year at 20% moisture content)

Climatic Zone	Lopping interval							
	Pepper			Coconut		Tea	Live fence	
	4 Months	6 Months	12 Months	6 Months	9 Months	6 Months	6 Months	12 Months
Mid country Intermediate Zone	0.258	0.326	0.178	0.278	0.231	-	0.350	0.243
Mid Country Wet Zone	0.242	0.263	0.242	0.242	0.243	0.194	0.312	0.181
Up country (WU/IU)	0.251	0.267	0.214	-	-	0.280	0.204	0.225
Duncan MRT (P=0.05)	P=0.05	P=0.05	P=0.05	P=0.05	P=0.05	P=0.05	P=0.05	P=0.05

Gliricidia Biomass Production in the Kandy district

The average weights of Gliricidia biomass produced under different cropping systems and the average number of Gliricidia trees planted in the systems (per ha) are given in the Table 5. Using these values production of Gliricidia per ha by different cropping systems was estimated.

Table 5: Production of Gliricidia woody biomass by different cropping systems (at 20% moisture content)

Cropping system	IM			WM			WU/IU			Avg. Weight per ha (tons)
	Avg. weight per tree (kg)	No. of trees per ha	Weight per ha (tons)	Avg. weight per tree (kg)	No. of trees per ha	Weight per ha (tons)	Avg. weight per tree (kg)	No. of trees per ha	Weight per ha (tons)	
Pepper	12.41	1682	20.87	10.76	1682	18.10	10.77	1682	18.12	19.03
Coconut	8.34	2160	18.01	8.81	2160	19.03	-	-	-	18.52
Tea	-	-	-	9.54	1076	10.27	8.82	1076	9.49	9.88
Live fence	5.95	840	5.00	6.89	840	5.79	7.69	840	6.46	5.75

Based on the data collected by the study (Table 5) and considering the extent of cultivation of different cropping systems under which Gliricidia is grown in the Kandy district, it can be estimated that 251,746 t of Gliricidia woody biomass (under 20% moisture content) can be produced. It was estimated by multiplying the average weights of Gliricidia wood produced under the

cropping systems per ha (see Table 5) by the extents of different cropping systems in the district. There are 6,661 ha of pepper lands, 7,888 ha of coconut lands and 22,599 ha of tea lands in Kandy district [12]. It is assumed that 5995ha of pepper lands (90% of the pepper lands) have used Gliricidia as the shade and vine support tree, 394 ha of coconut lands (5% of coconut lands) have intercropped with Gliricidia and 11300 ha of tea lands (50% of total) are using Gliricidia as shade trees. Further it is assumed that 3744ha (5% of the lands) in the mid country intermediate (IM) zone have planted Gliricidia as a live fences. Hence the amount of Gliricidia wood produced under pepper, coconut, tea and live fence cropping systems are 114,085 t, 7,297 t, 111,644 t and 18,720 t, respectively.

In addition to woody biomass about 66,713 t of Gliricidia green biomass is annually produced in the district to under these cropping systems. They can be used as green manure or production of compost. Gliricidia green manure is rich in plant nutrients and containing 3-4.5% nitrogen, 0.2-0.3% phosphorus, 1.5-3.5% potassium, 1.4% calcium and 0.4-0.6% magnesium [2].

Conclusions

The study shows that Kandy district has a large stock of Gliricidia wood (251,746 tones) that can be used to generate electricity. On average 1KW electricity can be generated using 2kg of Gliricidia under dendro thermal power generation. Hence, there is a potential to generate over 126 GW electricity annually using the stock of Gliricidia available in the Kandy district.

A high variation was observed in the biomass production across different sites and localities of the district. This indicates that climatic zone do not make a significant limitation on the growth and yield of Gliricidia and it can be cultivated successfully in most parts of the district except elevations above 1200m. It appears that soil related factors such as soil type, soil depth, graveliness, pH and soil moisture have a higher bearing on the biomass production of Gliricidia.

Appendix

Appendix 1: Categorization of lands of different Divisional Secretariat Divisions (DSD) in the Kandy Districts based on the agro ecological conditions.

DSD	Land Extents in ha			
	WM	IM	WU	IU
Akurana	2861	-	-	-
Delthota	248	1039	965	3182
Doluwa	5486	-	3529.4	554
Ganga Ihala Korale	6847	-	2409	-
Harispattuwa	5415	-	-	-
Kandy	4454	1256	-	239
Kundasale	2457	5598	-	
Medadumbara	2024	17064	-	4527
Minipe	-	10400	-	1853
Panvila	3706	5589	-	5478
Pasbage Korale	6833	-	5211	-
Pathadumbara	4225	644	-	09
Pathahewaheta	-	5296	-	2941
Poojapitiya	5738	-	-	-
Thumpane	1181	-	-	-
Udadumbara	-	28013	-	8601
Udapalatha	5879	-	3321	-
Udunuwara	6667	-	-	-
Yatinuwara	7095	-	-	-
Total	71116	74899	15435.4	27384

Source: [13]; Key: WM-Mid Country Wet Zone, IM-Mid Country Intermediate Zone, WU-Up Country Wet Zone, IU-Up Country Intermediate Zone

References

[1] Stewart JL. Utilization. In: *Gliricidia sepium,* Genetic Resources for farmers. Tropical Forestry Paper 33. Oxford Forestry Institute, U.K; 1996; p 33-44.

[2] Gunasena HPM. Gliricidia in Sri Lanka. The University of Peradeniya-Oxford Forestry Institute (UK) Forestry Research Link; 1997; 67p.

[3] Gunathilake HAJ, Joseph PG, Wickramasinghe H, Peiris TSG. Sustainable Biomass Production in Sri Lanka and Possibilities for Agro-forestry Intervention; 2015. [Online] Available:http://projects.nri.org/biomass/conference_papers/sustainable_biomass_production_in_srilanka.pdf (Accessed on 2015.06.22)

[4] Wickramasinghe H, Weaver BM. Dendro: Biomass Power From, By, and For the People of Sri Lanka. ASME 2006 International Solar Energy Conference (ISEC2006), July 8–13. Denver, Colorado, USA; 2006.

[5] Simons AJ, Dundson J.L. Evaluation of the potential for genetic improvement of *Gliricidia sepium*. ODA Forestry Research Report. Project R4525. Oxford Forestry Institute, UK; 1996.

[6] Hughes C.E. Biological considerations in designing a seed collection strategy for *Gliricidia sepium.* Commonwealth Forestry Review; 1987; 66: 31-48.

[7] Ford L.B. Experiences with *Gliricidia sepium* in Caribbea. In *Gliricidia sepium* Management and improvement. Proc. NFTA/CATIE Workshop, Costa Rica. June; 1987; p3-7.

[8] Glover N. *Gliricidia:* Production and Use. NFTA Publication. P.O. Box 680. Waimanalo, Hawaii. USA; 1989.

[9] Simons A.J. Ecology and Reproductive Biology. In: *Gliricidia sepium,* Genetic Resources for farmers. Tropical Forestry Paper 33. Oxford Forestry Institute, U.K.; 1996; p 19-29.

[10] Perera KKCK, Rathnasiri PG, Sugathapala A.G.T. Sustainable biomass production for energy in Sri Lanka. Biomass & Bioenergy; 2003; 25(5): 541-556.

[11] Capareda SC. Introduction to biomass energy conversions. Taylor & Francis Group LLC, CRC Press, USA; 2014.

[12] Department of Census and Statistics. Sri Lanka Census of Agriculture; 2002.

[13] Punyawrdena BVR. Rainfall and Agro-ecological Regions of Sri Lanka (in Sinhala). Department of Agriculture; 2008; 129p.

Introduction of saw dust ovens for the production of Maldive fish: Environmental benefits through productivity gains

Mudalige, N.K.
Soba Kantha Foundation

Abstract

Maldive fish is made by boiling fish and sun-drying it typically for nine days. This method, although prevalent in many places in the country, is unproductive and environmentally unsound. The Small Grants Programme of the Global Environmental Facility introduced ten sawdust ovens in Mirissa of Matara, and established a baseline of the environmental impact prior to the project and compared the impact after the introduction of the ovens. A single oven served the drying needs of five women, therefore the total beneficiaries was 50 women. A representative sample of 27 women was used for the study. After the introduction of ovens, the average Maldive fish production increased to 132 kg/month per woman, a 33% gain from the previous production level. Prior to the introduction of the oven, firewood was used to boil fish. With the introduction of the oven, fish was boiled on a sawdust stove, and dried in a sawdust fired oven. The specific CO2 emission prior to the introduction of the oven was 4.7 kg of CO2 per kg of Maldive fish made, which declined by 20% to 3.8 kg of CO2 per kg of Maldive fish made after the introduction of ovens. When firewood was used for boiling, typically 10 kg of ash was generated from 63 kg of firewood. But only 3 kg of ash was generated from sawdust to do the same work, marking a 70% reduction. The energy cost of Maldive fish prior to the introduction of ovens was LKR 29.78/ kg of Maldive fish, which declined to LKR 4.12 /kg of Maldive fish after the introduction of ovens, since sawdust was a waste resource available aplenty, unlike the commercial fuel wood used before. Nevertheless, the use of solar heat as an energy source in the Maldive fish industry ceased with the introduction of the oven. This must be further probed to find a technology which can use both solar and waste biomass resources to further increase the productivity and profitability.

Introduction

Fisheries Production

The fisheries industry plays an important role in the economy of Sri Lanka by providing livelihood for more than 2.5 million coastal communities as well as providing more than 50% of animal protein requirement of people in the country. The industry can be divided in to costal, offshore/deep sea, and inland and aquaculture sub sectors. Further, the share of fisheries to the Gross Domestic Production (GDP) of the country has remained unchanged and that was 1.7% with a stable contribution of inland (0.2%) and marine fisheries (1.5%) in 2011 [1]. In 2012 the share of fisheries to the GDP was 1.8% with a contribution of inland fisheries at 0.3% and marine fisheries at 1.5% [2]. Prior to the war on terrorism in 1985, the Jaffna district was a dominant fish producing district that contributed more than 25% to the total marine fish production. But at present, the Kalutara district is the dominant fish producing district in the country. With the end of the war, the fish production in the North and Northeastern provinces are gaining momentum. The study site of this report, the Matara district contributes by 14% [1] & [2].

Sri Lanka is the major fish produce importer in the South Asian region contributing more than 75% of the total imports of the region. But a large proportion of imported fish is re-exported to other countries and the rest is used for local consumption. Dried fish, Spats, Maldive fish, canned fish and edible fish are the major imported fish and fisheries products to the country [1].

According to the Sobha Kantha Environment and Community Development Foundation (2015) [3], the production process of Maldive fish constitutes of the following steps. First, the inedible parts such as intestines and head are severed. The fish is washed in cold water and then boiled for about 45 minutes, with an appropriate marinating mixture. Once the fish is boiled well, it becomes flaccid and is torn apart into four pieces. It is then dried in the oven for about six hours. Next, the skeleton is removed, and the balance is dried for three days, with manual turning of fish every six hours.

Saw dust as an energy source

Saw dust is an important industrial residue in the renewable energy industry and has varied applications in thermal energy generation [4]. Saw dust falls under the category of agro industrial residues [5]. It is estimated that a minimum of 52,000 tonnes of saw dust was produced from the timber milling industry. Of this, a very small quantity is used in the manufacturing industry and in the household sector as a cooking fuel. There aren't any detailed studies carried out on the use of saw dust in the

household sector. The available quantity of saw dust to be used in energy applications is 47,500 tonnes [4]. According to a study done by the Biomass Energy Association in Sri Lanka (2005) [6], a total of 52,298 tonnes of saw dust is available for various uses.

Objectives and Methodology

The objective of this study is to assess the environmental impact of the introduction of saw dust based ovens for the manufacturing of Maldive fish, with special emphasis on productivity gains.
Ten ovens among ten clusters had been distributed by the Sobha Kantha Environment and Community Development Foundation under a grant received from the GEF/SGP. Each cluster comprises of five women. The environmental impact study was carried out with a sample of 27 participants on May 23, 2015. Data was gathered through questionnaires, one to one interviews, field measurements and by extracting data from log books maintained by the user groups. Data on pre and post project methods of Maldive fish production were compared to calculate the specific carbon emissions.

Results and discussion

Data extracted from five log books indicated that the monthly average production of Maldive fish was 132 kg/month at present. When extrapolated to the entire population (ten ovens), the annual production amounts to 15,869 kg/annum of Maldive fish. Before the introduction of the oven, the production was around 33% less than the current production. The reasons for this reduction have been discussed below.

Figure 1 indicates that the average monthly production of Maldive fish peaks from July to September, and dips in February and March.

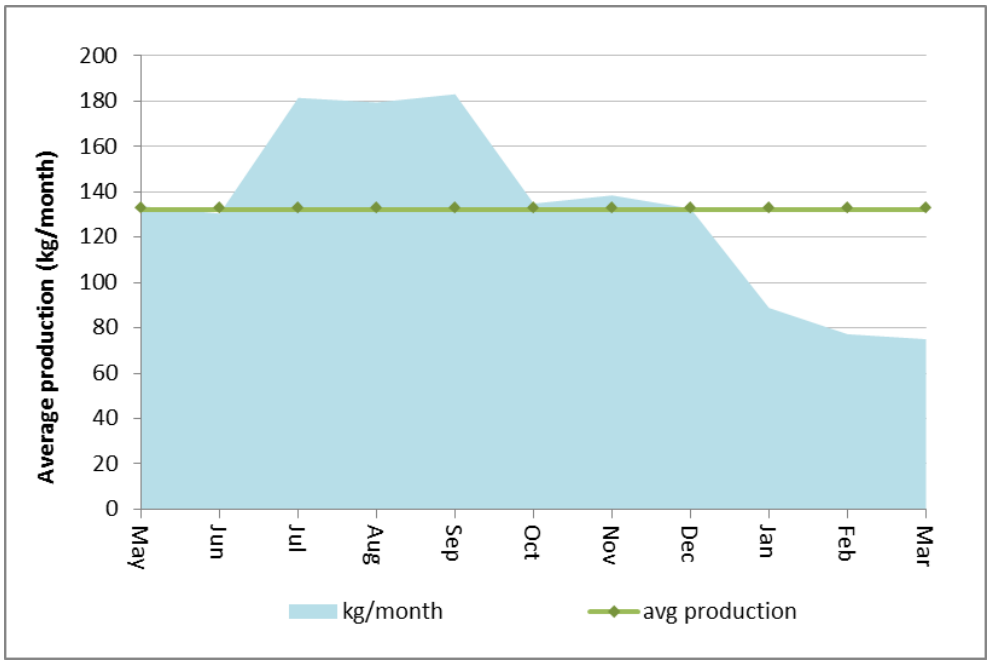

Figure 1: Average Maldive fish production (kg/month)

Calculation of the specific carbon emission

Based on data gathered from questionnaires and field measurements, the specific carbon emissions of the process prior to the introduction of the oven and after the introduction of the oven were calculated, as tabulated in Table 1.

Table 1: Comparison of specific carbon emission before and after the advent of the oven

	Without the oven	With the oven
Boiling - CO_2 emissions (kg/month)	7,531	2,945
Oven/ or sun drying - CO_2 emissions (kg/month)	1,208	8,890
Transport of fuel - CO_2 emissions (kg/month)	172	51
Total CO_2	8,911	11,886
Fraction of Maldive fish (marketable quality)	80%	100%
Increase in production (factor)	1	1.3
Maldive fish production (kg/month) – theoretical	2,375	2,375
Actual Maldive fish output (kg/month)	1,900	3,167
CO_2 emissions per kg of Maldive fish (kg CO_2/kg Maldive fish)	4.7	3.8

Before the introduction of the oven, firewood was used for boiling in open, three-stoned hearths. The women claimed that it was a tedious and messy process, because they had to stoke the fire often to keep it alight. With the introduction of the saw-dust stove however, this situation dramatically changed, allowing women to boil an increased capacity of fish, under improved, hygienic cooking conditions, with minimum effort to keep the fire burning. When the production records before and after the introduction of the oven was compared, it was calculated that the capacity of fish input has increased by a factor of 1.3. This too was considered in the above calculation. Also, prior to the oven, Maldive fish was sun-dried. But this led to a loss of 20% of the Maldive fish, owing to reasons such as them being carried away by stray dogs or being discarded owing to fly infestations resulting from unhygienic surroundings. The quality of the Maldive fish therefore, declined greatly. With the introduction of the oven, this situation changed for the better, where all the Maldive fish was dried under hygienic conditions and the total output was of high quality. This factor too was considered in the above calculation.

Before the introduction of ovens, saw dust produced in mills were dumped into the sea or incinerated in open dumps, which was an environmental hazard. But with the advent of ovens, this saw dust was used for the ovens, thereby providing a productive use for the waste and minimising environmental hazards. Saw dust was typically packaged in bags and transported in either tractors or three wheelers, from mills within close proximity to the ovens. Therefore, this marked a reduction in the distance transported, and accordingly a reduction in the quantity of CO_2 emitted, as indicated in Table 1.

The carbon footprint of the previous process was 4.7 kg of CO_2 per kg of Maldive fish made. This declined to 3.8 kg of CO_2 per kg of Maldive fish made, with the introduction of the oven. This is a 20% reduction. The conversion factors used for this calculation are tabulated below (Table 2).

Table 2: Conversion factors

CO2 emissions	Unit	Value	Source
Wood/ wood waste	kg/kg	1.51	[7]
Diesel	kg/l	2.74	[7]
Gasoline	kg/l	2.28	[7]
Diesel consumption in tractors	l/100 km	29	[8]
Gasoline consumption in three-wheelers	l/100 km	5.2	[8]

Also, during the period when firewood was used for boiling, typically 10 kg of ash was generated from 63 kg of firewood. But now, only 3 kg of ash is generated from saw dust used to do the same amount of work. This marks a 70% reduction in ash. Further, since firewood was burnt in an open hearth, the ash created environmental problems, by being blown away. But in the saw-dust stoves, the ash is retained within the vessel, till it is removed.

The saw dust is collected in polythene sacks when transported and stored. All saw dust sacks are stored in sheds, so that they are kept dry. Saw dust is manually filled into the sacks by the women, therefore the only cost incurred is for transporting them in a vehicle.

During the time Maldive fish was sun-dried, women had to take turns to watch over the Maldive fish to ward off stray dogs and scavenger birds. This was a very time consuming process. Now however, this time has entirely been released to be directed for other quality work.

Cost implication

Before the introduction of the oven, firewood was traded in tractors, which cost LKR 1,891 per month on average. According to Figure 2, the prices of firewood ranged between LKR 4/kg to LKR 12/kg. One recipient used her own firewood, which was gathered from her garden, therefore it incurred no cost. At present, there is no requirement for firewood, but saw dust. The cost for saw dust per month varies between LKR 0.11/kg to LKR 1.45/kg. One recipient supplies her own saw dust in her three-wheeler, therefore no costs are incurred.

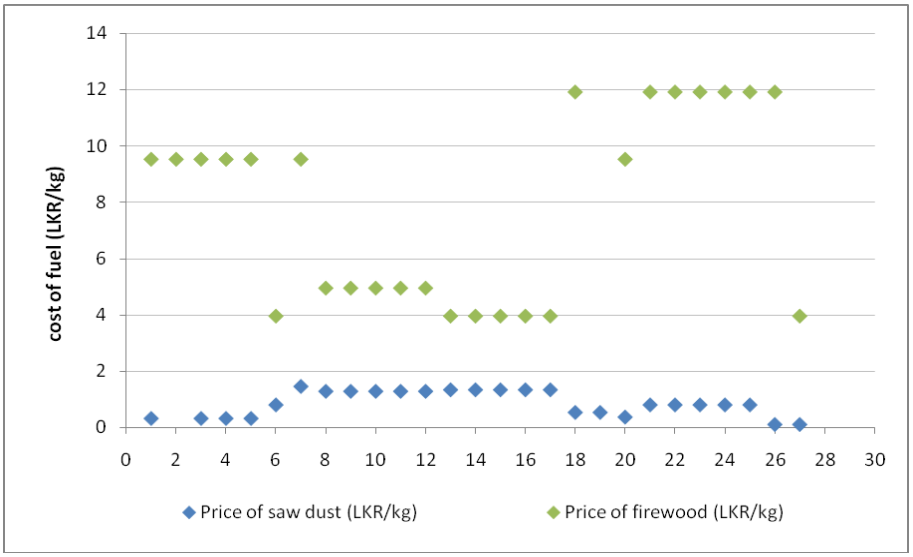

Figure 2: Costs of fuel before and after the introduction of the oven

Also, with the change of fuel, the mode of transport too has changed. During the period where firewood was used, only tractors were used for transport. But now, both tractors and three-wheelers are used to trasport saw dust sacks. On average, the distance transported by three-wheelers is 42.5 km/month, while the distance transported by tractors is 58.6 km/month. The reduced usage of tractors too has contributed to the reduction in CO_2 emissions.

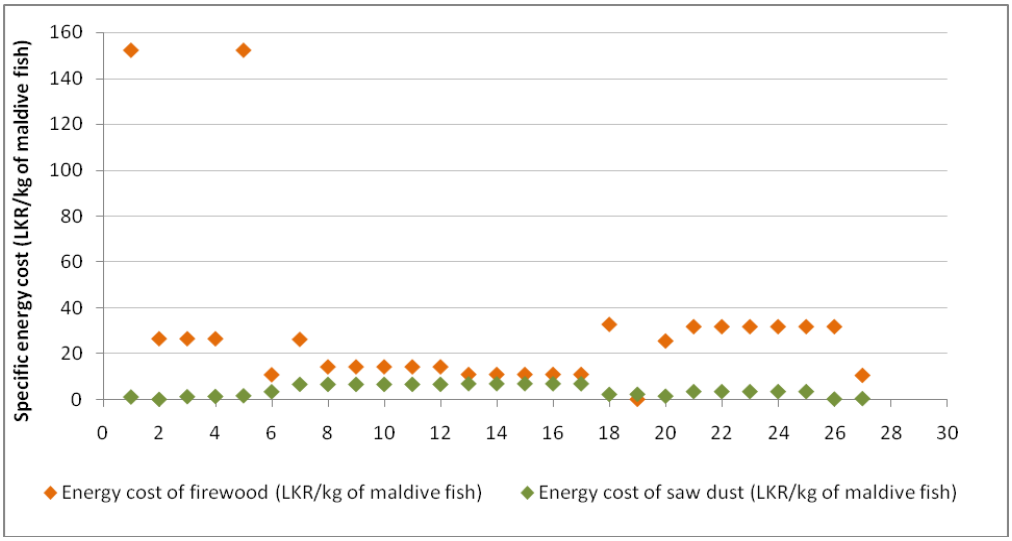

Figure 3: Specific energy costs in the usage of firewood and saw dust for the production of Maldive fish

From the above graph, it is evident that the change of process has reduced the specific energy cost of producing Maldive fish among all respondents. Accordingly, it will be a good intervention in terms of not only environmental benefits but also in terms of productivity and economic sense. Accordingly, the technology improvement in this sector requires the focussed attention of all concerned.

However, the technology introduced has replaced the use of solar energy with burning firewood, thereby lowering the environmental credentials of the new process on absolute terms. It will be prudent to seek a technical intervention where the utilisation of solar energy is continued, so that burning firewood or saw dust can function as a secondary source of energy.

Recommendations

Based on the findings of this study, the following measures are recommended to increase environmental benefits through productivity gains in the Maldive fish industry in the Matara district.

According to statistics of the District Fisheries Office (Matara), the average

production of Maldive fish is 75,000 kg per month. Therefore, if all this Maldive fish was produced under hygenic conditions, using saw dust ovens, the total quantity of saw dust required would be 22,727 kg of saw dust per month. The capacity of a single large oven is 750 kg (SKECDF, 2015). If all the Maldive fish were to be produced in saw dust ovens, 100 ovens would be needed for the Matara district. According to Figure 4, if saw dust ovens were introducted to the Matara district to streamline the production of Maldive fish, the reduction of CO_2 emissions would be 70 tonnes per month.

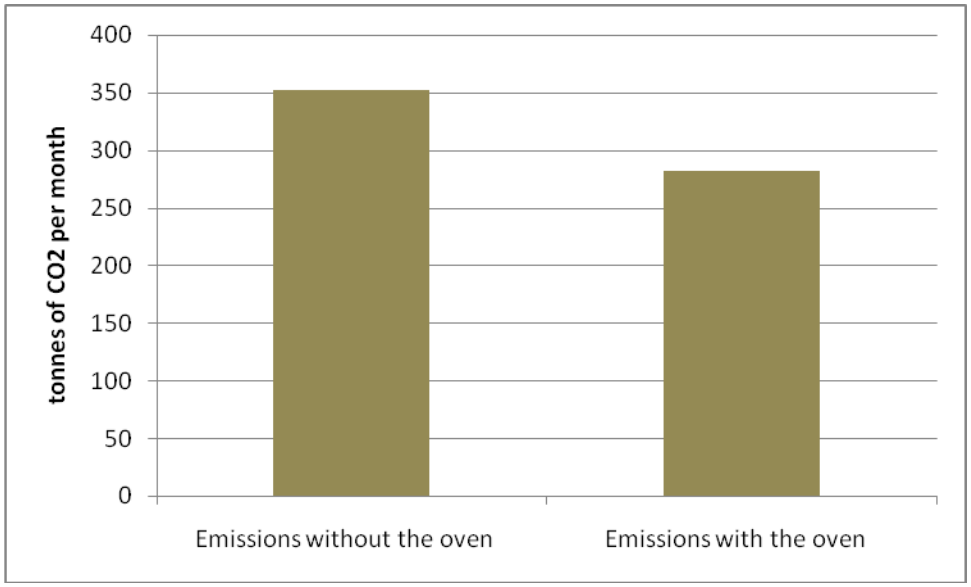

Figure 4: Likely emissions with and without saw dust ovens

Therefore, it is recommended to enhance the overall productivity of the Maldive fish industry by wider dissemination of the technology and by closely following the user groups to identify issues and opportunities for further technology improvement.

National impact

According to the Mahinda Chintanaya – a Vision for the Future, emphasis has been laid down to develop the fisheries industry to reach self-sufficuiecny. "*The fisheries development policy aims at exploiting the country's fisheries and aquatic resources in a sustainable manner, while conserving the coastal environment. The government is targeting self-sufficiency in the national fish supply and a significant increase in fish exports."*[9]

Accordingly, this study recomemnds to upgrade the Maldive fish industry to a self-sufficient level, to benefit the country as a whole.

The total annual consumption of Maldive fish in the country is 3,075 tonnes/annum (Table 3). If all this Maldive fish were produced within the country, a total of 10,148 tonnes of saw dust will be required per annum. The total avaialblity of saw dust for various applications is 52,298 tonnes [6], therefore, approximately 19% of this can be used as a clean energy source for Maldive fish production in the country.

Table 3: Benefits of producing Maldive within the country

Item	Unit	Value	Source
Per capita Maldive fish consumption	g/month	12.38	[10]
Midyear population	Nos. (million)	20.7	[11]
Total annual consumption	t/yr	3,075	Calculated
Saw dust requirement	t/yr	10,148	Calculated
No. of saw dust ovens (750 kg capacity)	Nos.	4,100	Calculated
No. of employees per oven	Nos.	7	[12]
Employment	Nos.	28,702	Calculated

According to Table 3, if the total requirement of Maldive fish is produced within the country, 28,703 people (women) will be provided employment. At present, 80% of Maldive fish is imported [1]. Therefore, if the Maldive fish industry is rendered self-sufficient within the country using saw dust ovens, 22,961 new employment opportunities would be created for processing Maldive fish. Many more employment opportunities will be created with manufacturing and maintenance of ovens and the supply chain of saw dust.

References

[1] National Aquatic Resources Research and Development Agency, Fisheries Industry Outlook, 2011.

[2] National Aquatic Resources Research and Development Agency, Fisheries Industry Outlook, 2012.

[3] Sobha Kantha Environment and Community Development Foundation, 2015

[4] Daranagama, U,. Availability of Fuelwood and Other Agricultural Residues as a Source of Energy in the Industrial Sector of Sri Lanka. National Engineering and Research Development Centre, Colombo, 1999.

[5] Lim, J. S., Manan, Z. A.,Wan Alwi, S. R. & Hashim, H. (2012). A Review on

Utilisation of Biomass from Rice Industry as a Source of Renewable Energy. Renewable and Sustainable Energy Reviews, 16, 3084–3094

[6] Biomass Energy Association of Sri Lanka, Biomass Energy Toolbox – The way forward for the use of wood and agricultural waste for energy production in S.Asia", Asia Pro Eco Programme. 2005

[7] IPCC Guidelines for National Greenhouse Gas Inventories, 2006

[8] Ministry of Environment and Natural Resource of Sri Lanka, Urban air Quality Management in Sri Lanka.

[9] Ministry of Fisheries and Aquatic Resource Development, and Midterm Policy Framework 2013 – 2016 for the Fisheries Sector Development, 2012.

[10] Department of Census and Statistics, Household Income and Expenditure Survey, 2015

[11] Central Bank of Sri Lanka, Annual Report 2014.

[12] Sobha Kantha Environment and Community Development Foundation, Project Proposal on Reduction of Carbon Dioxide Emissions through the Employment of Renewable Energy Technologies for Manufacturing Maldive Fish in Mirissa, 2015

A Comparative Study of the Combustion Characteristics of Diesel, Kerosene, Biodiesel and Biodiesel Blends Using Laminar Diffusion Flame

Wijesinghe, N.C., Prashantha, M.A.B., Jayaweera, P.M.
Department of Chemistry, University of Sri Jayewardenepura, Sri Lanka

Abstract

Biodiesel is arising renewable substitute for conventional diesel fuel. Therefore, this research has paid attention about the behavior of selected physical parameters of biodiesel when blends with diesel and compare the rate of soot formation, rate of fuel consumption and fuel to soot conversion percentage of diesel, kerosene, biodiesel and biodiesel- diesel blends using a laminar diffusion flame.

In this research, Soybean biodiesel was synthesized using transesterification reaction with the yield of 98% (v/v). Furthermore, biodiesel – diesel blends were prepared and their fuel properties such as density, kinematic viscosity, flash point, cetane index and fuel distillation temperatures were characterized following ASTM methods. Based on this experimental results, two mathematical relationships were developed to estimate the density and kinematic viscosity of any biodiesel-diesel blend. A linear relationship between density and blending ratio of biodiesel with diesel was found whereas the viscosity showed an exponential relationship with blending ratio.

According to the experimental results under steady laminar axisymmetric diffusion flame, the highest soot formation rate was found in diesel fuel and highest fuel consumption rate was found in kerosene. The fuel to soot conversion was highest in 6% biodiesel blend. However, the rate of soot formation, fuel to soot conversion percentage and rate of fuel consumption were lowest in biodiesel.

Keywords: soot, biodiesel, blends, laminar diffusion flame

Introduction

The decomposition of organic matters in died plants and animals throughout billions of years had led to form fossil fuels[1]. Fossil fuels became a unique material to change the conventional culture of civilization since it is a source for petroleum fuels and petrochemicals which use in numerous industries. The Hubbert theory of petroleum oil depletion states global production of petroleum oil follows a bell shaped curve over time since it is a non-renewable material[2],[3]. The slowdown of oil production is the key factor for a major energy crisis of the world. Therefore the development of biodiesel as an alternative energy source using plant oils has already become commercial interest. Transesterification (alcoholysis) is a reaction between triglyceride in oil and alcohol to form biodiesel and glycerol with the presence of catalyst. Alkali catalyzed transesterification is more efficient than acid catalyzed transesterification.[4] The presence of water in alkali catalyzed transesterification leads to soap formation through saponification reaction and hence anhydrous conditions are used to avoid saponification reaction [5].

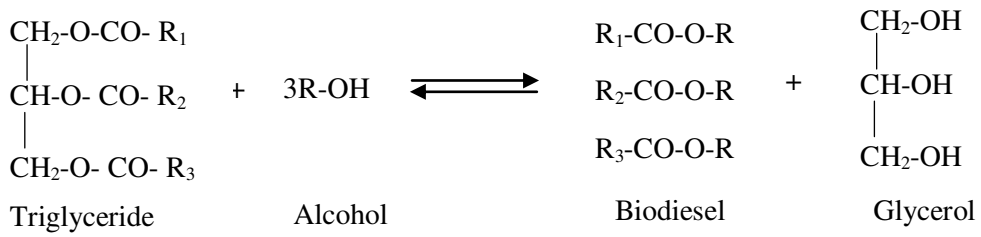

Figure 1: Transesterification reaction of triglycerides with alcohol (Smooke et al., 2005)

Biodiesel is blended with diesel to alter the properties of pure biodiesel in order to produce biodiesel based fuel for the existing internal combustion engines[6].A literature reported the density of the biodiesel blends is a linear function of the composition whereas the change in viscosity with the composition has agreed with $y= Ax^2 + Bx + C$ type equation [7].

Biodiesel combustion and their emission depend on the degree of unsaturation and the chain length of fatty acid side chain. Increment in the FAME side chain increases the total hydrocarbons (THCs), CO, volatile organic fraction (VOF) and soot formation[6].The laminar diffusion is one of the preliminary flame type which can use for the fuel combustion. Their flame length is proportional to the volumetric flow rate of fuel and it's inversely proportional to the availability of oxidizer[8]. For a given fuel under given air-fuel ratio, the flame height only depends on the fuel flow rate.

Soot formation basically occurs due to poor combustion conditions. Therefore it reduces the efficiency of the device and causes maintenance problems due to deposition of soot inside machineries. Emission of soot particles is caused in reduction of visibility of atmosphere and the presence of polycyclic aromatic hydrocarbons leads to adverse health effects by causing cancers and respiratory problems due to their breathability[9],[10]. Majority of large scale industrial combustion applications such as gas turbines, furnaces and internal combustion engines utilize diffusion flames rather than premixed[9]. Therefore, studies about the combustion characteristics of diffusion flames of biodiesel and blends of biodiesel with the petroleum fuel are very important.

This research project has carried out a comparative study on selected combustion characteristics (fuel consumption rate, soot formation rate and fuel to soot conversion as (w/w%)) using diesel, kerosene, soya bean oil based biodiesel and biodiesel blends during the combustion at steady laminar axisymmetric diffusion flame.

Methodology

In this study, commercially available Soy bean oil was used to produce biodiesel in the presence of KOH as base catalyst[11]. Methanol was used as alcohol, there molar ratio between alcohol and oil was kept to 6:1. Biodiesel synthesis was carried out in 1 L reaction flask equipped with reflux condenser, magnetic stirrer and thermometer. Transesterification reaction was carried out using anhydrous methanol for 1h at 55 ^{o}C [12],[13],[14]. The end of transesterification it was allowed to separate two phases and biodiesel was separated from glycerol[14]. Biodiesel was sufficiently washed by warm distilled water and it was heated up to 100 ^{o}C to remove excess alcohol and moisture[14]. Biodiesel was blended with diesel at 6% (B6), 10% (B10), 15% (B15), 20% (B20) and 60% (B60) on volume basis.

Commercially available diesel was purchased from Lanka Petroleum agent to prepare biodiesel- diesel blends. The fuel properties of diesel, kerosene oil, biodiesel and blends of biodiesel were characterized by determining there density (ASTM D1298), kinematic viscosity (ASTM D445), flash point (ASTM D93), calculated cetane index (ASTM D976) and fuel distillation temperatures (ASTM D86) in the Ceylon Petroleum Storage Terminal Limited laboratory, Kolonnawa, Sri Lanka.

Steady laminar axisymmetric diffusion flame was produced using a wick lamp to determine fuel consumption rate, soot formation rate and fuel to soot conversion as (w/w%) . The radius of circular nozzle was 7 mm and the flame height was adjusted to 5 cm. Metal sheet was placed perpendicularly to the axis of flame at a fixed level of 3cm above to the tip of flame in order to collect the soot. The wick was immersed in fuel around 24 hours before start the experiment. The mass of the wick lamp with fuel before and after 6 hours period

of combustion and mass of the metal sheet with and without soot were measured using analytical balance.

Results and Discussion

A volume of 1.96 L of biodiesel was synthesized using 2 L volume of soybean oil. Therefore the yield of the synthesized biodiesel is 98% (v/v%). According to literature 99% soybean based biodiesel yield (v/v) can be obtained under prescribed conditions used in transesterification reaction[12]. Therefore the experimental percentage yield of biodiesel was comparable with the value reported in literature.

Experimental results of the fuel properties of the synthesized soya bean based biodiesel and standard specification of biodiesel are given in Table 1.

*Table 1: Comparison of properties of synthesized biodiesel with standard fuel properties (*Ceylon Petroleum Storage Terminal Limited Specifications, 2014)*

Fuel Property	Synthesized Soya bean oil based biodiesel	Standard biodiesel specifications[15]	Standard diesel specifications*
Appearance	Clear, golden yellow	Clear, golden yellow	Clear, free from water and visible impurities
Density at 15 ^{o}C/ kg m^{-3}	885.3	875 at 15.5 ^{o}C	820 - 860
Kinematic viscosity at 40 ^{o}C / cSt	4.25	4.0 – 6.0	1.27 – 1.51
Flash point/ ^{o}C	140.56	Min. 93	Min. 38
Cetane Index	55.5	48 - 65	Min. 46
Distillation temperatures/ ^{o}C			
Initial Boiling Point	322	299	178
10% recovered (T10)	331	328	212
50% recovered (T50)	335	336	261
90% recovered (T90)	346	Max. 360	Max. 360

Viscosity, flash point, cetane index and distillation temperature range of the biodiesel produced from soya bean oil are highly comparable with standard biodiesel specifications. However, density of biodiesel is higher than standard diesel specifications. Density of fuel is important parameter to give directions to predict about the engine deposits and formation of exhaust smoke, because high dense biodiesel increase engine deposits as well as smoke due to incomplete combustion[6]. This is one of the major drawback of pure biodiesel.

Flash point of the biodiesel is high compare to diesel. So that, biodiesel has higher safety in storage and handling than diesel[15]. The higher cetane index of the biodiesel leads to low ignition delay and low combustion roughness[16],[17]. This is mainly due to absence of aromatic molecules in biodiesel.

Biodiesel has high viscosity compare to diesel. Therefore, viscosity of the biodiesel blend increases with increasing percentage volume of biodiesel in blend. Highly viscous fuels such as neat biodiesel can damage filters, pump and injectors. Also it negatively effects to spray properties and pave the way for a partial combustion in diesel engines due to poor atomization[18],[8].

The Figure 2 shows the linear relationship between the density of blends of biodiesel at 15 ^{o}C, and the composition as v/v%. It suggested the equation (1) having correlation coefficient at 0.9999.

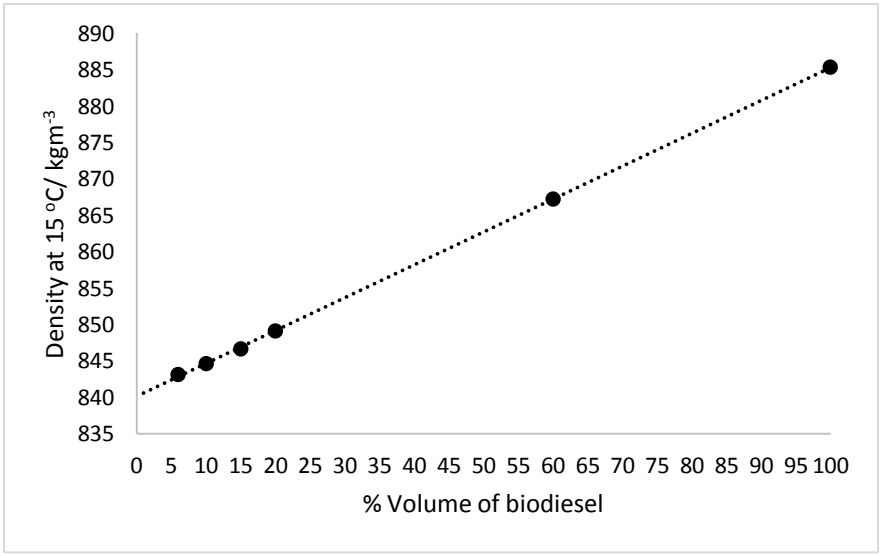

Figure 2: Variation of density with soybean biodiesel- diesel blend ratio

D = 0.4517 X + 840.1 Eq. 1

Here, 0.4517 and 840.1 coefficients are vary with the density of pure diesel and pure biodiesel used for the blend. Therefore those coefficients were replaced by density of pure diesel and pure biodiesel which is useful to estimate density of any Soy bean biodiesel- diesel blend at 15 ^{o}C.

Gradient = $\frac{D_{100}-D_0}{100}$ kg m^{-3}

Intercept = D_0 kg m^{-3}

D = $\frac{D_{100}-D_0}{100}\ v\% + D_0$ Eq. 2

Where D is density (kg m^{-3}) of any Soy bean biodiesel- diesel blend at 15 ^{o}C, D_{100} is density of neat biodiesel and D_0 is density of pure diesel and v% is percentage volume of biodiesel in the blend.

Table 2: Comparison between calculated densities of soybean biodiesel blends and literature (Alptekin & Canakci, 2008)

Biodiesel blend (v%)	Densities stated in literature [7] / kg m^{-3}	Calculated densities using Eq.(2)/ kg m^{-3}	% error of the results
B0	837.1	837.1	0.00
B10	841.9	841.8	0.01
B20	846.5	846.6	0.01
B75	872.4	872.6	0.02
B100	884.5	884.5	0.00

Table 2 shows the estimated density values using Eq. (2) and experimental density values obtain from the literature. The minute percentage errors and R^2 = 0.9999 are represent the excellent agreement between the estimated densities and the literature.

Figure 3 shows the exponential relationship between kinematic viscosity and the composition of blend of biodiesel as v/v% and it suggested the equation (3) where η is kinematic viscosity of soya bean oil based biodiesel blends at 40 ^{o}C. The coefficients 0.0042 and 2.7942 are in equation (3) vary with the viscosity of pure diesel and pure biodiesel used for the blend. Therefore, equation (4) is a modification of the equation (3) by replacing those coefficients by viscosity of pure diesel (K_0) and pure biodiesel (K_{100}) at 40 ^{o}C to estimate viscosity of any Soy bean biodiesel- diesel blends.

$$y = 2.7942e^{0.0042X} \quad \text{Eq. 3}$$

Where y is kinematic viscosity of biodiesel-diesel blend, 2.7942 and 0.0042 are coefficients and X is % volume of biodiesel in blend.

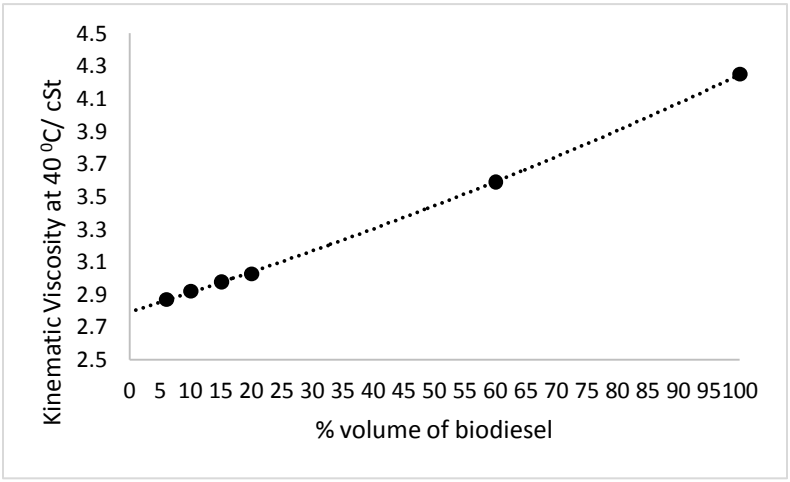

Figure 3: Variation of kinematic viscosity with soybean biodiesel- diesel blend

ln y = 0.0042x + ln 2.7942 Eq. 4

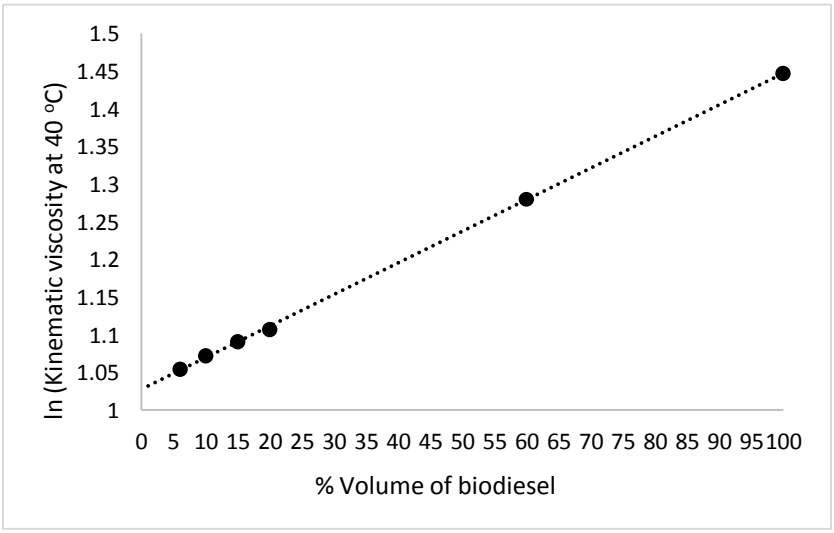

Figure 4: Plot of ln (kinematic viscosity at 40 °C) with the percentage of volume fraction of biodiesel in biodiesel blends

Here, 0.0042 and 2.7942 coefficients are vary with the viscosity of pure diesel and pure biodiesel used for the blend. Therefore, those coefficients were replaced by viscosity of pure diesel and pure biodiesel which is useful to estimate viscosity of any Soy bean biodiesel- diesel blend at 40 °C.

$$ln\ \mathrm{y} = \left(\frac{\ln K_{100} - \ln K_0}{100}\right)x + lnK_0$$

$$ln\,\eta = \left(\frac{\ln K_{100} - \ln K_0}{100}\right) V\% + lnK_0 \quad \text{Eq. 5}$$

The generalized viscosity equation is given by Eq. (6)

$$\eta = K_0 \times \left(\frac{K_{100}}{K_0}\right)^{V\%/100} \quad \text{Eq. 6}$$

Where η is kinematic viscosity of any Soy bean biodiesel- diesel blend at 40 ^{o}C, K_o is viscosity of pure diesel, K_{100} is viscosity of pure biodiesel and v% is percentage volume of biodiesel in the blend.

Table 3: Comparison between estimated kinematic viscosities and literature (Alptekin & Canakci, 2008)

Biodiesel Blend v%	Kinematic viscosities at 40 ^{o}C in literature[7]/ cSt	Calculated kinematic viscosities using Eq.(3.5)/ cSt	% error in the results
B0	2.71	2.71	0
B10	2.79	2.81	0.72
B20	2.88	2.92	1.38
B50	3.25	3.28	0.92
B75	3.56	3.60	1.12
B100	3.97	3.97	0

A comparison between estimated viscosity values using equation (6) and experimental viscosity values obtain from the literature shown in Table 3. In Table 3, the calculated viscosity values from equation (6) are validated by using viscosities mentioned in the literature. The low percentage errors and R^2 = 0.9998 are represent the acceptable agreement between the estimated viscosities and the literature.

Combustion characteristics were determined by using steady laminar axisymmetric diffusion flame. The Figure 4 illustrates the soot formation rate of different fuels at steady laminar axisymmetric diffusion flame conditions. According to experimental results maximum soot formation rate can be observed with diesel combustion and it is also possible to observe that the soot formation rate decreases with the increment of biodiesel percentage in the blend. Therefore minimum soot formation rate belongs to pure biodiesel combustion using laminar diffusion flame.

The oxygen content of the fuel, presence of aromatic species and kinematic viscosity hold a major role in soot formation during combustion[19]. Diesel fuel contains more aromatic species (31% vol. max)[20] than kerosene (25.0% vol. max) which leads to diesel to partial

combustion and formation of more soot precursors during combustion. Therefore soot formation rate of diesel is higher than kerosene. Biodiesel blends have lower soot formation due to reduction of aromatic species and increment of oxygen content in the fuel. The absence of aromatic species and the presence of higher oxygen content in pure bio diesel have lead the fuel for a complete combustion, thus the minimal soot formation was observed.

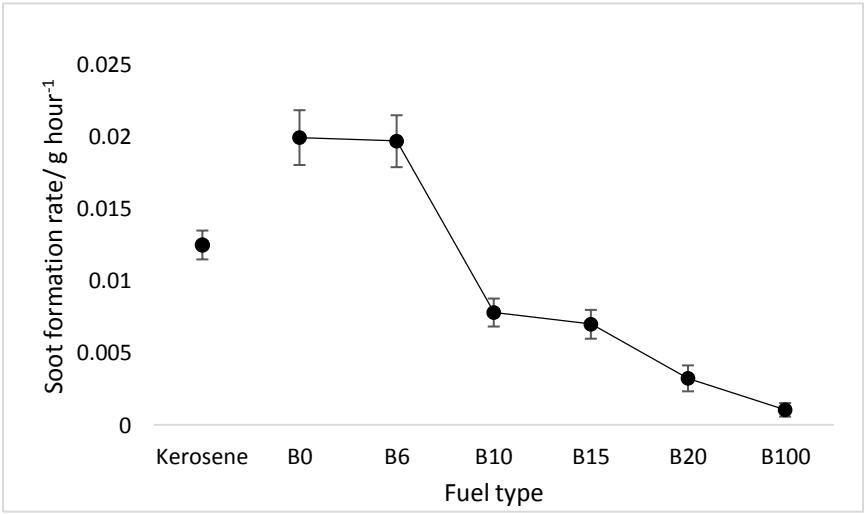

Figure 5: Variation of soot formation rate with fuel type

The Figure 6 shows fuel- soot conversion percentage of different fuel types when do the combustion using laminar diffusion flame.

Combustion products of a fuels can be CO_2, CO, water vapor, NO_x, soot precursors such as gaseous HC, HC radical species, PAH and soot etc. Here CO, soot precursors and soot form due to incomplete combustion of fuel. The fraction of soot and soot precursors (which adsorbed to soot particle surface) formed with the consumption of 100 g of different fuels under same combustion conditions were compared in Figure 6 Higher fuel-soot conversion implies the higher incomplete combustion of fuel by laminar diffusion flame.

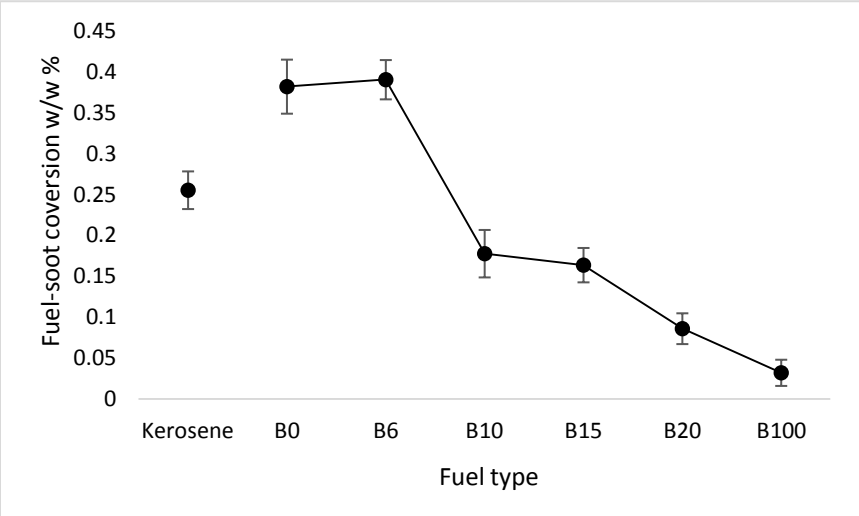

Figure 6: Variation of fuel-soot conversion with the fuel type

According to the experimental data in Figure 6, fuel- soot conversion (w/w%) is lower in kerosene fuel compared to diesel and fuel- soot conversion of B6 biodiesel blend slightly higher compare to diesel. Similar to soot formation rate in Figure 5, low aromatic content and low viscosity of kerosene compared to diesel may cause the fuel- soot conversion of kerosene to be lower than diesel. The B6 biodiesel blend contains 6% biodiesel, so there viscosity is slightly higher than diesel. Highly viscous fuels has ability to form large fuel droplets during combustion which reduce fuel- air mixing and enhance soot formation[8]. And small volume of biodiesel (only 6%) may not sufficient to increase oxygen weight fraction in B6 blend. Therefore soot formation rate of B6 blend is higher than diesel. Similar to soot formation rate in Figure 5 Soot- fuel conversion of biodiesel blends decrease with the increment of biodiesel volume in blend and thus the lowest conversion has achieved by pure biodiesel combustion using laminar diffusion flame. The complete combustion of the fuel facilitated by the oxygen content present within the fuel may be the cause for this reduction in the fuel to soot conversion.

The experimental results in Figure 7 illustrate a comparison of different fuel consumption per unit time in laminar diffusion combustion.

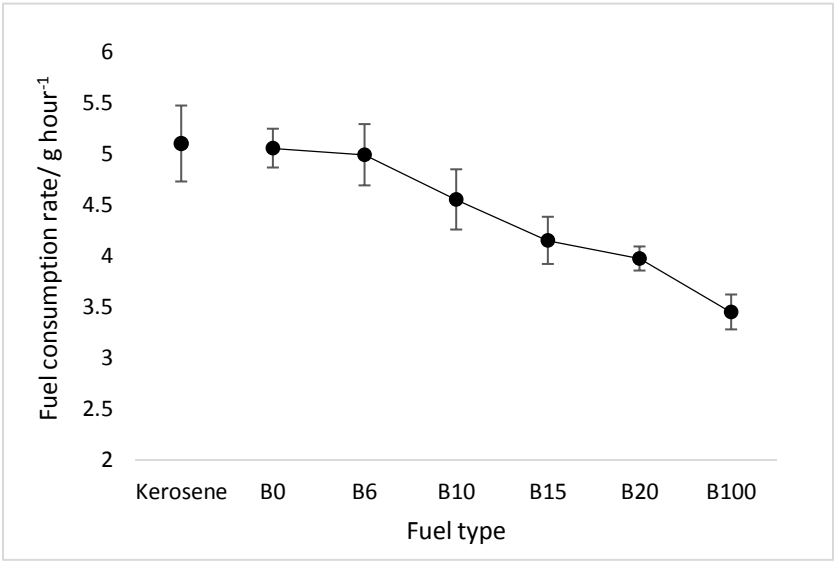

Figure 7: Variation of fuel consumption rate with fuel type

In a wick lamp, fuel moves towards the flame through the wick by the help of capillary action. Mainly three parameters are useful to determine the ability of a liquid to move through the capillary action. The three parameters are the cohesive forces (interaction between fuel molecules), adhesive forces (attraction between wick surface and fuel molecules) and surface tension (energy require to stabilize surface). The capillary action only occurs when adhesive forces are stronger than cohesive forces.

Petroleum fuels such as kerosene and diesel mainly consist of hydrocarbons. Therefore only weak Van der Waals interactions exist in between these hydrocarbons with representing weak cohesive forces. The wick is made up of cotton fabric having oxygenated polar groups which facilitate the movement of non-polar kerosene and diesel through the wick. So they can actively possess the capillary action and enhances the fuel consumption compared to biodiesel. Biodiesel has Van der waal interactions between fatty acid side chains and dipole interactions between ester groups. Therefore it has strong cohesive forces and high surface tension with producing highly viscous fuel compare to diesel and kerosene. It reduces the capillary action of biodiesel through the wick. Also strong dipole interactions between the polar groups in biodiesel and cotton fabric further decline the capillary action. So fuel consumption reduces with increasing biodiesel percentage in the blend and the lowest fuel consumption was achieved by neat biodiesel.

Conclusion

The purpose of this study is to do a comparative study on selected combustion characteristics using diesel, kerosene, soya bean oil based biodiesel and biodiesel blends during the combustion at steady laminar axisymmetric diffusion flame. Soya bean oil based biodiesel was prepared and basic fuel properties are comparable with the standards biodiesel specifications. Density and kinematic viscosity of biodiesel blends are important physical parameters. Two equations are developed to predict the density and kinematic viscosity of biodiesel blends. Density of biodiesel blend can be calculated using the density of diesel and pure biodiesel. Kinematic viscosity can be calculated using kinematic viscosity of diesel and pure biodiesel. Calculated values of density and kinematic viscosity well agree with the experimental values reported in literature.

And the soot formation rate, fuel consumption rate and fuel- soot conversion percentage of diesel, kerosene, biodiesel and biodiesel blends were compared using at steady laminar axisymmetric diffusion flame. According to the experimental results, the highest soot formation rate was found in diesel fuel and highest fuel consumption rate was found in kerosene. The fuel to soot conversion was highest in 6% biodiesel blend. However, the rate of soot formation, fuel to soot conversion percentage and rate of fuel consumption were lowest in biodiesel. Therefore, this study suggests that, biodiesel is also an environmental friendly renewable energy source for the combustion applications which govern by laminar diffusion flame.

Acknowledgement

This study was supported by Ceylon Petroleum Storage Terminal Limited, Kolonnawa, Sri Lanka and Department of Chemistry, University of Sri Jayawardenepura, Sri Lanka.

Appendix

Table 4: Mass of the soot formed and consumed fuel during combustion

Fuel type	Mass of the soot collected within 6 hrs/ g		Mass of fuel consumed within 6 hrs/ g	
	I replicate	II replicate	I replicate	II replicate
Kerosene	0.080	0.081	31.201	31.431
Diesel	0.123	0.109	30.898	29.760
B6	0.124	0.112	30.860	29.020
B10	0.050	0.046	26.431	28.212
B15	0.045	0.037	25.601	24.220
B20	0.022	0.019	23.288	23.411
B100	0.005	0.009	20.190	22.221

Table 5: Average fuel consumption rate

Fuel type	Average fuel consumption rate/ g hour^{-1}	Cumulative error
Kerosene	5.219	0.2300
Diesel	5.055	0.1896
B6	4.990	0.3066
B10	4.554	0.9683
B15	4.152	0.2302
B20	3.891	0.1872
B100	3.534	0.3385

Table 6: Average soot formation rate

Fuel type	Average soot formation rate/ g hour^{-1}	Cumulative error
Kerosene	0.013	0.0002
Diesel	0.019	0.0023
B6	0.020	0.0020
B10	0.008	0.0007
B15	0.007	0.0013
B20	0.003	0.0005
B100	0.001	0.0007

Table 7: Average fuel to soot conversion percentage

Fuel type	Average fuel-soot conversion (w/w%)	Cumulative error
Kerosene	0.249	0.001
Diesel	0.382	0.032
B6	0.394	0.016
B10	0.176	0.026
B15	0.164	0.023
B20	0.077	0.017
B100	0.033	0.016

Reference

[1] Speight, J. G., *The chemistry and technology of petroleum*. CRC press: 2014.

[2]Brandt, A. R., Testing Hubbert. *Energy Policy* 2007, *35* (5), 3074-3088.

[3] Philippi, G. T., On the depth, time and mechanism of petroleum generation. *Geochimica et Cosmochimica Acta* 1965, *29* (9), 1021-1049.

[4] Ramadhas, A. S.; Jayaraj, S.; Muraleedharan, C., Biodiesel production from high FFA rubber seed oil. *Fuel* 2005, *84* (4), 335-340.

[5] Foidl, N.; Foidl, G.; Sanchez, M.; Mittelbach, M.; Hackel, S., < i> Jatropha curcas</i> L. as a source for the production of biofuel in Nicaragua. *Bioresource Technology* 1996, *58* (1), 77-82.

[6] Pinzi, S.; Rounce, P.; Herreros, J. M.; Tsolakis, A.; Pilar Dorado, M., The effect of biodiesel fatty acid composition on combustion and diesel engine exhaust emissions. *Fuel* 2013, *104* (0), 170-182.

[7] Alptekin, E.; Canakci, M., Determination of the density and the viscosities of biodiesel–diesel fuel blends. *Renewable Energy* 2008, *33* (12), 2623-2630.

[8] Turns, S. R., *An introduction to combustion*. McGraw-hill New York: 1996; Vol. 287.

[9] Smooke, M.; Long, M.; Connelly, B.; Colket, M.; Hall, R., Soot formation in laminar diffusion flames. *Combustion and Flame* 2005, *143* (4), 613-628.

[10] Kumar, P.; Morawska, L.; Birmili, W.; Paasonen, P.; Hu, M.; Kulmala, M.; Harrison, R. M.; Norford, L.; Britter, R., Ultrafine particles in cities. *Environment International* 2014, *66* (0), 1-10.

[11] Agarwal, M.; Chauhan, G.; Chaurasia, S. P.; Singh, K., Study of catalytic behavior of KOH as homogeneous and heterogeneous catalyst for biodiesel production. *Journal of the Taiwan Institute of Chemical Engineers* 2012, *43* (1), 89-94.

[12] Borugadda, V. B.; Goud, V. V., Biodiesel production from renewable feedstocks: Status and opportunities. *Renewable and Sustainable Energy Reviews* 2012, *16* (7), 4763-4784.

[13] Ma, F.; Hanna, M. A., Biodiesel production: a review. *Bioresource Technology* 1999, *70* (1), 1-15.

[14] Elizabeth Funmilayo ARANSIOLA [1,] E. B., Stephen Kolawole LAYOKUN [1] and Bamidele Ogbe SOLOMON[1,2], Production of biodiesel by transesterification of refined soybean oil *International Journal*

of Biological and Chemical Sciences 2010, 1-9.

[15] Laboratory, N. R. E. *Biodiesel Handling and Use Guide* U.S. Department of Energy National Renewable Energy Laboratory, 2009; p 56.

[16] Murphy, M. J.; Taylor, J. D.; McCormick, R. L., *Compendium of experimental cetane number data*. National Renewable Energy Laboratory Golden, CO: 2004.

[17] J. Van Gerpen, B. S., and R. Pruszko; Clements, D.; Knothe, G. *Biodiesel Analytical Methods*; 2004; p 100.

[18] Corporation, M. A. I. *Biodiesel Fuel Testing*; 2011; p 2.

[19] Lemaire, R.; Bejaoui, S.; Therssen, E., Study of soot formation during the combustion of Diesel, rapeseed methyl ester and their surrogates in turbulent spray flames. *Fuel* 2013, *107* (0), 147-161.

[20] Monyem, A.; H. Van Gerpen, J., The effect of biodiesel oxidation on engine performance and emissions. *Biomass and Bioenergy* 2001, *20* (4), 317-325.

The potential for biodiesel from algae under Sri Lankan condition

Nagahawatta, I.A., Rupasinghe, C.P., Gammanpila, A.M.
Department of Agricultural Engineering, Faculty of Agriculture, University of Ruhuna

Abstract

The demand for energy will be greatly increased in the future as the current trends in technological progress and innovations continue. World is now moving toward renewable energy sources and environmental problems creates due to utilization of conventional energy sources. Algal biofuels have high potential as an alternative to fossil fuel due to high photosynthesis productivity, can be grown in abandon land and not competitive with edible sources. The objective of the study was to evaluate the effectiveness of two different culture systems for growing Nannochloropsis spp. for extracting oil for biodiesel production. Nannochloropsis pure cultures were grown in two different culture systems (20 L horizontal tank and 20 L vertical polybag) in outdoor shed under local Sri Lankan climatic conditions. Guillard and Ryther's modified F/2 medium was used to grow algae. The experiment was designed according to the RCBD and treatments were replicated three times. The harvested dry matter content of microalgae Nannochloropsis spp in polybag culture system and tank culture system were observed as 0.7440 g/L and 0.4568 g/L respectively and it was significantly higher($p < 0.05$) in poly bag culture system compared to tank culture system. The oil content of polybag and tank system were estimated as 10.76% and 10.68% in dry basis, respectively. The higher oil content was observed in polybag culture system. The free fatty acid content value of the extractable oil was tested as 3.26. The results revealed that Nannochloropsis spp can be successfully grown in polybag culture system to produce biodiesel under local conditions. The biodiesel from extracted oil of micro algae Nannochloropsis spp can be made in the presence of alkaline catalyst as free fatty acid level was within the acceptable limit (3-5). The biomass production of Nannochloropsis oil was observed as 57.1 g/m^2/cycle on dry basis in open tank culture system and 209.57 g/m^2/cycle on dry basis with 1.08 m height vertical poly bag culture system.

Keywords: biodiesel, micro algae, open tank culture system, poly bag culture system

Introduction

Biodiesel is a source of renewable energy and it has become more attractive recently because of its environmental benefits [1]. Use of fossil fuel in near future may be very problematic due to several reasons. Petroleum is a non-renewable energy source. Therefore increasing demand will cause increasing fuel prices. Excessive fossil fuel burning leads to long term global environmental problems.

As a solution for energy crisis, world is now moving forward for renewable energy sources. Micro algae have higher growth rates and productivities of biomass and lipids than conventional crops, which eventually results in a lower demand of land area. Furthermore, since microalgae can be cultivated in non-arable land, they do not compete with agriculture [2]. Microalgae cultivation is not seasonally limited and allows daily harvests. Microalgae can provide different types of renewable biofuels [3]. Biodiesel is produced from vegetable oils or animal fats [4]. Since vegetable oils may also be used for human consumption, there is a restriction from Sri Lankan government to use edible oil for producing biofuel [5]. There are no studies done for producing biofuel from marine microalgae in Sri Lanka under local conditions. The objective of the study was to evaluate two different culture systems for growing *Nannochloropsis* spp. for extracting oil for biodiesel production.

Methodology

The experiment was carried out at the Faculty of Agriculture, University of Ruhuna, Sri Lanka. The experimental site lies within latitude 6.06 °N and longitude 80.56 °E of the equator. The Faculty of Agriculture is located in agro-ecological region of Low Country Wet Zone (WL4) [6]. The average air temperature, relative humidity and light intensity was recorded as 30.9 °C, 81% and 3604.04 lux inside the green house. The Diluted sea water with Guillard & Ryther's modified F medium half concentration was used as growth medium to grow marine microalgae *Nannochloropsis spp.* The experiment was designed according to the RCBD and treatments were replicated three times.

The pure culture of *Nannochloropsis* spp. was inoculated to the 100 ml growth medium and it was transferred into 1 l bottle and established in the outdoor cultivation unit under normal light conditions. When the growth medium was changed into dark green colour in 2 weeks, it was transferred into bottles with 5 l culture medium.

The 5 l of culture medium was transferred into 20 l polythene bags (75 microns) (30 cmx108 cm) and 20 l tank culture (0.4×0.4×0.225cm^3) system. Each

culture system was provided with 3 aeration stones.

Electric Conductivity and pH of the medium was measured using EC meter (Oakton EC Tester 11) And pH meter at 24 hours interval (PCE-PH 22). The cell count was measured as the growth performance parameter of the micro algae culture by Absorbance Spectra values (ABS Value) with 650 nm wave length [7] using Spectrophotometer UVmini 1240. The data were collected in each treatment every other day for period of two weeks.

Well grown algae were harvested by flocculation using $FeCl_3$. Then samples were dried in oven at 105^0C. Algal oil was extracted by standard Soxhlet methods using petroleum ether as organic solvent. Percentage of oil was calculated. The free fatty acid content was measured by titration with 0.1% NaOH. The Free Fatty Acid Value was determined using equation 1-3.

Sample weight = density of the oil × Volume of oil taken Eq.1

$$\text{Acid Value (AV)} = \frac{\text{Reading} \times N \times 56}{\text{Sample weight}} \quad \text{Eq.2}$$

Free Fatty Acid % (FFA) = AV x 0.503 Eq.3

Where;

Reading = Amount of NaOH required for titration

N = Normality of NaOH (0.1%)

All the data was analyzed by Anova test using the software SAS 9.1.3.

Results and Discussion

A difference in growth performances of two cultivation methods was observed. According to the figure 1, maximum cell counts of the polybag system was observed as 27800 cell/ml on 10^{th} day after inoculation and as for the tank culture system it was 18300 cell/ml on 8^{th} day after inoculation. Even though the tank culture system completed the growth cycle earlier than the polybag culture system the cell count and the higher dry weight yield were observed in polybag culture system.

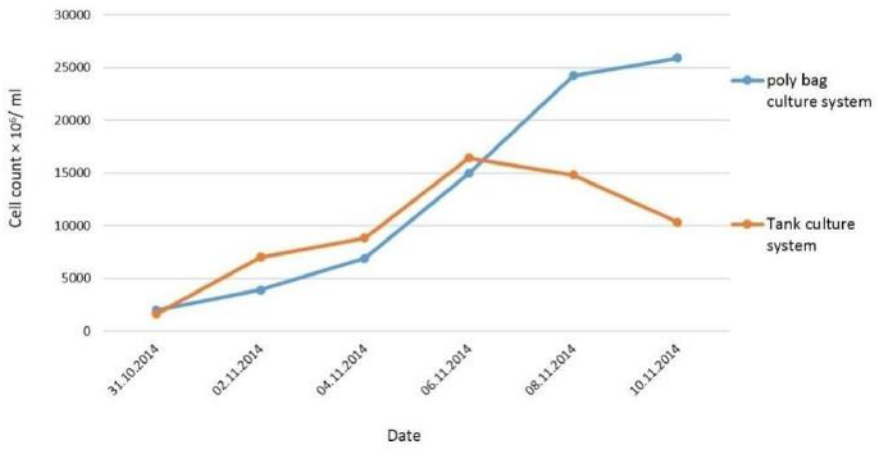

Figure 1: Comparision of growth performance of Nannochloropis spp after introducing to poly bag and tank culture systems

The harvested dry matter content of microalgae *Nannochloropsis* spp in polybag culture system and tank culture system were observed as 0.74 g/l and 0.48 g/l respectively.

The harvested dry matter content in poly bag culture system was significantly higher than the tank culture system ($P<0.05$) (figure 2). Chinnasamy *et al* (2010) observed higher biomass productivity of polybags (21.1 g m^{-2} d^{-1}) compared to Vertical Tank Reactors (8.1 g m^{-2} d^{-1}) and raceway ponds (5.9 g m^{-2} d^{-1}) in untreated waste water [8]. The light penetration of the polybag culture system was higher than tank culture system. These results may correlate with the differences of the light penetration in the culture medium.

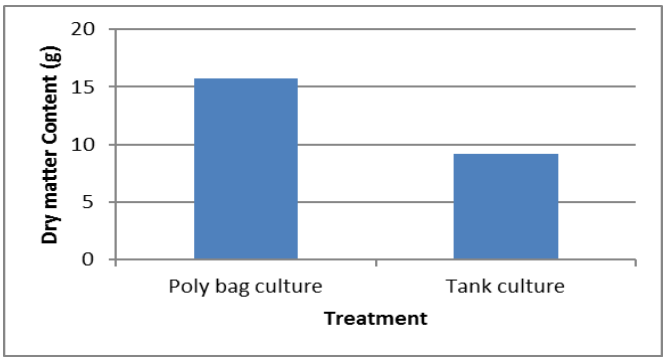

Figure 2: Average dry matter content of Nannochloropsis spp in different culture systems

The oil percentage of polybag and tank system was estimated as 10.76% and 10.68% respectively (figure 3). Oil percentages of both culture systems were nearly same. However no significant difference was observed between the two treatments.

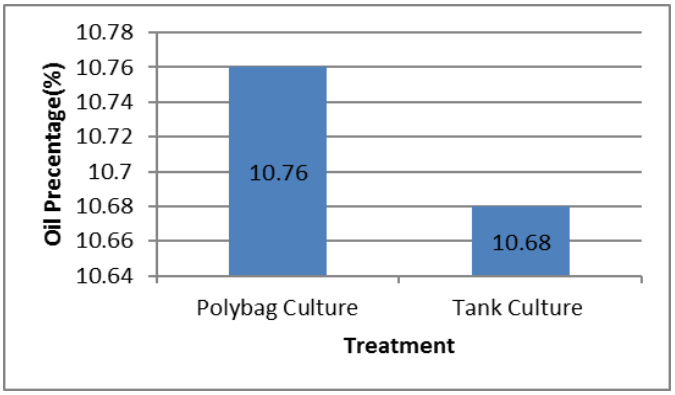

Figure 3: Oil percentages of Nannochloropsis spp grown in two culture systems

Though the growth cycle was completed earlier in tank culture system it showed the low oil content.

The titration for free fatty acid level determination test was done on 1ml of 0.1M NaOH. Free fatty acid value percentage of the extracted oil was calculated as 3.26 for both culturing systems. When producing biodiesel to obtain 98% diesel from oil, the free fatty acid content must be 3.5 or less than that. To carry the base catalyzed reaction to completion; a lower free fatty acid (FFA) value is needed. The higher the acidity of the oil, smaller is the conversion efficiency. Both, excess as well as insufficient amount of catalyst may cause soap formation [9]. Therefore, oil of *Nannochloropsis* spp. can be successfully utilized for producing biodiesel as content of free fatty acid level was in acceptable limit.

Conclusion

Marine microalgae *Nannochloropsis* spp was successfully grown in outdoor cultivation systems under local weather conditions. The harvested dry matter in poly bag culture system was significantly higher than tank culture system as the growth *of Nannochloropsis* spp is accelerated by the light penetration. Tank culture system completed the growth cycle earlier than the polybag culture system but cell count and the dry matter yield were significantly higher in polybag culture system. There was no significance difference in oil content in

two different culture systems. According to the results, *Nannochloropsis* spp can be successfully grown in polybag culture system under local conditions with lower price compared to tank culture system. Furthermore extracted algal oil can be successfully utilized for producing biodiesel as the content of free fatty acid level was in acceptable limit. The biomass production of Nannochloropsis oil was observed as 57.1 g/m^2/cycle on dry basis in open tank culture system and 209.57 g/m^2/cycle on dry basis with 1.08 m height vertical poly bag culture system.

Acknowledgement

This research was supported by National Research Council (NRC) with providing necessary funding.

References

[1] Fangrui Ma and Milford A Hannab, 1999, Biodiesel production: a review, Bioresource Technology, Vol 70 (1) October 1999, pp 1-15

[2] L. Gouveia, A.C.Oliveira, Microalgae as a raw material for biofuels production ,J.Ind. Microbiol. Biotechnol. 36 (2009) 269–274.

[3] Shariff A.B.M.H, Aishah S, Amur N.B, Partha C & Mohd N, 2008, Biodiesel Fuel Production from Algae as Renewable Energy, Vol. 4(3), pp. 250-254.

[4] Scarlat N, Dallemand JF, Pinilla FG. Impact on agricultural land resources of biofuels production and use in the European Union. In: Bioenergy: challenges and opportunities. International conference and exhibition on bioenergy; 2008.

[5] Chisti, Y, 2007, 'Biodiesel from microalgae', Research review paper: Biotechnology Advance, Vol 25, pp. 294-306.

[6] Weerasinghe, K. D. N. 1989. The rainfall probability analysis of Mapalana and its application to agricultural production of the area. J. Natn. Sci. Coun. Sri Lanka 1989 17(2):173-186

[7] Lucia H.R.R, Alexandre A, Maria T.R and Nelson F.F, 2011, 'Algal density assessed by spectrophotometry: A calibration curve for the unicellular algae Pseudokirchneriella subcapitata', Journal of Environmental Chemistry and Ecotoxicology, Vol. 3(8), pp. 225-228, Reviews.

[8] Chinnasamya, S., Bhatnagara, A., Claxtona, R. and Dasa, K.C. 2010, 'Biomass and bioenergy production potential of microalgae consortium in open and closed bioreactors using untreated carpet industry effluent as growth medium', Bioresource Technology, Vol 101 (17), pp 6751–6760

[9] Dorado MP, Ballesteros E, Almeida JA, Schellet C, Lohrlein HP and Krause R. An alkali-catalyzed 855 transesterification process for high free fatty acid oils. Trans ASAE 2002;45(3):525-9.

Challenges and concerns towards National energy security: Coal, Renewable and Electric vehicle additions

Jayaprathap, N., Kandeeban, K., Kohilavani, G., Kumara, J.R.S.S., Fernando, M.A.R.M.

Abstract

As in many other countries, the demand for electric power in Sri Lanka is also growing fast during recent years. Due to this, the power utility company i.e. CEB has the responsibility to cater the increased power demand and increases generation by conventional and non convetional methods such as coal and new renewable sources. With present tax reliefs, usage of electric vehicles has also been increased so that expected power demand will be even higher in future. In this paper, performance of Sri Lankan transmission network under above mentioned changes to the power system was studied by means of load flow analysis performed using PSS/E software package. Different cases i.e. (i) with and without coal power plants at Norochchole (ii) with and without 100 MW wind generation in Mannar (iii) with distributed PV and (iv) With distributed electric vehicles (EV) were considered for 2017 transmission network. Three different regions in daily load pattern were considered for each case to check any voltage violation, line overloading etc. It was found that some buses showed under-voltages for some of the analyzed cases. Further significant EV additions resulted increasing line losses and voltage violations. However, addition of shunt capacitors solved some of the obsevred problems. Finally it can be concluded that comprehensive load flow analysis may provide answers to the above challenges on the energy security of the country.

Keywords: Sri Lankan transmission network, Electric vehicles, Power flow, Reactive power Compensator, Voltage violations

Introduction

The Electricity sector in Sri Lanka is governed by the Ceylon Electricity Board (CEB). There are three major parts in power system. There are generation, transmission and distribution. Generation is owned by CEB as well as independent power producers (IPP). About 40% of total power generation is from large hydro plants in Mahaweli complex, Laxpana complex, Samanala Wewa and Kukule Ganga. Until recent years significant portion of the energy came from fossil fuel plants belongs to CEB as well as IPPs. Recent addition to the generation system is Puttalam Lakvijaya coal power which has a gross generation capacity of 900MW. The second coal power plant planned at Sampur will supply 500MW in the first phase [1]. However as Sri Lankan government has decided to have no more coal power plants, now CEB is trying to utilize more and more renewable resources. On the other hand, global trends towards sustainable energy concepts demand minimizing of fossil fuel based power plants. Then thermal power plants of 259.14 MW total capacity will retire from Sri Lankan power system.As renewable energy in 2016, 35MW broad lands and 125MW Uma Oya will connect to the national grid. And as the result in 2017, there will be 614 MW of renewable energy in Sri Lankan power system [2]. In addition to those relatively large renewable sources CEB is promoting domestic renewable generations such as roof top solar systems. This concept has gained some attraction among the public especially due to net metering system. A consumer with net-metering system will be provided credits for energy supplied to the CEB from the solar power system. These credits will be deducted from the consumer's monthly electricity bill.

After the civil war, now Sri Lanka develops rapidly and demand for electricity is continuously increasing. Also to reduce the fuel consumption and harmful gases released by vehicle, Sri Lanka government decided to promote Electric Vehicles (EV). The government planed 10 % of road transportation to electricity powered by 2020, compared to almost 100% percent fuel driven at present [3]. Power requirement of charging per EV is 3600W [4] and introduction of huge number of EVs will significantly increase the electricity demand and may need modification to the power system infrastructure itself. It is intended to generate that electricity through the production of green electricity.

This study was focused on predicting the changes in load flow and its consequences due to above mentioned changes in generation and loads. The load flow is the study of voltages, voltage angles, real power and reactive power at each bus bar and power flows in each line. Among different load flow software’s such as IPSA, PSS/E, FLOW ANALYSIS.SYSTEM 282, and CYME power engineering software and etc. For this study PSS/E was used to model

generation and transmission system of Sri Lanka and then to analyze load flow under various operating conditions.

Methodology

A. Sri Lankan Power system

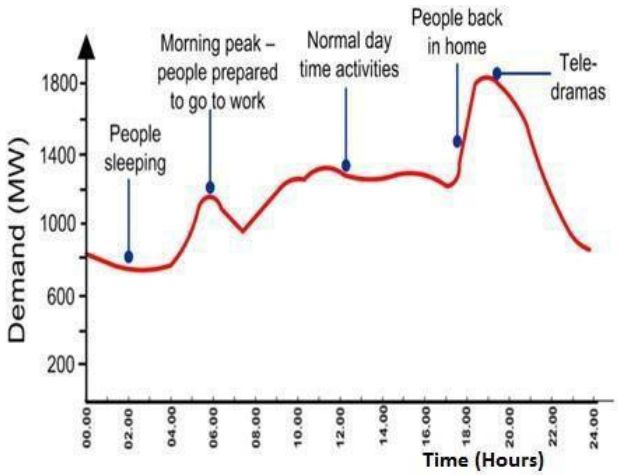

Figure 1: Daily load pattern (Source- public utility commission of Sri Lanka)

Figure 1 elaborates more clear idea about present daily load pattern of Sri Lanka. The night peak demand is approximately twice of the off peak value. Power generation capacity of the country should be enough to supply this night peak. Usually the base power is produced by coal plants whereas demand fluctuations especially in night peak are supplied by hydro and thermal plants sources.

As already mentioned in Section 1 power demand of Sri Lanka would be very high due to industrial developments and additions of electric vehicles in 2017. In order to fulfill this demand the power utilities have the responsibility to increase the power generation. According to this, renewable penetration and coal generations will be the dominant power generation in 2017. Accordingly the CEB has planned new power plants in 2017.They are, a Wind power plant in Mannar and Kerawalapitiya,hydro plant at Uma-oya at Mahiyangana power plants [2].

B. Power demand in 2017

To analyze the power demand values at night peak, day time and night time is required. Ideally calculation of these demand values, need information of new load additions and changes in

existing loads. Since this is practically impossible to predict those loads, an alternative method was used to estimate demand. First, information about the past peak demand were obtained from annual report of the public utility commission of Sri Lanka (PUCSL). Figure 2 shows the variation of average night peak demand over several years. Then the power demand value for 2017 was estimated by linear extrapolation. The estimated night peak demand in 2017 is 2534 MW.

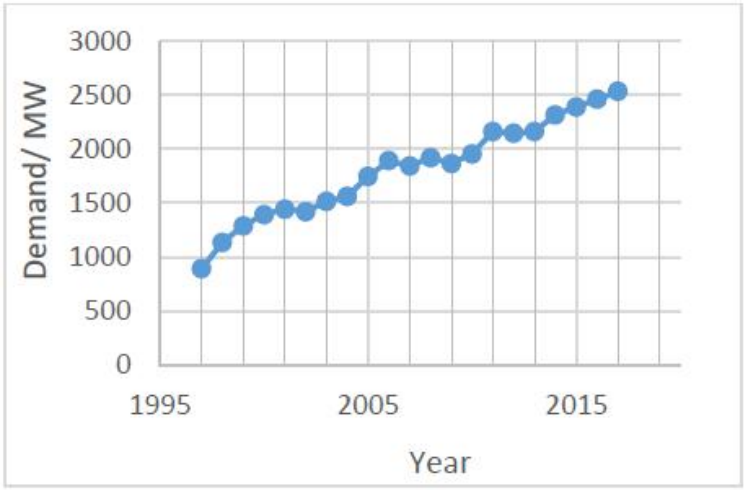

Figure 2 : Variation of night peak with year

According to [5] ration between night peak and night time demand is 2.2. Using this ration night time demand was estimated as 1152 MW. Figure 3 shows variation of ratio between the day time demand and night peak over last years. According to this variation the ratio for 2017 was estimated as 1.67. Thus corresponding day time demand is 1517 MW.

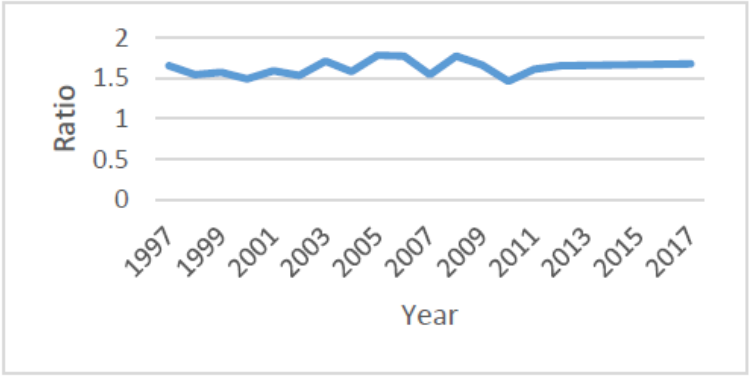

Figure 3: Variation of ratio between night peak and day time with year

C. Addition of Electric vehicles (EVs)

Usage of electric vehicles will be high in upcoming years [3]. It is needed to calculate the increasing power demand. The number of electrical vehicle in 2017 will be almost two hundred thousand (200,000). The power that required for charging of a electrical vehicle is about 3600 W [4]. Thus total new deamnd is about 720 MW. Generally, the usage of electrical vehicles are high mostly in developed cities.. However as it is very difficult to evaluate and predict demand changes in each place, total demand increase due to EV was distributed throughout the country proportional to other loads. After calculating the demand due to EVs and add this up with calculated power demand in 2017, the total power demand was estimated.

D. Photo voltaic (PV) additions

As already discussed in section 1, significant amount of PV power will add to the power system specially at customer end. So, the variation for day peak in daily load pattern was analyzed by assuming that 50% of the people use this PV in dry zone and 30% of people use PV in wet zone.

Results and Discussion

A. Power flow analysis for 2017 without Electric vehicles

Summary of the result for this study is given in Table 1. The estimated night peak demand in 2017 without EV addition was 2534 MW. Load flow calculations were performed for this peak demand and bus voltages/power flow results were obtained. Here Victoria bus was defined as the slack bus which generated 81.9 MW power. The transmission losses were estimated as 41.3 MW. It was observed that the voltage violations occured in Kappalthurai and, Trincomalee buses.

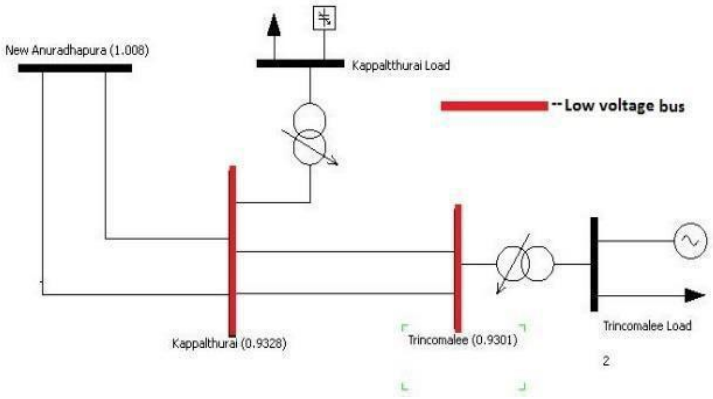

Figure 4: Portion of the simulated network: Anuradhapura, Kappalthurai and Trincomalee buses

As shown in Figure 4, the New Anurathapura bus voltage is 1.008 pu and it is healthy. There are two transmission lines each carries 40 MVA apparent power. There are several solutions to overcome this low voltage problems. The first one is adding reactive power compensator at the load bus to reduce reactive power flows and hence voltage drop in transmission lines. This method is effective if load is consuming significant amount of reactive power. Second one is connecting the kapalthurai bus to another grid closed by. Because Kappalthurai bus bar is now only connected to the New Anurathapura therefore,Kappalthurai bus voltage only depends on New Anurathapura bus Voltage. But, a small change in the New Anurathapura bus leads a huge effect on the Kappalthurai bus. So if this Kappalthurai bus is connected with another bus, this problem may be avoided. i.e Vavuniya Grid. This is practically possible. And the third one is Upgrading the transmission line voltage from 132 kV to 220 kV or 400 kV. This will reduce the current flow and hence voltage drop in lines.

For night time demand of 1152 Victoria slack bus gives 63.1 MW and transmission losses was 11.6 MW. There were no voltage violations and the power system is healthy.

For the day time demand of 1517 MW Victoria slack bus gives 20.7 MW and transmission loss was 24.25 MW. There were also no voltage violations and the power system is healthy.

Table 1: Case summary of without electric vehicles

	Day time	Night peak	Night time
Power demand (MW)	1517	2534	1152
Problems	No voltage violations	Voltage violations in below buses ◊.Kappalthurai ◊.Trincomalee	No voltage violations
Solutions		◊.Adding new compensator ◊.Connect Kappalthurai bus another grid ◊.Upgrade the transmission voltage 132 kV to 220 kV	

B. Power flow analysis for 2017 with Electric Vehicles

If the Electric vehicles are assumed to be charged during the night peak the total night peak demand will become 3254 MW. Power flow was run in the PSS/E software for this loading condition and results are summarized in Table 2. When the Victoria is defined as slack bus it gives 120 MW and transmission loss was 54.2 MW and voltage violation occurs in Kappalthurai, Trincomalee, Kurunaagela, Ukuwela, Pallekelle, Kiribathgumbara buses. And no line over loading occurred.

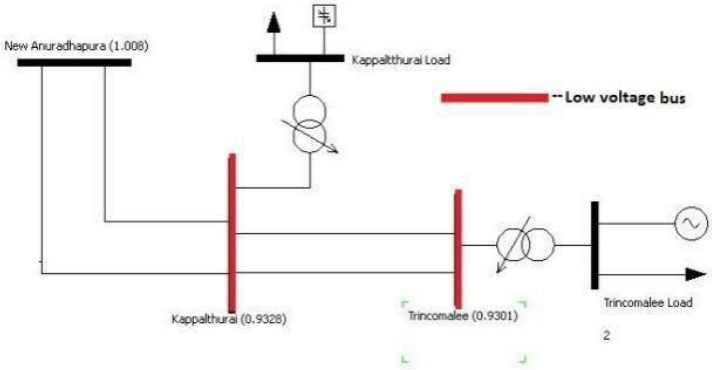

Figure 5: Network diagram of low voltage bus at night peak

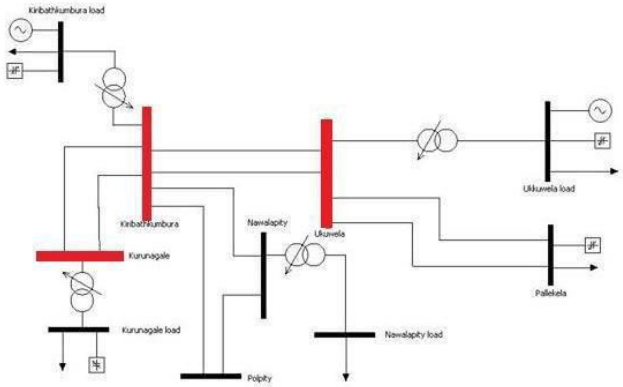

Figure 6: Network diagram of low voltage bus night peak

Following solutions can be applied to overcome this problems, (a)Adding 40 Mvars the compensator in Kappalthurai (Without EVs only 30 Mvars is enough).(b)In 2017 PSS/E model, there will be a 10 Mvars compensator is planned by C.E.B in Kurunagalle. So to overcome this problem compensator capacity should be increased to 20 Mvars. (c)In 2017 model, there will be a 20 Mvars compensator is planned by C.E.B in Pallekalle. So the compensator capacity should be increased by 5 Mvars to overcome this problem.

If the night time demand is considered, the power demand required for night time interval is the least compared to other intervals. Therefore the power generation should be also reduced. The coal power plants are run only 40 % of its full capacity during this interval and, if the electric vehicles are assumed to be charged during this interval, analyzed how the generation should be increased to fulfill the demand and challenges to be faced. The total demand is 1872 MW. For this loading condition slack bus gives 36.6 MW and transmission loss is 20.4 MW. Voltage violation occurs Trincomalee, Kappathurai, Kilinochchi, Chemmunai, Chunnakam buses. No line loading was observed.

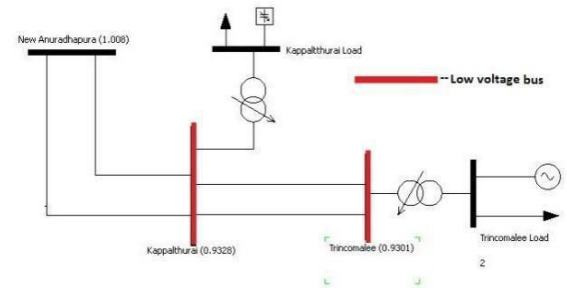

Figure 7: Network diagram of low voltage buses at night time

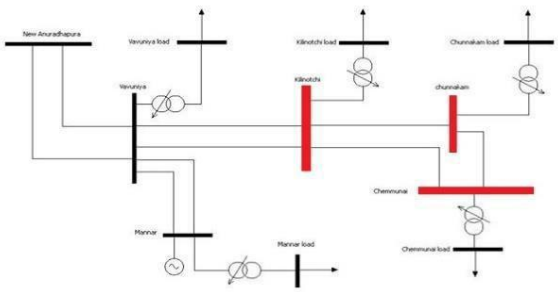

Figure 8: Network diagram of low voltage buses at night time

Above low voltage buses can be considered as two portions (a) Anurathapura, Kappalthurai and Trincomalee (b) Anuradhapura,Vavuniya, Kilinochi, chunnakam and chemmunai. For kappalthurai and Trincomalee solutions suggested fornight peak can be used. For Kilinochi, Chunnakam and Chemmunai low voltage buses if the Chunnakam power station bus voltage is maintained above 1.0 PU (but below 1.05 PU) then voltage violation can be solved.

Most of the electric vehicles are used to travel during the day time. While the travelling, there might be a chance to be charged. The analysis was done based on two constraints they were, 50 % of electric vehicles and 100 % of electric vehicles.
Here, it was considered that 50 % of electric vehicles are charged during the day time peak and the demand is 1877 MW while, obtaining the power flow results, slack bus gives 91.2 MW and transmission loss 26.7 MW. But, there were no voltage violations.

When 100 % EVs are considered the demand was raised to 2237 MW.Power flow results for this case was, slack bus produced 41.9 MW transmission loss was 36.3MW.The voltage violations occurred in Trincomalee, and Kappalthurai buses and no line over loading occurs.

Here again the same bus bars in Trincomalee and Kappalthurai are at the low voltage. These problems already occurred at night peak and night time. So to overcome this problem, same solutions can be applied.

Table 2: Case summary of with electric vehicle

	Day time		Night peak	Night time
Power demand (MW)	50 % EVS	100% EVs	3,254	1,872
	1,877	2,237		
Problems	No voltage violations	Voltage violations in below buses, ◊.Kappalthurai ◊.Trincomalee	Voltage violations in below buses, ◊.Kappalthurai ◊.Trincomalee ◊.Kurunagalle ◊.Pallakalle ◊.Kiribathkumpara	Voltage violations in below buses ◊.Kappalthurai ◊.Trincomalee ◊.Kilinochchi ◊.Chemmunai ◊.Chunnakam
Solutions		◊.Adding 40 Mvars capacity compensator	◊.Adding 40 Mvars capacity compensator ◊.Increasing the Kurunagale compensator capacity to 20 Mvars ◊.Increasing the Pallakelle compensator capacity to 25 Mvars	◊.Adding 40 Mvars capacity compensator in kappalthurai bus ◊.Chunnakam power station bus voltage should be maintained 1PU

C. Without coal power

Here it is considered that if an interruption occurs in the coal power plant during the night peak while coal power plants runs in the full load capacity and one generator can generate 285 MW power at its full capacity. If an interruption occurs for at least one generator, power system can be collapsed and slack bus cannot have the capability to manage the demand. Therefore it is required to turn on other power plant to manage the power demand so the schedule of the generation was changed. After scheduled this generation in different ways and ran the power flow in PSS/E for each different ways, there were no voltage violation occurred. But the power produced by the slack bus and transmission losses was varied.

Here it is considered that if an interruption occurs for Coal power plant during the night time, while coal power plant runs at 40 % of its full capacity so that one generator can produces around 150 MW power. But, the maximum capacity of the slack bus (Victoria) is 210 MW. If an interruption occurs for one generation coal power plant the required power demand can be only managed by slack bus if and only if slack bus produces the power below 50 MW before the interruption.

And also if an interruption occurs for more than one generator, the required demand cannot be managed by the Slack bus. So to manage the demand, other power plants should be turned on.

D. PV Additions

For this analysis, it was assumed that the PV usage in dry zone was 40 % and wet zone was 20 %. it was also assumed that PVs are in usage at day time peak. If the case of 100 % electric vehicles is considered at day time peak, the total required demand would be reduced due to PV additions. Earlier, the total demand was 2237 MW after the PV addition the total required demand is reduced to 1557 MW. It was observed that there were no voltage violations and the transmission loss also less to half while comparing with, without PV addition of 100% electric vehicle usage.

Discussion and Conclusion

Development of each year leads a huge power demand in 2017 and this power demand will be raised even more due to the usage of electric vehicles therefore, the power generation should be increased. The contribution of the coal power plant will be high to fulfill that demand. If the coal plant gives the required power, much power flows through the Norochchole transmission line, which leads to high transmission losses in the transmission line. So the buses which are far away and, connected with Norochchole have more possibility to become low voltage. If the transmission voltage in Norochchole will be upgraded from 220 kV to 400 kV or by increasing the number of transmission lines the problems can be avoided. Second thing observed in this study was that among the analyzed cases, some cases showed voltage violations where as some cases did not. Additionally it was noted that Kappalthurai and Trincomalee buses were always in low voltage. This is because, Trincomalee bus was connected to Kappalthurai bus, which was only connected to Anuradhapura bus, and they were long transmission lines. So if any changes occur in Anuradhapuara bus voltage due to other networks which are connected with it will greatly affect the Kappulathurai bus which should be connected more than one buses i.e Vavuniya to overcome the voltage violation occurrence. Other voltage violations in other buses are due to reactive power consumptions. If capacitor banks are installed, the consumption of the reactive power will be reduced and this problem can be avoided. Due to the usage of the PV additions, the required power demand will be reduced mostly in dry zone in Sri Lanka. Hence the power flow through the transmission lines will also be reduced and the transmission losses will be also reduced. So the most of the time buses in the power system are healthy and the possibilities for voltage violation are much less. It can be concluded that due to electric vehicle additions, kappalthuarai and Trincomalee buses gives a big challenge for the 2017 power system. Comprehensive load flow analysis and solutions will provide the

answers for the energy security of the country.

Acknowledgements

We sincerely thank to CEB for providing the relevant information about the Sri Lankan transmission network as in 2017 and for helping us in various circumstances. And our thanks go to the Department of Electrical and Electronic Engineering, University of Peradeniya for providing the platform for our research.

References

[1] LBO, web.[online]. Available: http://www.lankabusinessonline.com
[2] Transmission generation and planning branch, transmission division, CEB. Long term generation expansion plan 2013- 2032.
[3] Auto bay, web. [Online]. Available: http://www.autobay.lk
[4] Wikipedia, web. [Online]. Available: https://en.wikipedia.org/wiki/Charging_station
[5] Public Utility Commission of Sri Lanka. Study report on electricity demand curve and system
[6] Kundur P., "Power System Stability and control",
McGraw-Hill Inc. 1994.
[7] Ceylon Electricity Board (CEB), Sri Lanka, official website. *http://www.ceb.lk*
[8] wolf-Peter Schill, Clemens Gerbaulet. Power System Impacts of Electric Vehicles in Germany: Charging with Coal or Renewables.
[9] J. Arrillaga and C. P. Arnold. Computer analysis of power system. England: John Wiley and sons;1990.

Distribution Networks with Renewable Sources, Electric Vehicles and Reactive Power Compensators

Kehelpannala, K., Herath, T., Nadeekumari, N., Prof. Ekanayake, J.B., Liyanage, K.M.

Department of Electrical and Electronic Engineering, University of Peradeniya

Abstract

The use of rooftop and grid connected Photovoltaic (PV) panels are expanding due to its cost effectiveness. At the same time the use of Electric Vehicles (EVs) is also gradually increasing. The increment of EV penetration have some negative impacts on the distribution networks such as increase in line loading and hence increase in the voltage drop along the line. This paper discusses a solution based on the reactive power generation capability of PV systems to address the problem of increased voltage drop that will arise due to high EV penetration. The PV inverter can be used as a STATCOM (Static Var Compensator) to provide controllable reactive power to the system. This paper presents a case study done on an existing distribution feeder. From the observations it was concluded that when the reactive power sources with smaller capacity is distributed along the feeder, they provide a better improvement on the voltage profile. Simultaneously distributed reactive power sources reduces the current flowing in the feeder, which in turn resulted in lower I^2R losses.

Keywords: Grid Connected PV, reactive power compensation, STATCOM (Static Var Compensator)

Introduction

With the fast development and use of low carbon energy technologies, nowadays there is an increasing trend of electricity generation using renewable energy sources. Among renewable energy sources, Photovoltaic (PV) has captured interest among customers and power producers. Use of rooftop and grid connected PV panels are becoming larger due to their cost effectiveness [1]-[3]. At the same time use of Electric Vehicles (EVs) is also gradually increasing with the introduction of new models of EVs in the market and special tax reductions on them [4]. The increment of EV penetration have some negative impacts on the distribution network such as increase in line loading and hence increase in the voltage drop along the line. Voltages on a distribution system have to be maintained within an acceptable limit to provide satisfactory service to critical loads. But with the increasing penetration of EVs, it is challenging to maintain the voltage at a satisfactory level. This paper discusses an investigation of the effect of EVs on the voltage profile of a distribution network and how this problem can be addressed utilizing the available reactive power capability of the inverter of existing grid connected PV system.

The voltage drop due to increasing load can be reduced by reducing the reactive current component without affecting the real power transmitted. The conventional method to address this issue is to use reactive power compensation to reduce reactive power flow. Usually a capacitor bank installed at a site on the distribution conductor provides this reactive power compensation. However, this method has very little control of the reactive power [5].

The grid connected PV panels are being installed at an increasing rate. These PV panels are usually used only during day time to generate active power and they are inactive during night. But at night PV systems can support to produce their full reactive power generation capability. That is if a PV inverter is used as a STATCOM (Static Var Compensator) it can provide controllable reactive power to the system. A STATCOM is a Voltage Source Converter (VSC) based device with the voltage source behind a reactor which converts DC input voltage into an AC output voltage in order to compensate active and reactive power. It can act either as an AC reactive power sink or a source to an electricity system. If connected to a power source, like a PV panel, it can also provide active power. It can actively vary the reactive power or reactive and active powers with the change of voltage.

As the rooftop grid connected PV systems are usually distributed along the feeder and they have reactive power producing capability they can be used as distributed reactive power sources to improve the voltage variation of the distribution feeder.

The study presented in this paper has two major parts. The first part demonstrates the impact of EV

penetration on the voltage profile of a distribution feeder and how this issue can be mitigated using capacitor banks. The second part of the case study is a demonstration of how PV inverter can be used as a distributed reactive power source to mitigate the voltage issue.

Operation of a STATCOM for Reactive Power Compensation

The STATCOM consists of a VSC whose DC side is connected to a capacitor. The inverter is connected to the supply system via a transformer. A basic STATCOM circuit is shown in Figure 1, in which transformer leakage reactance is represented by X. If the fundamental of the phase output voltages of the inverter is in phase with the corresponding system voltage, the line current flowing into or out of the VSC is always at 90° to the network voltage due to the reactive coupling. When the fundamental of the inverter voltage is less than the ac system voltage, reactive power is absorbed by the STATCOM. On the other hand, when the STATCOM voltage is higher than the system voltage, reactive power flows from the STATCOM to the system. This is shown in Figure 1(b) and (c). The magnitude of the STATCOM output voltage can be varied by controlling the DC capacitor voltage. If the switching devices of the inverter are operated to obtain the fundamental of the STATCOM output voltage leading or lagging the ac system voltage by a small angle, a net amount of real power flows between the system and the STATCOM. This in turn decreases or increases the dc capacitor voltage.

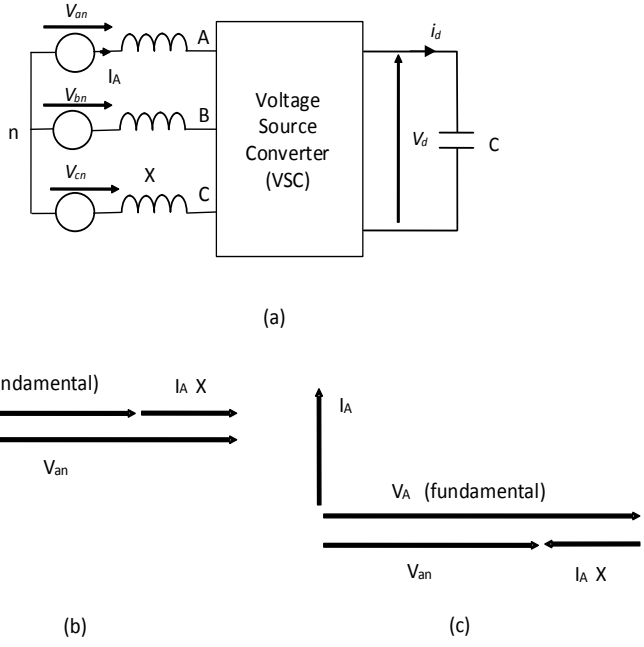

Figure 1: Operation of a STATCOM

Load flow studies of distribution feeders

One of the aims of the study is to analyze the behavior of the voltage profile of a distribution feeder under different loading situations. Therefore a simulation environment was developed to represent the feeder and analyze its voltage characteristics. The distribution system has some salient characteristics such as; radial structure, high R/X ratio and unbalance loads along with single phase and two phase laterals. Because of these features of distribution networks, the conventional load flow methods commonly used in transmission network power-flow studies such as Newton_Raphson method and Gauss-Seidal method generally fail to converge in solving such networks. Therefore, for analyzing a low voltage distribution system, an iterative technique specially designed for radial systems called 'Ladder Iterative Technique' was selected [6]. The Ladder iterative technique uses both Kirchhoff's Voltage Low (KVL) and Kirchhoff's Current Low (KCL) for finding each node voltages of a low voltage distribution feeder when power consumption at each node is known. The following is the procedure used:

a) Assume an initial nodal voltage magnitude and angle for each bus (nominal voltage is often used).
b) Start from the root and move forward towards the feeder and lateral ends while calculating the current in each branch using KCL
c) Start from the feeder and lateral ends towards the root while calculating the voltage in each node using KVL
d) Check the termination criterion
e) The forward/backward sweep is repeated until the criterion is met

Case Study I: EV connection with concentrated Reactive Power Compensator

For this analysis a distribution feeder belonging to Ceylon Electricity Board was used. Even though feeder has irregular distribution of loads, for the analysis purpose the total load on the feeder was represented by evenly distributed 10 point loads spaced at equal distances over the 1.8 km of full length of the feeder. Further single phase system was assumed for the study. The conductor of the selected feeder is All Aluminum Fly conductor (AAC) which has a current rating of 155A. The resistance of the AAC Fly conductor is 0.505 Ω/km and reactance is 0.293 Ω/km. Power factor of the feeder was taken as nominal maintained power factor, 0.88 to calculate the reactive loads corresponding to measured active power.

The developed load flow program in Matlab/ Simulink was used to analyze the voltage variation along the feeder. As the base case the current situation is

considered where there is no EV or rooftop PV panels connected. Figure 2 shows the voltage profile along the feeder.

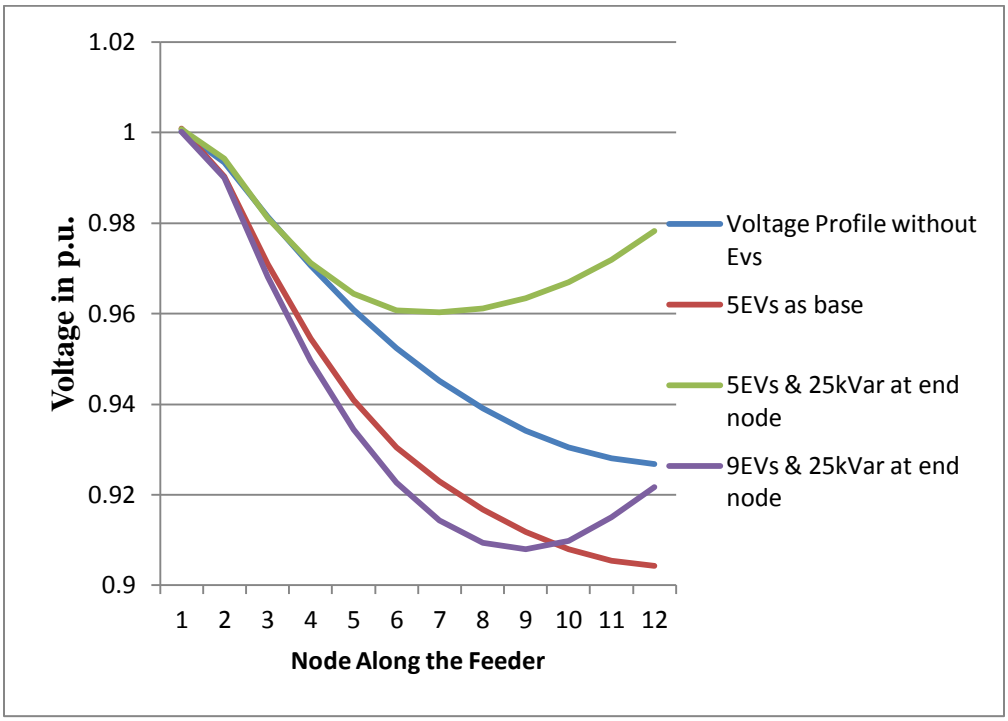

Figure 2: Voltage Profile of the Feeder for the base case, with EVs and with shunt capacitors

The usual practice of the Utility is to maintain the distribution feeder voltage variation within ±10% of nominal voltage, that is any node voltage can have a maximum drop up to 0.9 p.u.. According to the Figure it was observed that the last node voltage only drops up to 0.928 p.u.. Therefore there is room to increase the load until the maximum allowed voltage drop is reached. Even though the conductor has a current carrying capability of 155 A, from measurements it was found that the loading on the feeder is only 36.84 A even at the peak load. The voltage being above 0.9 p.u. along the feeder and current being less than the rated value of the conductor altogether means the maximum capacity of the feeder is not utilized. In order to harness this unutilized capacity, Nissan Leaf electric vehicles having charging load of 3.3 kW [7] was added to the feeder. It was observed that only 5 EVs can be connected and if more EVs are connected the last node voltage drops below 0.9 p.u.. Figure 2 also shows the voltage profile with EVs connected to the first 5 nodes starting from the transformer end.

The current with the 5 EVs added to the feeder was calculated to be 59.69 A, which is still below the rated current capability of the feeder. Therefore if the voltage can be improved by using a suitable technique it will provide the space to increase the loading capability of the feeder. Adding a reactive power compensator is a current practice to boost the voltage. Considering the payback period it was found that a 25 kVar capacitor at the end node is a value of an economically viable reactive power source which is to be connected at the end of the feeder. The improved voltage profile after introducing the reactive power source was found to be much better than the base case as also shown in Figure 2. Now the current flow was found to be 61.29 A, which is still less than the rated current carrying capacity of the conductor.

From simulations, it was found that 9 EVs can be connected in total to the feeder with the 25 kVAr capacitor at the end of the feeder and without violating the voltage or current carrying capacity constraints. In this case, a 25 kVar capacitor was considered as an economical option because when it is connected at end node, it enables addition of 4 more EVs to the feeder and if the capital of the capacitor bank is to be covered by these additional 4 EVs, the payback period for the capacitor bank is less than 12 months. The voltage profile after adding 4 more EVs is also shown in Figure 2.

Case Study II: EV connection with distributed Reactive Power Compensators

The effect of using capacitive reactive power sources in a distributed manner was also investigated. As can be seen, the distributed arrangement allows addition of one more EV. Even though this is not a considerable achievement, If PV inverters are used in the night as a STATCOM to provide reactive power then it becomes a cost effective solution. With income from the added EV it facilitates the ability to invest on a reactive power compensator with increased rating of 50 kVar. Figure 3 compares the voltage profile when a 50 kVar capacitor at the end of the feeder to that when a distributed reactive power compensation is used.

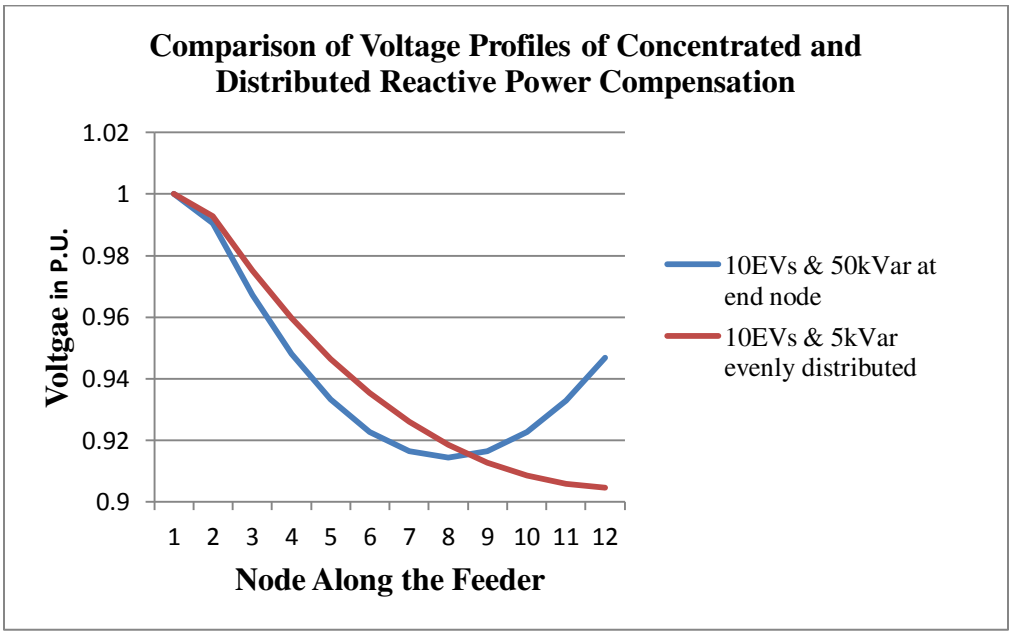

Figure 3: Voltage Profile with Distributed Reactive Power Sources

Furthermore, the addition of reactive power sources in distributed manner reduces the current flow in the line as shown in Figure 4. This in turn reduces the distribution line losses.

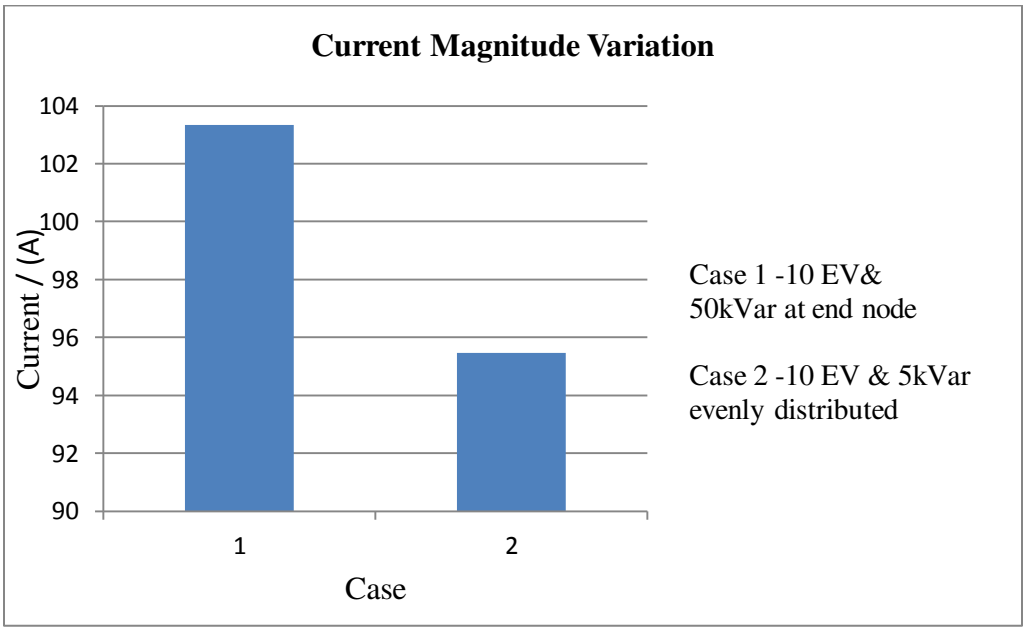

Figure 4: Variation of Current Magnitude

Conclusions

A simulation environment was developed to study the effect of EV connections on typical LV distribution feeders. Even though there was a room in the feeder to add more EVs without violating the voltage constraints, the full current carrying capability of the feeder was not utilized. As a measure of utilizing the full capacity of the feeder, reactive power compensation in a concentrated and distributed manner was investigated. Even though both enabled utilization of the full capacity of the feeder, the introduction of reactive power support in a distributed manner seems to be more attractive as it is not only reduces the line losses but also enables the utilization of PV inverters when they are idling.

As PV systems are inherently distributed along the feeder, the utilization of the reactive power compensation capability of PV inverter enabled to enhance the utilization of the feeder and the PV inverter. Utilizing PV inverter as a STATCOM is an attractive solution to adding capacitors as it is freely available during the time feeder demands more reactive power to boost the voltage.

Acknowledgements

Authors would like to acknowledge the support of Kandy City Area Office of Ceylon Electricity Board to obtain the feeder data. The authors would also acknowledge the financial support provided by the National Research Council, Sri Lanka under the research grant NRC 14-15.

References

[1] Meinhardt, M. , Cramer, G. Past, present and future of grid connected photovoltaic- and hybrid-power-systems, IEEE Power Engineering Society Summer Meeting, 2000, Seattle, WA

[2] Hui Li, Hao Zhang ; Fei Ma ; Weihua Bao, Modeling, control and simulation of grid-connected PV system with D-STATCOM, IEEE International Conference on System Science and Engineering (ICSSE), 2014, Shanghai

[3] E. Sortomme and M. a. El-Sharkawi, “Optimal Charging Strategies for Unidirectional Vehicle-to-Grid," IEEE Transactions on Smart Grid, vol. 2, no. 1, pp. 131-138, Mar. 2011.

[4] Goli, P. , Shireen, W. PV Integrated Smart Charging of PHEVs Based on DC Link Voltage Sensing, Smart Grid, IEEE Transactions on (Volume:5 , Issue: 3), Van der Geer J, Hanraads JAJ, Lupton RA. The art of writing a scientific article. J Sci Commun 2000; 163:51-9.

[5] Lars T. Berger, Krzysztof Iniewski, Smart grid applications, communications and security, First edition, John Wiley & Sons, INC., publication

[6] W. H. Kersting, Distribution System Modeling and Analysis, Third Edition. CRC Press, 2012.

[7] Nissan LEAF website [Online], Available: http://www.nissan.co.uk/GB/en/vehicle/electric-vehicles/leaf/charging-and-battery/charging-nissan-leaf-and-battery.html

Relationship between energy usage and thermal comfort in green buildings

Jayalath, J.R.D.K., Dr. De Silva, N.

Abstract

Contemporaneous concerns over global warming and escalating energy prices have rapidly emerged into public consciousness. Therefore, the concept of "sustainability" is happening in building sector as a solution to mitigate above issues in a rapid manner. Driven by the desire for sustainable building practices the "Green Building" concept is adopting by various organizations in Sri Lanka. LEED is one key prestige certificate which green building can achieve to market itself. In general, these rating, awards and standards are based on building design and its potential for low energy and sustainable operation, and their focus tend to be on technical aspects of building design. However, buildings that perform poorly from the users' point of view are unlikely to be sustainable in the long term. Thus it is stated that, measuring green buildings' performance from user point of view in a comprehensive manner is essential. By measuring green building's performance from user's views, this research study aims to identify relationship between energy usage and thermal comfort in green buildings.

By evaluating two LEED "Gold" rated green buildings with questionnaire survey and observation of temperature and relative humidity, final thermal comfort level was derived. Furthermore thermal comfort related issues were also identified using questionnaire survey. By evaluating past three months energy bills with level of thermal comfort relationship was derived. According to the findings both selected cases can increase averagely 1.5 ^{0}C and save energy nearly 7% while reducing dis-satisfied percentage of people by approximately 20%. Result showed that by enhancing thermal comfort of occupant's significant energy saving can be achieved in Sri Lankan green building sector. Furthermore, results showed that there is a considerable level of thermal dis-comfortness associated with symptoms of sick building syndrome in both green buildings. Derived results can be used to improve existing building energy performance and for future building designs by finding desirable set points and elements missing from current buildings. Also study encourages the need of thermal comfort benchmark in warm humid climate countries. Further study reassures the necessity of moderating green building rating systems with thermal comfort parameters in a deep manner.

Key Words: ASHRAE, Green Buildings, Health, LEED, Sick Building Syndrome, Thermal comfort

Introduction

Recent literature related to indoor environmental conditions have discovered that thermal comfort is ranked as first priority by building occupants compare to other comfort parameters [1]. Similarly Huang, Zhu, Ouyang and Cao [2] also described that thermal comfort is considered to be the environmental factor to which people pay the most attention. However, many researchers have revealed that numerous technologies used in green buildings can affect negatively for occupants' thermal comfort occasionally [3]. Cui, Cao, Ouyang and Zhu [4] proved that extremely high or low temperature set points of air conditioning system can deteriorate human performance. Moreover, Seppanen, Fisk and Faulkner (as cited Cui et al.) stated that increase in temperature by 1^0C resulted in 2% decrease in occupancy performance rate [4]. Puteh, Ibrahim, Adnan, Ahmad and Noh (2012) showed that either high or low humidity is detrimental to the health of normal people [5]. Besides, indoor air temperature indirectly affects on prevalence of sick building syndrome symptoms as well [6]. However, to ensure continuous growth in the adoption of green buildings, it is important to ensure occupants comfort parameters are being addressed such as thermal comfort [7]. Tom (2008) noted that many engineers and facilities managers focus on secondary objectives of controlling satisfied environment such as minimizing energy use, while ignoring primary objective of satisfying occupants [8]. Thus, discovering the relationship between energy usage and thermal comfort Sri Lankan green building sector is indispensable.

Thermal comfort assessment parameters

Assessment of thermal comfort is a complex topic as it is subjective to individuals' different expectations [9]. Further to authors, these expectations will be determined by varying parameters such as age, sex, health, origin of an individual, and clothing. Furthermore, it has been proven that, within an environment with the same characteristics and climate, the thermal sensation and preferences for the same differs among individuals [10].In assessing the thermal comfort two different techniques are used namely, the heat balance approach and the adaptive approach [11,12].

- Heat balance approach- The human body's thermoregulatory system is used to maintain an essentially constant internal body temperature is the key assumption of heat balance approach [12]. To apply this approach, ASHRAE used a seven-point thermal comfort scale as given in Table 1 [13]. This scale is used to measure the occupants' actual thermal sensations using "thermal sensation value (TSV)".

Table 1: ASHRAE seven point thermal comfort scale

Comfort Value	-3	-2	-1	0	+1	+2	+3
Description	Cold	Cool	Slightly cool	Neutral	Slightly warm	Warm	Hot

- PMV (Predicted Mean Vote)

PMV is an index, which is practiced by HVAC engineers used to predict whether a certain thermal environment would be acceptable to a large group of people [14]. Further to authors, it was derived by expanding the comfort equation to incorporate the seven-point ASHRAE thermal comfort scale.

$$PMV = f(t_a, t_{mrt}, v, M, I_{cl}) \quad \text{Eq. 1}$$

Table 2: PMV parameters description

		Symbol	Unit of Measurement
Environmental Variables	Air temperature	t	^0C
	Mean radiant Temperature	T_{mrt}	^0C
	Relative air velocity	v	m/s
	Air humidity/vapour pressure	p_a	kPa
Personal Factors	Activity level/ metabolic rate	M	W/m^2
	Clothing insulation	I_{cl}	Clo.

- PPD - Predicted Percentage of Dissatisfied

Based on experimental studies in which participants voted on their thermal sensations, an empirical relationship between PMV and the predicted percentage of dis-satisfied (PPD) was developed as follows:

$$PPD = 100\text{-}95 \times \exp(-0.03353 \times PMV^4 - 0.219 \times PMV^2) \quad \text{Eq. 2}$$

PPD Equation indicates that even at a thermal neutrality (PMV = 0), about 5% of the people can still be dissatisfied.

Research Methodology

This study resorted to the case-study method in order to research thermal comfort level of green building occupants. Hence, the unit of analysis of the study was “thermal comfort”. Two green buildings situated in Western Province were selected for the study. All two cases selected for this study has

awarded LEED "Gold" rating system. Both Case A and Case B is newly constructed office buildings with central AC. Façade of these buildings are glass with fixed windows. Thermal comfort information of occupants of the buildings was collected through a questionnaire survey at three time interval during the daytime. Thirty occupants from each case were participated. Further field temperature and humidity measurements were taken using thermo-hygro meter.

Findings

- Thermal comfort evaluation using Thermal Sensation Vote (TSV)

Table 3: ASHRAE seven point thermal comfort scale

	Cold	Slightly Cool	Cool	Neutral	Warm	Slightly Warm	Hot	MTSV	AVR.
CASE A	-3	-2	-1	0	+1	+2	+3		
9.00 AM	7	5	8	9	1	0	0	-1.267	-1.156
12.00 PM	8	4	4	12	2	0	0	-1.133	
3.00 PM	6	5	6	11	2	0	0	-1.067	
CASE B									
9.00 AM	4	6	10	9	1	0	0	-1.100	-1.100
12.00 PM	9	3	9	8	1	0	0	-1.367	
3.00 PM	3	6	7	11	3	0	0	-0.833	

TSV data showed that none of the occupants who felt 'hot' or 'warm' during the study. The mean thermal sensation vote (MTSV) varies between -2 and -1 in case A while in case B, this varies between -2 to 0. This implies that both buildings maintain slightly cool/cool environment according to their occupants.

Averagely 23.33% and 17.77% of the respondents considered the indoor thermal conditions to be cold (-3) in case A and case B respectively throughout the whole day; furthermore as an average 15.56% and 16.67% of them responded that the indoor temperatures were cool (-2) in case A and B subsequently. The ASHRAE 55-2010 specified that the thermal acceptability should be defined as the condition where 80% of occupants should have TSV between slightly cool (-1) and slightly warm (+1). However, in case A only 61.12% of average respondents replied with neutral (0, 35.56%), slightly cool (-1, 20%) or slightly warm (+1, 5.56%), This value is

noticeably lower than the value recommended in ASHRAE 55-2010 standard. In Case B, only 65.54% of the respondents have replied with neutral (0, 31.11%), slightly cool (-1, 28.88%) or slightly warm (+1, 5.55%). That value is also considerably lower than the value recommended in ASHRAE. Accordingly, both case A and B are not fulfilled the requirements of ASHRAE 55 – 2010 standard (AHSRAE, 2010).

Table 4: Data collected using Thermo-Hygro Meter

	Case A					Case B				
Time	09.00 a.m.	12.00 noon	3.00 p.m.	Range		09.00 a.m.	12.00 noon	3.00 p.m.	Range	
				Min. (^{0}C)	Max.(^{0}C)				Min. (^{0}C)	Max (^{0}C).
Air Temperature (^{0}C)	23.6	23.2	23.9	22.8	24	24	23.4	23.9	23.3	24.1
Mean Radiant Temperature (^{0}C)	23.4	23	23.7			23.8	23.2	23.7		
Air Speed (ms^{-1})	0.10	0.10	0.10			0.10	0.10	0.10		
Humidity (%)	48	51	54	48	55	57	56	54	54	58
	Air speed taken as average air velocity in Sri Lanka (0.1 ms^{-1})									
	Clo value for summer season according to ASHRAE 55-2010 is 0.5									
	The activity level is considered as Seating, quiet according to the ASHRAE.									
	Mean Radiant Temperature = 0.99T – 0.01									

In case A at 9.00 am PMV value is greater than MTSV value. According to the online tool used to evaluate in this study clearly says that situation at 9.00 am is not accordance with ASHRAE 55-2010 standard. Because according to the ASHRAE 55-2010 PPD value should be less than 10% and in this case it is

greater than even 20%. Main reason for this can be due to lower temperature of 23.6 ^{0}C and 48% relative humidity at that time. When consider about 12.00 p.m. situation PMV is (-1.09) and PPD is 30%. PMV value is considerably lower than PMV value at 9.00 am. PPD also increased from 25% to 30% from 9.00 am to 12.00 pm. MTSV for case A at 12.00 am is (-1.133). However PMV derived by objective evaluation is (-1.09). Although at 12.00 pm closely similarly PMV values derived, however PMV value is greater than MTSV value. According to the online tool used to evaluate in this study clearly says that situation at 12.00 pm is not accordance with ASHRAE 55-2010 standard. Main reason for this can be due to lower temperature of 23.2 ^{0}C and 51% relative humidity at that time. When consider about 3.00 p.m. situation PMV is (-0.81) and PPD is 19%. That result is the highest PMV and lowest PPD value for case A. However at 3.00 pm only 81% of people are satisfied with thermal environment according to the PPD. MTSV for case A at 3.00 Pm is (-1.067). However PMV derived by objective evaluation is (-0.81). In case A at 3.00 pm PMV value is greater than MTSV value. According to the online tool used to evaluate in this study clearly says that situation at 9.00 am is not accordance with ASHRAE 55-2010 standard. Because according to the ASHRAE 55-2010 PPD value should be less than 10% and in this case it is greater than even 15%. Main reason for this can be due to lower temperature of 23.9 ^{0}C at that time.

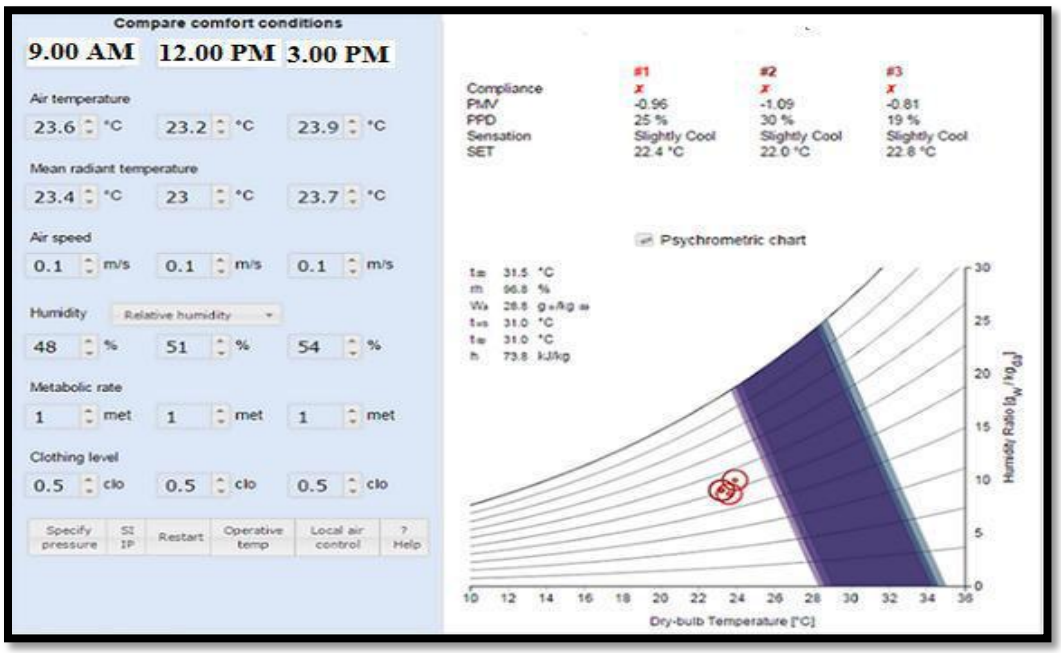

Figure 1: Case A – Thermo-Hygro Meter Data Analysis

Table 5: Case A – PMV, PPD and Compliance with ASHRAE

Case A	Pedicted Mean Vote	PPD	Satisfying ASHRAE comfort range (Yes/No)
9.00 A.M.	-0.96	25%	No
12.00 P.M.	-1.09	30%	No
3.00 P.M	-0.81	19%	No

According to the value derived from online software in case A none of the sessions were unable to satisfy with the ASHRAE 55-2010. Main reason for this can be the low temperature maintained inside the building more than the level stated in the standard. PMV is a widely used model to predict human thermal comfort. Many previous studies have indicated the inherent difference between PMV and TSV. In this study, the mean PMV value is (-0.953), while the overall TSV value for case A is (-1.156). The difference +0.2026 imply that the comfort temperature predicted by the PMV model is lower than the one indicated by the TSV.

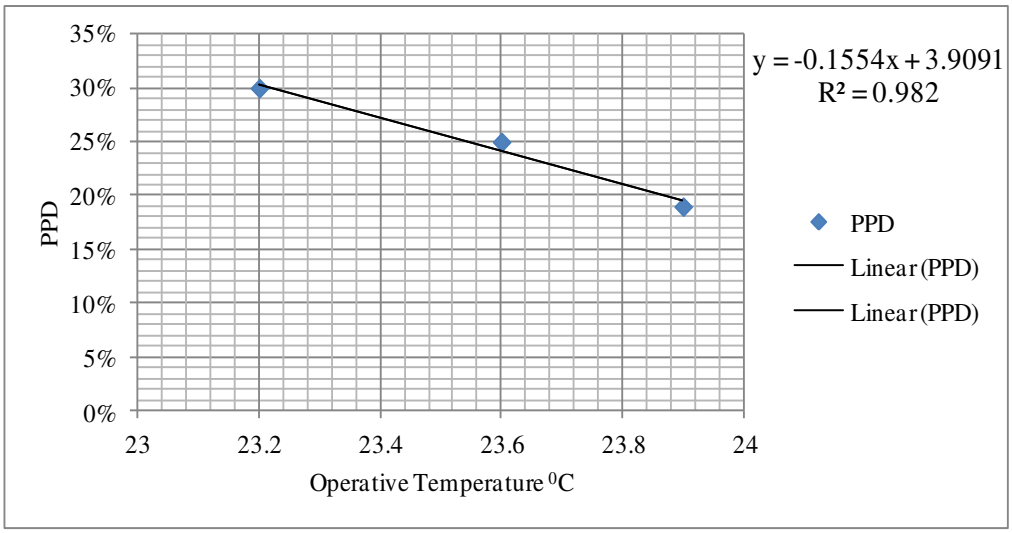

Figure 2: Case A- PPD vs Temperature

By illustrating operative temperature against PPD it has found that there is a linear regression (R^2 =0.982). With the increasing of temperature PPD value is decreasing. Decreasing PPD value indicates that satisfied percentages of occupants are going to be increased. That implies huge percentage of occupants is satisfied with the increasing temperature. Since Sri Lanka is a warm humid country people are usually prefer to be in slightly warm environment. The reason for satisfy more percentage of occupants with growing temperature is

"acclimatization" which was described in previous sub sections as well.

Furthermore this implies the building is overcooled. According to the literature, overcooling appears to be a common phenomenon in local offices in warm humid countries. Though local field studies in tropical countries have reported the phenomenon of overcooling in air conditioning offices for decades, little is known about the occupants' reactions to overcooling and the potential energy efficiency impact. Foo and Poon (as cited in Cheng & Chang, 2012) found that 60% of the occupants worked in air conditioned offices with air temperatures less than 24 ^{0}C, and they suggested that an air temperature of 27 ^{0}C might be good enough to satisfy more than 80% of the occupants. Previous studies discovered that overcooling might cause thermal discomfort and energy wastage in the building. Since case A is a green building both sustainability of workplace and sustainability of occupants is very crucial. By increasing temperature case A can save more energy more than existing level.

To find out the maximum temperature which case A can increase can be found as follows. According to figure 4.11 the equation is

PPD = -0.1554*Operative Temperature + 3.9091

Eq. 3

Where -0.1554 and 3.9091 are constant for case A.

According to the Equation 2.2 mentioned in literature review, 5% is the minimum dissatisfied percentage which a building can achieve. Applying minimum PPD value to equation 4.1, operative temperature is 24.83 ^{0}C. It is the maximum temperature which case A can have by satisfying maximum percentage of occupants (minimum dissatisfaction).

4.6 Case B –Thermo – Hygro Meter Data Analysis

When consider about case B - 9.00 a.m. situation PMV is (-0.75) and PPD is 17%. When compared with case A, PPD value is relatively low in case B at 9.00 am. That imply satisfied occupants percentage is relatively high in case B. MTSV for case B at 9.00 am is (-1.100). However PMV derived by objective evaluation is (-0.). According to the literature, both PMV and MTSV should be slightly similar. In case B at 9.00 am PMV value is greater than MTSV value. According to the online tool used to evaluate in this study clearly says that situation at 9.00 am is not accordance with ASHRAE 55-2010 standard. When consider about case B – 12.00 p.m. situation PMV is (-0.98) and PPD is 25%. PMV value is considerably lower than PMV value at 9.00 am. PPD also increased from 17% to 25% from 9.00 am to 12.00 pm. It can be due to increasing outside temperature and decreasing outside temperature. With increasing difference in between outside temperature and inside temperature make occupants uncomfortable. However at 12.00 pm only 75% of people are satisfied with thermal environment. MTSV for case B at 9.00 am is (-1.367). However PMV derived by objective

evaluation is (-0.98). Although at 12.00 pm closely similarly PMV values derived, however PMV value is greater than MTSV value. According to the online tool used to evaluate in this study clearly says that situation at 12.00 pm is not accordance with ASHRAE 55-2010 standard.

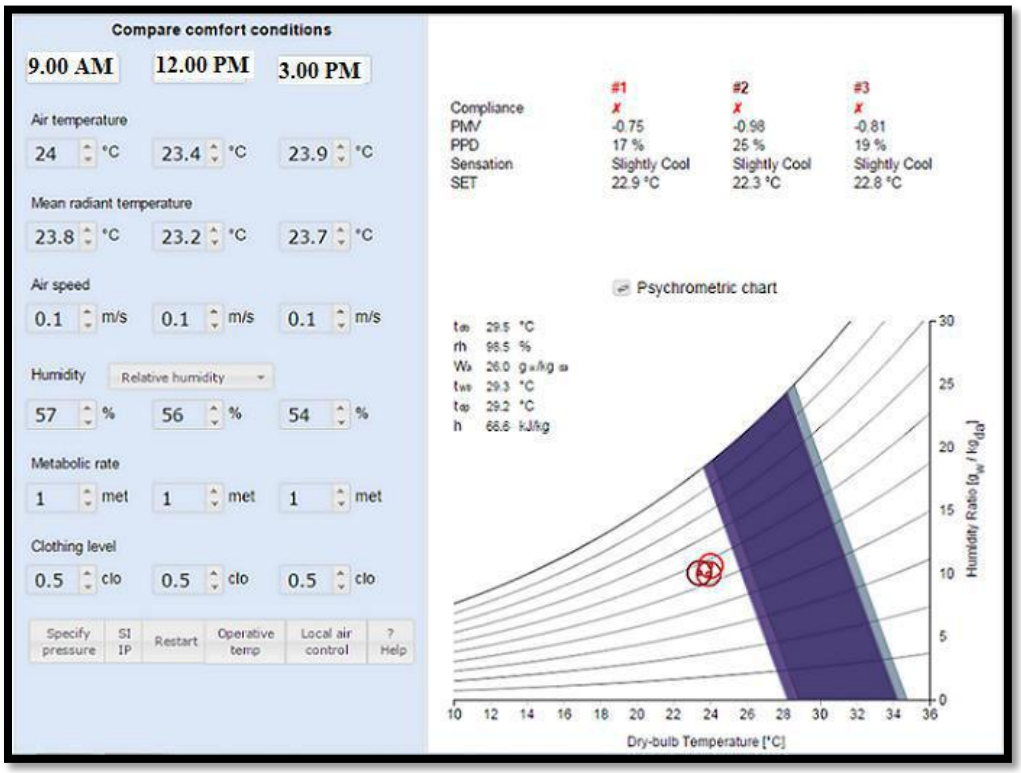

Figure 3: Case B – Thermo-Hygro Meter Data Analysis

When consider about 3.00 P.M. situation PMV is (-0.81) and PPD is 19%. Accordingly, at 3.00 pm only 80% of people are satisfied with thermal environment. MTSV for case B at 3.00 Pm is (-0.833). However PMV derived by objective evaluation is (-0.81). According to the online tool used to evaluate in this study clearly says that situation at 3.00 pm is not accordance with ASHRAE 55-2010 standard. Because according to the ASHRAE 55-2010 PPD value should be less than 10% and in this case it is greater than even 15%.

Table 6: Case B - PMV, PPD and compliance with ASHRAE

Case B	PMV	PPD	Satisfying ASHRAE comfortable range (Yes / No)
9.00 AM	-0.75	17%	No
12.00 P.M.	-0.98	25%	No
3.00 P.M.	-0.81	19%	No

In this case also with temperature increasing, the dis-satisfied percentage of occupants is decreasing. The maximum temperature which case B can have with minimum percentage of dissatisfied occupant percentage is 24.96^{0}C (According to the equation derived in figure 4.15 with 5% minimum percentage of dissatisfaction).

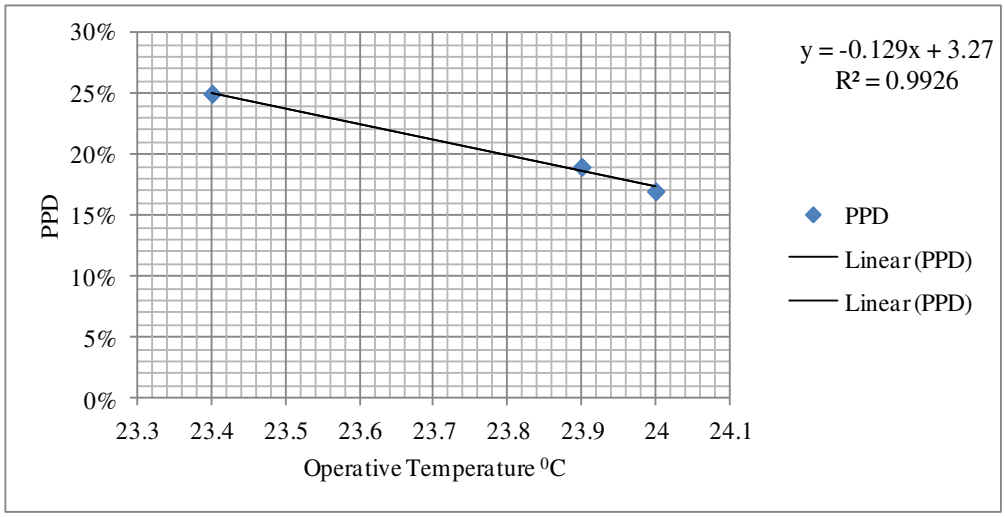

Figure 4: Case B – PPD vs Operative temperature

By illustrating operative temperature against PPD it has found that there is a linear regression (R^2 =0.9926). With the growing of temperature PPD value is decreasing accordingly. Decreasing PPD value indicates that increasing percentage of satisfied occupants (As mentioned in case A section 4.4.2). Also main reason for this is also acclimatization for warm humid climate of Sri Lanka. To find out the maximum temperature which case B can increase can be found as follows. According to figure 4.14 the equation is

PPD = -0.129*Operative Temperature + 3.27 Eq. 4

Where -0.129 and 3.27 are constant for case A.

According to the Equation 2.2 mentioned in literature review, 5% is the minimum dissatisfied percentage which a building can achieve. Applying minimum PPD value to equation 4.2, operative temperature value is 24.96 ^{0}C. It is the maximum temperature which case B can have by satisfying maximum percentage of occupants (minimum dissatisfaction).

Therefore maximum temperature is 24.96 ^{0}C which case B can have by satisfying maximum percentage of occupants.

Very similar results can be obtained by case A and case B. For case A maximum temperature with minimum PPD is 24.83 ^{0}C. For case B maximum temperature with minimum PPD is 24.96 ^{0}C. It can be concluded that both selected green buildings can maintain higher temperature than existing low level temperatures and can obtain more energy efficient results. Also increasing temperature indirectly affect to duration of air conditioning system as well. Furthermore, by making working environment more similar to familiar environment can increase productivity and performance of occupants as well.

Conclusions

Thermal comfort evaluation based on the ASHRAE TSV scale showed that many people in green buildings complain about overcooling. Higher percentage of occupants vote for -3.-2, or -1 while none of the occupants vote for +2 and +3 (slightly warmer or hot). This implies many occupants are feeling cooler with existing thermal environment condition. The reason for this is acclimatization for usual Sri Lankan warmer weather. Therefore occupants from warm humid countries can feel comfortable with higher temperatures. Therefore in order to enhance productivity or performance by reducing temperature is not applicable strategy to a country like Sri Lanka. Since none of the cases were unable to satisfy 80% occupant satisfaction level at any given time it can be concluded that Sri Lankan green buildings are not at a satisfactory level based on ASHRAE 55-2010.

According to the document review done during study shows, acceptable thermal conditions were maintained during initial stage of the building. However, maintaining acceptable level of thermal conditions is missing from any kind of building with its life time. Building owners, Facility Managers, Engineers should continuously monitor the working environment to provide a better environment for occupants, because ultimate business success is always relied upon occupants' satisfaction. Moreover green building rating systems should include thermal comfort as a key parameter with specified numerical values applicable to Sri Lanka in line with ASHRAE standard or any other thermal comfort standards.

According to the objective evaluation minimum humidity is 48% and minimum temperature is 22.4 ^{0}C for case A. This can be the reason for eye irritation and

stuffy nose problems under sick building syndrome category. According to the Sri Lankan usual weather condition outdoor temperature is 30 ^{0}C. And relative humidity is at 70%. In such scenario maintaining (-6) difference inside a building can cause for health issues like running nose, coughing etc.

By comparing PMV according objective measurement and TSV according subjective survey it is found the value of TSV is less than PMV in all cases. This finding is in agreement with adaptive theory that believes people in warm-humid region are adapted to warm weather and can tolerate condition more than people in other climate. Sri Lanka is located in a tropical region in South Asia. Being near the equator, Sri Lanka experiences a warm and humid climate, with constant high temperatures and relative humidity throughout the year. Therefore, people in country like Sri Lanka acclimatize to be in hot or warm weather conditions. In order to maintain indoor environment conditions at a standard level, many building managers, facilities managers are keeping indoor conditions such as temperature and humidity at specified by international standards (ASHRAE). Although those standards are internationally recognized, the applicability of such standards in a country like Sri Lanka is at a confusion level.

For case A, strong linear regression was identified PPD = -0.1554*Temperature + 3.9091 (R^2 =0.982) in between operative temperature and PPD. For case B, strong linear regression was identified PPD = -0.129*Temperature + 3.27 (R^2 = 0.9926).Accordingly it has identified for case A maximum temperature can be raised up to 24.83 ^{0}C with minimum level of dissatisfied occupants (5%). By increasing temperature to that level can lead to saving of Rs. 7493.62. In case B it is 24.96 ^{0}C. And increasing temperature to that level can save Rs. 25,845.96.

Acknowledgement

Special Thanks should goes to my family providing me strength all the time &heartfelt gratitude should goes to Dr. Nayanathara De Silva for her constant support encouragement and valuable guidance provided throughout the period of the research.

References

[1] Frontczak, M., & Wargocki, P. (2011). Literature survey on how different factors influence human comfort in indoor environments. *Building and Environment, 46*, 922 – 937. doi:org/10.1016/j.buildenv.2010.10.021

[2] Huang, L., Zhu, Y., Ouyang, Q., & Cao, B. (2012). A study on the effects of thermal, luminous, and acoustic environments on indoor environmental comfort in offices. *Building and Environment, 49*, 304 - 309. doi:10.1016/j.buildenv.2011.07.022

[3] Hossein, M.M., Jouzi S.E., Elmualim, A.A., Ellis, J., & Williams, M. (2013). Post-occupancy studies of an office environment: Energy performance and occupants' satisfaction. *Building and*

Environment, 69, 121-130. doi:org/10.1016/j.buildenv.2013.08.003

[4] Cui, W., Cao, G., Ouyang, Q., & Zhu, Y. (2013). Influence of dynamic environment with different airflows on human performance. *Building and Environment, 62*, 124 - 132. doi:10.1016/j.buildenv.2013.01.008

[5] Puteh, M., Ibrahim, M. H., Adnan M., Ahmad, C. N. C., & Noh, N. M. (2012). Thermal comfort in classroom: constraints and issues. *Procedia - Social and Behavioral Sciences, 46*, 1834-1838. doi:10.1016/j.sbspro.2012.05.388

[6] Fang, L., Wyon, D. P., Clausen, G., & Fanger, P. O. (2004). Impact of indoor air temperature and humidity in an office on perceived air quality, SBS symptoms and performance. *Indoor Air Quality, 14*, 74-81. doi:10.1111/j.1600-0668.2004.00276.x

[7] Paul, W. L., & Taylor, P. A. (2007). A comparison of occupant comfort and satisfaction between a green building and a conventional building. *Building and Environment, 43*(11), 1858–1870. doi: 10.1016/j.buildenv.2007.11.006

[8] Tom, S. (2008). Managing energy and comfort. *ASHRAE Journal, 8*(1) 18-26. Retrieved from https://www.ashrae.org/File%20Library/docLib/eNewsletter s/tom-062008--feature.pdf

[9] Corgnati, S. P., Filippi, M., & Viazzo, S. (2007). Perception of the thermal environment in high school and university classrooms: Subjective preferences and thermal comfort. *Building and Environment, 42*, 951–959. doi: 10.1016/j.buildenv.2005.10.027

[10] Nematchoua, M. K., Tchinda, R., & Orosa, J. A. (2014). Thermal comfort and energy consumption in modern versus traditional buildings in Cameroon: A questionnaire-based statistical study. *Applied Energy, 114*, 687–699. doi: 10.1016/j.apenergy.2013.10.036

[11] Buratti, C., Ricciardi, P., & Vergoni, M. (2013). HVAC systems testing and check: A simplified model to predict thermal comfort conditions in moderate environments. *Applied Energy, 104*, 117–127. doi: 10.1016/j.apenergy.2012.11.015

[12] Yang, L., Yan, H., & Lam, J. C. (2014). Thermal comfort and building energy consumption implications – A review. *Applied Energy, 115*, 164-173. doi:org/10.1016/j.apenergy.2013.10.062

[13] American Society of Heating, Refrigerating and Air Conditioning Engineers. (2010). Thermal environmental condition for human occupancy (ANSI/ASHRAE Standard 55-2010). Retrieved from http://www.ashraerp.com/files/ASHRAEStandard55-2013.pdf

[14] Buratti, C., Ricciardi, P., & Vergoni, M. (2013). HVAC systems testing and check: A simplified model to predict thermal comfort conditions in moderate environments. *Applied Energy, 104*, 117–127. doi: 10.1016/j.apenergy.2012.11.015

Making Realistic Predictions on Building Energy Performance through Coupled Energy Simulation and Computational Fluid Dynamics

Bandara, R.M.P.S.[1], Attalage, R.A.[2], Fernando, W.C.D.K.[3]
[1]*Department of Mechanical Engineering, General Sir John Kotelawala Defence University*
[2]*Department of Mechanical Engineering, University of Moratuwa*
[3]*Department of Civil Engineering, General Sir John Kotelawala Defence University*
[1]bandara@kdu.ac.lk, [2]dinu@mech.mrt.ac.lk, [3]kumari@kdu.ac.lk

Abstract

Buildings account for nearly 40% of the global energy consumption and hence presently high emphasize is made on improving the energy performance of buildings. Energy Simulation (ES) is the most widely used method in predicting the energy performance of buildings during the conceptual stage. However, it is observed that Energy Simulation tools show certain inherent deficiencies in predicting the energy performance of buildings. The said tools do not have the capacity to model air circulation through the building space explicitly. Energy Simulation tools mainly rely on the simplifying assumption that air within a thermal zone of a building is *well-mixed*. Furthermore, convective heat transfer coefficients of building surfaces are calculated using set empirical correlations. Hence, ES tools often find it difficult to make realistic predictions on energy performance of buildings. The literature also reveals that most Energy Simulation tools under-predict energy consumption in buildings, especially under sunny conditions. On the other hand, Computational Fluid Dynamics (CFD) tools are capable of predicting the indoor flow field comprehensively. However, CFD simulations need to be provided with the corresponding boundary conditions of the computational domain, which are readily available in the Energy Simulation approach. On this basis, the paper explains how Energy Simulation can be coupled with Computational Fluid Dynamics in predicting the energy performance of an actual building design more accurately through complementary data exchange between the tools. The analysis uses *EnergyPlus 8.0* and *Ansys Fluent 6.3* as the tools for conducting Energy Simulation and Computational Fluid Dynamics respectively. *MATLAB R2012a* establishes the coupling platform. The study shows that the coupled scheme predicts considerably higher energy consumption for the building design compared to that given by the conventional Energy Simulation using *EnergyPlus*.

Keywords: Energy Performance, Energy Simulation, Computational Fluid Dynamics

Introduction

Buildings consume nearly 40% of the global energy, 16% of the world's fresh water, 25% of the forest timber while emitting almost 70% of oxides of sulphur and 50% of carbon dioxide gas annually [1]. Hence, presently high emphasize is made in improving the performance of buildings in terms of energy consumption and carbon footprint on the environment.

A building is a complex system with multiple interacting physical processes taking place simultaneously. Performance of buildings can be analysed based on the following criteria:

- Energy performance
- Indoor environment for human comfort and health
- Environmental degradation
- Economic aspects

Energy Simulation (ES) is the most widely used method in predicting the energy performance of buildings during the conceptual stage. This is an approach that analyses thermal aspects, day-lighting, moisture, acoustics, airflow and indoor air quality of buildings [2]. A whole building energy simulation tool can serve this purpose. Energy Simulation is based on the principles of energy and mass conservation. Inputs for the process mainly consists of the building geometry, weather data, Heating, Ventilation and Air Conditioning (HVAC) systems and components, internal loads, operating strategies and schedules and simulation specific parameters. Building geometry is represented in terms of a solid model or Computer Aided Drafting (CAD) format and the building model is divided into multiple thermal zones to facilitate modelling of different components and processes. Properties and characteristics of building materials, glazing and shading aspects also have to be provided as inputs. Internal and external thermal loads provide vital inputs for an energy balance in a thermal zone. External thermal loads are strongly influenced by weather and hence, statistically assembled weather data are used in energy modelling [3]. Weather data files are created for a large number of cities and regions in the world to be used particularly for building performance modelling purposes. Weather files do not represent a specific year, but provide statistical reference for the typical weather parameters of a specific location [3]. Internal loads represent thermal loads due to lighting, occupancy and equipment. The workflow for Energy Simulation is illustrated in Figure 1.

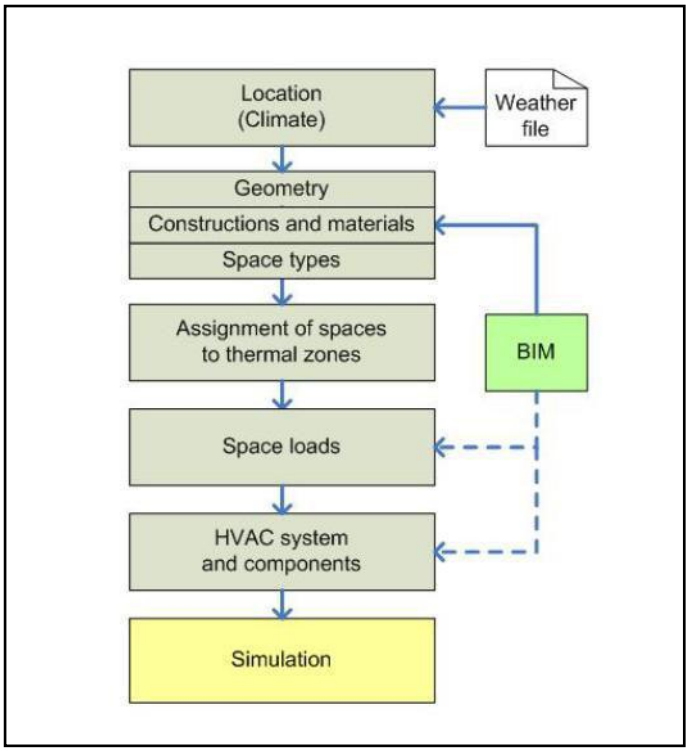

Figure 1: Workflow for Energy Simulation [3]

ES tools are capable of predicting space-averaged indoor conditions, cooling/heating loads and energy consumption etc on an hourly or sub-hourly basis for a particular design day, a specific time period or for a reference year or more.

However, it is observed that Energy Simulation tools show certain inherent deficiencies in predicting the energy performance of buildings. ES tools assume a uniform air temperature within the thermal zone due to the application of the *well-mixed* model. This assumption may be appropriate for small buildings. However, for moderate and large buildings, those typically produce non-uniform air temperature distributions within the occupied space, such as displacement ventilation systems, the said tools cannot accurately predict the energy consumption [4]. Moreover, convective heat transfer coefficients utilized by the Energy Simulation tools are generally determined through set empirical correlations and hence have limited applicability. They are unable to provide information on the airflow field introduced by building spatial configurations especially through natural ventilation [4]. ES tools do not have the capacity to model air circulation through the building space explicitly. Knowledge on the airflow field is vital in predicting

the temperature field of building air and heating and/or cooling load and hence the energy consumption. Also spatially-averaged thermal comfort predictions are not sufficient to satisfy advanced design requirements at present [4]. Hence, ES tools often find it difficult to make realistic predictions on energy performance of buildings. It is observed that many Energy Simulation tools under-predict energy consumption in buildings, especially under sunny conditions [5]. Some studies [6, 7] suggest that this discrepancy of energy consumption may even reach up to 37%.

On the other hand, Computational Fluid Dynamics (CFD) tools can predict airflow paths, velocities, relative humidity and contaminant concentrations within an occupied space of a building extensively and accurately. Also, they are capable of determining the temperature distribution in the building space and convective heat transfer coefficients of the building envelope. The predictions can be further extended to determine thermal comfort indices such as Predicted Mean Vote (PMV), Percentage of People Dissatisfied (PPD) due to discomfort, Percentage Dissatisfied (PD) due to draft and ventilation effectiveness [4]. For CFD, boundary of the solution domain is the inside surface of the building envelope. Hence, it is difficult to predict the corresponding boundary conditions for CFD simulations since they depend on many parameters such as construction details of the building envelope, outside weather conditions etc. However, this information is readily available with ES tools.

On this basis, it is clear that if Energy Simulation and Computational Fluid Dynamics are coupled, more accurate predictions for building energy consumption can be made through complementary data exchange between the said tools. On this basis, the paper explains how Energy Simulation can be coupled with Computational Fluid Dynamics in predicting the energy performance of an actual building design to be constructed in Ratmalana more accurately.

Governing Principles

Energy balance equations for building zone air and surface heat transfer are two essential equations that an ES tool should solve [4]. The energy balance equation for building air is in the form [4]:

$$\sum_{i=1}^{N} q_{i,c} A_i + Q_{\text{other}} - Q_{\text{heat\_extraction}} = \frac{\rho V_{\text{building}} C_p \Delta T}{\Delta t} \qquad \text{Eq.1}$$

where

$\sum_{i=1}^{N} q_{i,c} A_i$ - Convective heat transfer from enclosure surfaces to building air

$q_{i,c}$ - Convective flux from surface i

N - Number of enclosure surfaces

A_i - Area of surface i

Q_{other} - Heat gains from lighting, occupants, appliances, infiltration etc.

$Q_{heat\_extraction}$ - Heat extraction rate of the building

$\frac{\rho V_{building} C_p \Delta T}{\Delta t}$ - Rate of change of energy in building air

ρ - Air density

$V_{building}$ - Volume of building

C_p - Specific heat capacity of air

ΔT - Change of building air temperature

Δt - Sampling time interval

When the building air temperature is kept constant (ΔT = 0) heat extraction rate is equal to the cooling and/or heating load.

The convective heat fluxes are determined from the energy balance equations for the corresponding surfaces as shown in Figure 2.

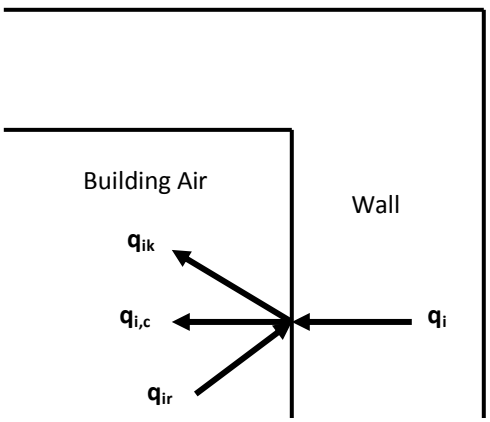

Figure 2: Energy balance of a surface in a building [4]

A similar energy balance is performed for each surface.

The surface energy balance equation can be written as [4]:

$$q_i + q_{ir} = \sum_{k=1}^{N} q_{ik} + q_{i,c} \quad \text{Eq.2}$$

where

q_i - Conductive heat flux on surface i

q_{ir} - Radiative heat flux from internal heat sources and solar radiation

q_{ik} - Radiative heat flux from surface i to surface k

q_{ic} - Convective heat flux from surface i

q_i can be determined by transfer functions or by solving the discretized heat conduction equations of the surfaces using finite difference schemes.

Convective heat flux is determined by [4]:

$$q_{i,c} = h_c \left(T_i - T_{\text{building}}\right) \quad \text{Eq.3}$$

where

h_c - Convective heat transfer coefficient

$T_{building}$ - Building air temperature

T_i - Building internal surface temperature

The convective heat transfer coefficient, h_c is not known. ES tools such as *EnergyPlus* estimate h_c by empirical equations or taken as constants.

The simple natural convection model uses constant coefficients for different configurations as given in Table 1.

Table 1: Simple natural convection model [8]

Configuration	h_c (W/m^{2}K)
Horizontal surface with reduced convection	0.95
Horizontal surface with enhanced convection	4.04
Vertical surface	3.08
Tilted surface with reduced convection	2.28
Tilted surface with enhanced convection	3.87

The detailed natural convection model in *EnergyPlus* correlates the convective heat transfer coefficient (h_c) to the surface orientation and the temperature difference between the surface and zone air (ΔT) as follows [8]:

- If ΔT = 0 or a vertical surface, then

$$h_c = 1.31\|\Delta T\|^{1/3} \quad \text{Eq.4}$$

- If ΔT < 0 with an upward facing surface or ΔT > 0 with an downward facing surface, then

$$h_c = \frac{9.482\|\Delta T\|^{1/3}}{7.283 - \|\cos \Sigma\|} \quad \text{Eq.5}$$

where Σ is the surface tilt angle.

- If ΔT > 0 with an upward facing surface or ΔT < 0 with an downward facing surface, then

$$h_c = \frac{1.810\|\Delta T\|^{1/3}}{1.382 - \|\cos \Sigma\|} \quad \text{Eq.6}$$

The ceiling diffuser model in *EnergyPlus* correlates convective heat transfer coefficient to the supply mass flow rate (ACH) as shown in Table 2.

Table 2: Ceiling Diffuser model [8]

Building Element	h_c (W/m^{2}K)
Floors	$3.873+0.082(ACH)^{0.980}$
Ceiling	$2.234+4.099(ACH)^{0.503}$
Walls	$1.208+1.012(ACH)^{0.604}$

If the building air temperature, $T_{building}$, is assumed to be uniform and known, the interior surface temperatures, T_i, is determined by simultaneously solving the surface heat balance equation (2). Building thermal load is then calculated from the convective heat transfer from enclosure surfaces using equation (1)

In Computational Fluid Dynamics numerical techniques are applied for solving Navier-Stokes equations for fluid flow and heat transfer. Navier-Stokes equations are derived through the application of the conservation laws of mass (continuity), momentum and energy (first law of thermodynamics) to a control volume of a fluid. In addition to the aforementioned basic set of governing equations, different models such as turbulence, radiation, combustion etc. may be incorporated depending on the problem being handled. The general form of the governing equations takes the following form [4]:

$$\frac{\partial \phi}{\partial t} + (\boldsymbol{V} \cdot \boldsymbol{\nabla})\,\phi - \Gamma_\phi \nabla^2 \phi = S_\phi$$

Eq.7

where

t - Time

ϕ - General transport variable

V - Velocity vector

Γ_ϕ - Diffusion coefficient

S_ϕ - Source term

The governing equations in CFD are highly non-linear in nature. Hence, they are solved by discretizing the equations using finite volume methods converting them to a set of algebraic equations. The spatial domain is divided into a finite number of discrete cells (or nodes) creating a computational mesh of acceptable resolution. Appropriate boundary conditions are assigned for the computational domain depending on the problem being handled. All transport equations are solved at each node point of the mesh at each time step through an iterative process until the solution meets a preset convergence criterion.

The accuracy of the CFD solution is highly sensitive to the boundary conditions assigned for the domain. Hence, in modelling indoor flows in buildings, boundary conditions related to air supply, air exhaust, envelope surfaces and internal objects highly influence the CFD solution. On this basis, supply air temperature, velocity and level of turbulence comprise the inlet boundary conditions. The interior surface temperatures and/or heat fluxes of the

building envelope establishes the vital thermal boundary conditions for the problem.

Coupling Strategy

Many attempts have been made for coupling Energy Simulation and Computational Fluid Dynamics tools mainly since 1990. Negrao [9] performed a complete iterative coupling between ES and CFD. A full iterative strategy was implemented, where coupled variables were exchanged at each iterative step until a convergence criterion was reached at each time step. Beausoleil-Morrison [10, 11, 12] continued the work of Negrao [9, 13] with the investigation of the coupling between ES and CFD. A conflation controller was established to configure the CFD model at each time step.

Bartak et al. [14] conducted an empirical validation of the coupled model of Beausoleil-Morrison [11]. Djunaedy et al. [15, 16], Chen et al. [17] and Zhai et al. [4] analysed the pros and cons of internal coupling of the ES and CFD. Zhai et al. [18, 19, 20] investigated the different coupling strategies extensively. Their results revealed that for rooms of moderate size, without significant temperature stratification, coupling of ES and CFD gives marginal improvement in energy performance predictions. However, those with large temperature stratification, the discrepancy between the coupled approach and ES alone can be as high as 42%. Wang [21] and Wang and Chen [22] proved that the combined ES and CFD approach has a unique solution. Wang and Wong [23] developed a text-based interface for automated coupling for exchanging information between TAS (ES tool) and Fluent (CFD tool). According to Djunaedy [24], coupling between ES and CFD is categorized as follows:

- Internal coupling (Hard coupling) - Two or more sets of equations are combined and solved at the same time (Conjugate heat transfer method)
- Internal coupling (Loose coupling) - Two or more sets of equations are solved separately, and exchange data during calculation
- External coupling (Loose coupling) - Two or more set of equations solved separately, in ES and CFD programs, and exchange data during calculation

The application of the conjugate heat transfer approach has several disadvantages. The difference in stiffness of the fluid and the solid side of the model leads to difficulties in obtaining a converged solution [25]. It is computationally expensive since the computing time increases drastically due to the difference in the time scale related to dynamics in fluids (few seconds) and dynamics in solids (few hours) encountered in buildings [4]. Although Internal coupling (Loose coupling) solves some of the issues in the first method, internal coupling approach

as a whole is a computationally expensive approach [24].

Benefits of external coupling include [26]:

- Computationally less expensive
- ES and CFD models can be maintained and updated individually

Moreover, building simulation research [27] reveals that the difference in results between internal and external coupling is not significant.

Methodology and Approach

EnergyPlus [28] v. 8.0 is used as the ES tool during present work. It is a new generation building energy modelling tool based on *DOE* (U.S. Department of Energy) – *2* and *BLAST* (Building Loads Analysis and System Thermodynamics), with numerous capabilities and was first released in 2001. It can model heating, cooling, lighting, ventilation, other energy flows, water usage etc. in buildings and includes many innovative simulation capabilities [28]. *Ansys Fluent* v. 6.3 [29] is used as the CFD tool for the study. *Fluent* is one of the most widely used and extensively validated software available for flow modelling. It is capable of modelling turbulence, heat and mass transfer, combustion, multi-phase flow etc. *MATLAB* R2012a forms the coupling platform for ES and CFD tools. It is a high-level language and interactive environment for numerical computation, visualization, and programming [30]. *MATLAB* utilizes a comprehensive collection of toolboxes that extend its potential to solve a variety of problems.

The L-shape single-storey office building under consideration has overall dimensions 14.0 m x 12.0 m x 2.7 m. ES computational model of the building was created using *Google SketchUp* v. 8.0 with *OpenStudio* plug-in v. 1.0.7 and is shown in Figure 3. It consists of two thermal zones. The ES computational model of the building is generated using inputs through both *Google SketchUp* and *IDF Editor* of *EnergyPlus*. Weather information was incorporated to the model through the .epw file available for Ratmalana area. Tables 3 and 4 give the details of thermal and electrical loads and construction details of the building respectively.

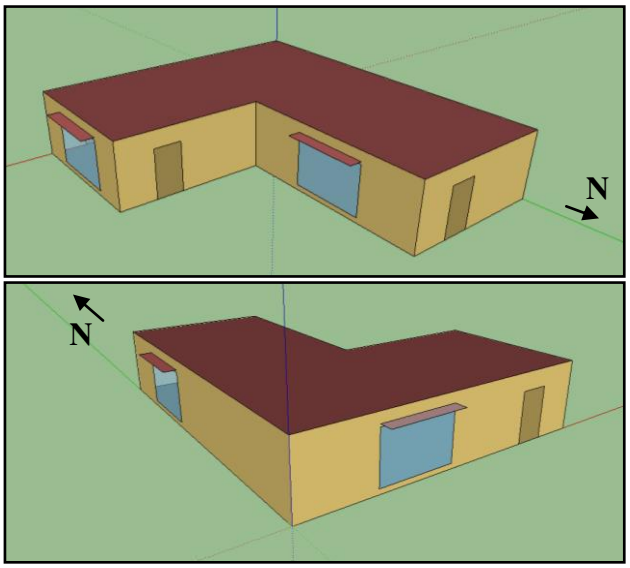

Figure 3: Computational model of office building for energy simulation

Table 3: Thermal and electrical loads of the building

Load / System	Rating and Description
Occupancy	20 nos. of occupants involved in general office work with the specified occupancy schedule.
HVAC system	Temperature control through dual set point, where 20 ^{0}C for heating and 24 ^{0}C for cooling effective from 7.00 to 19.00 hrs. Maximum indoor air velocity is 0.2 ms^{-1}.
Artificial lighting	200 W
Electrical equipment rating	750 W
Building lighting control mechanism	Continuously dims artificial lights to match an illumination set point of 400 lx at two reference points at a working plane of 0.8 m above the floor level, with the variation of day light.

Table 4: Construction details of the building

Element	Construction Details
Walls	9” thick standard brickwork
Flat Roof	150 mm thick reinforced concrete slab
Floor	10 mm thick ceramic tiles on a 150 mm thick reinforced concrete slab
Doors	Each of 1.1 m x 2.0 m, made of plywood
East Windows	02 nos. of 3.0 m x 2.0 m double pane windows with 4 mm thick glass and 2 mm thick air space. There exists 0.2 m of wall below the windows and 0.5 m of wall above the windows. The edge of the two windows is located 1.5 m and 2.5 m from the corresponding wall edges respectively.
West Window	3.0 m x 2.0 m double pane window with 4 mm thick glass and 2 mm thick air space. There exists 0.2 m of wall below the window and 0.5 m of wall above the window. Edge of the window is located 2.5 m from the corresponding wall edge.
South Window	3.0 m x 2.0 m double pane window with 4 mm thick glass and 2 mm thick air space. There exists 0.2 m of wall below the window and 0.5 m of wall above the window. Edge of the window is located 3.0 m from the corresponding wall edge.
Shading overhangs on all windows	Depth 0.5 m with 0.1 m height above the window. Tilt angle is 90^0.

The CFD model of the building was created using the solid modelling software *GAMBIT* v. 2.2 [31] and is shown in Figure 4. It consists of 405,502 tetrahedral/hybrid mesh volumes in the computational domain. Separate boundary meshes were created for each solid surface of the building.

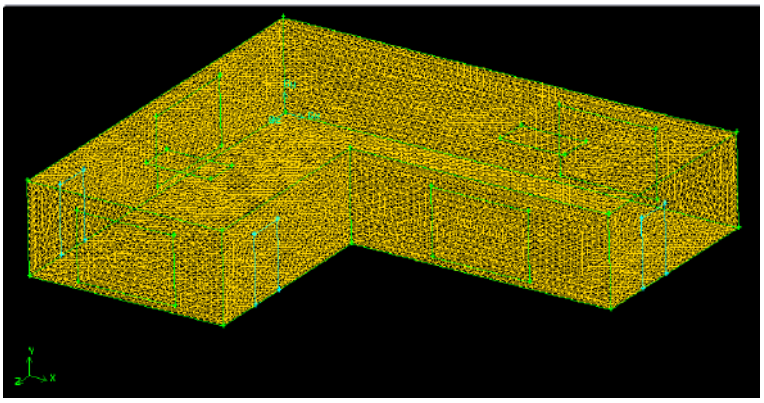

Figure 4: Computational model for CFD

The *k-ε RNG* turbulence model and *QUICK* discretization scheme have been used in the CFD model. Enhanced wall treatment methodology was applied in

order to take care of the boundary layer interactions at the solid surfaces of the building. Pressure-velocity coupling was adopted to improve convergence of the solution.

Simulation Setup

External coupling (Loose coupling) approach is adopted for combining ES and CFD on *MATLAB* platform in the present study. Hence, individual simulation tools achieve the status of convergence before exchanging the variables between them. Internal surface temperatures of the building (T_w) generated by *EnergyPlus* and surface convective heat transfer coefficients (h_c) predicted by *Ansys Fluent* are the exchange variables for the coupled simulation. Workflow of the coupled simulation is shown in Figure 5. Since execution of the coupled simulation to predict energy consumption of the building is highly computationally expensive, simulations are conducted only for the following cases with time step for complementary data exchange taken as 1 hour:

- Case 1 - Day recording the maximum dry bulb temperature
- Case 2 - Day recording the minimum dry bulb temperature

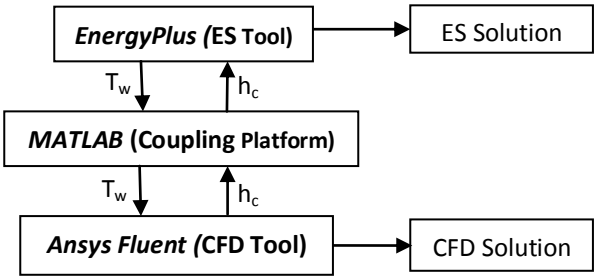

Figure 5: Workflow of coupled simulation

Simulation Results:

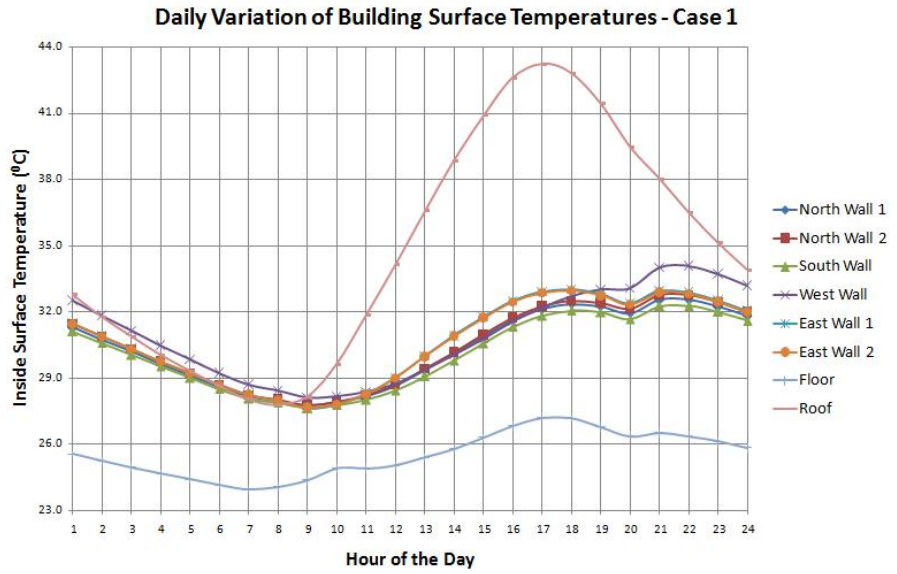

Figure 6: Daily variation of inside surface temperatures of the building – Case 1

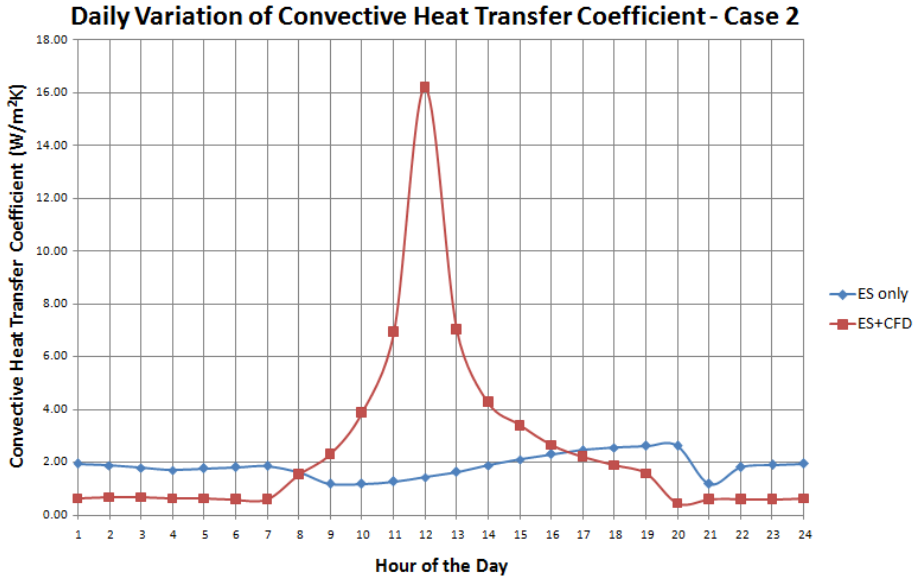

Figure 7: Daily variation of the south wall convective heat transfer coefficient related to ES and coupled approach – Case 2

The coupled ES and CFD simulations were run on an Intel Core i5 3.2 GHz workstation of 4.0 GB RAM. It took 6 hours and 10 minutes for each coupled simulation to complete. Figure 6 illustrates the daily variation of inside surface temperatures of the building predicted by *Energy Plus* for Case 1. Figure 7 shows the daily variation of the south wall convective heat transfer coefficient related to ES and coupled approach for Case 2. Figure 8 illustrates the velocity fields at the air supply and discharge port mid-planes of the building predicted by the CFD tool.

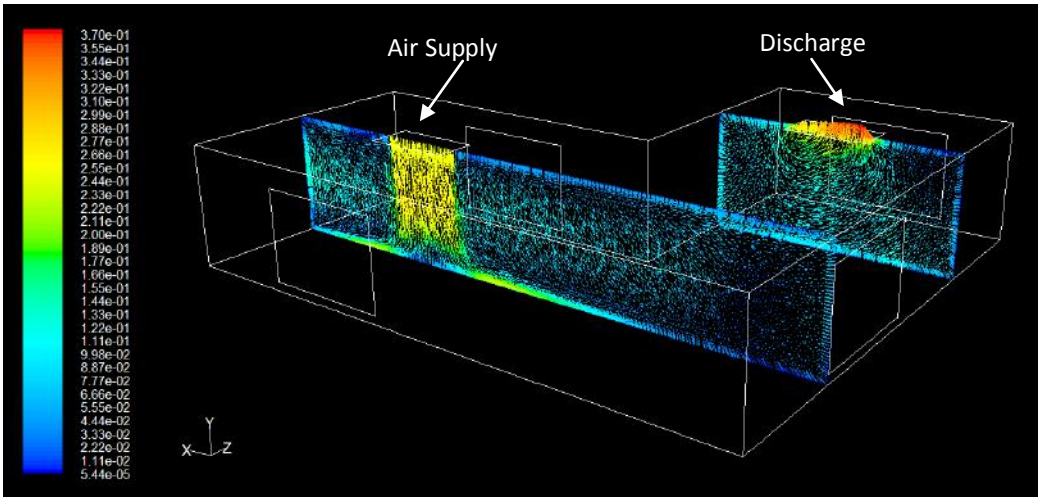

Figure 8: Velocity fields at the air supply and discharge port mid-planes

Table 5 gives a comparison of building energy consumption related to the two approaches for Cases 1 and 2.

Table 5: Building energy consumption

Case	Energy Consumption (MJ)		Discrepancy	
	ES only	ES + CFD	Value (MJ)	(%)
1	392.36	480.12	87.76	22.4
2	256.30	328.46	72.16	28.2

According to Table 5, it is observed that Case 1 and Case 2 report a discrepancy of 22.4% and 28.2% respectively. In the proposed model, the respective convective heat transfer coefficients were calculated based on the temperature of a point located just outside the thermal boundary layer of the corresponding surface of the building. Hence, the value of the convective heat transfer coefficient is strongly dependent on the location of this point. Also, the influence due to movement of occupancy was not considered during the analysis.

Conclusion

The study considered only two cases for the analysis since it is not feasible to

perform the coupled simulation for the entire 365 days of the year due to the high computational cost involved. It is seen that for both cases (this is the sample) considered, the discrepancy related to energy consumption between ES and coupled approach is significant. This is in good agreement with the previous studies conducted by different researchers. Hence, it is reasonable to expect that the same trend prevails for the entire year (this is the population). However, this needs to be further justified through an appropriate statistical approach. It is essential to analyse whether similar results are obtained for different air supply configurations of the building. Furthermore, validation of the model needs to be conducted through appropriate measurements. This will be the next step of the present effort.

References

[1] Ghiaus C, Inard C. Energy and environmental issues of smart buildings, A Handbook for Intelligent Building, 26-51. [Online]. Available: http://www.ibuilding.gr/handbook/

[2] Mumovic D, Santamouris M. A Handbook of Sustainable Building Design and Engineering: An Integrated Approach to Energy, Health and Operational Performance, Earthscan, 2009.

[3] Maile T, Fischer M, Bazjanac V. Building Energy Performance Simulation Tools: A Life-Cycle and Interoperable Perspective, Stanford University, 2007.

[4] Z. Zhai, Q. Chen, "Strategies for Coupling Energy Simulation and Computational Fluid Dynamics Programs", in *Proc. 7th International IBPSA Conference*, Rio de Janeiro, August 13-15, 2001.

[5] Loutzenhiser PG et al. An empirical validation of window solar gain models and the associated interactions, International Journal of Thermal Sciences 2009:48:85–95.

[6] Spitler JD. Pedersen CO, Fisher DE. Interior Convective Heat Transfer in Buildings with Large Ventilative Flow Rates. ASHRAE Transactions 1991:97:505-515.

[7] Lomas KJ. The U.K. applicability study: an evaluation of thermal simulation programs for passive solar house design. Building and Environment 1996:31-3:197-206.

[8] *EnergyPlus* Engineering Reference, University of Illinois & Ernest Orlando Lawrence Berkeley National Laboratory, September 2014.

[9] Negrao COR. Conflation of Computational Fluid Dynamics and Building Thermal Simulation, *PhD Thesis*, University of Strathclyde, 1995.

[10] I. Beausoleil-Morrison, J.A. Clarke, "The implications of using the standard k-ε turbulence model to simulate room air flows which are not fully turbulent", in *Proc.* ROOMVENT, 1998, pp. 99-106.

[11] Beausoleil-Morrison I. The Adaptive Coupling of Heat and Air Flow Modelling Within Dynamic Whole-Building Simulation, PhD Thesis, Energy Systems Research Unit, Department of

Mechanical Engineering, University of Strathclyde, Glasgow, UK, 2000.

[12] I. Beausoleil-Morrison, J. A. Clarke, J. A. Denev, A. Melikov & P. Stankov, "Further developments in the conflation of CFD and building simulation", in *Proc. 7th International IBPSA Conference*, Rio de Janeiro, Brazil, 2001, pp. 1267-1274.

[13] Negrao COR. Integration of Computational Fluid Dynamics with building thermal and mass flow simulation. Energy and Buildings 1998: 27:155-165.

[14] Bartak M et al. Integrating CFD and Building Simulation, Building and Environment 2002:37:865-871.

[15] Djunaedy E, Hensen JLM, Loomans MGLC. Towards external coupling of building energy and airflow modelling programs. ASHRAE Transactions 2003:109-2:771-787.

[16] Djunaedy E, Hensen JLM, Loomans MGLC. Selecting an appropriate tool for airflow simulation in buildings. Building Services Engineering Research and Technology 2004:25-3:289-298.

[17] Chen Q, Peng X, Van Passen AHC. Prediction of room thermal response by CFD technique with conjugate heat transfer and radiation models. ASHRAE Transactions 2003:101:50-60.

[18] Zhai Z et al. On approaches to couple energy simulation and computational fluid dynamics programs. Building and Environment 2002:37-8:857-864.

[19] Zhai Z et al. Solution characters of iterative coupling between energy simulation and CFD programs. Energy and Buildings 2003:35-5:493-505.

[20] Z. Zhai et al, "Pressure boundary conditions in a multi-zone and CFD program coupling", in *Proc. 1st IBPSA-USA Conference*, Boulder, Colorado, USA, 2004.

[21] Wang L. Coupling of multi-zone and CFD programs for building airflow distribution and contaminant transport simulations, PhD Thesis, Purdue University, 2007.

[22] L.Z. Wang, Q.Y. Chen, "On solution characteristics of coupling of multi-zone and CFD programs in building air distribution simulation", in *Proc. 9th International IBPSA Conference*, Montreal, Canada, August, 2005.

[23] Wang L, Wong NH. Coupled simulations for naturally ventilated residential buildings. Automation in Construction 2008:17:386-398.

[24] Djunaedy E. External coupling between building energy simulation and computational fluid dynamics, PhD Thesis, The Eindhoven University of Technology, Netherlands, 2005.

[25] Chen Q, Peng X, Paassen AHCV. Prediction of room thermal response by CFD technique with conjugate heat transfer and radiation models. ASHRAE Transactions 1995:101-2:50-60.

[26] Zhang R, Lam KP, Yao S, Zhang Y. Coupled *EnergyPlus* and computational fluid dynamics simulation for natural ventilation. Building and Environment 2013:68:100 -113.

[27] E. Djunaedy, J.L.M. Hensen & M.G.L.C. Loomans, "Comparing internal and external run time coupling of CFD and building energy simulation software", in *Proc. 9th ROOMVENT*

International Conference on Air Distribution in Rooms, Coimbra, 2004, pp. 393 -396.
[28] Crawley D et al. *EnergyPlus*: creating a new-generation building energy simulation program. Energy and Buildings 2001:33:319-331.
[29] *Ansys Fluent* v. 6.3, Fluent Inc., 2006.
[30] The MathWorks, *MATLAB* program v. 2012b. Natick, MA: The MathWorks, Inc., 2012.
[31] *GAMBIT* v. 2.2, Fluent Inc., 2006.

Present situation and future energy usage in government sector offices

Maldeniya P.S., Sakaraja S.J.R.J., Elvitigala S.J., Ekanayake W.M.V.
Sri Lanka Sustainable Energy Authority

Abstract

Government sector is one of the largest employers in Sri Lanka. One fifteenth of Sri Lankan is a government employee in Sri Lanka. Out of the total government workforce larger share works in office environments, with typical pattern of energy use and typical set of equipment's. Although circulars are in place to curb the energy use, lack of sense of belongingness has made energy wastage considerably high in government sector office buildings. Since the budget spent by the government improvement of office environment has been increasing, it possible to reduce energy usage through replacement of older inefficient systems with newer more efficient ones. And there is potential for reduction of energy wastage through increasing employee awareness. In considering above factors present situation and future forecast for productive government sector are discussed in this research paper.

Key words: Government, Energy audit, Specific energy consumption

Introduction

According to the report of labour statistics published in 2014 state sector employees in Sri Lanka are 1,330,456 [1]. State sector includes Ministries, Departments and other Institutions under the Central Government, all the Institutions under provincial councils included in public sectors, and Semi-government sector includes corporations, statutory boards, authorities and public-private bilateral companies. The figure excludes labourers of state owned estates and active members of armed forces. This figure is a dramatic increase when compared to year 2006, where the number is 835,798. Of this number, large numbers of employees work in offices. Total annual electrical energy usage in Sri Lanka is 11063 GWh [2], and due to the large number of employment considerable percentage of energy usage is by government sector offices. In light of the energy crisis faced by Sri Lanka, government has taken steps to control the energy usage in government sector offices issuing circular SP/CS/30/12, with several measures to curb the energy usage and insisting the appointment of energy management officers to government sector office. But due to various factors discussed in following sections still there exists considerable saving potential in most of the offices in certain areas, while the lighting level has to be increased to meet the standards.

Methodology

Sri Lanka Sustainable Energy Authority (SLSEA) and other Energy Service Companies (ESCOs) have conducted several energy audits during the period 2014-2015. Seven detailed energy audits were conducted by SLSEA. Four audits conducted by ESCOs which employs at least one accredited energy auditor was also chosen for the study. Serial Nos. 1-7 corresponds to the Kandy district offices and 8-11 corresponding to Colombo district offices. Following information was analyzed to estimate the present energy usage and improvement strategies.

1. Basic data (floor area, number of employees, and energy bills)
2. Record of statistical information obtained from the energy audits (list of equipment and usage hours) or the energy balance when such information is not available
3. Actual measured energy consumption data of the equipment
4. Other measurements such as illuminance
5. Load profiles presented in the reports
6. Energy saving potentials and Recommendations given in the reports

Specific energy consumption and energy balance

Electrical energy is the main source of energy. In organization 8 and 10, 4% and
2% of electricity has been generated by the backup diesel generators. The specific energy consumption was analyzed per floor area basis and per employee basis and is presented in Figure 01 and Figure 02. Comparison between the organizations was not possible as percentage of air conditioned area of each office was different. The minimum percentage was 0 and maximum was 81%. Weighted average specific energy consumption per employee is 54 kWh/ month and on floor area basis 3.7 kWh/m^2/month. Specific energy consumption value (3.7 kWh/m^2/month) obtained in this audits is well lower than benchmark value of 136.55 kWh/m^2/year (11.4 kWh/m^2/month) for commercial buildings according to Energy Consumption Benchmark Analysis of SLSEA [4].

Table 1: The basic information

No.	kWh (monthly)	Number of employees	Floor area (m2)	AC floor area percentage	Tariff category
1	615	42	335	28%	GP1
2	525	32	612	0%	GP1
3	4500	131	2313	11%	GP1
4	1640	71	696	20%	GP1
5	1150	50	645	29%	GP1
6	2050	138	1547	4%	GP1
7	933	50	844	43%	GP1
8	9250	26	435	81%	GP2
9	28676	550	5426	60%	GP2
10	20160	181	5574	24%	GP2
11	2316	67	970	25%	GP2
Total	71815	1338	19396		

Energy Balance

The energy balance shown indicate that for Kandy district government offices computers are the most significant load with 30.6% of energy consumption was for computing. Air conditioning (27.6%) and lighting (20.6%) are other major loads. The Colombo district case is slightly different. The major loads are the same but the percentages are different. Here air conditioning load is 51.1% while computers and other office equipment contribute to 19.7% while lighting

accounted for 13.7%. The energy balances for both districts are presented in Figure 1.

Table 2: The cumulative energy balance for Kandy district offices

Equipment type	Energy (kWh/month)	Percentage
Air conditioners	3120	27.3
Computers (monitor, cpu,ups)	3491	30.6
Lighting	2305	20.2
Kettles	1020	8.9
Fans	796	7
Printers,fax,photocopy,scanners etc.	323	2.8
Other equipment (refrigerators,televisions etc.)	359	3.1
Total	11414	100.0

Table 3: Cumulative energy balance for Colombo district offices

Equipment type	Energy (kWh/month)	Percentage
AC	30875	51.1
Lighting	8303	13.7
Office equipment	11909	19.7
Kettles ,water dispensers	1644	2.7
Fans	5357	8.9
Other	2314	3.8
Total	60402	100.0

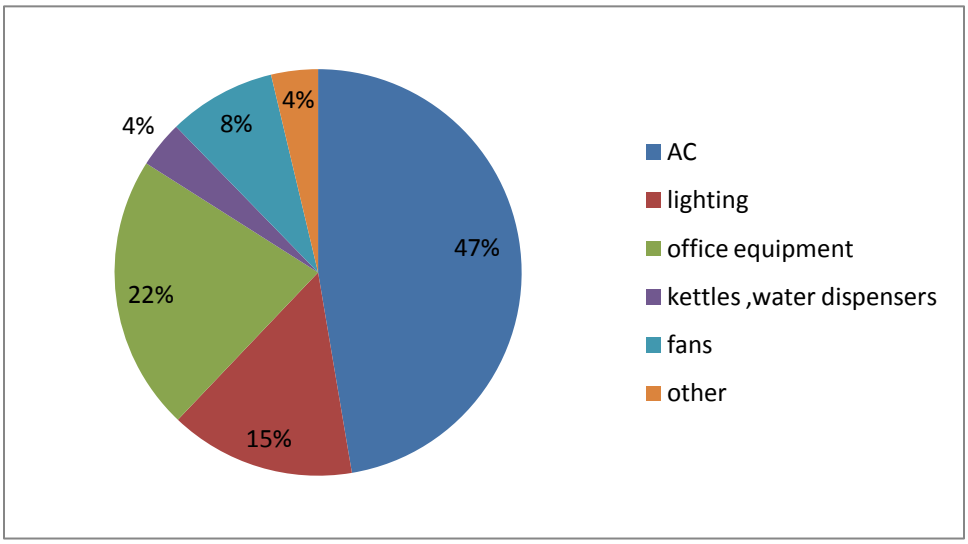

Figure 01: Cumulative energy balance

Daily load curve

In most of the audits load variations for one week was studied, with typical nearly flat working hour load was observed for week days. Figure 2 shows such a daily load curve. It is important to note that the night time load is significantly higher than that was predicted by using data provided by the organizations. This was observed in the daily load curve of the office with significant energy use.

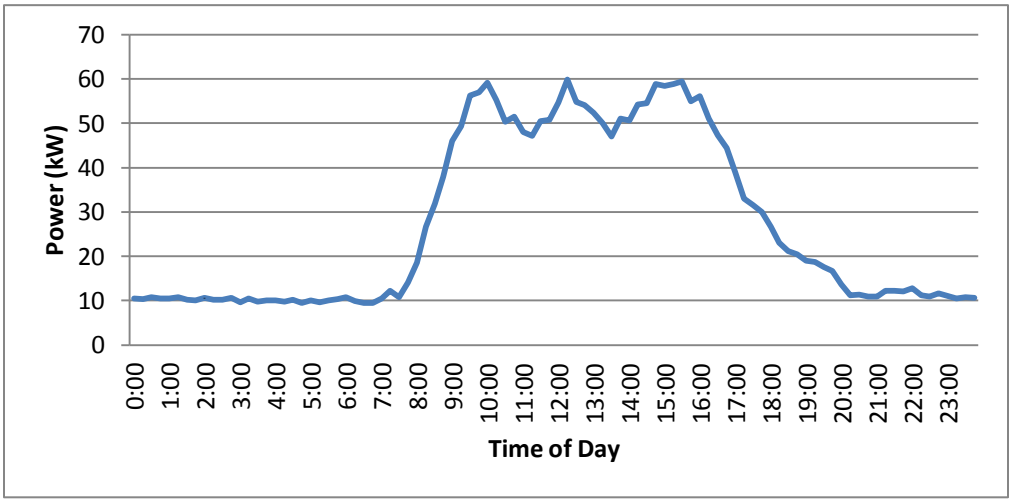

Figure 2: Typical daily load profile of an office building

Major findings

Night time load

Especially in large organizations considerable night time and non working day load is present. This is attributed to employees not turning off the equipment after they leave the office. Relevant details are given in Table 4. Per employee loss in this way is estimated to be about 8 kWh/month.

Table 4: Estimation of loss due to night non working time loads

No	Non working hour load (W)	Number of employees	Monthly energy loss (kWh)
1	negligible	42	negligible
2	negligible	32	negligible
3	1500	131	840
4	400	71	224
5	50	50	28
6	800	138	448
7	negligible	50	negligible
9	6000	550	3360
10	10000	181	5600
11	negligible	67	negligible
∑		1312	10500

Air conditioning

Air conditioning is the major load in the Colombo district government offices and second major load in Kandy district government offices (central provincial council offices). In all of the audited organizations split type air conditioners had been installed. The average efficiency (kW/Ton value) of air conditioners was 1.23. Arbitrary sizing of air conditioners is another problem to be found. Table 5 presents the average sizing for 3 categories of rooms found. As per our studies, If the solar heat gain through glasses can be controlled. Roughly 60 BTU/hr/sqft is sufficient for a general office, with less solar heat gain. However for a conference room the load is heavily dependent on the number of occupants, so under sizing and over sizing is evident.

Table 5: Present air conditioning sizing

Location	BTU/hr/Sqft
Managers room	85
General office	83.5
Conference room/meeting room	87.6

Wastage in electrical energy due to improper partitioning and re-partitioning was observed in two offices. Replacement of the air conditioners with low COP value with inverter type air conditioners, servicing of air conditioners, proper partitioning were the steps suggested in reducing the air conditioning load.

Computers and UPS

Computer load has increased due to the increased use, but due to the improvements in technology the energy efficiency has significantly improved. Figure 4 indicates the decrease of computer power according to the year of manufacture. At present with LED backlit technology, the computer consumes about 40-60 W, while the power for CPU has not changed in such manner. Average power value found for the CRT monitor was 64 W. For a LCD monitor it was 21 W and for a LED monitor it was 11 W. average power for a computer was 74 W Summary of power details of computer measurements are mentioned in table 5. The CPU power corresponding to CRT and LCD monitors is roughly same of about 55 W; However CPUs tend to break down more often so the CPUs for CRTs may have been replaced with new ones, which could not be verified during the survey. Largest share of monitors were LCD type which was 75% of total in Kandy district offices while LED monitors was 15.5% and CRT monitors were 9.5%. For the western province percentage of CRT monitors observed was 5%. LCD and LED monitors were 82% and 13% respectively.

Table 6: comparison of desktop computer types

Technology	Screen size (inches)	Year of manufacture	Average power (W)	Corresponding CPU power (W)
CRT	14-17	2002-2007	64	54
LCD	15-20.5	2006-2013	21	55
LED	15.6-19	2011-2014	11	36

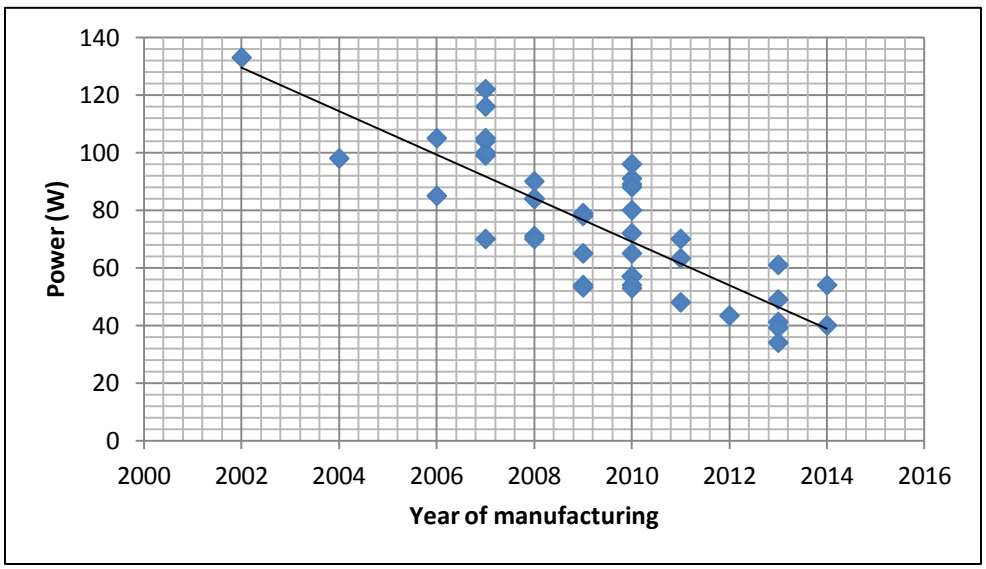

Figure 4: Decrease of computing power according to year of manufacture

UPS was major source of energy loss in most of the organizations and generally 650-700 VA capacity UPS are used to supply backup power. Available brands consumed 13-25 W. Most common types consumed about 18 W in average. Larger UPS found in some offices consumed about 30 W. Replacement of CRTs with LED monitors, use of standby mode, replacement of larger UPS with smaller UPS were the suggestions given in audit reports.

Lighting

Although lighting is a considerable load, in most offices the illuminance level (lux level) was not up to the standards. In 3 offices the illuminance level had been measured and found to be around 100 lux, which is well below the recommended value according to most standards. Fluorescent tube lamps and CFLs were the main source of lighting, with only small number of lamps were incandescent lamps. Lighting power densities (installed) are far below the maximum allowed value of 10.8 W/m^2 [3]. Out of 11 in 10 offices the lighting power density is below 5W/m^2. Fluorescent lamps were the main source of lighting with 72% of lighting power installed. CFLs accounted for about 18%, while LED penetration was about 7%. Incandescent and mercury lamps were found to be of negligible value. Detailed values are presented in Table 7 and 8.

Table 7: Lighting power densities and illuminance

Organization	LPD installed (W/m2)	LPD used (W/m2)	Average illuminance level (lux)
1	1.43	1.43	100
2	1.87	1.75	106
3	4.84	4.19	
4	5.15	4.00	
5	4.40	3.51	
6	1.18	0.64	112
7	8.31	2.65	
8	10.54	9.63	170
9	2.69	2.69	
10	3.42	2.93	
11	1.56	1.41	

Energy saving options in lighting is mostly seen in replacement of magnetic ballasts and in some cases incandescent lamps with CFLs. Options for replacement with LEDs are also suggested but due to high cost of replacement these is less likely to be implemented.

Table 8: Installed lighting power percentages based on technology

	CFL	Fluorescent	LED	Incandescent	Mercury
Kandy	15.5	80.9	0.0	3.6	0.0
Colombo	20.2	65.6	12.3	0.6	1.3
Total	18.3	71.9	7.2	1.9	0.7

Printers, Photocopy, Fax machines and other similar equipment

This is not found to be a significant load of the offices studied. However some old dot matrix printers consumed about 15W in standby mode. Other printers used less than 10 W in standby mode .The average value is 7 W. Fax machines used 3 W in standby mode. Photocopy machines used about 20W in standby mode.

Prediction of future energy usage in a more productive and efficient environment

By considering the technology improvements in the most important loads Viz. Air conditioning, lighting and computers and awareness creation following estimate for productive and most efficient office environment is calculated. For Air conditioning inverter type air conditioners with Specific energy consumption of 0.95 kW/ton is assumed, whereas the present average is 1.23 kW/Ton. Lighting level has been increased up to 10 W/m^2 and hence the lighting load. Replacement of computers with LED technology is assumed with improvement from 71W present average to 47 W for LED. Since in section 4.1, it was found that 8 kWh were lost per employee due to negligence at present for an specific energy consumption of 54 kWh/month, factor of 46/54 has also been used to get rid of the energy lost due to employee negligence. After that A/C load was corrected to the increased other loads. The final predicted energy consumption values for the offices selected are presented in Table 9. The predicted energy consumption is higher than the present value with Specific energy consumption of 49.2 kWh/m^2/year.

Table 9: Comparison between present and improved office environment

Equipment type	Present energy consumption (kWh/month)	Predicted energy consumption (kWh/month)
AC	33,995	29,551
Lighting	10,608	30,720
Office equipment	15,723	9,463
Kettles ,water dispensers etc.	2,664	2,269
Fans	6,153	5,242
Other	2,673	2,277
Total	71,816	79,521

Discussion

In most government organizations a common set of problems related to energy use are found. Except for lighting, in other areas energy efficiency can be improved. The existing lighting levels have to be increased and the efficiency can be improved by technologies such as efficient fluorescent lamps. The air conditioning load can be reduced by 25% by replacing with newer efficient systems. Proper sizing of air conditioners is important in reducing the air conditioning load however due to inadequate data the reduction in that respect cannot be calculated. Computing power will continue to decrease as the presently used once are aged. Slightly higher energy consumption level can be maintained with more productive environment with the improvements discussed in the paper.

References

[1] *Annual Report 2014*. pp. 97, Central Bank of Sri Lanka

[2] *Statistical Digest 2014*, Ceylon Electricity board

[3] *Code of practice for energy efficient buildings in Sri Lanka 2008,* Sri Lanka Sustainable Energy Authority

[4] *Energy Consumption Benchmark Analysis,* Sri Lanka Sustainable Energy Authority (2014)

Performance Comparison of Energy Recovery Systems for Internal Combustion Engine Applications

Wijewardane, M.A.1, Stobart, R.K.2,
[1]*University of Moratuwa, Sri Lanka*
[2]*Loughborough University, United Kingdom*

Abstract

Today, the investigation of fuel economy improvements in internal combustion engines (ICEs) has become the most significant research interest among automobile manufacturers and researchers. The scarcity of natural resources, progressively increasing oil prices, carbon dioxide taxation and stringent emission regulations all make fuel economy research relevant and compelling. The enhancement of engine performance solely using in-cylinder techniques is proving increasingly difficult and as a consequence the concept of exhaust energy recovery has emerged as an area of considerable interest. Vapour power cycles, turbo-compounding devices and thermo-electric generators have been identified as the main energy recovery systems applicable for ICE applications.

Performance comparison of these energy recovery systems was performed using a one dimensional (1-D) engine simulation software. The modelling work was performed to understand the steady state performance of energy recovery systems, for real exhaust gas boundary conditions generated by a validated 1-D engine simulation model developed to represent a heavy-duty diesel engine.

It was found that the vapour power cycles (VPCs) are capable of recovering more energy for the similar exhaust gas characteristics compared with the turbo-compounding (TC) devices and thermoelectric generators (TEGs). However, considering the complexity, weight penalty and controllability of the systems, TEGs have been identified as the most promising energy recovery system compared to vapour power and turbo-compounding devices.

Keywords: Energy recovery, internal combustion engines, vapour power cycle, turbo-compounding, thermo-electric generation

Introduction

The world energy consumption rate is rapidly increasing due to the extensive energy usagefor global industrialization. The American Energy Information Administration (AEIA) predictsa 37% increase of the world energy consumption from 2014 to 2040 [1]. Further, it has been predicted that the world-wide energy consumption will increase by 1.1% annually (the predictions were made assuming the 'business-as-usual trend' and the 'current laws and regulations are maintained throughout the projections'). According to AEIA predictions, the transportation sector contributes approximately 1/3rdof the total energy consumption in the world and it increases by 1.1% annually from2010 to 2040.

In developed countries, road transportation sector is the most energydemanding sector within the transport sector and it consumes around 85% of the totalwhereas, the maritime and the air transport sectors consume only 7% and 8% respectively.However, road transport sector in the Europe contributes only 20% of the total [1]. More than 95% of the road transport sector entirely depends on conventional energy sources; such as gasoline and diesel, which are not promising due to lack of availability and the envisaged energy crisis. The need to reduce both the oil dependency and fuel consumption is particularly acute in the road transport sector. The majority of the automotive industry is currently investigating the enhancement of the performance of ICEs while exploring for alternative energy sources and technologies that will ultimately replace the conventional ICEs.

Currently, almost all the automobiles in the world are driven by ICEs and a small percentage by electrically driven motors and hybridized systems. It is stated in the second law of thethermodynamics, the impossibility of any thermodynamic cycle (i.e. Otto, Diesel, Rankine and Gaspower) to convert the thermal energy input, solely into work or mechanical energy.Hence, all energy conversion processes are associated with heat rejection to cold sinks,typically the environment.

Taking a broader view, three energy conversion steps; well-to-tank, tank-to-wheel and wheel-to-mile, can be identified for a comprehensive analysis of the energy consumption ofautomobiles. Figure 1 shows the efficiencies of 12 different power trains technologies thatare used in present road transportation sector [2].

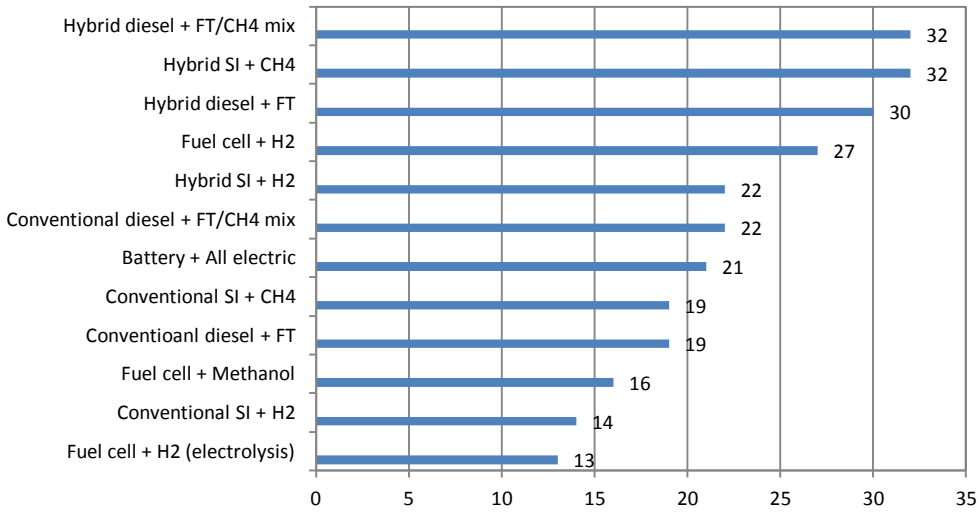

Figure 1: Well-to-wheel efficiency data of automobile systems [2]

Where,
FT – Fisher-Tropsch diesel, CH_4 – Methane, H_2 – Hydrogen and SI – Spark Ignition.

Typical thermal efficiency of small ICEs ranges from 10%-35% where, large diesel enginescan reach 50% and above. If the maximum in-cylinder gas temperature for a diesel engine isapproximately 2500K and the lowest temperature during the cycle is, the ambienttemperature, approximately 300K; and then the ideal Carnot heat engine working betweenthese two reservoirs would have an efficiency of 88%, which is approximately twice thehighest efficiency actually achieved by any practical engine. The differences are attributableto several factors.

Normally, it is only 1/3rd of the energy content of the fuel that ends up as useful shaft work.The remainder appears as exhaust and coolant enthalpy. Heat transfer to the exhaust andcoolant affects engine performance, efficiency and exhaust emissions. The heat transferfrom the hot combustion gases is comprised of forced convection through the hot gasboundary layer, conduction through the cylinder walls and convection into the engine coolantin the cylinder head, cylinder walls, piston rings, engine blocks and manifolds. There is asmall radiative component (less than 5%) of heat transfer from the hot gases to the cylinderwalls. Heat transfer takes place from hot cylinder walls to cold charge during the intakeprocess. During the compression, expansion and exhaust processes, heat flows from hotgases to cooler cylinder walls and heat transfer rates to cylinder walls become highest duringthe expansion process. Small amount of energy produced is also wasted as friction lossesarising from piston rings, shaft bearings and valve-

train. Auxiliary devices such as waterpump, oil pump and alternator also consume a fraction of the useful work output of the engine [3].

The overall first law energy balance of an ICE at steady state operation is defined by Eq (1);

$$\left.\begin{matrix}\text{Total fuel}\\ \text{conversion}\\ \text{power}\end{matrix}\right\} = \left.\begin{matrix}\text{Brake}\\ \text{power}\end{matrix}\right\} + \left.\begin{matrix}\text{Coolant}\\ \text{heat}\\ \text{transfer}\end{matrix}\right\} + \left.\begin{matrix}\text{Radiation}\\ \text{heat transfer to}\\ \text{environment}\end{matrix}\right\} + \left.\begin{matrix}\text{Exhaust heat}\\ \text{transfer due to}\\ \text{incomplete}\\ \text{combustion}\end{matrix}\right\} + \left.\begin{matrix}\text{Exhaust}\\ \text{gas enthalpy}\end{matrix}\right\} \quad \text{Eq.1}$$

Approximate breakdown of the various forms of energy resulting from the combustion of fuels in air for different classes of engines is given in Table 1.

Table ***Error! No text of specified style in document.****: Energy balance for automotive engines at maximum power [4]*

	P_b(%)	P_c(%)	P_{o+e} (%)	P_{ic} (%)	P_e(%)
SI (Gasoline)	25-28	17-26	3-10	2-5	34-45
CI (Diesel)	34-38	16-35	2-6	1-2	22-35

Where,

P_b – Brake power, P_c – Coolant, P_{o+e}– Oil and environment, P_{ic} – Waste heat due to the incomplete combustion and P_e – Exhaust enthalpy

The operational energy percentage (fuel cost) of a typical ICE is found to be 89% out of the total life cycle cost. This value may vary according to the application and can be as high as 95% in marine and rail applications. So that the low efficient ICEs adversely affect the fuel consumption of the vehicle and as a result global energy efficiency iscompromised. Even though more than 100 years has passed since the invention of the ICE, over 60-70% of the fuel energy is still lost to the environment without being used. In order to recover otherwise lost thermal energy and convert it into shaft power, a thermally managed engine has to be developed and introduced. By adding an innovative heat recovery system to the exhaust system and with the implementation of an engine coolant energy recovery system, very significant gains in efficiency could be achieved.

Thermal efficiency enhancement of ICEs is more convincing due to the exhaust emissions of ICEs have become the major contributors for global air pollution, greenhouse effect and eventually global warming. With a large increase in traffic volumes, it becomes increasingly important to keep ICE emissions to a minimum. During recent years, environmental concerns have led to the development of stringent emission standards for restricting carbon monoxide (CO), nitrogen oxide (NOx), and unburned hydrocarbons (HC) emissions. Presently, a number of emission control strategies are used to control the tail pipe emissions. These include Exhaust Gas Recirculation (EGR),

Selective Catalytic Reaction (SCR), Catalytic Converter (CAT) and Diesel Particulate Filter (DPF) and all those systems are fitted to the exhaust system of the vehicle. Current automobile research interest is gradually diverting to investigate on Super Ultra Low Emission Vehicle (SULEV) and Zero Emission Vehicle (ZEV) technologies such as electric, fuel cell and hybrid vehicles, with the aim of reducing the air pollution due to the increased traffic volumes in urban areas.

In this context, with the concerns of world energy crisis and the global warming trends due to the Green House Gas (GHG) emissions, recovering the waste heat of ICEs has been identified as vital.

Importance of waste heat recovery and heat recovery methods

ICEs reject approximately 30-40% of the energy supplied by the fuel to the environment through exhaust gases. So that, there is a possibility for further considerable improvement of ICE efficiency with the utilization of exhaust gas energy and its conversion to mechanical energy or electrical energy (direct energy conversion). Menchen [5] suggested that the overall efficiency of a heavy duty diesel engine has to be improved by 5-10% in order to enhance the fuel economy by 10%. Ikoma et al. [6] emphasized that even 3% recovery of the waste heat from a radiator or exhaust system expelling 60kW might be adequate for displacing an alternator assembly in a passenger vehicle.

Figure 2 and Figure 3 show the exhaust temperature profile of SI and CI engines of BMW 3-series motor cars [7]. Generally, the exhaust temperatures of SI engines are much higher than that of CI engines. However, the amount of energy that can be recovered depends on the availability of the exhaust gases. The availability is a state property which quantifies the maximum work that could be produced by a fully reversible work producing device. Availability mainly depends on both the upstream fluid properties (i.e. temperature and mass flow rate) and ambient conditions (i.e. temperature and pressure). Exhaust gas mass flow rate and temperature vary with the engine torque and the RPM (Revolution per Minute).Availability of a light duty naturally aspirated SI engine (Ford Sigma 1.4 litre engine), light duty turbo-charged CI engine (VW 1.9TDi 1.9 litre engine) and a heavy duty turbo-charged CI engine (Caterpillar 6.6 litre engine)were calculatedfrom experimentally measured data (from the test engine facility available atpowertrain laboratory, Loughborough University, UK) and range from 2-45 kW, 2-65 kW and 2-70 kW respectively.This indicates thata very significant amount of energy flux is rejected to the surrounding without being recovered.

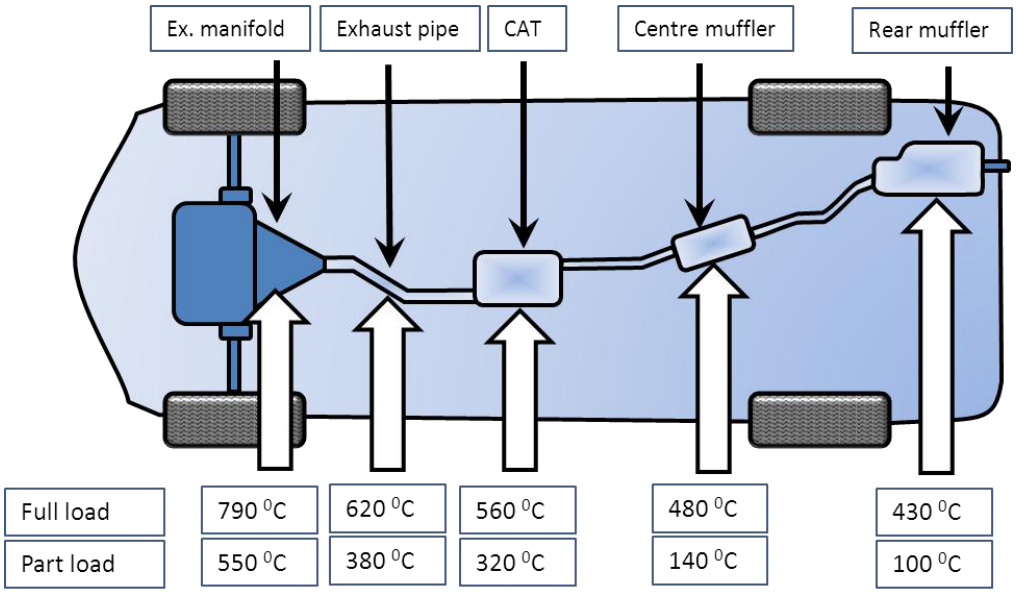

Figure 2: BMW 3-series exhaust temperature profiles of a Spark Ignition (SI) engine [7]

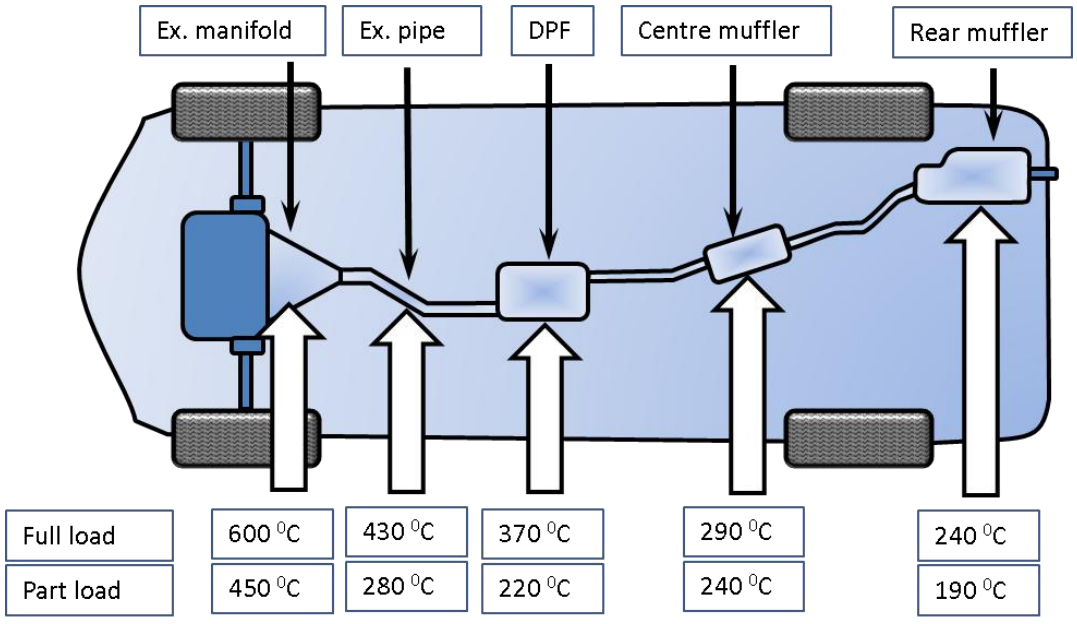

Figure 3: BMW 3-series exhaust temperature profiles of a Compression Ignition (CI) engine[7]

However, to date, the automobile researchers have identified the following technological solutions for energy recovery: turbo compounding devices, bottoming cycles (i.e. Rankine cycle with various working fluids, i.e. organic and inorganic), thermo-electric generators

(TEGs), thermo-acoustic systems and thermo-chemical systems [8].

Comparison of energy utilization and the degree of complexity of each technology for automotive applications has been illustrated in Figure 4. This comparison makes it easy to choose the best heat recovery system for a particular application.

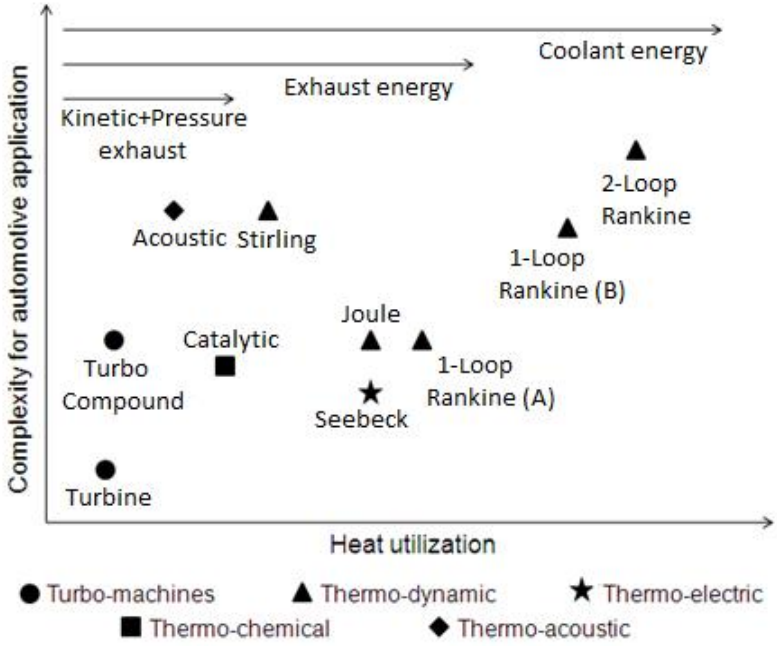

Figure 4: Energy utilization vs. complexity of different heat recovery systems [9]

As turbines can only use the pressure gradient and kinetic energy for energy recovery, the conversion efficiency and heat utilization is in a very low range. Other technologies can capture much larger amount of waste heat as they utilize the temperature difference of the exhaust gas and the coolant. High source temperatures are much more critical for devices based on the thermo-acoustic effects or the Stirling cycle. The heat transfer by gas-to-gas of the Joule process and thermo-acoustic, and by gas-to-material of a thermo-electric device, makes the heat utilization for a given heat exchanger surface more difficult in comparison to the conventional evaporator and condenser of thermo-dynamic cycles. Although, the thermo-chemical heat recovery systems utilize exhaust heat and coolant heat, their poor heat utilization and complexity are even greater than thermo-electric systems. In general, with increasing heat utilization or a greater amount of thermal energy recovery, the bigger the complexity of the energy recovery system [10]. The thermal energy recovery is highest with the implementation of a Rankine cycle.

According to previous studies, with increasing driving speed, more power is needed and results in higher waste heat flows providing an ideal basis for thermal energy recovery. At this stage in the development of this review, it is appropriate to note that the absolute heat flux changes significantly with the driving speed, the engine power and the fuel.

In practically, some of these energy recovery systems can behave differently to the potential heat utilization performances given in the Figure 4. For example, the thermo-electric devices have been identified as excellent devices for heat utilization. However, the realistic performance of these devices has been constrained with the thermo-electric material performance and hence, exhibits poor heat utilization characteristics in practise.

Energy recovery from the exhaust is much easier than from the coolant. Since the cylinder heat transfer process is periodic and the engine speed is usually high, the temperature fluctuations only penetrate about a millimetre into the cylinder wall. Making advantage of this, “insulated engine” or “adiabatic engine” concept has been evolved. Heat transfer to the cooling system can be significantly reduced by insulating the engine walls using an advance ceramic materials and by coatings of a perfectly IR (Infra-Red) radiation reflecting materials [11]. As a result, the available thermal energy in the exhaust stream can be increased and hence, recovered easily while enhancing the overall thermal efficiency of the engine.

Previous studies [9 and 10] revealed that the vapour power cycle is the most efficient thermal energy recovery technique for ICEs, and also revealed that the evaporator (boiler) of the Rankine cycle system can recover more than 90% of exhaust thermal energy (in the form of steam), a performance that outdoes other candidate heat recovery systems. Ideal Rankine cycles or vapour power cycles basically consist of four components; boiler, turbine, condenser & pump, and can be divided into four processes; heat addition (heat in), isentropic expansion (work out), isobaric heat rejection (heat out) and isentropic compression (work in), and each associated with a phase change of the working fluid.Diego et al. [9] proposed a vapour power cycle to recover energy from the exhaust gas and engine coolant. In his study, the conventional engine cooling system was eliminated and as a replacement, the engine block and exhaust gas were used as the evaporator of the Rankine cycle with water as the working fluid. Waste heat of the engine block was used to boil the working fluid and the high temperature exhaust gases were used to superheat the working fluid. It was found that the system can recover up to 8.1% from total input. But the back pressure constraint imposes a significant limitation to the complexity of the heat exchanger of the exhaust gasses. Simulations on vehicle

thermal energy recovery carried out by Hounsham et al. [12] reported that more than 6% of fuel economy could be achieved and overall efficiency of the engine can be enhanced by implementing a vapour power cycle. Further, the findings revealed that the future work should mainly concern on the dynamic behaviour of the heat exchanger and the formulation of an optimal control system to make it realistic.

Turbo compounding technology is another well-known technology used to increase the combustion efficiency, power output and reduce the fuel consumption of ICEs by recovering waste energy in the exhaust gas. In a turbo-compound engine, turbocharger is supplemented with a power turbine. Unlike in naturally aspirated (NA) engines, the combustion air of the turbo-compound engine is compressed and cooled before being supplied to the combustion chamber by a compressor which is driven by an exhaust gas powered turbine. Hence, the engine aspirates the same volume of air, but due to the high pressure, more air mass is supplied into the combustion chamber and increases the combustion efficiency while recovering the exhaust energy. Previous studies revealed that the Brake Specific Fuel Consumption (BSFC) can be improved up to 5-6% by implementing a turbo-compounding system in an IC engine [13]. Unlike other energy recovery systems used in ICEs, turbo compounding devices can only use the pressure gradients and/or kinetic energy fractions of the exhaust gas; hence efficiencies are much lower than other processes [10]. Turbo-compounding devices are of low complexity, small size, low cost and high power to weight ratio devices. The main disadvantage of turbo-compounding is the increase of the engine backpressure and pumping losses which result a reduction in net engine power [14]. Further, the turbo-compounding engines could face refinement questions for passenger car applications as they tend to make high noise due to rotor-dynamic devices. Hence, turbo-compounding devices essentially are used in heavy duty diesel engines, racing cars and marine applications where the noise emissions can be managed.

TEGs have been identified as a reliable solid state technology for power generation [15]. TEGs have many advantages in comparison to other thermal energy recovery methods, i.e. no moving parts, produce no noise and vibration, low maintenance, more environmentally friendly and direct conversion of low quality thermal energy into high quality electrical energy. Because of these properties, it has been traditionally used in places where other methods of reliable power generation systems are not feasible such as: deep-space missions (as RTGs – radioisotope thermo-electric generators) and, gas pipe lines. A TEG consists of a number of Thermo-Electric Modules (TEMs) which are sandwiched between a hot thermal

reservoir and a cold thermal reservoir. Thermalenergy is converted into electrical energy due to the changes of internal quantum structure ofthe TE material. In order to realize the practical importance as a generator in heat recoveryunits, it is necessary to increase the conversion efficiency of the TE material and to improvethe heat transfer from exhaust gas to the TEM.Stobart et.al [16] developed a vehicle model to predict the fuel consumption rates for range of vehicles with TEGs (modelled the TEG as a replacement of an engine-driven alternator) and predicted a fuel saving of 3.9-4.7% for passenger vehicle application. It further revealed that the transit busses are capable of 7.4% fuel saving for range of drive cycles with a pay back of 6 years with current thermo-electric materials and costs. Thacher et al. [17] also tested the performance of an exhaust mounted TEG in a full size truck with a 5.3litres V-8 gasoline engine. The device generated around 180W at 113km/h and zero grades. It was estimated that the recovered energy corresponded to a 1-2% fuel economy improvement and concluded that to extract more power either a larger unit was necessary or the heat exchanger design needed improvements.

Performance comparison of energy recovery systems

In the present work, performance comparison of three different energy recovery systems; vapour power cycles, turbo-compounding devices and thermoelectric generators was performed using the modelling facility available in 1-D engine simulation software, GT-Power. The modelling work was performed to understand the steady state performance of energy recovery systems, for real exhaust gas boundary conditions generated by a validated 1-D engine simulation model developed to represent a Caterpillar 6.6litre heavy-duty diesel engine.All calculations were performed assuming the R245fa as the working fluid of the vapour power cycle. Heat rejection needed at the condenser, heat addition required at the boiler, required pump work and capacity of the turbine were designed to capture the maximum available energy at downstream of the turbine of the engine. Figure 5 illustrates the vapour power cycle modeled in GT-Power.

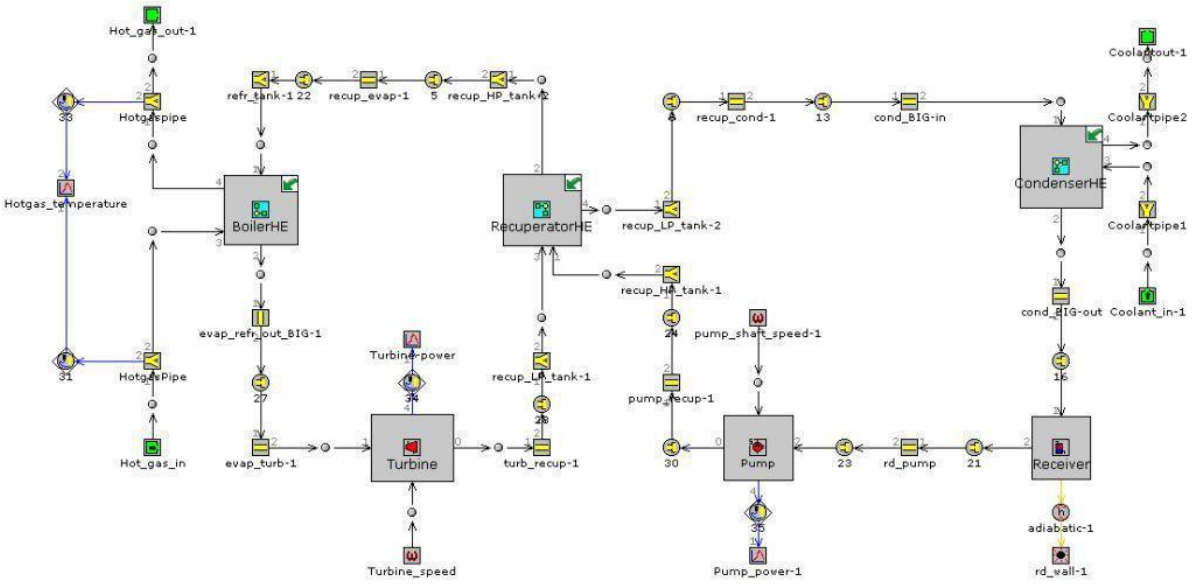

Figure 5: Vapour power cycle modelled in GT-Power

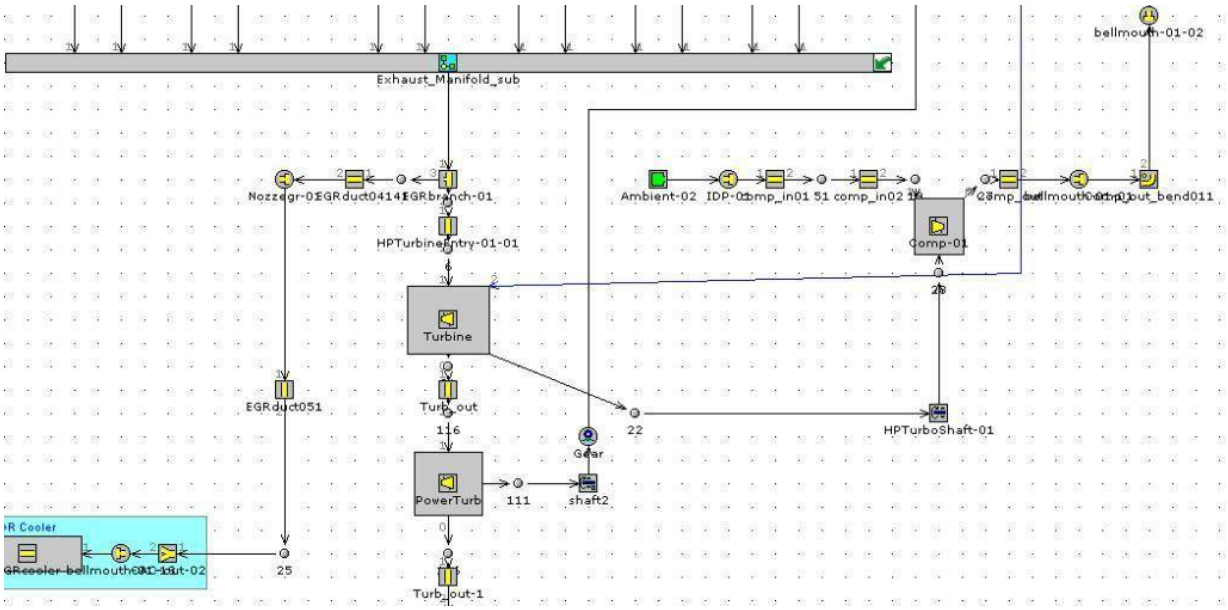

Figure 6:Turbo-compounding device modelled using GT-Power

Figure 6 illustrates the turbocharger section of the exhaust and intake systems of the engine model of the exhaust and intake systems of the engine model of the Caterpillar 6.6 litre engine. As shown in the figure, the power turbine of the turbo-compounding device can be located after the turbine of the turbocharger and recovered energy redirected to the engine via shaft and gear objects. The turbine and compressor maps were obtained from Garrett Turbochargers [18].

As illustrates in Figure 7, the TEG was designed as a 3-layer plate-fin heat exchanger to accommodate 24 TEMs (8 TEMs per row). The Seebeck coefficient of the TE material and the total module resistance of a TEM were defined as *ZT*=1 and 0.15 Ω respectively.

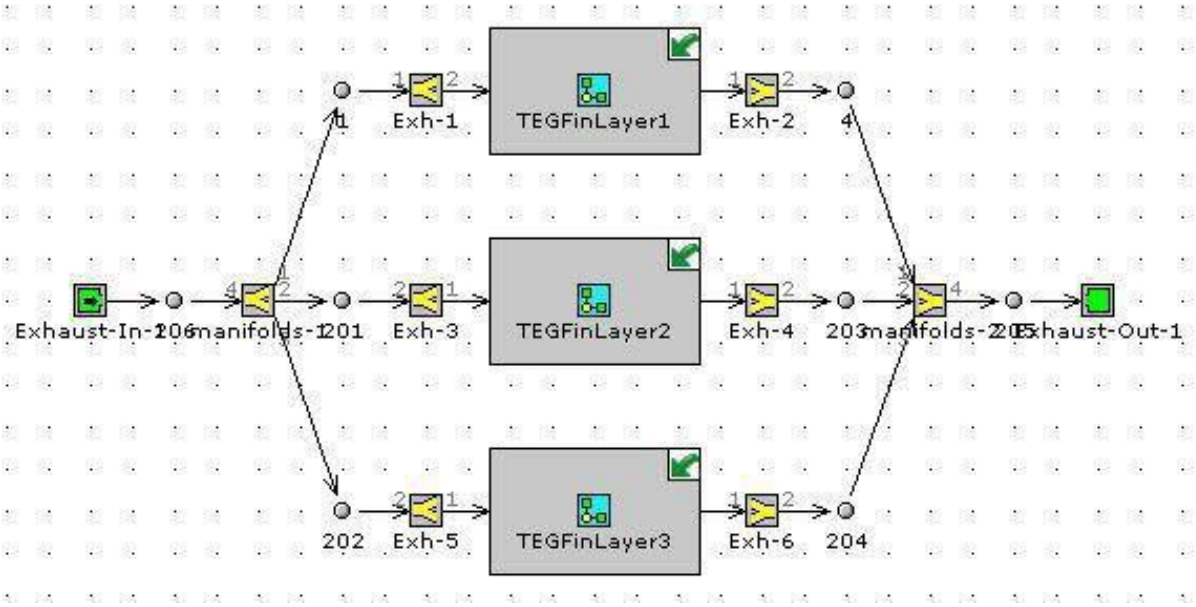

Figure 7: Thermo-electric generator modelled in GT-Power

Energy recovered by the vapour power cycle, turbo-compounding device and the thermo-electric generator, located in the main exhaust stream of the Caterpillar 6.6 litre engine was obtained for the same engine operation conditions as given in the Table 2.

Table 2: Performance comparison of energy recovery systems

Engine operation conditions				Exhaust gas characteristics				Energy recovery		
Mode	N_e (rpm)	Γ_e (Nm)	P_b (kW)	$\dot{m}$ (kg/s)	$p_{turb,in}$ (bar)	$T_{pre,turb}$ (K)	$T_{post,turb}$ (K)	$P_{Rankine}$ (kW)	P_{TEG} (kW)	P_{Tc} (kW)
1	1175	523	64	0.090	1.350	779	766	2.536	0.614	0.831
2	1550	449	73	0.116	1.460	670	630	2.578	0.339	1.066
3	1550	677	110	0.168	1.877	707	641	3.965	0.393	2.519
4	1175	271	33	0.062	1.159	655	647	1.117	0.288	0.336
5	1175	398	49	0.078	1.254	721	716	2.582	0.462	0.564
6	1175	139	17	0.054	1.110	543	536	0.412	0.123	0.272
7	1550	796	129	0.194	2.113	721	640	7.431	0.398	3.175
8	1550	234	38	0.077	1.207	587	565	1.025	0.188	0.439
9	1925	722	145	0.219	2.361	724	622	7.603	0.361	3.634
10	1925	189	38	0.090	1.260	567	554	1.272	0.185	0.655
11	1925	540	109	0.177	1.929	688	613	4.974	0.334	2.669
12	1925	362	73	0.127	1.512	644	603	2.468	0.293	1.307

Where, N_e-engine speed, Γ_e-engine torque,P_b-engine brake power,$\dot{m}$-air-mass flow rate,$p_{turb,in}$-inlet pressure at turbine, $T_{pre,turb}$-inlet temperature at turbine, $T_{post,turb}$-outlet temperature at turbine,$P_{Rankine}$- Power generated by a Rankine Cycle, P_{TEG}- Power generated by a TEG, P_{TC}- Power generated by a turbo-compounding system

As shown in the Table 2, modelling results show that the vapour power cycle recovers a significant amount of energy than the turbo-compounding device and the TEG device. As discussed above, vapour power cycles can be integrated with engine coolant to preheat the working fluid, which will be eventually results in significantly enhance the overall thermal efficiency of the engine. However, due to the number of heat exchangers and turbo-machines involved in the system, the vapour power cycle becomes complex, bulky and requires more control strategies integrated into the engine control unit (ECU) of the engine. If the weight penalty is very significant, vapour power cycles would be more desirable to install in heavy duty and medium duty vehicle applications rather than the light duty vehicle applications.

On the other hand, turbo-compounding devices mainly recover the kinetic energy of the exhaust gas. Therefore, the turbocharger and the power turbine needs to be specifically matched for an engine to obtain the required boost pressure for a given engine operation condition. Overall engine performance of the engine will significantly deteriorate if an un-matched power turbine was installed after the turbine of the

turbocharger, due to the increased back pressure generated by the turbine. Having proposed efficient turbo-machines with a variable geometry turbines(VGT) capability, a substantial amount of energy can be recovered from the turbo-compounding devices as shown in Table 2. Even though, the turbochargers are commonly used in both light duty and heavy duty applications of CI and SI engine, turbo-compounding devices are only used in CI heavy duty engines.

Solid state TEGs have been identified as the simplest energy recovery devices those can be easily adapted to the existing exhaust systems of both SI and CI engines. The rated power of the TEG can be easily improved by increasing the number of TEMs in the device. Moreover, the efficiency of the TEG system can be significantly increased by augmenting the heat transfer rate across the TEG heat exchanger and utilizing more efficient thermo-electric materials, which promise the ability to recover similar amount of energy as vapour power cycles. Results shown in Table 2 reveal that, a significant amount of energy can be easily recovered by implementing a simple TEG heat exchanger device in the exhaust system, unlike the vapour power cycles and turbo-compounding devices.

Conclusions

Thermal energy recovery of ICEs has been identified as a vital and attractive research interest among the researchers and automobile manufacturers all over the world, aiming to reduce the CO_2 emission from power-trains. The available energy flows in different power-trains were studied and it was found that, a significant amount of fuel energy is rejected to the environment. Although, the number of energy recovery systems is being investigated for deployment in passenger cars and other types of vehicle, none of that research activity has yet encompassed the comparative performance of available energy recovery systems.

A vapour power cycle, turbo-compounding device and thermo-electric generator were modeled in a 1-D software code, to compare the performance of main energy recovery systems that can be used in automobile applications. It was found that the vapour power cycles are capable of recovering more energy for the similar exhaust gas characteristics compared with the turbo-compounding devices and TEGs. However, when considering the complexity, weight penalty and controllability of the systems, TEGs have been identified as the most promising energy recovery system when compared to vapour power and turbo-compounding devices.

Acknowledgements

Authors would like to thank the co-researchers of the low carbon technology group of Dept. of Aeronautical and Automotive

Engineering, Loughborough University, UK.

References

[1] "International Energy Outlook 2013, U.S. Energy Information Administration". Internet:http://www.eia.gov/forecasts/ieo/pdf/0484(2013).pdf, [Date accessed: Aug, 02, 2015]

[2] Kreith, F. and West, R.E. "Gauging Efficiency, Well to Wheel". Internet: http://www.memagazine.org/supparch/mepowerr03/gauging/gauging.html, [Date accessed: June 15, 2009]

[3] Borman, G. and Nishiwaki, K. "Internal Combustion Engine Heat Transfer". *Progress in Energy and Combustion Sciences*, Vol. 13, Issue 1, 1987

[4] Heywood, J.B. *Internal Combustion Engine Fundamentals.* New York: McGraw-Hill Inc, 1988

[5] Menchen, W.R., Osmeyer, W.E. and McAlonan, M. "Thermoelectric Conversion to Recover Heavy Duty Diesel Exhaust Energy". *Proc. of the Annual Automotive Technology Development Contractors Meeting - SAE*, 1991

[6] Ikoma, K. "Thermoelectric Module and Generator for Gasoline Engine Vehicle". *Proc. of 17th International Conference on Thermoelectric - Nagoya,* pp. 445-449, 1998

[7] LaGrandeur, J., Crane, D. and Eder, A. "Vehicle Fuel Economy Improvement through Thermoelectric Waste Heat Recovery". Deer Conference, Chicago, IL, 2005

[8] Hountalas, D.T., Katsanos, C.O. and Lamaris, V.T. "Recovering Energy from the Diesel Engine Exhaust Using Mechanical and Electrical Turbo Compounding", SAE Technical Paper, 2007-01-1563, Detroit, MI, 2007

[9] Diego, A.A., Timothy, A.S. and Ryan K.J. "Theoretical Analysis of Waste Heat Recovery from an Internal Combustion Engine in a Hybrid Vehicle", SAE Technical Paper, 2006-01-1605, Detroit, MI, 2006

[10] Ringler, J., Seifert, M., Guyotot, V. and Hübner, W. "Rankine Cycle for Waste Heat Recovery of IC Engines", SAE Technical Paper, 2009-01-0174, Detroit, MI, 2009

[11] Assanis, D.N. "Effect of Combustion Chamber Insulation on the Performance of Low Heat Rejection Diesel Engine with Exhaust Heat Recovery". *Heat Recovery Systems and CHP*, Vol. 9 No.5, 1989

[12] Hounsham, S., Stobart, R.K., Adam, C. and Peter, C. "Energy Recovery Systems for Engines". SAE Technical Paper, 2008-01-0309, Detroit, MI, 2008

[13] Ulrich, H. and Marcelo, C. A. "Diesel Engine Electric Turbo Compound Technology". SAE Technical Paper, 2003-01-2294, Detroit, MI, 2003

[14] Hountalas, D.T., Katsanos, C.O. and Lamaris, V.T. "Recovering Energy from the Diesel Engine Exhaust

using Mechanical and Electrical Turbo-compounding". SAE Technical Paper, 2007-01-1563, Detroit, MI, 2007

[15] Quazi, E. H., David, R. B. and Clay, W. M. "Thermoelectric Exhaust Heat Recovery for Hybrid Vehicles". SAE Technical Paper, 2009-01-1327, Detroit, MI, 2009

[16] Stobart, R., Wijewardane, A. and Allen, C. "The Potential for thermo-electric devices in passenger vehicle applications". SAE Technical Paper, 2010-01-0833, Detroit, MI, 2010

[17] Thacher, E.F., Helenbrook, B.T., Karri, M.A. and Richter, C.J. "Testing of an Automobile Exhaust Thermoelectric Generator in a Light Truck". *Proc. of the IMechEPart D: Journal of Automobile Engineering*, Vol. 221, 2007

[18]https://www.turbobygarrett.com/turbobygarrett/ [Date accessed: 28th March 2010]

Numerical Analysis of Aerodynamic Performance of a Ceiling Fan

Rajapakshe, P.D.M.P., Mapa, M.H.H.G., Thanushan, R., Ranasinghe, R.A.C.P.[1]
[1]*University of Moratuwa, Katubedda, Sri Lanka*

Abstract

Ceiling fans are often used in both the industry and the domestic sector for ventilating indoor environments. However, at present the overall efficiency of an average ceiling fan is only about 7.0-12.5%. Therefore, improving aerodynamic performance of ceiling fans has a significant contribution in creating an enhanced thermal comfort level at a reduced energy cost. Growing concern on energy labelling for electrical appliances, including ceiling fans, also highlights the need for more investigations on ceiling fan performances. The aim of this study is to analyse the flow field around a ceiling fan occurring under different operating conditions. Consequently, the performances were investigated for different rotational speeds and ceiling heights. Rotational speed is directly proportionate to electrical consumption thus proper use of speed can aid in achieving greater energy efficiencies and desirable occupant comfort level. In addition, the gap between the fan and the ceiling also significantly affect the volumetric air flow rate, thus the thermal comfort level. In this work, computational fluid dynamics (CFD) tools combined with an experimental program was used for the quantitative and qualitative assessment of service values, average velocities, velocity profiles and mass flow rates. In the first stage the present CFD approach was successfully validated against experimental measurements and subsequently used for the prediction of fan performance at various rotational speeds and ceiling heights. The effect of ceiling gap on flow rate and torque was calculated using the simulation and it was found that maximum service value is obtained when the gap is around a radius of the rotor. Best operating speed was identified as regulator setting two depending on the service value criterion.

Introduction

Ceiling fans are often used in both the industry and the domestic sector for ventilating indoor environments. Due to simplicity in design, low cost, ease of installation and less maintenance, ceiling fan usage is higher. Also the less power consumption compared to air conditioning units makes ceiling fans more popular. Growing concerns in saving energy have made it mandatory to evaluate performance of electrical appliance, prior to market launch. Further, governments are providing financial incentives for manufacturers to implement high efficient fan which consumes less than half of energy of typical fans in the market [1].

Moreover, it has identified in a study [2] that ceiling fans accounted for about 6% of residential primary energy usage in India in 2000, and this figure is expected to grow up to 9% by 2020. A detailed assessment on this matter shows that using available technologies, ceiling fan efficiency can be cost-effectively improved by at least 50% and if these improvements are implemented in all ceiling fans sold by 2020, 70 terawatt hours per year and 25 million metric tons of CO_2 could be avoided [3]. Consumer education on selection, installation and operation of ceiling fans also contribute significantly in obtaining potential benefits of ceiling fan usage, as identified in [4].

Efficiency of ceiling fans can be enhanced through improving manufacturing methodologies and implementing electrical and aerodynamic modifications. Indian Super-Efficient Equipment and Appliance deployment (SEAD) initiative has identified that use of efficient blades would save the annual electricity consumption per fan by 33 kWh with incremental manufacturing cost of US$ 3.50 [3]. It has also been shown that thermal comfort level can be increased in an air-conditioned room by using ceiling fans, emphasising the need for more energy efficient ceiling fans [5]. All these facts encourage the investigation of flow field around ceiling fans as a basis for performance improvements.

To investigate potential improvements, flow field around a ceiling fan resulting from different geometrical and operating parameters needs to be analysed thoroughly. Experimental, analytical and numerical methods can be utilized on this regard. In an experimental study [6], it was identified that winglets and spikes attached to the tip of blade (there by disturbing the formation of tip vortices) can increase the downward air flow by 13% without increasing the power consumption.

Analytical methods are rigorous and exact, but obtaining solutions for complex scenarios using this method is always not possible. Theoretical model using actuator disk theory has been proposed in [7] [8] to analyse the ceiling effect on performance of ceiling fans, mentioning the difficulty in modelling upstream wall effect using analytical methods. In [8], ratio of volume flow rate between at presence of ceiling and without ceiling was analysed as ratio

between ceiling gap (H) to radius of span of rotor (R) varies. When ratio of H/R below one, higher reduction in volume flow rate can be seen in with ceiling flow scenario compared to without ceiling scenario. Due to the versatility available with numerical tools such as in computational fluid dynamics (CFD), flow field analysis can be done with more flexibility, nevertheless to date, research done on particular matter is not adequate. With the assistance of CFD, it has been identified in [9], that ceiling fan guard which encloses the rotor, would create a wider air flow distribution but with lower velocity output.

As mentioned previously, research done on ceiling fan performance is limited. Modelling and analysis on the influence of ceiling fan geometrical parameters to the air flow distribution are very few [10].Therefore, In this work, CFD tools combined with an experimental program was used for the quantitative and qualitative assessment of service values, average velocities, velocity profiles and mass flow rates. In the first stage the present CFD approach was validated against experimental measurements and subsequently used for the prediction of fan performance at various rotational speeds and ceiling heights.

The test setup

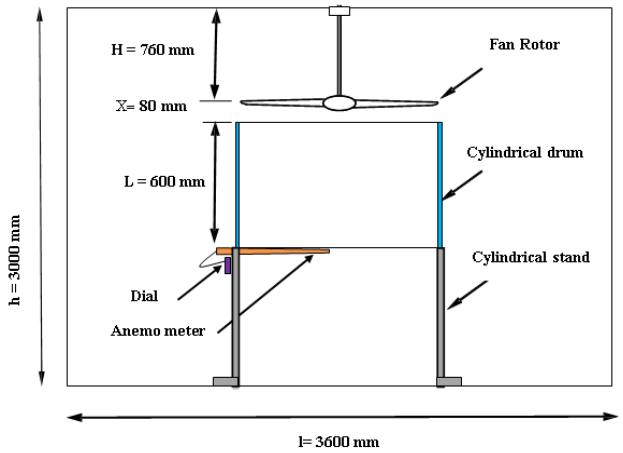

Figure 1: The experimental setup used for data acquisition

Experiments were carried out in order to develop a basic understanding about the flow field and to aid in numerical method validation process. Experimental setup shown in Figure 1 was utilized as recommended by the Sri Lanka Standard (SLS) No. 814 for ceiling fan testing. Test chamber has dimensions of 3600 mm x 3600 mm x 3000 mm, which is equivalent to a room of a single person. Axial velocities were measured at different axial stations and velocity distribution was plotted against radial distance. Twenty reading at 10 seconds time intervals were obtained at one point and average was taken as the

velocity measurement of that particular point.

Computational modelling

Three dimensional analysis was performed using ANSYS 15.0 – Fluent code. Reynolds averaged transport equations and Spalart Allmaras (SA) turbulence model with moving reference frame (MRF) technique was employed obtain the time averaged flow field. Entire computational domain was discretised using tetrahedral mesh elements. A sensitivity analysis for the mesh structure was performed and identified that most economical and effective mesh for the analysis is approximately 3 million cells, where 64% of the mesh elements cover the MRF domain as indicated in Figure 2. Aspect ratio of elements were kept around 1 along with skewness value below 0.7 for greater accuracy while maintaining a refined mesh region near rotor to capture the effect of geometry on the flow field variation in an accurate manner.

SA turbulence model: a one equation model, is specifically design for aerodynamic applications [11]. Equation for transport variable $\tilde{v}$, the turbulent kinematic viscosity, in SA model is given by the following equation;

$$\frac{\partial(\rho\tilde{v})}{\partial t}+\frac{\partial(\rho\tilde{v}u_i)}{\partial x_i}=G_v+\frac{1}{\sigma_{\tilde{v}}}\left[\frac{\partial}{\partial x_j}\left\{(\mu+\rho\tilde{v})\frac{\partial\tilde{v}}{\partial x_j}\right\}+c_{b2}\rho\left(\frac{\partial\tilde{v}}{\partial x_j}\right)^2\right]-Y_v+S_{\tilde{v}} \quad \text{Eq. 1}$$

Where,

G_v	-	Production of turbulent kinematic viscosity
Y_v	-	Destruction of turbulent kinematic viscosity
x_i	-	Three coordinate directions$(i=1,2,3)$
u_i	-	Velocity components in three directions
μ	-	Molecular dynamic viscosity
ρ	-	Density of the fluid
$S_{\tilde{v}}$	-	User defined source term
$\sigma_{\tilde{v}}, c_{b2}$	-	model constants which have the values 2/3 and 0.622

The governing equations for a moving reference frame can be defined as below,

Conservation of mass

$$\frac{\partial\rho}{\partial t}+\nabla.\rho\overrightarrow{v_r}=0 \quad \text{Eq. 2}$$

Conservation of momentum

$$\frac{\partial \rho \overrightarrow{v_r}}{\partial t} + \nabla.(\rho\, \rho \overrightarrow{v_r} \overrightarrow{v_r}) + \rho[\overrightarrow{\omega} \times (\vec{v} - \overrightarrow{v_t})] = -\nabla p + \nabla.\bar{\bar{\tau}} + \vec{F} \qquad \text{Eq. 3}$$

Conservation of energy

$$\frac{\partial \rho E}{\partial t} + \nabla.(\rho \overrightarrow{v_r} H + p\vec{u}_r) = \nabla.(\mathrm{k}\nabla \mathrm{T} + \bar{\bar{\tau}}.\vec{v}) + S_h \qquad \text{Eq. 4}$$

The symbols have following definitions.

$\vec{v}$ - Absolute velocity

$\vec{F}$ - Force vector

H - Total enthalpy

T - Temperature

$\vec{u}_r$ - Velocity of the moving reference frame relative to inertial reference frame

$\overrightarrow{v_r}$ - Relative velocity (velocity viewed form the moving frame)

$\overrightarrow{\omega}$ - Angular velocity

$\bar{\bar{\tau}}$ - Stress tensor

E - Total energy

k - Kinetic energy per unit mass

The Figure 2 given below illustrates the computation domain used for the simulations.

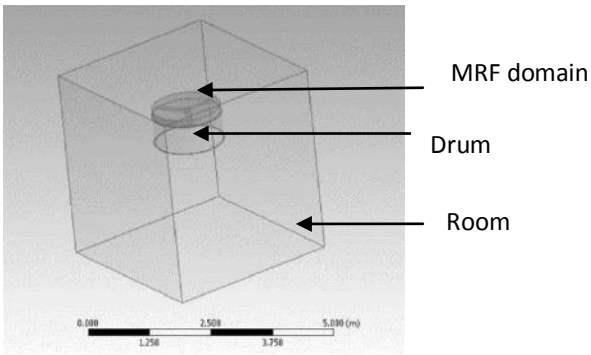

Figure 2: Computational domains

Results and Discussion

Figure 3 illustrates a comparison between simulated results at different axial stations and their respective experiment results. Note that these simulations have also been performed with a drum placed below the rotor, as described. A reasonable agreement can be seen between simulated and experimental results. It should be noted here that the standard model constants have been used for the SA model without any fine tuning.

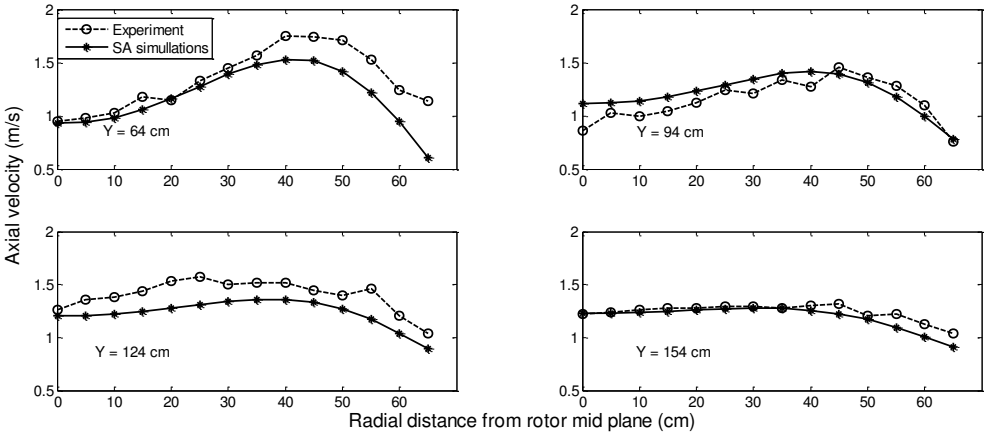

Figure 3: Comparison of simulated and experimental velocity profiles at different heights

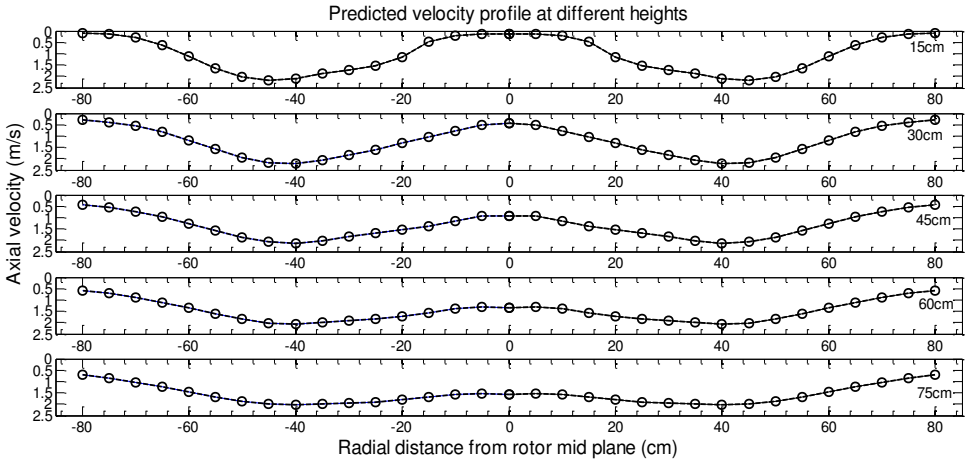

Figure 4: simulated flow profile at different axial stations at 239 rpm (without the drum)

Figure 4 demonstrates the velocity profiles and their variations as the flow reaches the floor. Further, figure has depicted velocity variation in radial direction from centre of the hub, when fan operates in regulator setting 3. Effect of the hub can be clearly seen with the low velocity region in the middle. Moreover, Flow profile is characterized by the higher velocity near middle of the blade. These two findings highlights the significance of developing more aerodynamically sound blade designs which can incorporate whole length of the rotor effectively in imparting downward flow.

When evaluating performance of the given fan under varying rotational speed and at different ceiling heights, quantification of performance done with parameters; mass flow rate, average velocity, torque and service coefficient as shown in Table 2. Here, service value (η) is defined as,

$\eta = (Mass\ Flow\ Rate\ (\dot{m}))/(Torque\ (\tau))$

where torque here is referred to torque exerted on the blade and hub by air, which is calculated using simulated results. Flow coefficient (

$\phi) = (Average\ axial\ flow\ velocity)/(D/2 \times \omega)$

where D is diameter of fan; is a measure of how effective a ceiling fan in transferring the tangential velocity of the fan blade to the axial velocity component of air.

Effect of rotational speed variation

Table 1- Fan speed at different regulator settings

Regulator setting	RPM(rad/s)
1	116
2	164
3	239
4	263
5	294

Ceiling fan used in the experiment runs at speed shown in the Table 1 under each regulator setting. Figure 5 shows the vector plots obtained under each regulator setting for the fan. Further, from these plots, it is identifiable that the with the RPM increase, centre of flow circulation travels downwards creating a more downward flow. Moreover, Increase of this downward flow increase the level of comfort for occupants. Thus it is desirable to have the centre of flow circulations at bottom part of the room in order to obtain higher downward flow rate. Further, even if the speed of rotor increases, directly downward flow occurring below rotor is confined approximately to cylindrical shape volume without showing any divergence. Effective area of seating is limited to this particular area, which is normally considered as a comfort zone. If a design can incorporate diverging flow cone with a sufficient downward wind speed, number of fans need to be installed in a given space can be reduced since one fan can impart cooling effect over wider area.

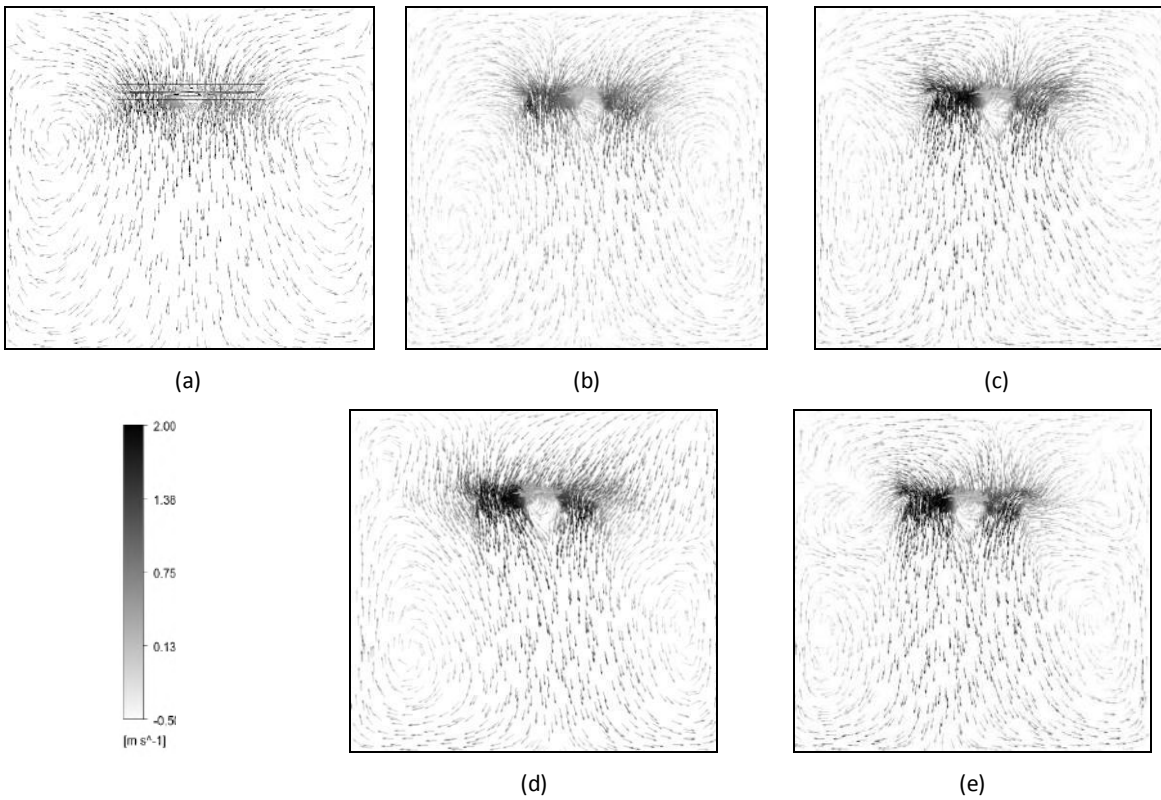

Figure: 5 variation of flow field under regualator settings 1 to 5 [(a) to (e)]

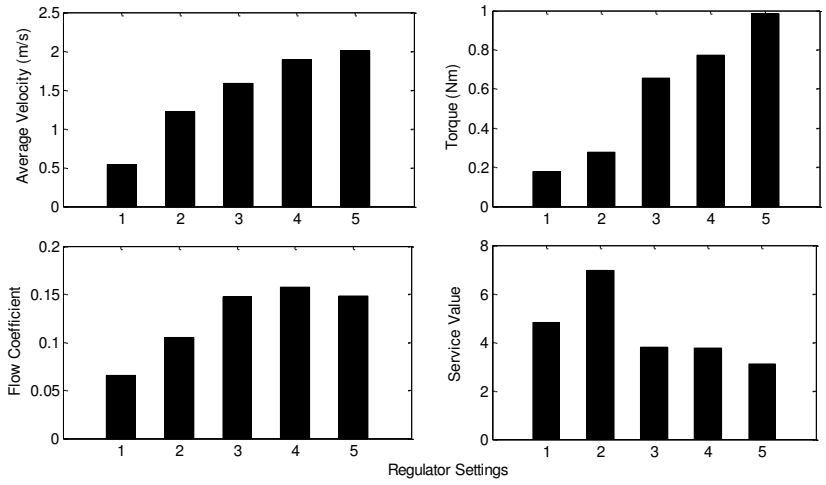

Figure: 6 Performance variation at different regulator settings

According to simulations above performance measurements values were obtained as shown in Figure 6 .The greater the rotational speed is the

greater the kinetic energy of the rotor that is transferred to air resulting in greater velocity component downwards, thus increasing the average velocity. As a consequence, mass flow rate increases with regulator setting.

It can be seen that flow coefficient increases with the regulator setting but decreases after regulator setting 4. Blade design should be able to direct a considerable volume of air downward to create cooling effect, for this blade angle plays an important role. When rotational speed increases, for a given blade angle, blade can push air strongly downward than lower regulator setting.

Even though the best flow coefficient and service value is obtained at regulator settings 4 and 2 respectively, the best regulator setting depends on the user's requirements; higher flow rate, low energy consumption and etc. On average it can be concluded that the ceiling fan operates fairly well at regulator setting 3.

Effect of the gap between Ceiling Height and the fan

To analyse the effect of upstream solid wall on the performance of ceiling fan, distance between rotor plane and ceiling was varied and air flow motion inside the room was predicted using simulations (note that this set of simulations were done without the cylindrical drum). Minimum distance was selected as 30 cm and maximum gap was limited to 90 cm due to practical limitations given that the height of modelled room geometry is only 3 m.

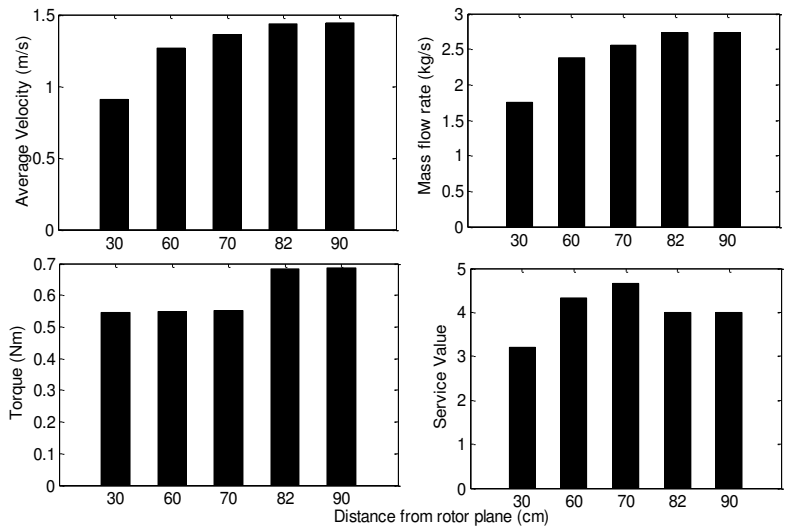

Figure 7: Performance evaluation as ceiling gap varies

Table 2: Performance variation with ceiling gap

Height	Mass Flow Rate (kg/s)	Avg. velocity (m/s)	Torque (Nm)	Service val.
30	1.747	0.911	0.546	3.197
60	2.376	1.267	0.550	4.320
70	2.560	1.362	0.551	4.651
82	2.734	1.438	0.684	4.000
90	2.732	1.444	0.685	3.990

Figure 7 shows that the average velocity measured at the bottom of MRF domain increases with the ceiling height. As the ceiling height is increased the volume of air above the rotor is increased which results in increase of suction pressure on the ceiling. This ultimately increases the momentum transferred to downward flow which results in increase of average velocity.

When the ceiling height decreases, flow tends to direct upwards below the hub area. As the ceiling gap reduces it restrict upstream air volume and reduces suction pressure. This reduction of pressure creates greater pressure jump and ultimately creating an upwards flow right below the hub, as identified through the simulation results.

The torque on the blades increases with the increase of ceiling height. As the ceiling height increases the gap between the floor and the rotor reduces which results in more resistance from floor to thrust air downwards. Thus, the torque increased with the ceiling height.

The best service value is achieved at 70 cm ceiling height which is around half of the rotor diameter. The explanation for this service value variation is done later on. The above flow profiles have been achieved by varying the ceiling height from 30 cm to 90 cm. Results show that mass flow rate, average velocity and torque have increased with the increase of ceiling height. The service value has increased up to 70 cm and then decreased. The service value is low at lower ceiling heights as there is less amount of air in the upper stream. The insufficient amount of air above the rotor results in restricted air flow across the blade, thus requiring higher torque to move air downwards. The service value decreases when the ceiling height is further increased since when the rotor becomes closer to the floor it becomes difficult to thrust air downwards requiring greater torque. Therefore 70 cm is the optimum ceiling height that gives results in greater service value predicting better performance.

Conclusions

Main objective of this research work is to identify the flow patterns around the ceiling fan and thereby determine the effective operating parameters based on quantitative and qualitative assessment.

Maximum velocity can be seen around at the middle point of rotor and low velocity region can be seen around hub. Investigations for aerodynamically sound designs can eliminate these drawbacks while obtaining a wider uniform flow region below rotor. More research need to be done in order to identify

geometrical and operational parameters which aid in developing wider downward flow area. As the speed increases, centre of the flow circulations due to near wall boundaries moves downward direction producing more downward flow, which is desirable for cooling.

When the ceiling height decreases, flow tends to direct upwards below the hub area. Optimum ceiling height based on service value is found to be around half of the rotor diameter. When distance between rotor plane and ceiling is less or greater than the optimum value, service value tends to decrease.

Acknowledgements

Authors wish to acknowledge the support of Dr. A.G.T. Sugathapala, Mr. Harsha Wickramasinghe, Mr. K.K.M.N.P. Samaraweera, Mr. T.P. Miyanawala and Dr. H.K.G. Punchihewa during this project.

References

[1] D. Singh, A. Barve and G. Sant, "Ceiling Fan: The Overlooked Appliance in Energy Efficiency Discussions," prayas energy group, India,Pune.

[2] N. Zhou, J. Sathaye, M. McNeil, V. Letschert and S. D. l. R. d. Can, "Residential and Transport Energy Use in India: Past Trend and Future Outlook," Ernest Orlando Lawrence Berkeley National Laboratory, 2009 January.

[3] N. Sathaye, A. Phadke, N. Shah and V. Letschert, "Potential Global Benefits of Improved Ceiling Fan Energy Efficiency," Ernest orlando lawrence berkerly national laboratory, 2012 October.

[4] D.S. Parker and j. Sonne, "Measured Ceiling Fan Performance and Usage Patterns: Implications for Efficiency and Comfort Improvement," 1998.

[5] S. H. Ho, L. Rosario and M. M. Rahman, "Thermal comfort enhancement by using a ceiling fan," *Applied Thermal Engineering,* vol. 29, p. 1648–1656, 2009.

[6] J. Ankur, R. Rochan, C. Samarth, S. Manish and K. Sunil, "Experimental Investigation of the Flow Field of a Ceiling Fan," in *ASME Heat Transfer/Fluids Engineering Summer Conference*, Charlotte,NC,USA, 2004.

[7] A. G. T. Sugathapala, "Preparation of Performance Standards and Test Procedures for Energy Performance Tests of Ceiling Fans," Sri Lanka Sustainable Energy Authority, 2008.

[8] A. Sugathapala, "Wall effects on the perfomance of the ceiling fans : A two dimentional model," in *ERU Research symposium, University of Moratuwa, Sri Lanka*, 1999.

[9] S.C Lin and M.Y Hsieh, "An Integrated Numerical and Experimental Analysis for Enhancing the Performance of the Hidden Ceiling Fan," *Advances in Mechanical Engineering,* p. 15, 27 February 2014.

[10] R. Bhortake, P. S. Lachure, S. R.

Godase and V. More, "Experimental analysis of air delivery in ceiling fans," *Emerging Technology and Advanced Engineering,* vol. 4, no. 6, pp. 247-251, June 2014.

[11] P. Spalart and S. Allmaras, "A One-Equation Turbulence Model for Aerodynamic Flows," *Recherche Aerospatiale,* vol. 1, pp. 5-21, 1994.

Assessment of the Available Potential in Paddy Husk for Power Generation in the Ceylon Electricity Board – Minneriya Region

Fernando K.N.A.[1], Prof. D. de Silva[2], Wickramasinghe, H.K.[1]
[1]*Sri Lanka Sustainable Energy Authority,* [2]*Faculty of Science, University of Colombo*

Abstract

Paddy husk, the outer layer of the seed of *Oryza sativa* is used as an agro-industrial residue in many thermal applications, including parboiling, usage in brick and lime kilns and in biomass based power generation. Although paddy husk has competing uses, there is no established methodology to assess its available potential for power generation. This study established a methodology for the assessment of the same, through a pilot study carried out in the Minneriya Ceylon Electricity Board (CEB) Region. The main objective of the study was to assess the power generation potential of biomass resources, for the preparation of renewable energy resource maps by the Sri Lanka Sustainable Energy Authority. The specific objectives were, to assess the theoretical potential of paddy husk generated in the country, to assess the uses of paddy husk in the Minneriya CEB region, to generate a resource flowchart based on the uses of paddy husk in the Minneriya CEB Region and to establish a methodology for the assessment of paddy husk available for power generation in a given site.

The theoretical potential of paddy husk was estimated from rice production statistics obtained from the Department of Census and Statistics, while the paddy husk production was estimated using the RPR of 0.2. Electricity consumption of the rice mills in the study site were obtained from the CEB. Mills were classified as bulk consumption (14 Nos.) and regular (159 Nos.) mills. The available potential for power generation in the study site was deuced through a field survey, which established the usage factors of paddy husk, and by extrapolating the results for bulk consumption and regular mills obtained from the CEB. The resource flow chart for paddy husk was generated through a simulation model on MS Excel (2007). Both, static (analytical) and dynamic (simulation) models were used to establish the methodology for the assessment of paddy husk in a given site.

The availability of paddy husk for power generation was 7%, while the highest use of paddy husk was for parboiling (86%). Only paddy husk generated at bulk consumption mills were available for power generation. The quantities of paddy husk available for power generation and other applications vary each year, therefore the study proposed a methodology for the assessment of available potential of paddy husk for power generation, by considering the location of the resource, inter-district transfer of paddy husk and area specific usage factors of paddy husk. The study did a scenario analysis and concluded that the Captive Generation Scenario is the most profitable method to utilise paddy husk for power generation with net metering, in a given area. Additionally, the study recommends including the economic potential for the methodology of assessing the availability of paddy husk, which would estimate the cost of biomass resources at the field.

Introduction

The botanical name of paddy is *Oryza sativa L.*, belonging to the Gramineae family. Paddy is a self-pollinated crop. A complete seed of rice is called paddy and contains one rice kernel. The outer layer of the rice shell is called the 'husk', while the next layer is called 'rice bran'. The innermost part is called rice kernel (Khullar, 2005). Paddy husk is an important agro industrial residue in the renewable energy industry and has varied applications in thermal energy generation (Daranagama, 1999).

The Government of Sri Lanka envisages developing New Renewable Energy (NRE) technologies such as hydro, wind, solar and biomass, to reach a 10% target in power generation by 2015 (Ministry of Power and Energy, 2008). *Mahinda Chintana: Vision for the Future* envisions further extending this goal to reach 20% by 2020. According to the Sri Lanka Sustainable Energy Authority (SEA) (2013), at present, a grid connected to a paddy husk based power plant of a capacity of 12 MW exists in Trincomalee. It generated 22 GWh in 2012, using an estimated 36 thousand tonnes of paddy husk resource in 2012 (SEA, 2013).

The study was carried out in the Minneriya region of the Ceylon Electricity Board (CEB) of the Polonnaruwa district, which has the second highest turnover in paddy production (Department of Census and Statistics, 2013). The main objective of the study is to assess the power generation potential of biomass resources, for the preparation of renewable energy resource maps by the Sri Lanka Sustainable Energy Authority. The specific objectives are (1) To assess the theoretical potential of paddy husk (agro industrial residue) generated in the country, (2) To assess the uses of paddy husk and available potential in power generation in the Minneriya CEB are, (3) To generate a resource flowchart for paddy husk that is available for power generation in the Minneriya CEB Region and (4) To establish a methodology for the assessment of paddy husk available for power generation in a given site.

The rice milling industry consists of two sectors, namely commercial and custom milling, according to the types of mills and technologies used for rice processing (Daranagama, 1999). The total number of rice mills presently operating is approximately 7,000 (Daranagama, 1999, Perera *et al.,* 2005, and Kannan *et al.,* 2013). Of these mills, 77% are custom mills. The balance (23%) is commercial mills. It is estimated that only 50% of the rice is produced in the commercial mills, and other 50% in the custom mills (Senanayake *et al.,* 1999; cited in Perera *et al.,* 2005).In 1997, it was estimated that 447,000 tonnes of paddy husk was produced. In majority of rice processing areas, rice husk is considered as a waste material and its disposal often created environmental problems. Many of the rice mills burned considerable quantities of husk to heat

water or generate steam for parboiling and steaming.

A study conducted by Perera *et al.,*(2005), revealed that in Anuradhapura and Pollonnaruwa districts, approximately 50% of the paddy husk produced is utilised as fuel for steam generation while 44% is left unutilised. But in other areas, 54% of paddy husk produced in commercial mills is used for energy applications, 7% is used for other applications and therefore the excess amount available is estimated to be 39%.

Estimating the theoretical potential of paddy husk generated in the country

Paddy production figures from 1955 to 2010 were obtained from the Department of Census and Statistics (2013). The quantity of paddy husk produced during rice production was estimated using the conversion factor, Residue to Product Ratio (RPR), obtained from published literature. The estimates on the husk availability were made taking into account that husk production is 20% (Daranagama, 1999 and Perera *et al.,* 2005).

Assessment of paddy husk available for power generation in the Minneriya CEB area

Paddy production in a given mill can be correlated to the units of electricity consumption of the mill. Details of electricity consumption of mills in the study site were obtained from the CEB. Data included aggregated consumption of 173 mills, in two classes, namely, Bulk consumption mills (above 42 kVA) – 14 mills and Regular mills (below 42 kVA) – 159 mills. The mills were classified according to their paddy rice milling capacity into the following category. Regular mills (2,000 kg – 25,000 kg of paddy milled per day) and Bulk consumption mills (over 25,000 kg of paddy milled per day). Data was obtained for a period of 28 months, for the period from 2011 January to 2013 April. In the field, out of the total mills, 15% (26 mills) were sampled representatively, to determine the usages of paddy husk using questionnaires.

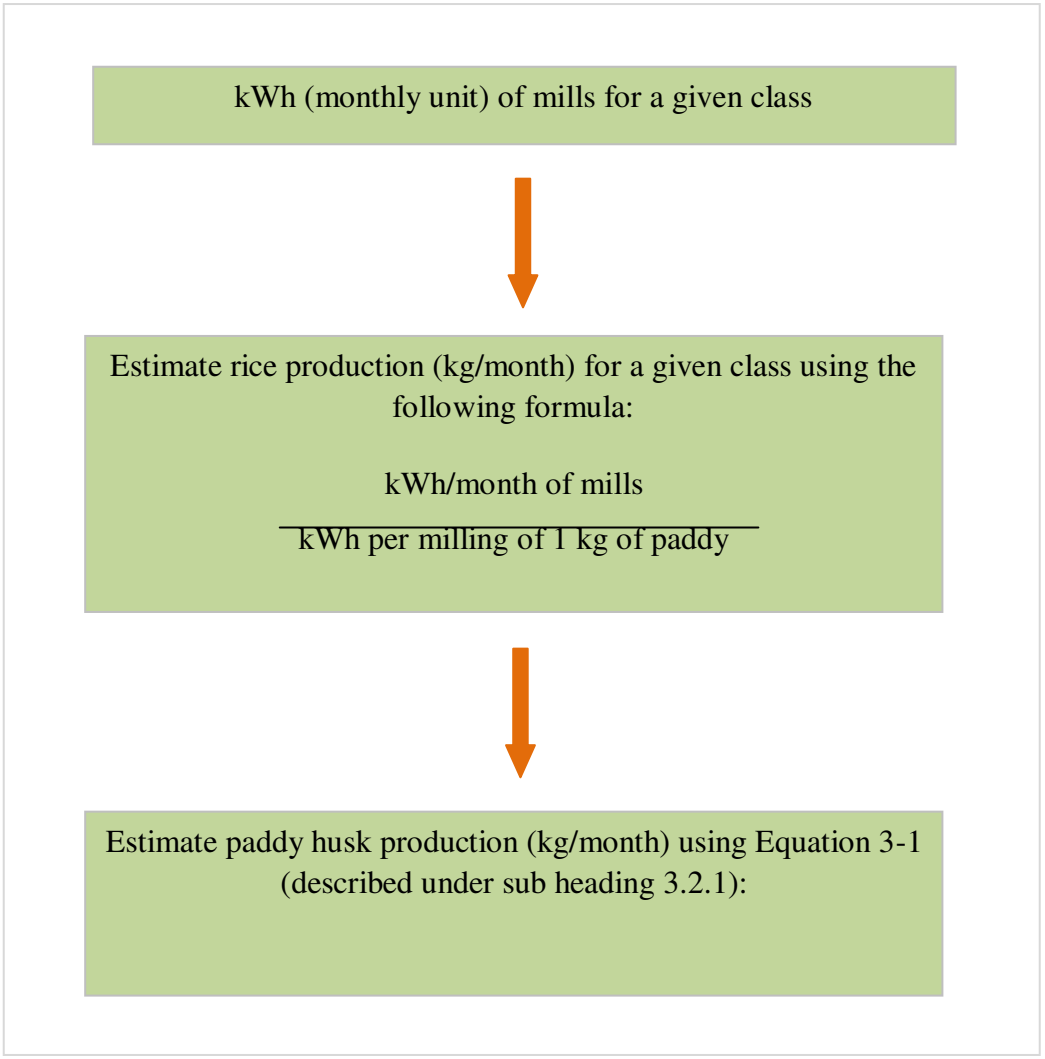

Figure 1: Methodology for determining paddy husk production

The probable income of paddy husk based power generation was calculated using the contemporary tariff applicable for biomass categories (Agricultural and Industrial Waste), LKR 17.71 per kWh (PUCSL, 2013). The plant cost was taken as 243 million and the price of paddy husk was taken as LKR 3.33/kg. The price of electricity for bulk consumption mills was taken as LKR 12.50/kWh (CEB, 2013).

The theoretical potential in paddy husk generated in the country

The highest paddy production is in the Ampara district (615,291 tonnes), in both seasons, Yala and Maha combined, followed by Polonnaruwa (459,201tonnes) and Anurdhapura (427,971 tonnes), respectively. The trend analysis performed for data from 1955 to 2010, indicates that the paddy husk production is estimated to rise upto 790 thousand tonnes by 2013

Assessment of Paddy Husk Available for Power Generation

Of the 26 mills, 4 mills were bulk consumption mills, and 22 mills were regular mills. 5,739 tonnes of paddy husk is generated in the Minneriya CEB area per month. The total monthly paddy husk production in the Polonnaruwa district is estimated to be 7,653 t/month. The Polonnaruwa district contributes by 12% to the national total paddy husk generation, while the Minneriya CEB region contributes by 9% and the Minneriya CEB region contributes by 75%. Results indicate, that, of26 mills, 3,315 tonnes of paddy husk is generated in Minneriya per month, in both types of surveyed mills combined. The bulk consumption mills generated 1,677 tonnes, out of which 1,343 tonnes per month (80%) is used for parboiling, while 11% and 2% exported to kilns (brick and lime) and paper mills, respectively. Only 120 tonnes per month (7%) of the paddy husk supply is available for biomass power generation plants. The total paddy husk supply from regular mills is 1,104 tonnes/month. 95% of this paddy husk supply is used for parboiling (1,118 tonnes/month), while only 5% is exported to brick and lime kilns (64 tonnes/month). There was no contribution for power generation from regular mills. A quantity of 286 tonnes/month is imported to be used in parboiling in regular mills.

The average generation of paddy husk in bulk mills was 3,824 tonnes/ month. In regular mills, the average paddy production is 10 thousand tonnes per month.

Paddy production figures in a given district do not necessarily mean that the entire paddy produced in the district will be milled in the same district. Perera *et al.,* 2005 explains that, it is difficult to estimate the theoretical paddy husk potential on a district-wise basis, using data from the district paddy production figures of the Department of Census and Statistics only, as there exists a considerable transfer of paddy between districts (Perera *et al.,* 2005). Therefore, the theoretical potential of paddy husk for a given district will vary significantly from the available potential of paddy husk, based on whether paddy is exported or imported into the district of concern.

When extrapolated to the actual population of bulk consumption mills, 7% from the average production of 3,824 tonnes of paddy husk per month, gives 268 tonnes of paddy husk for power generation each month. On average, 268 tonnes of paddy husk for power generation is available each month. During peak seasons, upto 370 tonnes per month would be available for power generation. Assuming that 1.64 tonnes of paddy husk is consumed in generating a single MWh, on average, 163 MWh of electricity would be generated from the paddy husk in the Minneriya CEB region.

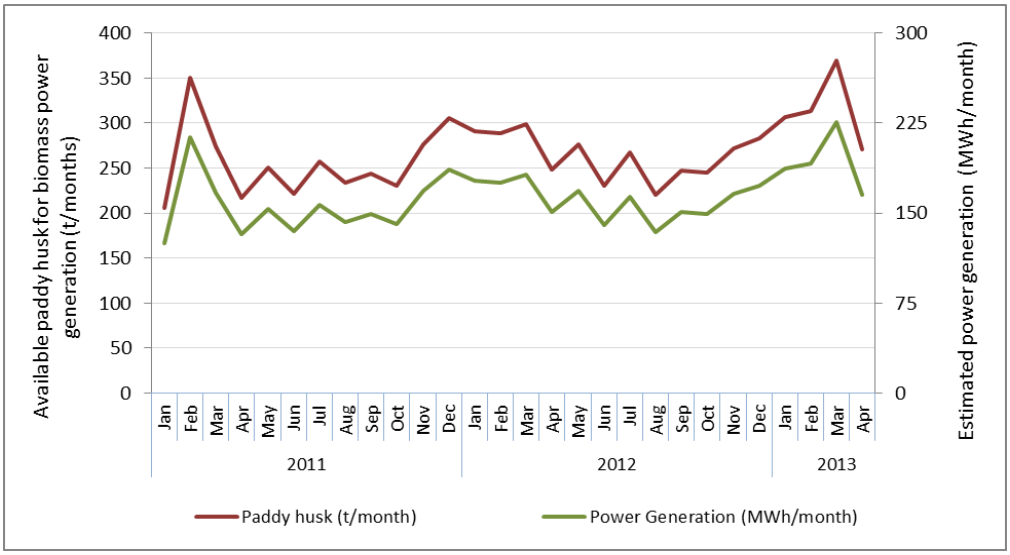

Figure 2 : Available potential of paddy husk for power generation (t/month) and estimated power generation (MWh/month)

In the Central and Eastern districts, paddy is usually parboiled before milling, while in the Southern districts parboiling is not common (Perera *et al.,* 2005). Therefore, it could be assumed that the majority of paddy husk generated in the Southern districts is available for power generation, if it is not used for other applications.

Resource flow chart

This resource flow chart was mapped taking into account the entire quantity of paddy husk generated and its usages deciphered from the 26 sampled mills. 0.9 of the input of paddy husk is generated in the mills, while 0.1 is imported. According to the resource flow chart, only 0.04 is available for power generation. The majority of paddy husk (0.86) is consumed in parboiling. Minor quantities are despatched to brick and lime kilns and a paper mill.

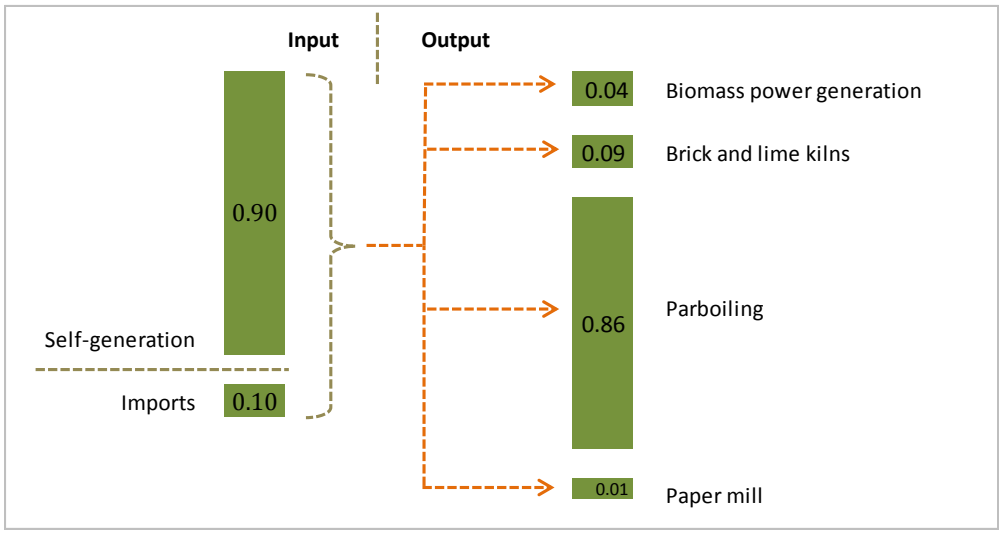

Figure 3 : Annual flow chart of paddy husk in the Minneriya CEB Area

Theoretical potential (Overend, 2008) – the theoretical potential of paddy husk in the Minneriya CEB region was derived from the electricity consumption values obtained from the CEB. Electricity consumption was converted into corresponding paddy husk production figures using established conversion factors. The Technical potential (Overend, 2008) – the actual potential for paddy husk available for power generation in the Minneriya CEB region was deduced by conducting a representative field survey on usage factors of paddy husk and by extrapolating the field results to the actual population of mills. Competition analysis (LDJ 2011) – the competing uses of paddy husk in the Minneriya CEB region was deduced from the field survey and results were extrapolated to the actual population of mills. Uses of paddy husk were also quantified and included in the resource flowchart.

Income generation options from the utilisation of paddy husk under three scenarios in the Minneriya CEB region

The income generation from usage of paddy husk was analysed under three scenarios, (1) Business as Usual scenario, (2) Captive generation scenario and (3) Small power producer scenario. The BaU scenario was considered as the base case, assuming that no power generation projects will be mooted and the prevalent market prices and percentage consumption by traditional users like brick and lime kilns will remain unchanged. The captive generation scenario assumes that millers will use all excess paddy husk available in the region to run a small generator in net metering mode, to reduce their electricity bills. Paddy husk, under this scenario, will be used only for parboiling and for the

captive generation plant. The small power producer scenario assumes that all paddy husk available for other than parboiling in the region will be consumed in a power plant operated by a different investor.

Captive generation

86% of the total paddy husk generated in the Minneriya CEB region is consumed for parboiling. If the balance paddy husk (14%) was used for power generation, it would support a power plant of 823 kW, as calculated below, based on the following assumptions.

Assumptions:

The plant factor of the paddy husk based power plant is 0.8 (M/P&E, 2006)

1.64 kg of paddy husk is consumed in generating a single kWh (SEA, 2013)

Total paddy husk available for power generation in the Minneriya CEB region

= 9,456,428 kg

Power plant capacity (kW)

= 9,456,428/1.64/0.8

= 823

If this power plant (823 kW) operated as a captive generation plant in the Minneriya CEB region, the millers would only have to pay LKR 24.17 million per month on average to the utility (CEB) for electricity consumption, in milling operations. They would save LKR 6.01 million/per month on the bill.

Table 1: Reduced Electricity Bill warranted by the 823 kW Captive Generation Plant

Parameter	Unit	Calculation
Average monthly consumption of bulk consumption mills	MWh/month	2,414.23
Energy charge	LKR million	30.18
Average monthly generation of the captive generation plant (823 kW)	MWh/month	480.51
Energy Charge	LKR million	6.01
Reduced bill	LKR million	24.17

If the power generated from the plant is utilised as a net metered scheme, millers would be able to save LKR 6.01 million per month, on their cumulative electricity bill. This profit is earned by generating energy from the resource (paddy husk) and providing it to the grid. This profit could be shared equitably

among millers, who contribute by supplying paddy husk to the plant.

Small power producer scenario

The tariff applicable is LKR 17.71/kWh at the time of the study (PUCSL, 2013). With a paddy husk price of LKR 3.33/kg, on average, the income of the millers in bulk consumption mills in the Minneriya CEB area would be LKR 31.49 million per annum.

Income = Total available paddy husk (kg) x price (LKR/kg)
= 9,456,428 kg * 3.33 LKR/kg * 12/ 10^6
= LKR 2.62 million

The present investment of a 822 kW paddy husk based power plant would be LKR 200 million. With the investment of LKR 200, investors would be able to enjoy a return of LKR 20.27 million per annum, even after servicing a 60% debt on investment. If an investor constructed a power plant using this paddy husk, the return on investment would be 22% per annum to the investor. This scenario analyses the benefits of the sale of paddy husk to an investor, therefore, the millers would earn only by selling the resource (paddy husk) and the profit they would gain is less than in the previous scenario (LKR 2.62 million).

Proposed methodology for the assessment of the annual availability of paddy husk for power generation in a given area

The methodology established through this study, for the assessment of paddy husk availability for power generation in a given site, on an annual basis. The proposed methodology is two faceted.

Step 1:

a) The total generation of paddy husk of a given site was derived from the electricity consumption data of mills, obtained from the CEB.

b) Based on the kVA values, mills are classified as bulk consumption mills (above 42 kVA) and regular mills (below 42 kVA).

c) The corresponding paddy milled in each category of mills is obtained by using the conversion factor, *i.e.,* 4.2 kWh is consumed to mill 50 kg of paddy, which was based on information gathered from the questionnaire survey. This gives the milled quantity of rice.

d) Subsequently, the Residue to Product Ratio of 0.2 is used to estimate the quantity of paddy husk generated in the paddy milling process. (Each 1 kg of paddy milled generates 0.2 kg of paddy husk.) This gives the total quantity of paddy husk generated in each mill category.

Step 2:

a) A field survey was designed to sample paddy husk usages of the site of concern.

b) Mills were classified as regular mills and bulk consumption mills based on their daily milling capacity. Mills that milled paddy rice between 2,000 kg – 25,000 kg per day were classified as regular mills, whereas mills that milled paddy rice above 25,000 kg per day were classified as bulk consumption mills.

c) The representative field survey was used to derive;
   - usage factors (usages) of paddy husk
   - the electricity consumption to (kWh) to mill 50 kg of paddy rice (used in step c) of Step 1 above)

Step 1 and Step 2 were done in parallel. Forecasting in this study was done using simulation modelling on spread sheets (MS Excel 2007 version).

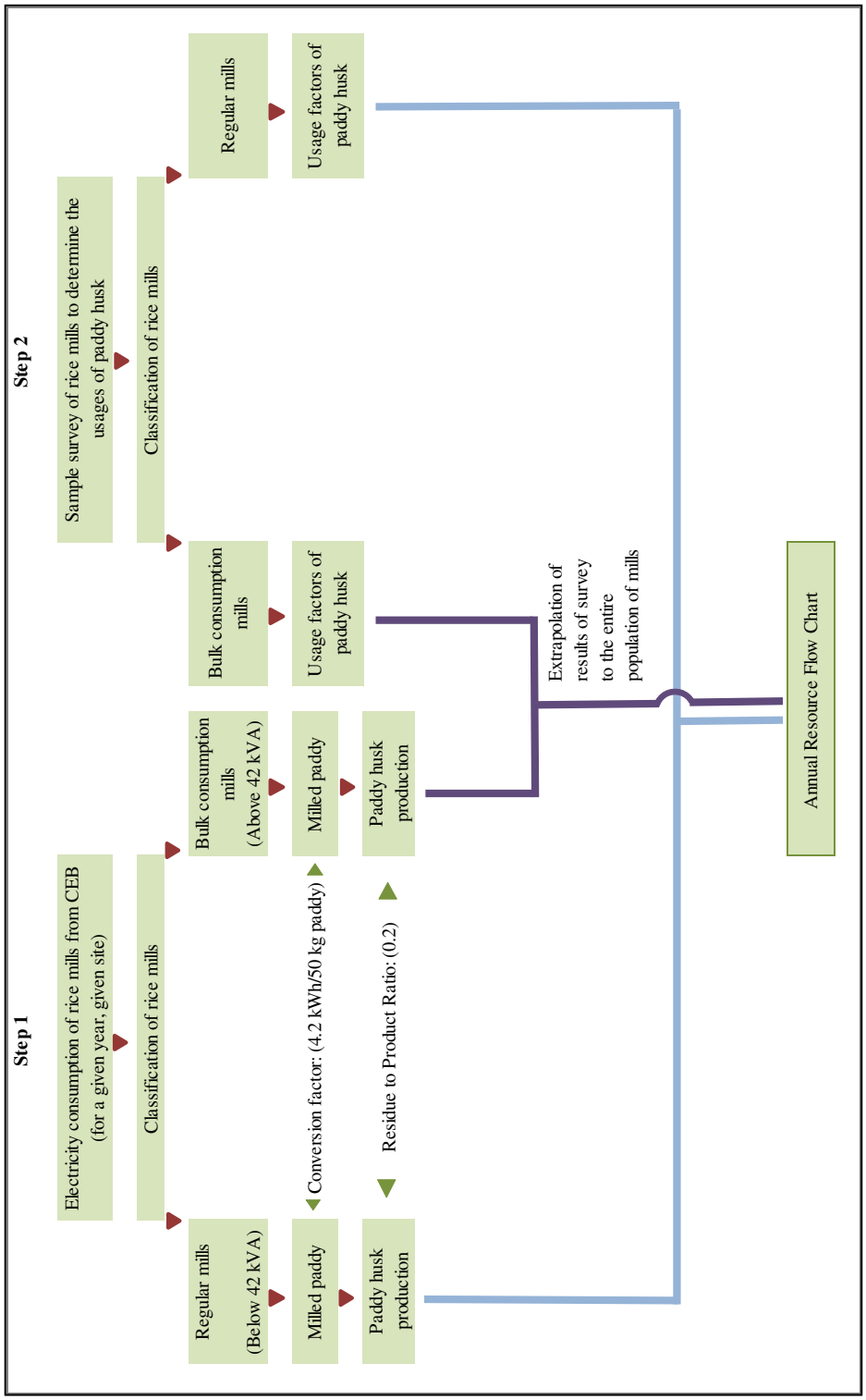

Figure 4: Methodology for the assessment of the annual availability and usage of paddy husk in a given area

In summary, the methodology proposed by this study, considers the following. The (1) Location of the resource (GIFT, 2013) – the results of this study is specific to the Minneriya CEB region and the Polonnaruwa district by large. (2) Paddy husk production figures for a given district cannot be derived from the district paddy production figures published by the Department of Census and Statistics alone, since there is a considerable inter-transfer of paddy rice within districts (Perera *et al.,* 2003). Hence, the total quantity of paddy rice produced in a district may not be milled within the district, rather, a considerable portion could be transferred to other districts for milling. But the total paddy husk generated in the district of concern can be deduced by analysing the electricity consumption figures of the operational rice mills in the given district. (3) The paddy usage factors vary among districts. Accordingly, the availability of paddy husk for power generation too varies. The actual availability of paddy husk for power generation can only be deduced through a site-specific (*i.e.,* district or region specific) survey conducted in the area of concern.

Conclusion

This study deduced the theoretical potential and technical potential of paddy husk available for power generation in the Minneriya CEB region, and also performed a competitive analysis to derive the competing uses of paddy husk in the area. The availability of paddy husk for power generation was 7%, while the highest use of paddy husk was for parboiling (86%). Only paddy husk generated at bulk consumption mills were available for power generation. The quantity of paddy husk available for power generation and other applications vary each year. The study proposed a methodology for the assessment of available potential of paddy husk for power generation, by considering the location of the resource, inter-district transfer of paddy husk and area specific usage factors of paddy husk. Additionally, the study recommends including the economic potential, which would estimate the cost of biomass resources at the field. The study concludes that the Captive Generation Scenario is the most profitable method to utilise paddy husk for power generation with net metering, in a given area. This profit could be shared equitably among millers, who contribute by supplying paddy husk to the plant.

References:

[1] Daranagama, U. (1999). *Availability of Fuelwood and Other Agricultural Residues as a Source of Energy in the Industrial Sector of Sri Lanka*. National Engineering and Research Development Centre, Colombo.

[2] Global Institute for Tomorrow. (2013). *Rice Husk to Electricity: Power Generation from 100% Biomass in Cambodia*

[3] Kannan, N., Dharmasena, D. A. N. & Mannappruma, J. D. (2013). Effects of Aerated Cold Water Soaking on Effluent Generation, Milling Yield and Sensory Characteristics of Cooked Parboiled rice. *Abstracts of Papers,*2nd Sri Lankan Roundtable on Sustainable Consumption and Production, Colombo, Sri Lanka, 2013.

[4] Khullar, V. (2005). *Post Harvest Profile of Paddy/Rice.* Ministry of Agriculture, India

[5] LD Jellison, Inc. (2011). *Biomass Fuel Resource Study; Clark County Central Campus – District Heating Co-Generation*. Clark County Public Services Center, Washington, USA.

[6] Ministry of Power and Energy. (2008). *National Energy Policy and Strategies of Sri Lanka (2008).* Sri Lanka.

[7] Ministry of Power and Energy. (2006). *Discussion Paper on Non-Conventional Tariff Methodology.* Sri Lanka

[8] Overend, R, P. (2008). *Survey of Biomass Resource Assessments and Assessment Capabilities in APEC Economies.* National Renewable Energy Laboratory (NREL). Colorado, USA

[9] Perera, K.K.C.K., Rathnasiria, P. G., Senaratha, S. A. S., Sugathapala, A. G. T., Bhattacharyab, S. C. & Salam, A. (2005) Assessment of Sustainable Energy Potential of Non-plantation Biomass Resources in Sri Lanka. *Biomass & Bioenergy*, in press

[10] Sri Lanka Sustainable Energy Authority. (2012). *Sri Lanka Energy Balance 2012*. Sri Lanka Sustainable Energy Authority, in press.

[11] Senanayake, D. P., Daranagama, U. & Fernando, M. D. (1999). *Availability of Paddy Husk as a Source of Energy in Sri Lanka.*National Engineering Research and Development Centre, Sri Lanka.

Design of a Radio Frequency Energy Harvesting Circuit for Sustainable Electronic Application

Balasooriya, B.M.N.[1], Edirisooriya, E.M.G.C.[2], Gedarakumbura, U.D.K.[3]
Dr. Wijekulasooriya, J. V., Dr. Suraweera, S. A. H. A., Dr. Godaliyadda, G. M. R. I.
Department of Electrical and Electronic Engineering, Faculty of Engineering, University of Peradeniya, Sri Lanka
[1]jump2narada@live.com, [2]gayanc91@gmail.com,
[3]uthpala.dkg@gmail.com

Abstract

In this paper we present study of ambient energy harvesting techniques in urban and semi urban environments. Ambient energy harvesting, also known as energy scavenging, the process where energy is obtained and converted from the environment and stored for use in electronics applications. Usually this method is applied to energy harvesting for low power devices, such as wireless sensor networks, or portable electronic equipment. In some applications, where the power supply is embedded into the structure, making battery replacement impossible without destroying it, RF power harvesting could be very useful. Therefore, the ability of RF power harvesting device to replace the batteries and provide a unique and independent energy source to save on the operation and maintenance cost has made it a favorite alternative sustainable source of energy, and has brought much attention and care for development. Some of the advantages are maintenance fee due to no battery replacement, environment friendly and even can develop applications that could work underwater. A prototype has been built showing good agreement with the simulated results. There an output of 4.4 V was achieved using 5 stage voltage doubler circuit which can power up LED and clock.

Keywords: Radio Frequency, Energy Harvesting, Low Power Devices, Ambient Energy Harvesting, GSM, Wi-Fi, Antenna, Microstrip Patch Antenna

Introduction

The use of wireless devices has increased in past few years. The most of applications in the mobile phones, sensor networks which are difficult to reach for changing batteries. There are number of sources that can use for energy harvesting such as solar power, thermal energy, wind energy, kinetic energy and RF energy. In our study we use RF energy as the source of energy harvesting since it is available all the time in the day. Mainly we use RF frequencies in the range of GSM900, GSM1800 and Wi-Fi.

Radio frequency energy is emitted by sources that generate high electromagnetic fields such as TV signals, wireless radio networks and cell phone towers, but through using a power generating circuit linked to a receiving antenna this free flowing energy can be captured and converted into usable DC voltage. Most commonly used as an application for radio frequency identification tags in which the sensing device wirelessly sends a radio frequency to a harvesting device which supplies just enough power to send back identification information specific to the item of interest. Depending on concentration levels which can differ through the day, the power conversion circuit may be attached to a capacitor which can disperse a constant required voltage for the sensor and circuit when there isn't a sufficient supply of incoming energy.

The design we use for RF energy harvesting comprised with four major components which are namely the antenna, resonator circuit, conditioning circuit and storage unit. The antenna is to receive the different frequencies from the ambient then the resonator circuit will response accordingly to that bandwidths, thereafter the conditioning circuit will improve the output voltage and finally the storage unit will manage that harvested energy.This paper is divided into the following sections. The antenna design is presented in Section 4. Section 5 presents the resonator implementation. In Section 6.1, simulation results. A prototype is made for validating the simulated results for a five stage voltage doubler circuit design. Finally, conclusions are given.

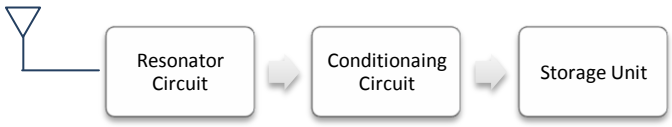

Figure 1: Block diagram of energy harvesting circuit design

Antenna Design

Antenna is a significant component in RF energy harvesting design as an efficient RF signal power receiving circuit. Main function of antenna is to grab RF energy and convert that RF energy into electrical form. Depending on the frequencies which are interested, the antenna design requirements are different. There are several factors that have to be concerned when designing an antenna such as gain, efficiency, bandwidth, center frequency and size.

And the use of Micro strip patch antennas made the outcome portable and handy. Micro strip patch antennas consist basically of three layers, a metallic layer with the antenna element pattern, a dielectric substrate and another metallic layer as the ground plane [1, 2]. These types of antennas are relatively easy to manufacture because of their simple planar configuration and the compact structure. They are light in weight and have the capability to be integrated with other microwave circuits. The volume constraints, often combined with large bandwidth and high efficiency specifications, make the antenna design a challenging task.

Currently many researches started to design MPAs which cover GSM900, GSM1800, UMTS, WIFI, WiMAX, etc...A simple MPA can be fabricated with the following calculations.

$$W = \frac{c}{2f_0\sqrt{\frac{\varepsilon_r+1}{2}}} \quad \text{Eq.1}$$

Where *W* is the width of the MPA, $f_0$for the resonance frequency, ε_r the relative Permittivity of the dielectric substrate and *c* for the speed of light respectively.

$$L = L_{\text{eff}} - 2x0.412h\left(\frac{(\varepsilon_{\text{eff}}+3)\left(\frac{W}{h}+0.264\right)}{(\varepsilon_{\text{eff}}-0.258)\left(\frac{W}{h}+0.8\right)}\right) \quad \text{Eq.2}$$

Where *L* for the length of the patch antenna and *h* express the height of the substrate and $\varepsilon_{\text{eff}}$is defined as

$$\varepsilon_{\text{eff}} = \frac{\varepsilon_r+1}{2} + \frac{\varepsilon_r-1}{2}\frac{1}{\sqrt{1+12\left(\frac{h}{W}\right)}} \quad \text{Eq.3}$$

The performance of the rectangular shaped MPA with the dialect height of0.762mm and a dielectric constant of 3.2 (Fig. 2(a)) is analyzed. The MPAs were simulated to 910MHz, 953 MHz, 1767.5MHz, 1.2GHz, 2.4 GHz and 10GHz. (Fig. 2(b)). This analysis were done using HFSS software. As shown in Fig. 2(c) and the rectangular shaped MPA has a reflected power radio of -24.30dB.

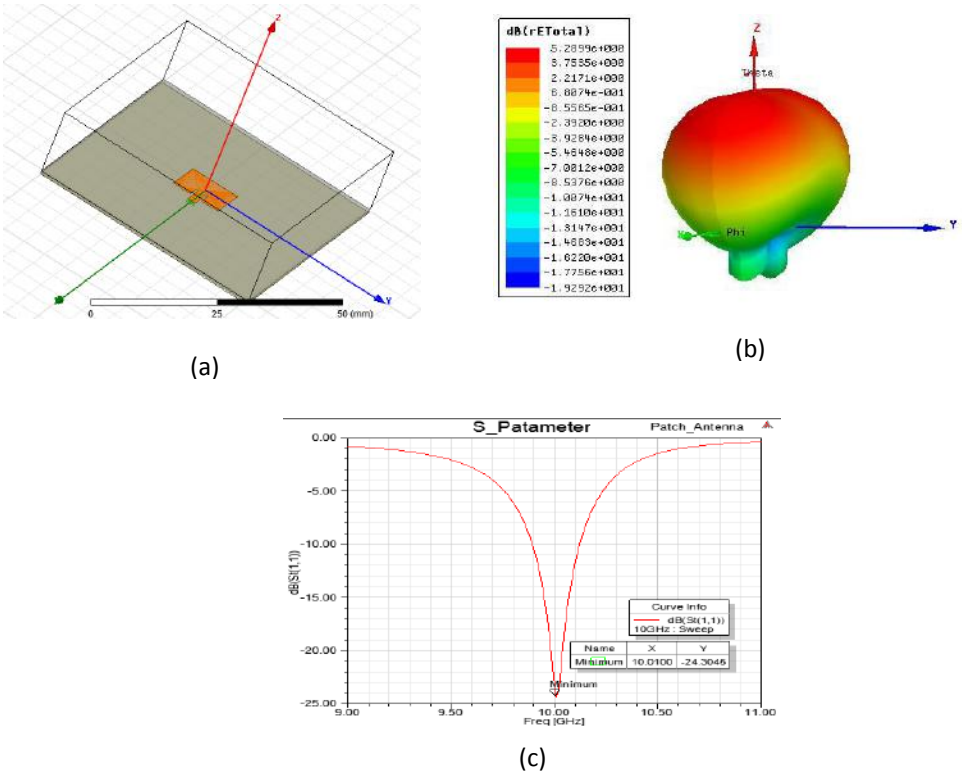

(a) (b)

(c)

Figure 2: Simulation top view of the MPA (a), Far Field radiation Pattern (b), reflected power ratio (c)

After the fabrication process the simulated results were compared with the actual results and close values were obtained. Then the MPAs were used in the harvesting process.

Resonator Implementation

A resonator is a device that exhibits resonance that is, it naturally oscillates at some frequencies, called its resonant frequencies, with greater amplitude than at others. Voltage doubler circuit exhibits nonlinearity because impedance of the circuit varies with the input signal frequency. So the maximum power transfer occurs when circuit matched with the antenna. Variation of magnitude and phase of impedance were obtained using spectrum analyzer and required impedance was calculated to design impedance matching circuit.

Along with the resonance the impedance matching was done, to get the input impedance of the conditioning circuit with the variance of the frequencies for single & five stages (Fig. 3(a)).

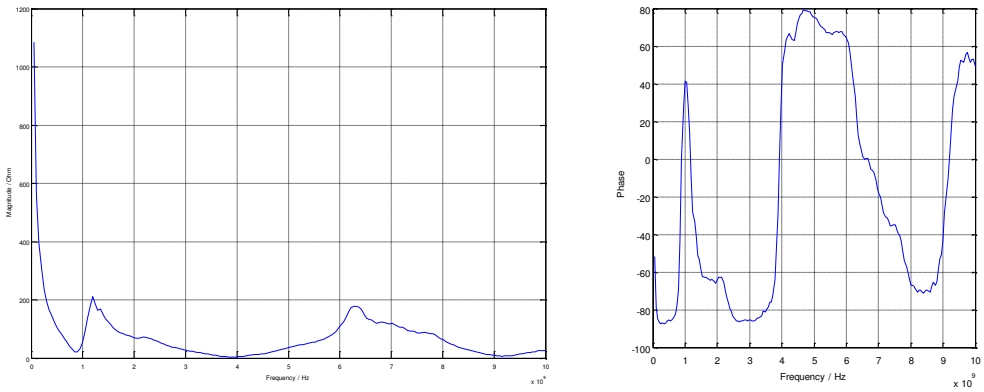

Figure 3: impedance variation of single stage voltage doubler circuit with the input signal frequency

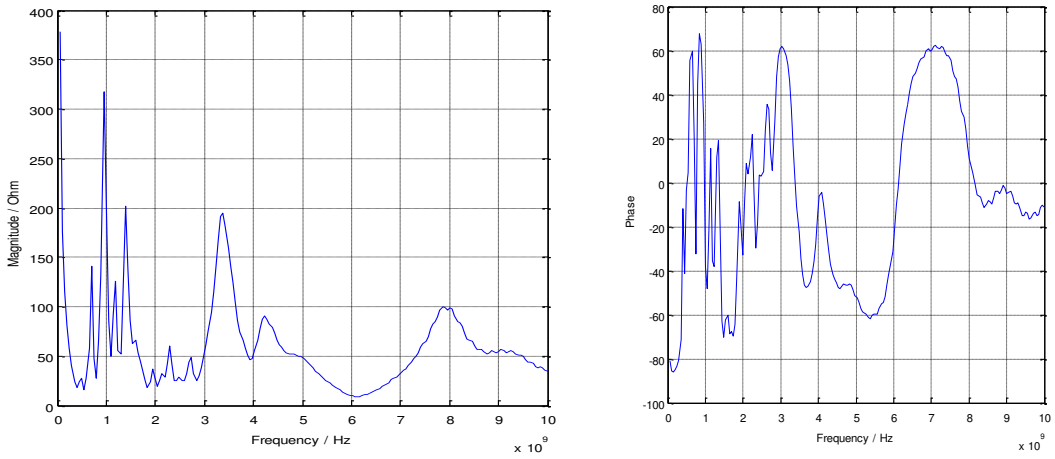

Figure 4: impedance variation of five stages voltage doubler circuit with the input signal frequency

The impedance matching circuit parameters were logged with frequency (Table.1) that is obtained from the MPAs.

Table 1: Impedances for antenna designed frequencies

Frequency	Single stage		Five stage		Rectangular form	
	Magnitude	Phase	Magnitude	Phase	1	7
910 MHz	23.84	7.85	184.5	52.43	23.62+j3.26	112.5+j146.24
953 MHz	36.12	30.37	299.3	17.06	31.16+j18.26	286.13+j87.81
1.2 GHz	209.1	-11.54	116.8	-35.84	204.87-j41.83	94.68-j68.39
1.767 GHz	85.3	-63.28	30.61	-67.12	38.35-j76.19	11.9-j28.2
2.4 GHz	61.12	-79.78	25.4	-13.56	10.84-j60.15	24.69-j5.96
10 GHz	25.88	48.5	34.65	-11.16	19.14+j21.63	33.99-j6.71

Conditioning circuit

Voltage appears after RF to DC conversion at the end of the antenna is not considerably large amount. Also it is a nearly similar to a sinusoidal signal. In that case conditioning circuit is more important to make that signal in an appropriate way to use before store it. Here we used voltage doubler as RF to DC converter.

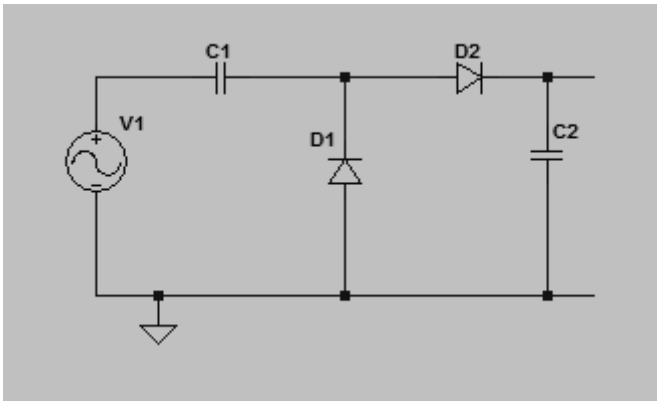

Figure 5: Voltage Doubler Circuit

Voltage Doubler is a voltage multiplier circuit which has a voltage multiplication factor of two. This simple diode-capacitor pump circuit gives a DC output voltage equal to the peak-to-peak value of the sinusoidal input.During the negative half cycle of the sinusoidal input waveform, diode D1 is forward biased and charge the capacitor C1 to the peak value of the input voltage V1. Because there is no path for capacitor C1 to discharge, it remains fully charged and acts as a storage device in series with the voltage supply. At the same time, diode D2 conducts via D1 charging up capacitor C2.

During the positive half cycle, diode D1 is reverse biased blocking the discharging of C1 while diodeD2 is forward biased charging up capacitor C2. But because there is a voltage across capacitor C1 already equal to the peak input voltage, capacitor C2 charges to twice the peak voltage value of the input signal (2V1). It is difficult to smooth out this large ripple frequency in much the same way as for a half wave rectifier circuit, but it captures the power from both negative and positive half cycles. So it is more efficient than simple half wave rectification circuit.

Simulation

Simulation on voltage doubler circuit was done using *LTspice IV* software. *LTspice IV* is freely available software. *LTspice IV* is a high performance SPICE simulator which gives schematic capture

and waveform viewer. The enhancements to SPICE have made simulating switching regulators extremely fast compared to normal SPICE simulators, allowing the user to view waveforms for most switching regulators in just a few minutes.

A good advantage with voltage doubler circuit is we can cascade stages in series. Figure 4 shows two stages of voltage doubler cascade in series.

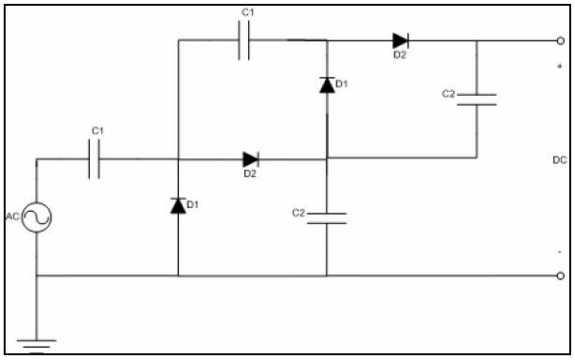

Figure 6: Two stage voltage doubler

Increasing of stages of voltage doubler circuit has high effect on the output voltage. The capacitance, both in the stages and at the end of the circuit, affects the speed of the transient response and the stability of the output signal.

The number of stages is essentially directly proportional to the amount of voltage obtained at the output of the system. Generally, the voltage of the output increases as the number of stages increases.

Table 2: Output voltage variation with the number of stages

Number of stages	Output DC voltage/ V
1	0.72
2	1.35
3	2.00
4	2.70
5	3.35
6	4.00
7	4.70
8	4.75
9	5.40

Storage unit

It is required to have efficient and reliable storage unit to give continuous output. When selecting storage unit there are several facts has to be considered such as capacity, life time, discharging ability, internal impedance and cost. As the storage unit we have used a super capacitor. They are unique, ultra-high capacitance devices utilizing Electrochemical Double Layer Capacitor (EDLC) construction combined with new high performance materials. Super capacitor differs from a regular capacitor in that it has a very high capacitance.

Table 1: Specifications of Super Capacitor

Specifications	
Working Voltage	5.0V
Surge Voltage	6.0V
Capacitance	0.1F to 1F
Capacitance tolerance	-20% to +80%(200C)
Operating Temperature Range	-250C to 700C

Conclusion

This paper presents simulated and experimental investigations for Radio Frequency Energy Harvesting to energize low power devices placed in remote areas. Circuit implementations to obtain effective output voltage were studied. Also to get maximum power output impedance matching circuit between antenna and voltage doubler circuit was designed since conditioning circuit exhibits non linearity in different input signals. Grabbing RF energy is more important in our studies. Therefore receiving antennas for GSM bands and Wi-Fi were designed. Super capacitors were used as energy storage device to get reliable output. With help of simulations and designs output of 4.4 V was achieved using 5 stage voltage doubler circuit which can power up LED and clock.

References

[1] Balanis, C. A., Modern Antenna Handbook, 1st Edition, John Wiley and Sons, Inc., 2008.

[2] Pozar, D. and D. Schaubert, Microstrip Antennas: The Analysis and Design of Microstrip Antenna Arrays, Wiley-IEEE Press, 1995.

[3] S. Sudevalayam and P. Kulkarni: Energy Harvesting Sensor Nodes: Survey and Implications, IEEE Communications Surveys & Tutorials, vol. 13, no. 3, pp. 443-461, Third Quarter 2011.

[4] A. Kansal, J. Hsu, S. Zahedi, and M. B. Srivastava: Power Management in Energy Harvesting Sensor Networks, ACM Transactions on Embedded Computing Systems, vol.6, no.4, article 32, Sep. 2007.

[5] C. M. Vigorito, D. Ganesan, and A. G. Barto: Adaptive Control of Duty Cycling in Energy-Harvesting Wireless Sensor Networks, Proc. of 4th IEEE Conference on Sensor, Mesh and Ad Hoc Communications and Networks (SECON 2007), pp. 21-30, San Diego, CA, June 2007.

[6] Manuel Piñuela, Student Member, Paul D. Mitcheson, Senior

Member, and Stepan Lucyszyn, Senior Member, Ambient RF Energy Harvesting in Urban and Semi-Urban Environments. IEEE transactionsonmicrowavetheoryand techniques,Vol.61,No.7,July2013.

[7] T. Le, K. Mayaram, T. Fiez; Efficient Far-Field Radio Frequency Energy Harvesting for Passively Powered Sensor Network. IEEE 2008

[8] Roundy, S. J., "Energy scavenging for wireless sensor nodes with a focus on vibration to electricity conversion," PhD Thesis, University of California, Berkeley, USA, 2003.

[9] Sabate, J. A., Kustera, D. and Sridhar, S., Cell-Phone Battery Charger Miniaturization. IEEE Journal 2000.

[10] T. Ungan, L. M. Reindl; Concept for Harvesting Low Ambient RF-Sources for Microsystems Laboratory for Electrical Instrumentation, IMTEK, University Freiburg, Germany

[11] "Intel Demos RF Energy Harvesting Technology," TreeHugger. [Online]. Available: http://www.treehugger.com/clean-technology/intel-demos-rf-energy-harvesting- technology.html.

[12] "RF energy harvesting circuit - Patent application." [Online]. Available: http://www.faqs.org/patents/app/20090152954.

[13] "Tune In Charge Up RF Energy Harvesting Shows its Potential | DigiKey." [Online]. Available: http://www.digikey.com/en/articles/techzone/2013/may/tune-in-charge-up-rf-energy- harvesting-shows-its-potential

Characterization of Municipal Solid Waste in Western Province, Sri Lanka: Way Forward to Waste-to-Energy

Dilhani J.A.T.[1], Subasinghe G.[1], Athapattu B.C. L.[2], Jayampath S.D.U.[3]

[1]*Sri Lanka Sustainable Energy Authority*

[2]*Department of Civil Engineering, The Open University of Sri Lanka*

[3]*Department of Town & Country Planning, University of Moratuwa*

Abstract

Characteristics and amounts of municipal solid waste depend on the socio-economic level of a country (Levien van Zon and Nalaka Siriwardena, 2000). With the changing socio-economic status of a country it is expected that the municipal solid waste's organic share gradually decreases while inorganic and combustible fractions progressively increases. Waste- to- energy (WTE) incineration is one of the option of solid waste management, which recovers energy from MSW and produces electricity or steam for heating. Therefore, understanding of characteristic of solid waste is utmost important as MSW is recognized as a renewable source of energy. This study focuses on detailed composition analysis of municipal solid waste and the characteristics of solid waste collected within the Colombo municipality. Further the results were compared with composition analysis obtained in 2004 in order to investigate perspective on MSW as a Waste- to- energy (WTE) option in renewable energy sector.

Background

Sri Lanka ranked among the lower-middle-income country category has an increasing urban population like many other developing countries. In 2012, Colombo district accommodate approximately 2.3 million persons apart from the large number of people daily travelling to the city because their work places are located in Colombo and suburbs or for other administrative purposes. These hosts and visitors generate significant amounts of solid waste which has now become huge burden to the local authorities. Composition and characteristics of Municipal Solid Waste (MSW) changes with the income level of the people. A MSW characterization had been conducted in 2004 by the Central Environmental Authority when the per capita Gross Domestic Production (GDP) was USD 1,250. Now the country's per capita GDP is approximately USD 3,400 indicating the requirement for a new MSW characterization within Colombo municipality. The characterization has been conducted under an internationally recognized methodology as such reliable information is needed in aligning waste management activities.

Available data indicates that the per capita solid waste generation in the country ranges between 0.4-0.85kg/day. The total waste generation is estimated to be 6,400 tons/day whereas waste collection is only about 3,700 tons/day. Western province accounts for more than 60% of the country's daily waste generation. There are two major garbage dump sites in western province; Meethotamulla and Karadiyana. Average daily MSW delivered to Meethotamulla dump site is approximately 800 tons/day while Karadiyana site receives400-450 tons/day. It is estimated that around 250-300 tons/day of the solid waste is treated as composting or organic fertilizer in the Western province, and the rest is diverted to 16 non-engineered open-dump sites.

Sri Lanka Sustainable Energy Authority (SEA), which is guiding the development of various indigenous energy resource of the country, receives considerable number of wastes-to-energy project proposals based on main dump sites of Colombo municipalities. Majority of these project proposals are not technically sound due to lack of understanding of the local waste characteristics. Therefore, it is proposed to conduct a waste characterization analysis in order to facilitate and streamline waste management activities through appropriate technology selection and providing project developers with crucial information of local waste characteristics.

Research objective

The main objective of this research is to detailed characterization of Municipal Solid Waste (MSW) which include composition analysis, and thermal characteristics (proximate, ultimate analysis and calorific value)

Location and Waste Receiving

This waste characterization analysis will be based on waste disposal at Meethotamulla open dumpsite which is located in the municipal council area of Kolonnawa in Colombo district. The location coordinates of this site is 6°56'17.9"N 79°53'26.0"E, and the area is demarcated in figure 01. The Colombo municipality includes six administrative districts namely D-01, D-02A, D-02B, D-03, D-04 and D-05. Waste generation within Colombo municipality is collected by the Colombo Municipal Council (CMC) through private contracted such as Abans Pvt Ltd. The collected wastes are directed to Meethotamulla dump site which handles approximately 40 % of waste collection of the district. Above six administrative districts and corresponding waste collections are shown in Figure 02.

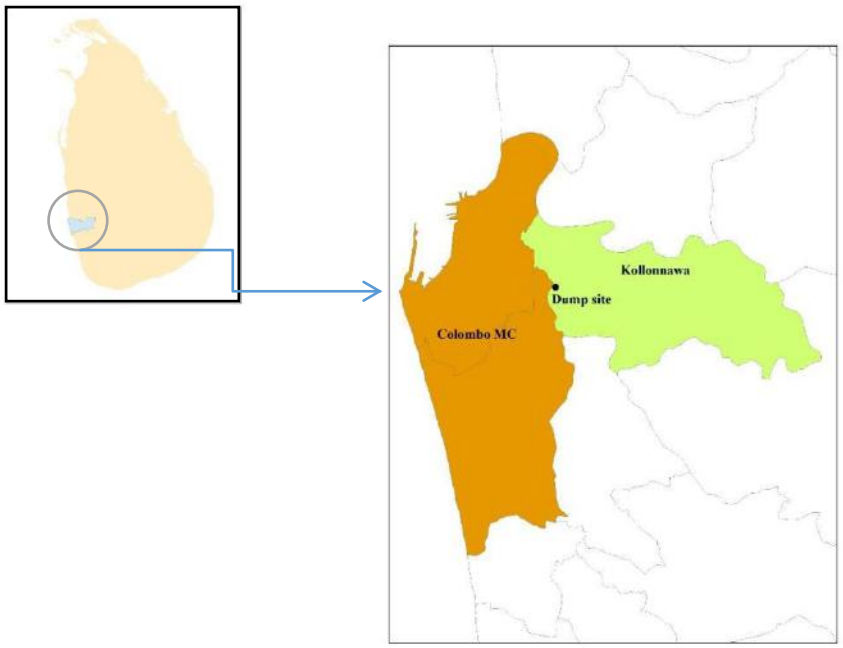

Figure 01: Location of Meethotamulla solid waste dump site

Other than the above six administrative areas, Kollonnawa municipality and waste generates from military camps located in the Colombo city are directedto Meethotamulla dump site.

Table 01 summarizes the various types of solid waste receiving to the dump site classified as Debris (DE), Earth (EA), Garbage (GA), Red Earth (Red EA), Pruning Trees (TR) and other materials.

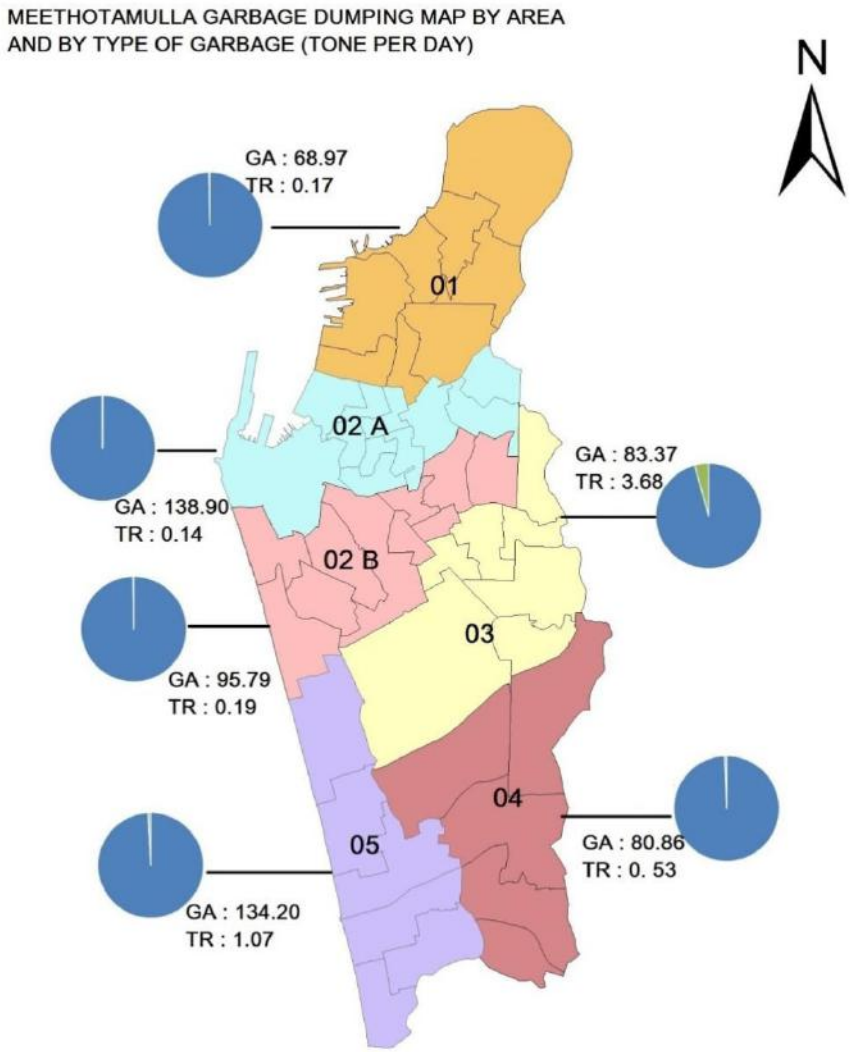

Figure 02: Administrative areas of CMC and amount of waste receiving to Methotamulla dump site

Table 01: Details of MSW of various locations received by Methotamulla dump site

Area	Debris (DE)	Earth (EA)	Garbage (GA)	Red Earth (RED EA)	Trees (TR)	Other	Grand Total
District 1	0.30	1.02	68.97	0.01	0.17	0.22	70.69
District 2A	2.30	1.17	138.90	0.10	0.14	0.38	142.98
District 2B	1.58	1.37	95.79	0.21	0.19	0.28	99.42
District 3	3.08	2.05	83.37	0.05	3.68	0.17	92.40
District 4	4.76	2.20	80.86	0.05	0.53	0.23	88.62
District 5	3.80	2.87	134.20	0.03	1.07	0.43	142.40
Military Camps	41.80	10.28	16.52	0.03	0.71	0.01	69.36
Kollonnawa MC	0.17	0.39	34.96	0.03	0.08	0.09	35.72
Other	38.11	29.56	22.47	5.26	1.33	0.37	97.10
Total	95.91	50.90	676.03	5.76	7.92	2.17	838.69

Methodology

Waste characterization study is based on ASTMD5231 – 92 – 2008 methodology which is a standard test method in determining the composition of unprocessed municipal solid waste by the American Society for Testing and Materials.

Since the composition of the waste stream varies during the calendar year due to cyclical patterns of local climate, social activities, demography and trade or commerce the generator based residential study was planned to collect MSW throughout the year. The number of samples to be analysed was decided based on the statistical calculation assuming organic as the main component of MSW. The details of statistical analysis are given in Annex 01. The minimum number of samples for the year (36) was statistically representative of the waste stream for the year and reflect cyclical patterns and seasonal variation. However this paper summarizes the results of 22 samples, which have been analyzed to date.

According to the percentage of waste received to the dump site, 36 number of samples were divided among different administrative districts and regions. The sampling schedule is given in Annex 02.

The MSW was collected randomly during each day. At the Meethotamulla dump site, the designated MSW loaded vehicle was directed to the specific area for secured unloading. Out of the load about 400kg was selected and discharge to a flat surface with swept clean area. After well mixing, using the cone quarter method, 100kg of sample was picked for composition analysis. A comprehensive list of waste components for sorting was carried out to select among 46 categories according to the given table in Annex 03 and net weights of different waste components were recorded.About 5kg was separated out of theremaining sample for moisture and chemical analysis such as calorific value, volatile

matter, fixed carbon content and ash content.

If there are many identical composite items (eg. plastic – sheathed aluminum electrical conductor etc), they were collected into the waste component containers corresponding to the materials present in the item, and in the approximate proportions according to the estimated mass fraction of each material in the item and were recorded.

Results and Discussion

Solid waste can be classified into 12 major categories which can be further categorized into 46 sub-categories (Annex 03). Above ASTM methodology indicates that 36 sample is needed to be analysed. Nonetheless only 22 waste samples have been analysed by the month of October 2015. The MSW composition of Municipal councils in 2015is presented in Figure 03 while the same in 2004 is shown in Figure 04. The 2004 composition analysis was conducted by the Central Environment Authority. When composition characteristics both studies are compared, it is clearly noticed that the biodegradable organic component has reduced whereas plastics including polythene, paper and cardboard percentages have increased over the time. The biodegradable percentage has dropped from 65% to 52% between 2004 and 2015. Polythene and plastics percentages have increased to 12% from 5.4% as well as paper and cardboard percentage has increased to 11.35% from 7% during the last decade.

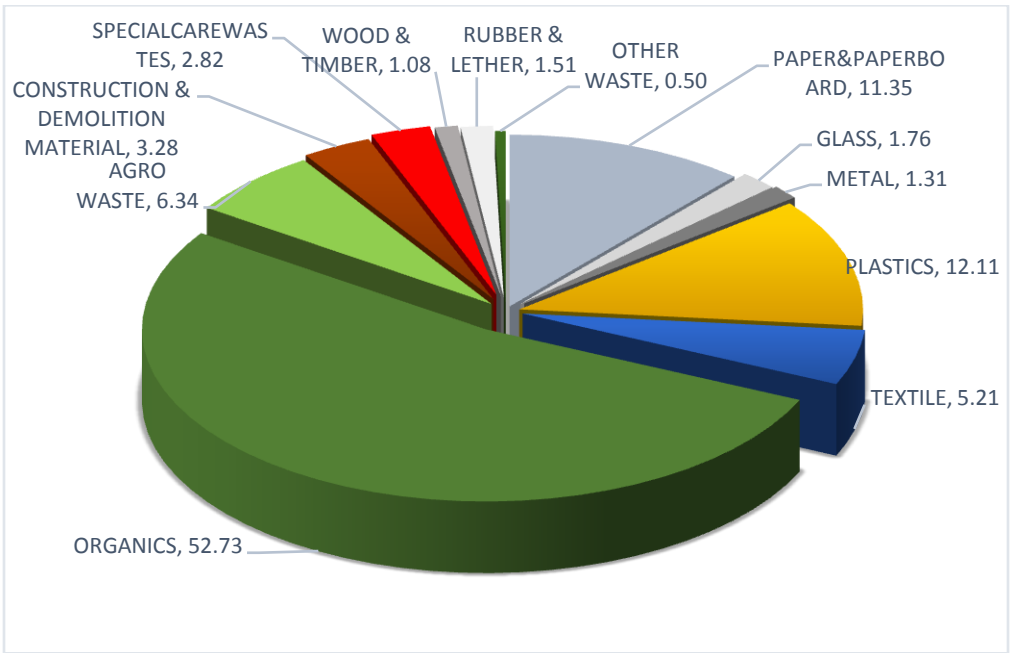

Figure 03: MSW composition of Municipal Councils in 2015

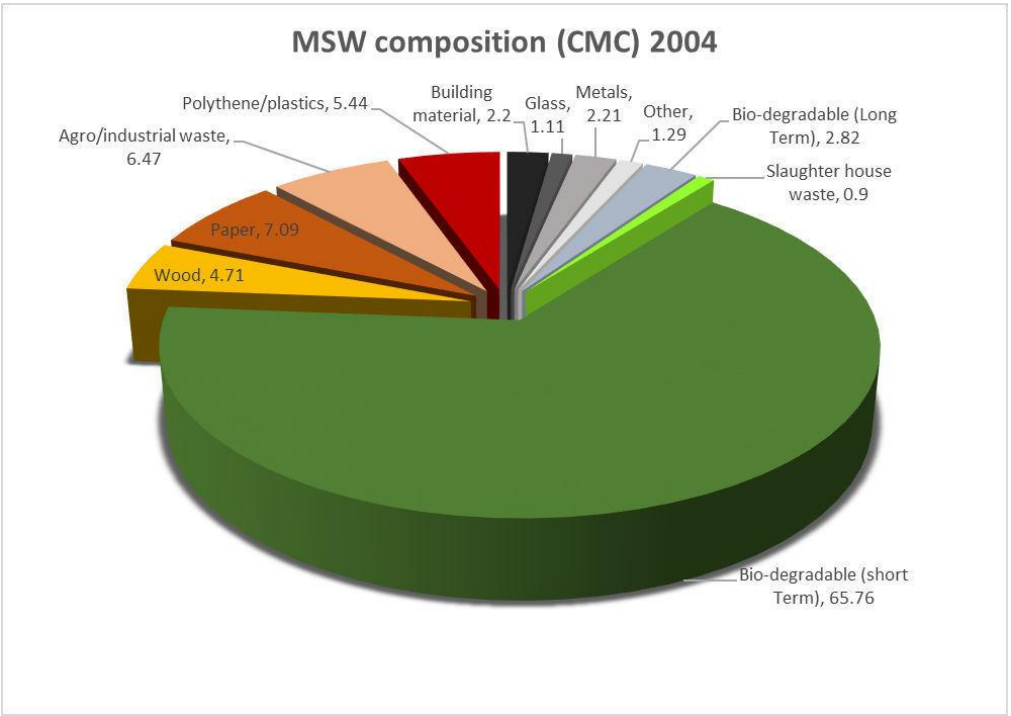

Figure 04: MSW composition of CMC in 2004
(Source: Central Environmental Authority, Sri Lanka)

Another significant characteristic of this analysis is that almost 85% of these organic wastes component are food wastes whereas the remaining share is garden waste except for insignificant amounts of abattoir waste and other composite organics which are not even 1% of total organic component.

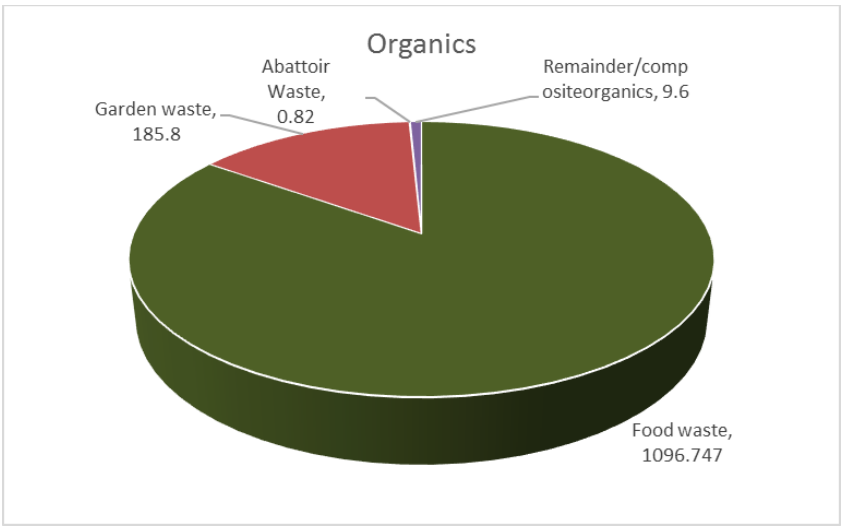

Figure 05: Percentage composition of organic waste

The combustible share (paper, cardboard, textile, rubber and leather, wood and timber, polythene and plastics) of MSW receiving in 2004 was only 17% while this share represents 31% in this latest analysis.

The moisture content variation of 15 samples is shown in Figure 06, and corresponding calorific values are shown in Figure 07. Average moisture content of these samples is 60% whereas average calorific value is 13.35MJ/Kg.

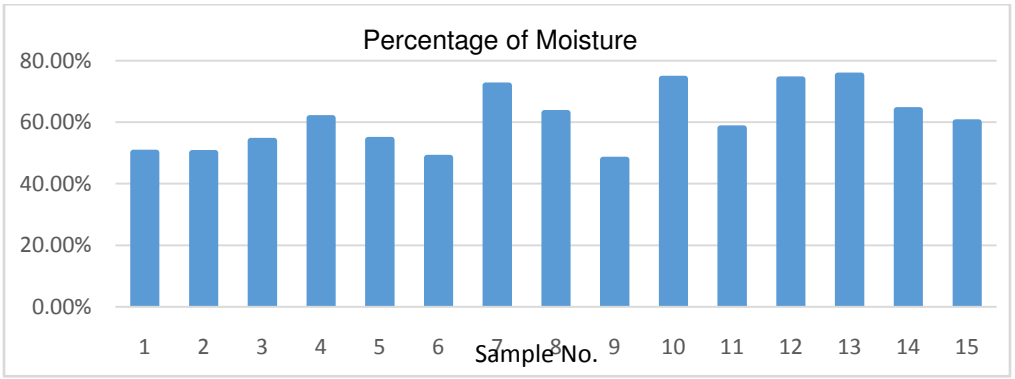

Figure 06: Moisture content of MSW

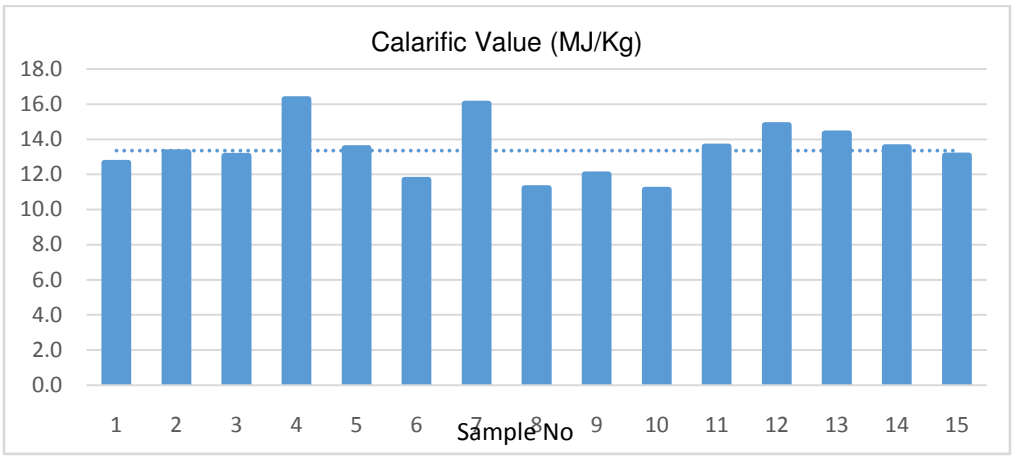

Figure 07: Calorific values of MSW in 2015

Table 2: Variation of average moisture content and calorific values based on the administrative area in CMC

Administrative Area in CMC	Calorific value (MJ/Kg)
1	13.65
2A	11.99
2B	12.06
3	11.77
4	14.55
5	14.31

According to the Table 2, solid wastes which are collected from administrative area 4 and 5 have significantly higher calorific value than the other solid waste collection areas of CMC. Area 4 and 5 comprise with Bambalapitiya, Wellawatta, Kirillapone, where high income residences, commercial and business entities are established.

Conclusion and Recommendation

This analysis reveals that the MSW compositions have slightly changed from the previous analysis conducted in 2004. Organic percentage has fallen to 52% from 2004's 65% whereas paper, cardboard and plastic shares have increased in significant margins. However, the average moisture content of these MSW still remains unchanged as 60%. Some inconsistency is noticed in the testing results of calorific value as it is not substantiated whether these samples are moisture-free basis or not. The significant share of this organic waste is food waste, and this is approximately 45% of incoming solid waste which implies that the need of biological treatment for the organic component of MSW. The segregation MSW of selected districts of CMC could be a way of supporting Waste- to-Energy (WTE) project which are having multiple benefits.

Acknowledgement

The authors acknowledge the sincere support provided by the Colombo Municipal Council and Kollonnawa urban council and the management of Meethotamulla waste disposal site, office staff and labourers for their commitment. The technical assistance of the Industrial Training Institute (ITI) and Ms NPM Rajaguru, Department of Civil Engineering, Open University of Sri Lanka are acknowledged.

We would like to express our gratitude to Mr. M.M.R. Pathmasiri, Director General, Mr. Vimal Nadeera, Deputy Director General (Operation) and Mr. Harsha Wickramasinghe, Deputy Director General (Strategy) of SLSEA for their guidance and directives for the successful completion of this study. Finally, we are also grateful to Mr. N.G.R.P Aberathne, executive of SLSEA and Ms A.D.C. Surathilini, University of Sri Jayawardhanapura University who coordinated field activities at the beginning of the project.

Reference

[1] Levien van Zon and Nalaka Siriwardena, 2000, Garbage in Sri Lanka [ONLINE] Available at: http://environmental.scum.org/slwaste/. [Accessed 14 October 2015].

[2] Open Journal of Civil Engineering_Engineering_Journals_SCIRP. 2015. Open Journal of Civil Engineering_Engineering_Journals_SCIRP. [ONLINE] Available at: http://www.scirp.org/journal/ojce. [Accessed 14 October 2015].

[3] Municipal Solid Waste Generation, Composition, and Management: The World Scenario (PDF Download Available). 2015. Municipal Solid Waste Generation, Composition, and Management: The World Scenario (PDF Download Available). [ONLINE] Available at: http://www.researchgate.net/publication/230806748. [Accessed 14 October 2015].

Annex 01: Statistical determination of number of MSW samples to be analyzed

$$n = \left(\frac{t*s}{e\bar{x}}\right)$$

t* = Student t statistic corresponding to the desired level of confidence

s = estimated standard deviation

e = desired level of precision

$\bar{x}$ = estimated mean

For 95% level of confidence, 10% level of precision assuming organic as the main component of MSW;

$n_{20} = [(2.093 * 0.03) / (0.1*0.1)]^2$

$= 39$

$n_{36} = [(2.03*0.03) / (0.1 * 0.1)]^2$

n = 37

n = 36

Annex 02: Required samples from each district in CMC and others

Area	Garbage ton per day	Percentage from each district	Required samples from each district (Percentage from each district * Total number of sample
District 01	70.69	8.43	3
District 02A	142.98	17.05	6
District 02B	99.42	11.85	4
District 03	92.40	11.02	4
District 04	88.62	10.57	4
District 05	142.40	16.98	6
Military Camps	69.36	8.27	3
Kolonnawa	35.72	4.26	2
Other	97.10	11.58	4
Total	**838.69**	**100**	**36**

Annex 03: Different Categories and Sub-categories of MSW

	Sample No :	
	PAPER&PAPERBOARD	
1	Newspaper	
2	Cardboard/boxboard	
3	Magazines/catalogues	
4	Office paper	
5	Other/miscellaneous paper	
	GLASS	
6	Clear containers	
7	Green containers	
8	Amber containers	
9	Remainder/composite glass	
	METAL	
10	Tin/steel containers	
11	Aluminum containers	
12	Other ferrous metal	
13	Othernon-ferrousmetal	
14	Major appliances	
	PLASTICS	
15	Clear PET Bottles/containers	
16	Green PET Bottles/Containers	
17	Amber PET Bottles/containers	
18	HDPE containers	
19	Film plastics	
20	Other plastics	
21	Rig foam	
	TEXTILE	
22	Textiles	
	ORGANICS	
23	Food waste	
24	Garden waste	
25	Abattoir Waste	
26	Remainder/composite organics	

	AGRO WASTE	
27	coconut, king coconut	
28	Agricultural waste	
	CONSTRUCTION & DEMOLITION MATERIAL	
29	Concrete	
30	Remainder/composite& D	
31	Debris	
32	Ceramics	
	SPECIALCAREWASTES	
33	Paint	
34	Hazardous materials	
35	Biomedical	
36	Batteries	
37	Oil Filters	
38	Remainder/composite S.C. Waste, sanitary	
39	Diapers	
40	Waste Electrical Products (WEEE)	
	WOOD & TIMBER	
41	Furniture (wood)	
42	Lumber	
	RUBBER &LETHER	
43	rubber	
44	Lether	
45	Tyre	
	OTHER WASTE	
46	other	
	Total	

Methods to improve the efficiency of a typical solar panel in the importance of green energy for a country in the scale of Sri Lanka

Gamage, M.V.

Abstract

Concentrated photovoltaics are able to harness the power of the sun at greater efficiencies than typical solar panels with the use of methods, concentrated sunlight, solar tracking and different types of material in solar panels. The purpose of this project was to find a cheaper alternative to concentrated photovoltaics to be installed in a local garments factory. In the process it has been investigated whether it is possible to achieve a higher power output from a conventional solar panel with the use of off the shelf mechanical parts and inexpensive microcontrollers.

The output of a smaller scale, solar panel was measured with various types of reflectors. And also the reflectors were strategically placed in a way that it would help cool down the solar cells with the use of aerodynamics. Then temperature of the solar cell was then recorded at different wind speeds and with each different reflector and was compared with each other.

Even though the combination of using aluminium coated paper was the best option as reflectors based on the readings, due to the problems that might occur in the longer run, it was decided to use conventional mirrors in the final design instead.

The payback period analysis was conducted between a conventional design and the proposed design and it was found that the design proposed in this project had the shortest payback period and also the best price to performance ratio.

Introduction

Solar power market had a rapid expansion in the recent years mainly due to the plummeting prices of solar PV panels, (Solar Electricity Cost vs. Regular Electricity Cost, 2015). But most of the PV panels only convert less than 20% of the sunlight in to electricity. (Solar contact, 2015). Although multi junction concentration PV systems that has efficiencies as high as 40% exists the cost of production still makes them out of reach for small businesses and homes. (Solar contact, 2015)

The subjected PV installation site for this project is the main building of Sun Queen Garments (Pvt) Ltd, Sri Lanka. The facility is situated in the coastal area of Panadura, 25 kilometres from the city of Colombo. Employing over 400 people, it produces wide variety of garments and houses a range of machinery mainly operating on national electricity grid. The monthly electricity usage of the facility is around32000kWh and based on the output readings of their backup electrical generator the facility has a peak electricity demand of around 200kW. As the first step it has been decided to implement a solar panel array which would have the capacity to serve up to a 50% (100kW) of the company's peak electricity need. The final design had to be suited for this particular application and it had to be an affordable option for the company.

There have been numerous research papers published on the subject of increasing the efficiency of a solar panel. Notably in the paper, More efficient use of photovoltaic solar panel using multiple fixed directed mirrors or aluminium foils instead of solar trackers in rural perspective of Bangladesh (Ahmed, S. et al, 2014) set out to find if the output of the PV panels increase with the use of reflectors. But focusing sunlight on to the small area via reflectors tend to cause other problems with the sun tracker system. And the focused sunlight might also cause the PV panel temperature to elevate. In the paper Photo voltaic cell efficiency at elevated temperatures (Ray, 2010) discusses about the importance of keeping the temperature of a photo voltaic panel to ensure that the photo voltaic cells operates at the optimum conditions. The paper finds that higher temperature might even permanently damage the solar cells. The final design will have to address all these issues while meeting the company requirements.

The aim of this project is to find the best value for the money by implementing the most suitable method of solar power installation. Since solar power installation is already a significant investment, designing a system that uses the most out of a conventional photo voltaic panel array by keeping them at their peak efficiency for as long as possible was essential.

The design has to be affordable, effective and reliable. All these objectives must be met while staying within the resources that are available on the site such as the roof top area the structural strength of the roof and also the design will have to withstand the environmental conditions during its lifetime. Most importantly the

final design would need to be affordable for the company in the scale of Sun Queen Garments (Pvt) Ltd.

Several methods will be proposed and tested in this project that will allow the PV panel to work at optimum conditions for a longer period of time. Considering the fact that the forth mentioned factory is only 300 metres from the cost, the investigation was more focused on developing a design that harnesses the power of wind to passively cool down the PV panels. The output power and the PV panel temperature was recorded at different wind speeds and was finally compared to find out its effectiveness.

A small scale (1:16) model was fabricated to find the effectiveness of the design under the same conditions. Although every precaution that's possible has been taken to keep the model in the same conditions as the proposed concept. The significance of this study is to exploit affordable solar power implementations, in the context of Sri Lanka and to find out the feasibility of improving the output of stationary PV panels, for a little extra cost.

Methodology

The sunlight hitting on the surface of the solar panel can be intensified by the use of parabolic shaped reflectors and flat panel reflectors. Since the manufacturing cost of curved reflectors are higher than that of flat panel reflectors (Dallakyan, Vardanyan, n.d.) the methods proposed in this section will utilize the use of flat panel reflectors. And since the solar intensifier only works at a certain spot in a certain direction the solar panels and the reflectors are in need of a solar tracker system. Although implementing such a system to focus the sunlight on to a smaller area will cause a rise in the temperature and a separate cooling system will also be needed. The concept will utilize two mirrors which will be at fixed angles and they each would reflect additional sunlight on to a half of the solar PV panel. The cooling will be done by a passive air cooling method. As illustrated in the figure 1mirrors will be fixed on to the frame leaving a small gap between the solar panel and itself. By adding some wind deflectors on each side the whole structure will act as a giant funnel to direct the naturally flowing wind in to the air gap thus cooling down the solar panel.

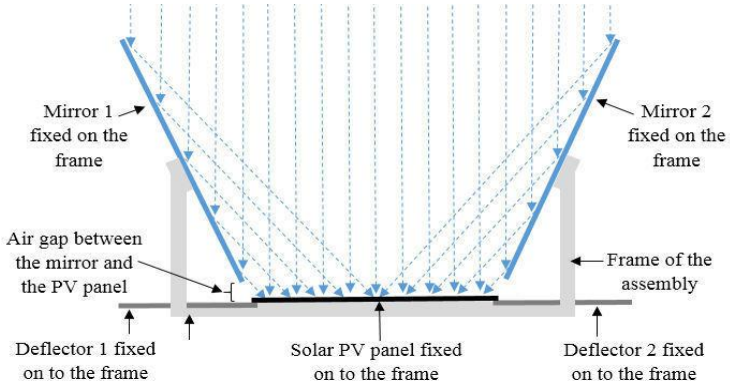

Figure 1: Design of the concept 3.This design exercises the fact that the sun queen garment company is situated in a location where wind resources are plenty.

Although Sri Lanka being a country that is very close to the equator and the path of the sun does not get very far off to north or south as much as in northern or southern countries, having two separate automated tracking mechanisms to track the sun in both axis would dramatically increase the payback period of the whole system. Therefore the concept 3 will have a single automated axis sun tracking mechanism to track the sun west to east, and a manual (human operated) tracker to change the north-south angle every couple of weeks.

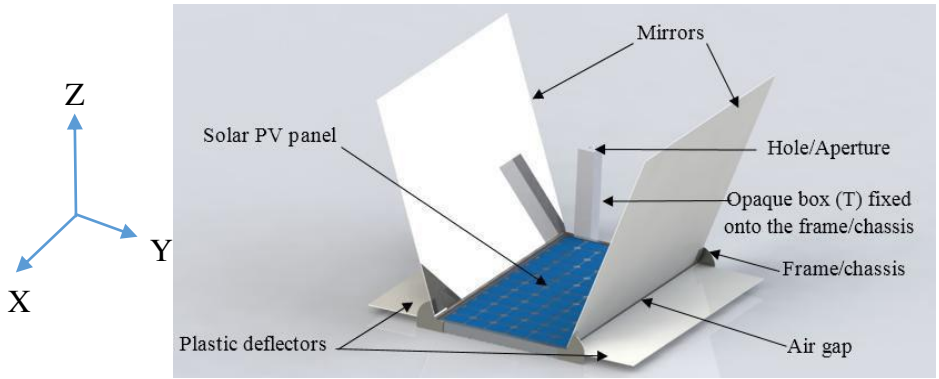

Figure 2: A 3-D rendering of the mirror, PV panel and the deflector assembly

The mechanism for the manual adjustment of the solar PV panel (north-south wise) uses a threaded shaft and a nut that runs along with it. When the thread shaft is rotated by the handle the nut will run along the thread bar, raising the arm that supports the PV assembly.

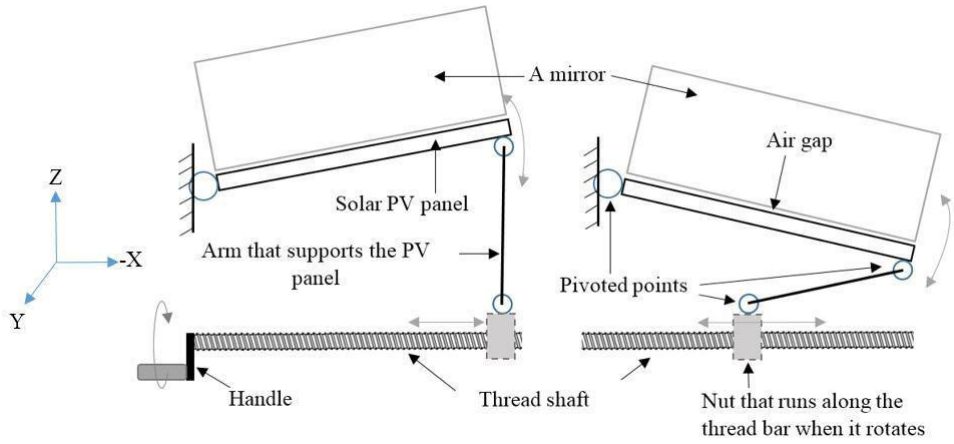

Figure 3: A side view of the solar panel assembly mounted on a threaded shaft.

The handle is only meant to turn once every couple of weeks as the angle of the sun rise gradually changes over the seasons in a calendar year. This unique design will allow an array of solar panels to be connected together and they all will be turned by a single thread shaft and a motor. The whole assembly will be pivoted as the sun moves from east to west during the day with the use of a linear motor. The PV panel, mirrors and the wind deflector assembly is pivoted through its centre of mass reducing the torque required to pivot the assembly.

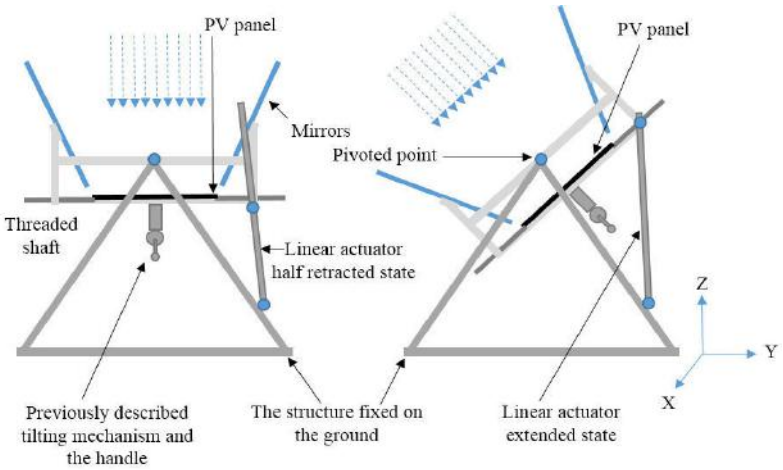

Figure 4: The mechanism that pivots the assembly (PV panel, mirrors and the deflectors) which is controlled by a linear actuator. The front view.

Analysis

The solar PV panel that will be subjected for the calculations is IBC PolySol 250 GX. The basic dimensions are $1654\text{mm} \times 989\text{mm} \times 40\text{mm}$. The panels are made out of polycrystalline solar cells which have and efficiency of 15.6%. (IBC Solar, 2015)

The first step of the design is to add the mirrors to focus additional sunlight on to the solar panel. In this design two mirrors will be used, each reflecting sunlight on to a half of the PV panel. The original area that the sunlight can be collected is only $1654\text{mm} \times 989\text{mm}$.

Following are the diagrams illustrates the utilisation of the mirrors to maximise the solar panel output at a mirror angle of θ^0. Following are the calculations carried out to find the angles between the PV panel and the mirror and the required length of the mirror, and to select the best angle, considering the cost of the mirror and additional effective width that the mirror creates.

The sunlight hitting the additional effective area will be reflected on to a half of the PV panel (other half will be covered by the mirror on the opposite side).

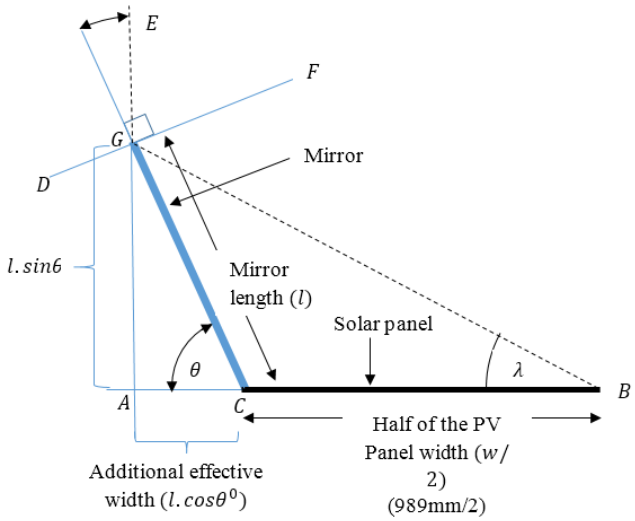

Figure 5: Illustration for the geometrical calculation

$$\text{Since } A\hat{C}G = \theta \ , \quad D\hat{G}C = 90^0 \ , \quad D\hat{G}A = \theta$$

since $D\hat{G}A$ and $E\hat{G}F$ are opposing angles

$$E\hat{G}F = \theta$$

since $E\hat{G}F$ and $F\hat{G}B$ are angles of the reflecting sunrays they also have to be euqal

$$\text{therefore } F\hat{G}B = \theta$$

$$F\hat{G}B + B\hat{G}C = 90$$

$$B\hat{G}C = 90 - \theta$$

Considering the triangle ofCGB;

$$\mathrm{B\widehat{G}C} + \mathrm{GCB} + \mathrm{CBG} = 180^0$$

$$\text{since} \quad \mathrm{B\widehat{G}C} = (90^0 - \theta), \qquad \text{and} \qquad \mathrm{GCB} = (180^0 - \theta)$$

$$(90^0 - \theta) + (180^0 - \theta) + \mathrm{CBG} = 180^0$$

$$\mathrm{CBG} = \lambda = 2\theta - 90^0$$

And using the law of sins for the same triangle

$$\frac{\text{mirror length (l)}}{\sin(2\theta - 90^0)} = \frac{\text{half of the PV panel width } \left(\frac{w}{2}\right)}{\mathrm{Sin}(90^0 - \theta)}$$

$$\frac{\text{mirror length (l)}}{-\cos(2\theta)} = \frac{w}{2\cos\theta}$$

$$\text{mirror length (l)} = \frac{-w\cos(2\theta)}{2\cos\theta}$$

Notice that the θ always has to be between 45 and 90 degrees for the last equation to be true. By applying various values for θ the following table can be created. The width of the mirror which is equal to the length of the solar panel which is 1654mm. The area of the mirror is calculated by multiplying (l)mm by the length of the solar panel (1654mm) and the effective area of the mirror is calculated by multiplying additional effective width (x) mm by 1650mm.

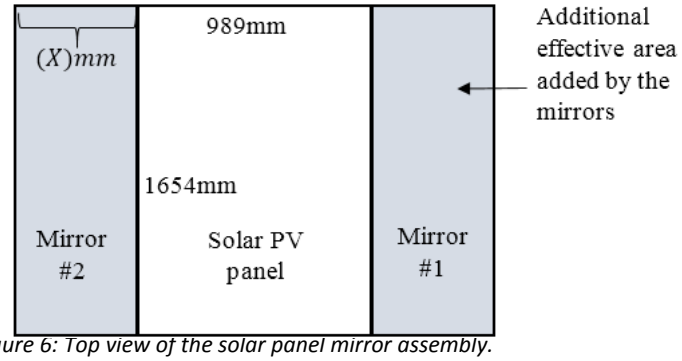

Figure 6: Top view of the solar panel mirror assembly.

Table 2: Calculation to find the effective area of the mirrors.

θ^0	l(mm)	Additional effective width achieved through the use of mirrors (x)= $lcos\theta$ (mm)	Additional effective area (m^2) $lcos\theta \times 1.654$	Cost with the average price of US $2.128 per square metre
45	0	0	0	-
50	135.074	86.82	0.143	0.475
55	298.146	170.92	0.281	1.049
60	500.000	250.00	0.413	1.75
65	760.482	321.18	0.530	2.67
70	1119.88	383.02	0.633	3.94
75	1673.03	433.01	0.716	5.88
80	2705.73	469.84	0.775	9.52
90	∞	-	-	-

With that information following graph can be plotted with the cost values against the additional area that the mirrors provide. The cost threshold has selected to be $4 for this application. And the corresponding θ value that is closest is 70^0 degrees and the length of the solar panel is 1119.88mm. The design will be carried forward with these values.

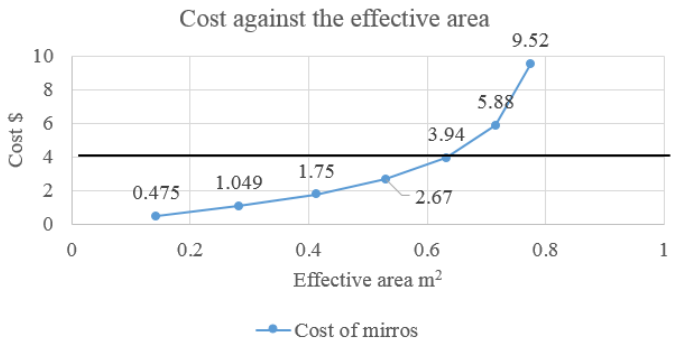

Figure7: The cost of mirrors plotted against their effective area.

The selected cost threshold has been marked at $4.

Following are the calculations for the mechanism to adjust the tilt of the solar panel. Since the sun rises at different angles year around, due to the tilt of earth's rotational axis, the angle of the solar also has to change year around. The tilt in the earth's rotational axis is 23.5 degrees (Tilt of the earth, 2015) and that causes the path that the sun travels vary by 23.5 degrees to the north and 23.5 degrees to the south throughout the year. In this mechanism this angle variation is achieved through the following design. The arm will control the tilt of the PV panel. Rotating the thread shaft will therefore tilt the PV panel to a desired tilting angle. Since this mechanism is being developed in Sri Lanka the angles have to be set according to the geological location of Sri Lanka. Being situated at a latitude of 7 degrees north would mean the variation of the rising angle of the sun will be 7 degrees off from the centre. This is illustrated in the figure 9:

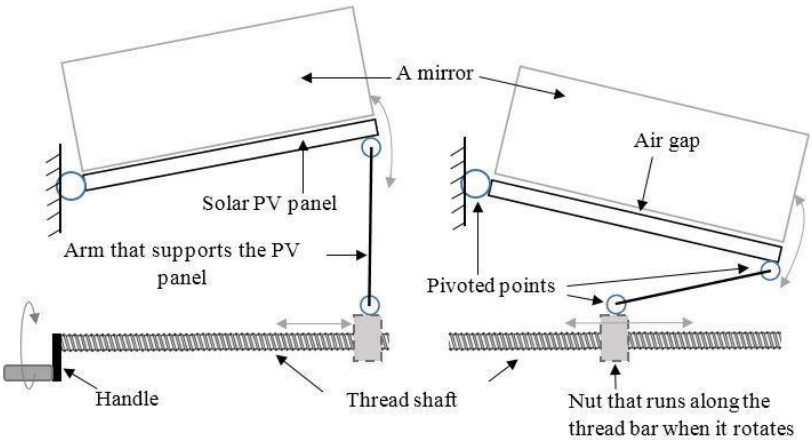

Figure 8: An illustration of the different tilt positions of the same solar panel.

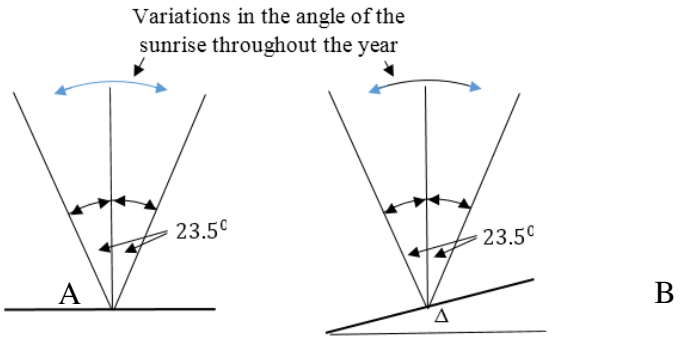

Figure9: Variations of the angles of sunrise throughout the year.Country on the equator (A) versus a country in the latitude of Δ, (B). Since Sri Lanka is situated at a latitude of 7 degrees the azimuth angles that are required for the mechanism would be as follows.

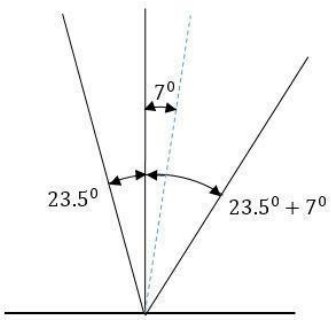

Figure 10: Illustration of the variation of the angle of the sunlight observed from a latitude of 7 degrees throughout the year.

Therefore the dimension in the parts of the tilting mechanism has to be as follows.

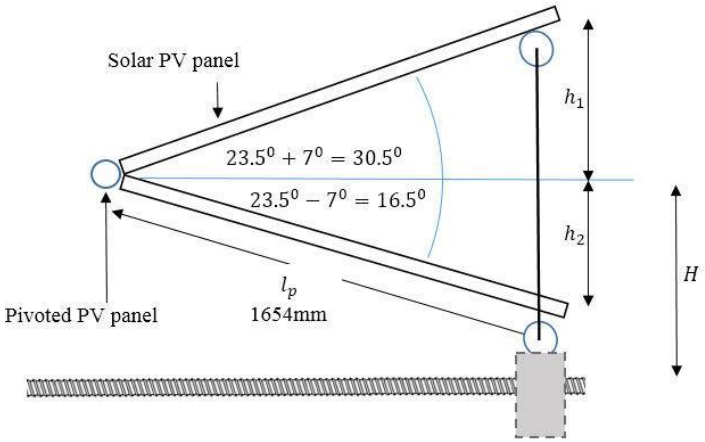

Figure 11: The dimensions of the mechanism that tilts the PV panel. The mechanical arm that connects the threaded nut that runs along the thread bar to the PV panel.

$\mathrm{h}_1 = 1654\mathrm{mm} \times \sin 30.5 = 839.5\mathrm{mm}$
$\mathrm{h}_2 = 1654\mathrm{mm} \times \sin 16.5 = 469.8\mathrm{mm}$

H = the gap between the pivoted PV panel end and the threaded shaft. This includes the $\mathrm{h}_2$value plus the height of pivoted nut at minimum. This gap has to be higher than h_2 or the PV panel will collide with the thread shaft at certain angles. Length of the mechanical arm has to exceed $\mathrm{h}_1 + \mathrm{h}_2$ minus the height of the nut that runs along the threaded shaft.

$$\begin{aligned}\text{length of the mechanical arm} &= 839.5\mathrm{mm} \\ &+ 469.8\mathrm{mm} \\ &+ \sim 10\mathrm{mm} \\ &= 1319\mathrm{mm}\end{aligned}$$

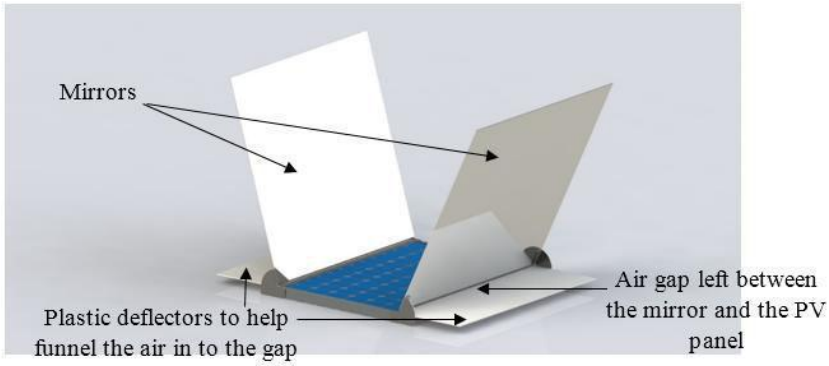

Figure 12: A rendered model of the proposed design.

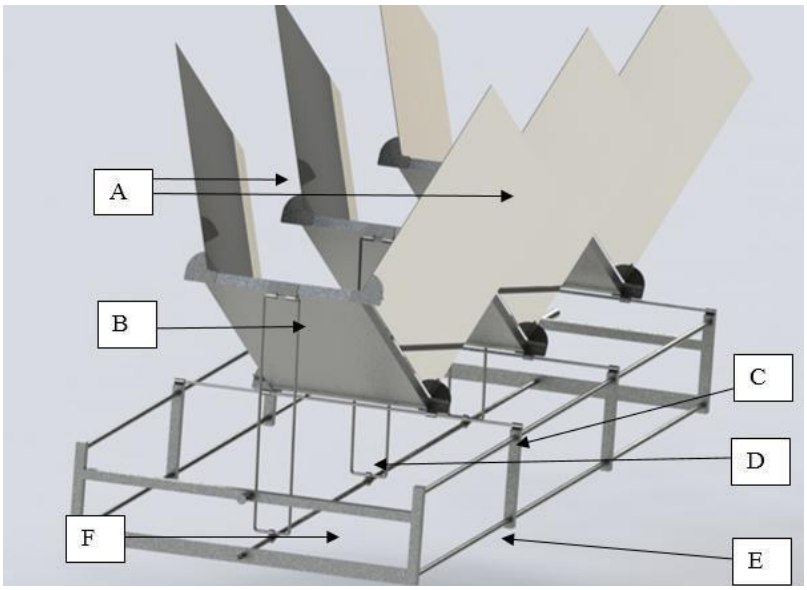

Figure 13: A rendered image of the tilting assembly.

A = Mirrors on either side of the PV panel
B = Bottom side of the PV panel
C = Screw thread that tilts the PV panel
D = The mechanical arm that links the nut (F) to the solar panel.
E = The railing frame that holds the whole assembly together.
F = Nut that is linked to the mechanical arm and runs along the screw shaft when the screw shaft rotates.

Since this design focuses the sunlight on to a precise area it is required to keep the solar panel facing the sun at all possible times. The pivoting mechanism is to follow the sun during the day time from dawn to dusk and it

has to be adjusted every couple of minutes. This is done through a logic controller and an electric motor. In the model however a programmed micro controller (Arduino) will be used instead of a PLC. Finding the centre of mass of the system and putting the pivoting axis through that would help reduce the torque required to roll the system. The figure 14 illustrates the pivoting mechanism in action.

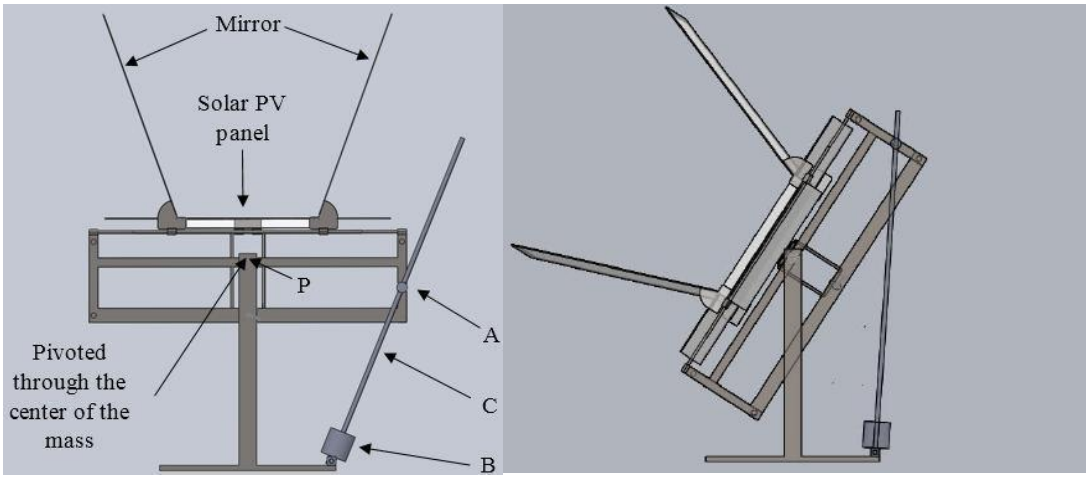

Figure 14: Illustration of the pivoting mechanism for the system.

C is a second thread shaft (mentioned as a linear motor previously) used in the same way as the first thread shaft and connected to the solar PV assembly. Instead of tilting the panel this thread bar pivots the whole assembly about the point P. when the electric motor B turns the thread shaft the nut at point A travels along the thread bar thus pulling/pushing the whole assembly with it.

Figure15: The model during the testing

Results and observations

The solar cell that was used for the experiment is a 21.8%% efficient $125\text{mm} \times 125\text{mm}$ monocrystalline "Sunpower Maxeon" solar cell that has a rated maximum open circuit voltage of 0.574V and a maximum rated short circuit current of 5.83A.

Therefore,

$$\text{Maximum rated current possible} = V_{max} \times I_{max} \quad \text{Eq. 1}$$
$$= 0.574\text{V} \times 5.83\text{A}$$
$$= 3.346\text{W}$$

This is generally unachieved in real world conditions although it has to be mentioned that each IBC PolySol 250 GX's power output of 250W is tested under lab conditions of 1000Wm^{-2} radiation at 25^0C. (IBC Solar,2015).

Readings for the open circuit voltage and short circuit current were taken every half an hour from 0800h to 1700h for 3 days, under the conditions in table 4. All the observations are averaged by the readings from 3 separate days with similar weather conditions.

Table 3: The conditions under which the solar cell was tested

	Cooling method				
	No aided cooling method	Passive cooling with deflector	Active cooling with deflector		
			Electric fan 2m away	Electric fan 1m away	Electric fan 0.5m away
Power output with no solar tracking, no reflectors	A	B	C	D	E
Power output with solar tracking with no reflectors	F	G	H	I	J
Power output with solar tracking and conventional mirrors and	K	L	M	N	O
Power output with solar tracking and aluminium foil used as reflectors	P	Q	R	S	T
Power output with solar tracking and aluminium coated paper used as reflectors	U	V	W	X	Y

Power output calculations was done using the equation 1. The values can be found in the tableH1 in the appendix H which are then used to plot the graph 10.

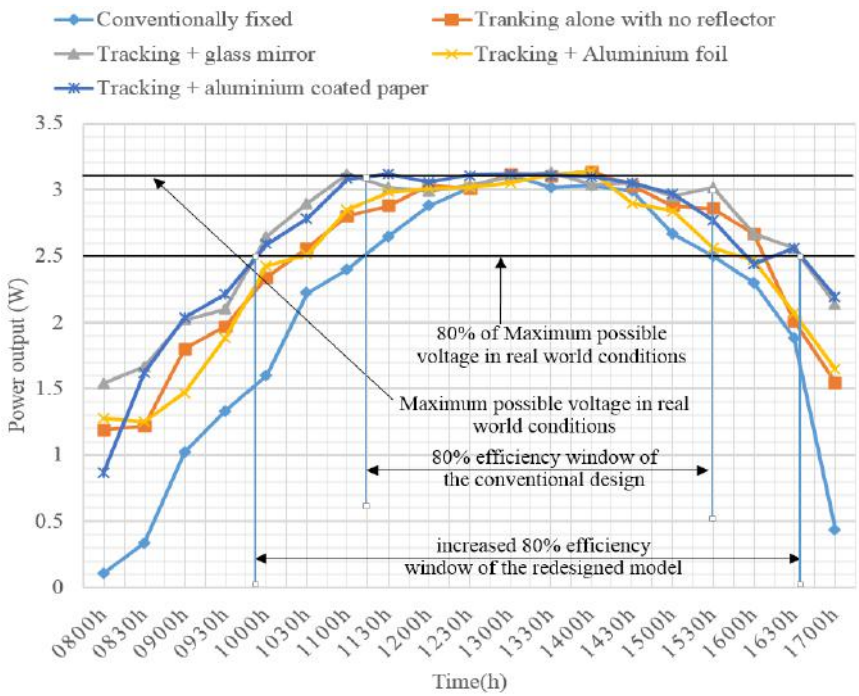

Figure 16: Outputs of redesigned solar panels vs the fixed panel

In the graph 10 it can be seen that adding a reflector to an already sunlight saturated PV panel does not make any difference, except increasing the temperature (see graph 12) which tends to reduce the lifespan of the solar cells. But the objective of the reflector here was to keep the solar panel at saturated levels even when the sunlight is not at its peak is the benefit which it has achieved. (1000h to 1630h instead of1115h to 1530h in graph 10). Surprisingly it seems that having an aluminium foil as a reflector does not make any significant difference at all and an aluminium coated papers being a fraction of the cost of a glass mirror, served just as well has a glass mirror itself. Building upon these findings the effectivity of the wind deflector calculations will be carried out only for mirror and Al coated paper reflectors using the data from the same table A2 in the appendix.

As it seen on the graph 11 the wind deflectors had not affected the power output of the solar panel in any significant manner either. But with the temperature data available on the graph 12 and IBC PolySol 250 GX's nominal operating cell temperature of 40^0C(IBC Solar, 2015) it is seems that the lower temperature in the model that had Aluminium coated paper would be the best technical option. But considering the longer lifespan of a glass mirror and its ability to resist extreme weather conditions far

outweighs the advantages of the aluminium coated paper.

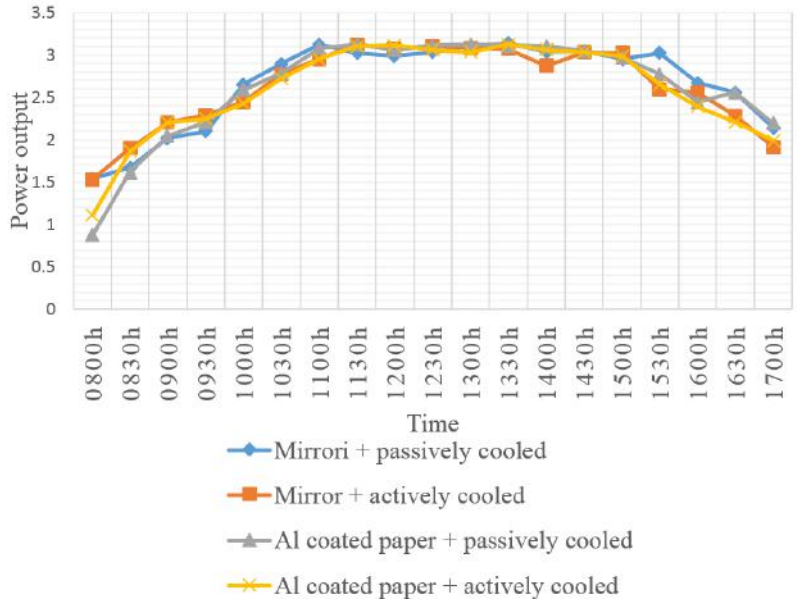

Figure 17: Different power output values of a solar panel under different wind speeds

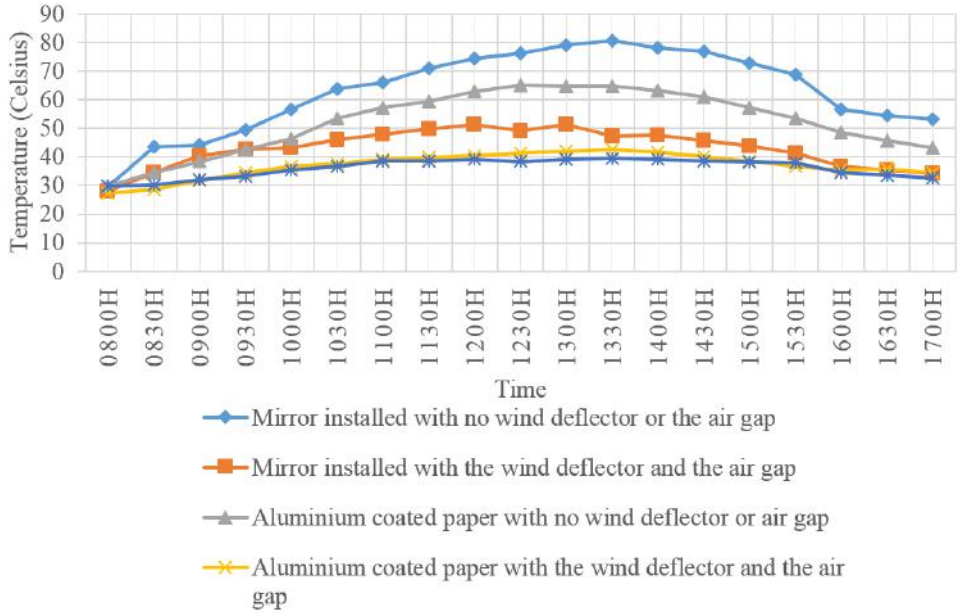

Figure 18: Temperature readings for mirror and aluminium paper reflectors. Values were taken under passive and active cooling. Note: the active cooling wind speed was approximately set to be as the same speed as the rooftop of the factory. The values can be found in the table A3 in the appendix A.

The breakeven analysis was done using the pricings and net metering pricings available in Sri Lanka. The Sun Queen garment has an energy requirement of 1020kWh in peak hours and 675kWh in off peak hours per month and a peak electrical demand of 200kW (value taken from the backup generator output values, which was outdated and a data sheet was not available). The solar panels are set to initially produce 50% of the company's peak electricity demand which is 100kW.

The inverter proposed for the solar system is Sunny Mini Central10000T of which the maximum DC power input from the solar panels is 10350W and had a price tag of 1378$ (SMA sunny mini central, 2015) and therefore it is decided to use 10 of them along with 400 (250W) solar panels. The panel array will be configured in 20 rows of 20 panels each, due to the narrow and long roof shape. Therefore 20 sets of proposed mechanical rails will be used along with 20 linear actuators.

Table 4: Calculated total system cost for the proposed solar array.

	Quantity	Unit Cost	Total
IBC PolySol 250 GX 250 watt solar panels	400	$ 138	$ 55,200
Sunny Mini Central 10000T	10	$ 1,378	$ 13,780
Mirrors	800	3.94	$ 3,152
Structure of the solar panels	20	$ 1,129	$ 22,580
Linear motor	20	$ 96	$ 1,920
Copper wire and junction box	20	$ 350	$ 7,000
Grounding wire	1	$ 150	$ 150
System Cost Total			$103,782

Table 5: Payback period calculation for the proposed system. (Weather averages for Colombo, 2015)

Number of Panels	400	
Watts Per Panel	250	W
Total watts per hour assuming optimum conditions	100,000	W
Number of hours that has adequate amount of sunlight*	7.0	h
Estimated kilowatt hours per day output	700	kWh
Number of days per month with bright day light estimated	20	
Estimated kWh per month output	14000	kWh
Leaving 5% to power the tracking mechanism	13300	kWh
Buying rate of a kWh in peak time (from the grid) converted to USD	0.16	$
Money saved from an average month	2128	$
Total payback period of the system	48.77	months

Table 6: Calculated total system cost for a conventionally mounted solar PV array.

	Quantity	Unit Cost	Total
IBC PolySol 250 GX 250 watt solar panels	400	$ 138	$ 55,200
Sunny Mini Central10000T	10	$ 1,378	$ 13,780
Mirrors	0	3.94	$ -
Structure of the solar panels	20	$ 321	$ 6,420
Linear motor	0	$ 96	$ -
Copper wire and junction box	20	$ 350	$ 7,000
Grounding wire	1	$ 150	$ 150
System Cost Total			$82,550

Table 7: Payback period calculation for a conventionally mounted solar PV array

Number of Panels	400
Watts Per Panel	250 W
Total watts per hour assuming optimum conditions	100,000 W
Number of hours that has adequate amount of solar power*	4.3 h
Estimated kilowatt hours per day output	430 kWh
Number of working days per month with bright day light	20
Estimated kWh per month output	8600 kWh
Buying rate of a kWh in peak time (from the grid) converted to USD	0.16 $
Money saved from an average month	1376 $
Total payback period of the system	75.42 months

*The number of hours is increased by the use of reflectors. The window of the maximum efficiency has widened.

Conclusions

- Implementing a solar tracker mechanism does improve the power output of a conventional solar panel during the morning and the evening hours.
- Adding a reflector to harness additional sunlight on to the panel makes a difference only when the solar panel has not yet reached its peak performance.
- The objective of the design which was to widen the window in of maximum power output has been achieved.
- Adding a reflector increases the temperature of the PV panel and it seems that having a wind deflector to funnel the air in to the air gap and then onto the solar panel does seem to reduce the temperature marginally. The temperature of the PV panel did not have an immediate effect on the solar panel output. But the increased temperature might affect the efficiency of the solar panel in the longer run.

- Implementing the design has reduced the payback period of the solar array. And based on the calculations, the redesigned array will continue to produce significantly higher amount of power even after the payback period.
- Having a mechanised solar panel that tracks and follows the sun instead of a fixed panel which does not have any moving parts, might introduce the chance of mechanical a failure. In a chance of a solar tracker failure the power output will plummet as the mirrors might cast a shadow on the solar panel.
- And also the mechanised solar panel and its almost vertical mirrors will not hold as much as a permanently mounted solar array under extreme weather conditions and it might require some maintenance time to time.

References

[1] Aliexpress. (2015) Aliexpress's website. Available at: http://www.aliexpress.com/item/Sunpower-Maxeon-Solar-Cell-21-8-Efficiency-3-34W-Semi-flexible-125x125mm-Mono-1pcs-Solar-Cell/ (Accessed: 05 April 2015).

[2] Solar Electricity Cost vs. Regular Electricity Cost. (2015) Solar Electricity Cost vs. Regular Electricity Cost's website. Available at: http://solarcellcentral.com/cost_page.html. (Accessed: 25 April 2015).

[3] Solar Contact. (2015) Solar Contact's website. Available at: http://uk.solarcontact.com/photovoltaic/technology/photovoltaic-efficiency. (Accessed: 05 April 2015).

[4] Ahmed, S. et al.(2014) 'More efficient use of photovoltaic solar panel using multiple fixed directed mirrors or aluminium foils instead of solar trackers in rural perspective of Bangladesh. International journal of scientific & technology research volume 3, issue 4, april [Online]. Available at: http://www.ijstr.org/final-print/apr2014/More-Efficient-Use-Of-Photovoltaic-Solar-Panel-Using-Multiple-Fixed-Directed-Mirrors-Or-Aluminum-Foils-Instead-Of-Solar-Trackers-In-Rural-Perspective-Of-Bangladesh.pdf (Accessed: 05 April 2015)

[5] Ray, K. L (2010) 'Photo voltaic cell efficiency at elevated temperatures'. NA [Online]. http://dspace.mit.edu/bitstream/handle/1721.1/59937/676836192.pdf?1 (Accessed: 05 April 2015)

[6] Dallakyan, V. Vardanyan, R. (n.d.) 'Mirror reflecting cost effective pv solar energy concentrating system' 4th International conference on solar concentrators for the generation of electricity or hydrogen N.A. [Online]. Available at: http://www.ies.upm.es/fileadmin/contenidos/programas/sistemas_integracion/El_Escorial/Session_3A_2.pdf

[7] Yupeng, W. Eames, C. and Smyth, M (2005) 'Optical analysis of asymmetric compound parabolic photovoltaic concentrators (ACPPVC) suitable for building façade integration' 4th

International conference on solar concentrators for the generation of electricity or hydrogen N.A. [Online]. Available at: http://www.ies.upm.es/fileadmin/contenidos/programas/sistemas_integracion/El_Escorial/Session_3A_2.pdf

[8] (Leutz, R and Fu, L. (2005) 'Segmented cone concentrators: optical design' 4th International conference on solar concentrators for the generation of electricity or hydrogen N.A. [Online]. Available at: http://www.ies.upm.es/fileadmin/contenidos/programas/sistemas_integracion/El_Escorial/Session_3A_2.pdf

[9] Tripanagnostopoulos, Y. (N. D.) 'Linear Fresnel lenses with photovoltaics for cost effective electricity generation and solar control of buildings' 4th International conference on solar concentrators for the generation of electricity or hydrogen N.A. [Online]. Available at: http://www.ies.upm.es/fileadmin/contenidos/programas/sistemas_integracion/El_Escorial/Session_3A_2.pdf

[10] U.S. Energy Information Administration (EIA). (2015). U.S. Energy Information Administration (EIA). 's website. Available at: http://www.eia.gov/todayinenergy/detail.cfm?id=18871. (Accessed: 15 April 2015).

[11] Solar Choice. (2015). Solar Choice's website. Available at: http://www.solarchoice.net.au/blog/solar-trackers/. (Accessed 26 April 2015).

[12] Photovoltaic Trackers. (2015) Photovoltaic Trackers's website. Available at: http://www.pvresources.com/PVSystems/Trackers.aspx. (Accessed 11 April 2015).

[13] Greentech. (2015)Greentech's website. Available at: http://www.greentechmedia.com/articles/read/Soitec-SunPower-and-Suncore-The-Last-CPV-Vendors-Standing. (Accessed 10 April 2015).

[14] ISE 2014, ISE's website Available at: http://www.webcitation.org/6SFRTUaBS. (Accessed 10 April 2015).

[15] IBC Solar.(2015) IBC Solar'swebsite.Availble at: http://soenen.info/media/zonnepanelen_dat/DatasheetIBC_PolySol_255_GX.pdf (Accessed 10 April 2015).

[16] Tilt of the Earth. (2015) Tilt of the Earth's website. Available at: http://www.universetoday.com/26778/tilt-of-the-earth/. (Accessed 16 April 2015).

[17] Weather Averages for Colombo 2015. Weather Averages for Colombo's website Available at: http://www.holiday-weather.com/colombo/averages/. (Accessed 15 April 2015).

[18] SMA Sunny Mini Central.(2015) SMA Sunny Mini Central's website. Available at: http://www.europe-solarshop.com/inverters/sma-sunny-mini-central-10000tl-10.html. (Accessed 18 April 2015).

[19] PV systems - steel supporting structures for PV modules. (2015) PV systems - steel supporting structures for PV modules' website. Available at: http://www.avextrade.cz/en/kategorie/pv-systems.aspx. (Accessed 19 April 2015).

[20] Support and Framing Systems for Solar Panels - JMC Steel Group. (2015) Support and Framing Systems for Solar Panels - JMC Steel Group's website. Available at: http://www.jmcsteelgroup.com/markets/support-and-framing-systems-for-solar-panels#click-for-product-options. (Accessed 19 April 2015)

Appendix

Table A1: The power output of the model under different conditions in the table 4.

(Watts)	The condition of the experiment												
	No tracking with no reflectors					Tracking with no reflectors					Tracking with mirrors		
Time of the day	A	B	C	D	E	F	G	H	I	J	K	L	M
0800h	0.11	NA	NA	NA	NA	1.19	1.28	1.17	1.31	1.23	1.44	1.54	1.53
0830h	0.34	NA	NA	NA	NA	1.22	1.35	1.24	1.40	1.29	1.66	1.67	1.90
0900h	1.02	NA	NA	NA	NA	1.80	1.67	1.80	1.78	1.92	1.89	2.02	2.20
0930h	1.33	NA	NA	NA	NA	1.97	1.88	1.97	2.09	1.99	1.98	2.10	2.29
1000h	1.60	NA	NA	NA	NA	2.34	2.43	2.34	2.53	2.50	2.57	2.65	2.44
1030h	2.22	NA	NA	NA	NA	2.56	2.51	2.56	2.49	2.52	2.92	2.90	2.87
1100h	2.40	NA	NA	NA	NA	2.80	2.88	2.75	2.86	2.83	3.11	3.12	2.95
1130h	2.65	NA	NA	NA	NA	2.88	2.87	2.88	2.92	2.89	3.10	3.02	3.11
1200h	2.88	2.93	2.88	2.92	2.90	3.03	3.01	3.06	3.21	3.01	3.03	2.99	3.02
1230h	3.01	3.09	3.01	3.07	3.09	3.01	3.04	3.01	3.10	2.95	3.07	3.03	3.13
1300h	3.11	3.12	3.10	3.09	3.11	3.12	3.03	3.10	3.01	3.11	3.03	3.10	2.84
1330h	3.02	3.09	3.03	3.12	3.11	3.11	3.10	3.11	3.03	3.15	3.12	3.13	3.07
1400h	3.03	3.02	2.98	3.08	3.12	3.14	3.03	3.14	3.07	3.04	3.07	3.04	3.12
1430h	2.99	NA	NA	NA	NA	3.03	3.02	3.00	3.04	3.08	2.98	3.05	3.08
1500h	2.67	NA	NA	NA	NA	2.88	2.78	2.88	2.84	2.88	2.94	2.95	3.03
1530h	2.50	NA	NA	NA	NA	2.86	2.80	2.86	2.56	2.78	2.86	3.02	2.45
1600h	2.30	NA	NA	NA	NA	2.67	2.48	2.67	2.52	2.76	2.77	2.67	2.73
1630h	1.88	NA	NA	NA	NA	2.01	2.22	2.01	2.22	2.16	2.44	2.56	2.22
1700h	0.44	NA	NA	NA	NA	1.55	1.04	1.55	1.34	1.60	2.15	2.14	1.97

(Watts)	The condition of the experiment											
			Tracking, with Aluminium foil					Tracking with Aluminium coated paper				
Time of the day	N	O	P	Q	R	S	T	U	V	W	X	Y
0800h	1.67	1.53	1.16	1.28	1.19	1.16	0.66	0.81	0.87	0.93	1.23	1.11
0830h	1.80	1.90	1.28	1.25	1.34	1.34	1.25	1.78	1.62	1.87	1.99	1.86
0900h	2.25	2.20	1.78	1.47	1.42	1.56	1.74	2.22	2.04	2.22	2.27	2.20
0930h	2.28	2.29	1.91	1.88	1.53	1.73	1.81	2.19	2.21	2.33	2.24	2.25
1000h	2.67	2.44	2.34	2.43	1.80	2.41	2.22	2.65	2.59	2.47	2.54	2.43
1030h	2.75	2.77	2.55	2.51	2.22	2.23	2.37	2.74	2.78	2.85	2.67	2.72
1100h	2.87	2.95	2.76	2.85	2.60	2.54	2.71	3.00	3.08	2.95	2.95	2.95
1130h	3.10	3.12	2.91	2.98	2.75	2.88	2.95	3.11	3.12	3.11	3.10	3.10
1200h	3.06	3.07	3.03	3.01	2.86	2.98	3.02	3.08	3.06	3.04	3.04	3.11
1230h	3.13	3.10	3.04	3.02	3.03	3.01	3.09	3.07	3.11	3.13	3.08	3.06
1300h	3.12	3.09	3.08	3.05	3.11	3.04	3.11	3.11	3.12	3.12	3.01	3.03
1330h	3.05	3.07	3.10	3.11	3.04	3.12	3.10	3.10	3.11	2.87	3.06	3.12
1400h	3.12	2.87	3.12	3.14	3.06	3.11	3.07	3.08	3.10	2.95	3.10	3.06
1430h	2.98	3.03	3.05	2.90	2.97	3.01	2.85	3.07	3.05	3.08	2.97	3.03
1500h	3.03	3.02	3.04	2.84	2.69	2.84	2.81	2.93	2.97	3.03	3.01	2.99
1530h	2.49	2.60	2.76	2.56	2.40	2.34	2.42	2.85	2.77	2.47	2.58	2.65
1600h	2.29	2.56	2.65	2.47	2.36	2.21	2.56	2.32	2.44	2.43	2.72	2.39
1630h	2.10	2.28	2.18	2.07	2.14	2.03	2.05	2.35	2.56	2.22	2.55	2.21
1700h	1.54	1.92	1.45	1.65	1.59	1.56	1.67	2.10	2.19	1.96	1.92	1.99

Table A2: Performance of the solar cell in the model under different wind conditions.

(*Celsius*)	The condition of the experiment												
	No tracking with no reflectors					Tracking with no reflectors					Tracking with mirrors		
Time of the day	A	B	C	D	E	F	G	H	I	J	K	L	M
0800h	0.11	NA	NA	NA	NA	1.19	1.28	1.17	1.31	1.23	NA	1.54	1.53
0830h	0.34	NA	NA	NA	NA	1.22	1.35	1.24	1.40	1.29	NA	1.67	1.90
0900h	1.02	NA	NA	NA	NA	1.80	1.67	1.80	1.78	1.92	NA	2.02	2.20
0930h	1.33	NA	NA	NA	NA	1.97	1.88	1.97	2.09	1.99	NA	2.10	2.29
1000h	1.60	NA	NA	NA	NA	2.34	2.43	2.34	2.53	2.50	NA	2.65	2.44
1030h	2.22	NA	NA	NA	NA	2.56	2.51	2.56	2.49	2.52	NA	2.90	2.87
1100h	2.40	NA	NA	NA	NA	2.80	2.88	2.75	2.86	2.83	NA	3.12	2.95
1130h	2.65	NA	NA	NA	NA	2.88	2.87	2.88	2.92	2.89	NA	3.02	3.11
1200h	2.88	2.93	2.88	2.92	2.90	3.03	3.01	3.06	3.21	3.01	NA	2.99	3.02
1230h	3.01	3.09	3.01	3.07	3.09	3.01	3.04	3.01	3.10	2.95	NA	3.03	3.13
1300h	3.11	3.12	3.10	3.09	3.11	3.12	3.03	3.10	3.01	3.11	NA	3.10	2.84
1330h	62.3	3.09	3.03	3.12	3.11	3.11	3.10	3.11	3.03	3.15	NA	3.13	3.07
1400h	3.03	3.02	2.98	3.08	3.12	3.14	3.03	3.14	3.07	3.04	NA	3.04	3.12
1430h	2.99	NA	NA	NA	NA	3.03	3.02	3.00	3.04	3.08	NA	3.05	3.08
1500h	2.67	NA	NA	NA	NA	2.88	2.78	2.88	2.84	2.88	NA	2.95	3.03
1530h	2.50	NA	NA	NA	NA	2.86	2.80	2.86	2.56	2.78	NA	3.02	2.45
1600h	2.30	NA	NA	NA	NA	2.67	2.48	2.67	2.52	2.76	NA	2.67	2.73
1630h	1.88	NA	NA	NA	NA	2.01	2.22	2.01	2.22	2.16	NA	2.56	2.22
1700h	0.44	NA	NA	NA	NA	1.55	1.04	1.55	1.34	1.60	NA	2.14	1.97

(Watts)	The condition of the experiment											
			Tracking, with Aluminium foil					Tracking with Aluminium coated paper				
Time of the day	N	O	P	Q	R	S	T	U	V	W	X	Y
0800h	1.67	1.53	NA	1.28	1.19	1.16	0.66	NA	0.87	0.93	1.23	1.11
0830h	1.80	1.90	NA	1.25	1.34	1.34	1.25	NA	1.62	1.87	1.99	1.86
0900h	2.25	2.20	NA	1.47	1.42	1.56	1.74	NA	2.04	2.22	2.27	2.20
0930h	2.28	2.29	NA	1.88	1.53	1.73	1.81	NA	2.21	2.33	2.24	2.25
1000h	2.67	2.44	NA	2.43	1.80	2.41	2.22	NA	2.59	2.47	2.54	2.43
1030h	2.75	2.77	NA	2.51	2.22	2.23	2.37	NA	2.78	2.85	2.67	2.72
1100h	2.87	2.95	NA	2.85	2.60	2.54	2.71	NA	3.08	2.95	2.95	2.95
1130h	3.10	3.12	NA	2.98	2.75	2.88	2.95	NA	3.12	3.11	3.10	3.10
1200h	3.06	3.07	NA	3.01	2.86	2.98	3.02	NA	3.06	3.04	3.04	3.11
1230h	3.13	3.10	NA	3.02	3.03	3.01	3.09	NA	3.11	3.13	3.08	3.06
1300h	3.12	3.09	NA	3.05	3.11	3.04	3.11	NA	3.12	3.12	3.01	3.03
1330h	3.05	3.07	NA	3.11	3.04	3.12	3.10	NA	3.11	2.87	3.06	3.12
1400h	3.12	2.87	NA	3.14	3.06	3.11	3.07	NA	3.10	2.95	3.10	3.06
1430h	2.98	3.03	NA	2.90	2.97	3.01	2.85	NA	3.05	3.08	2.97	3.03
1500h	3.03	3.02	NA	2.84	2.69	2.84	2.81	NA	2.97	3.03	3.01	2.99
1530h	2.49	2.60	NA	2.56	2.40	2.34	2.42	NA	2.77	2.47	2.58	2.65
1600h	2.29	2.56	NA	2.47	2.36	2.21	2.56	NA	2.44	2.43	2.72	2.39
1630h	2.10	2.28	NA	2.07	2.14	2.03	2.05	NA	2.56	2.22	2.55	2.21
1700h	1.54	1.92	NA	1.65	1.59	1.56	1.67	NA	2.19	1.96	1.92	1.99

Table A3: Temperature readings from the solar cell in the model at different wind speeds.

(*Celsius*)	Conditions			
Time of the day	Mirror with passive cooling	Mirror with Active cooling	Aluminium coated paper with passive cooling	Aluminium coated paper with active cooling
0800h	29.4	28.1	29.8	27.2
0830h	43.6	34.5	34.6	28.5
0900h	44.2	40.4	38.4	31.8
0930h	49.4	42.6	42.7	34.4
1000h	56.6	43.2	46.3	36.6
1030h	63.9	46.1	53.6	37.5
1100h	66.1	47.9	57.3	39.3
1130h	71.1	49.7	59.5	39.8
1200h	74.3	51.4	62.8	40.5
1230h	76.4	49.1	64.9	41.5
1300h	79.2	51.2	64.7	41.9
1330h	80.5	47.4	64.8	42.5
1400h	78.2	47.6	63.3	41.8
1430h	76.8	45.8	61.1	40.2
1500h	72.9	43.9	57.3	38.7
1530h	68.7	41.5	53.5	36.6
1600h	56.5	36.6	48.5	35.3
1630h	54.4	35.4	45.7	35.8
1700h	53.1	34.2	43.2	34.4

An Insight into Combustion Optimisation of Batch-fed Biomass Boilers

Rasanga, G. V. C. [1,2], Wickramasinghe, I. P. M. [1], Karunasena, H.C.P. [1]

[1] *Department of Mechanical and Manufacturing Engineering, Faculty of Engineering, University of Ruhuna, Hapugala, Galle, Sri Lanka.*

[2] *Department of Electrical Engineering, Faculty of Engineering, University of Moratuwa, Moratuwa, Sri Lanka.*

Abstract:

Industrial energy demand of Sri Lanka is continuously increasing due to the intense industrialisation and economic development. In this context, mainly due to the cost concerns, the industrial sector is rapidly moving towards biomass-based solutions to meet their thermal, electricity and other forms of energy demands.Although this move can save foreign exchange and minimise the net carbon emissions as a country, there are indications that Sri Lankan biomass based systems in generalmay not beoperating optimally. Particularly in the case of small and medium scale biomass combustors, advanced process control is seldom used. The operations are semi-automated or completely manual so that the combustion efficiencies can be as far below as 20% from the optimal levels. Majority of such systems are batch-fed combustion processes, where the combustion process is highly complex and advanced control methods are required in order to maintain higher overall performance throughout the combustion process. Further, the batch-fed combustion process has not been widely studied compared to continuously-fed counterparts, which are more popular in developed countries. In this background, this paper presents a qualitative study on the combustion process of a batch-fed biomass boiler with the objective of drawing useful insights in order to improve the overallperformance. The study finds that, during the batch-fed biomass combustion, the three stages of combustion; drying, devolatilisation and char burning, have to be considered to gain complete understanding of the batch-fed combustion process. Additionally, it was found that several process parameters are needed to be measured or estimatedin order to optimise the batch-fed biomass combustion process. The insights drawn from this study will lead to a better understanding of the combustion process of batch-fed biomass combustors, which would positively contribute for the sustainability of the biomass energy applications in Sri Lanka and eventually will reduce specific biomass requirement for generating a unit thermal power.

Keywords: Batch feeding of biomass; Biomass combustion; Biomass boiler; Combustion modelling; Combustion efficiency

Biomass combustion applications in Sri Lanka

As a whole, the biomass combustion technology currentlyused in the Sri Lankan industry is still in theprimitive stage, where only a handful of industries have invested to use advanced combustion control in biomass combustors. Since converting to biofueltypically cuts down fuel cost by two third, most of biofuel system operatorsdo not pay attention tocombustion efficiency. Particularly, the biomass system operators inSri Lankan tea industry record low combustion efficiencies due to poor combustion process control.

The sustainability of biomass fuel is still in question due to rapid growth of demand and depletion of biofuel sources. Biomass fuel can be a limited natural resource in near future and the shortage of biomass supply can lead to a fuel crisis unless some planning is put in place in advance. Therefore, more attention needs to be drawn on improving the biomass combustion processes to get the maximum usage of combusted mass.For all such improvements, a detailed study on the underlying fundamentals is indispensible and this particular research intends to contribute to that purpose. Therefore, sections below present details on biomass combustion processes, applications and room for improvements, particularly focusing the batch-fed biomass combustors, which are well popular in Sri Lanka although not have subjected to comprehensive research and development focus in the scientific world.

Biomass combustion is a thermochemical conversation, which can be of the form of: direct combustion, gasification or pyrolysis. The biomass fuel can mainly be in the forms of wood logs, densified wood pellets or briquettes, saw dust, wood chips and wood chops.Wood logs of the biomass can be categorized as thermally thick and the combustion of such thermally thick materials has very complex series of phases of combustion.

The widely used combustion techniquesare: fixed bed type, fluidized bed type and grate furnaces, which can be either: pile burners, stationary sloping grate burners, traveling grate burners or vibrating grate burners. Table 1 below summarises key boiler applications, combustion techniques involved and fuel types used in those [1].

Table 1: Biomass combustion techniques[1].

Applications	Type	Capacity (kW)	Fuel	Ash (%)	Moisture content (%)
Manual	Wood stoves	2 - 10	Dry wood logs	<2%	5-20%
	Log wood boiler	5 - 50	Log wood, sticky wood residues	<2%	5-30%
Pellets	Pellet stoves and boilers	2 - 25	Wood pellet	<2%	8-10%
Automatic	Unterstoker furnaces	20 - 2,500	Wood chips, wood residues	<2%	5-50%
	Moving Grate furnaces	150 - 15,000	All wood fuels	<50%	5-60%
	Per oven with grate	20 - 1500	Dry wood	<5%	5-35%
	Unterstoker with rotating grate	20,000 - 5,000	Wood chip	<50%	40-65%
	Cigar burner	3,000 - 5,000	Straw bales	<5%	20%
	Whole bale furnaces	10 - 5,000	Whole bales	<5%	20%
	Straw furnaces	100 - 5,000	Straw bales	<5%	20%
	Stationary fluidized bed	5,000 - 15,000	Various biomass, d<10mm	<50%	5-60%

State of the art of biomass combustion research

Some existingresearch on biomass combustion hasfocused on improving the overall combustionprocess efficiency by optimizing chambergeometry, mode of heat transfer and the properties of the fuel. Only recently, there has been a shift of focus to concentrate on improvements of efficiencies of combustion systems. Such efforts require biomass combustion modelling and understanding in order to use modern control principles to improve the process. Generally, the biomass combustion can be characterised using the key physical, chemical, mechanical and thermodynamic properties involved. Recently, the influence of differentbiomass propertiessuch as bulk density, geometry as well as environmentalfactors such as harvesting season has been studied [2].There,it is further revealed that the level of emissionis affected bythe fueltype and shape of the fuel particles. For instance,pellets can reduce CO emissions by 27-86%, compared to wood chops of the same wood type. Further, the efficiency of combustion significantly varies with the ash content of the fuel as shown in Figure 1, below[2].

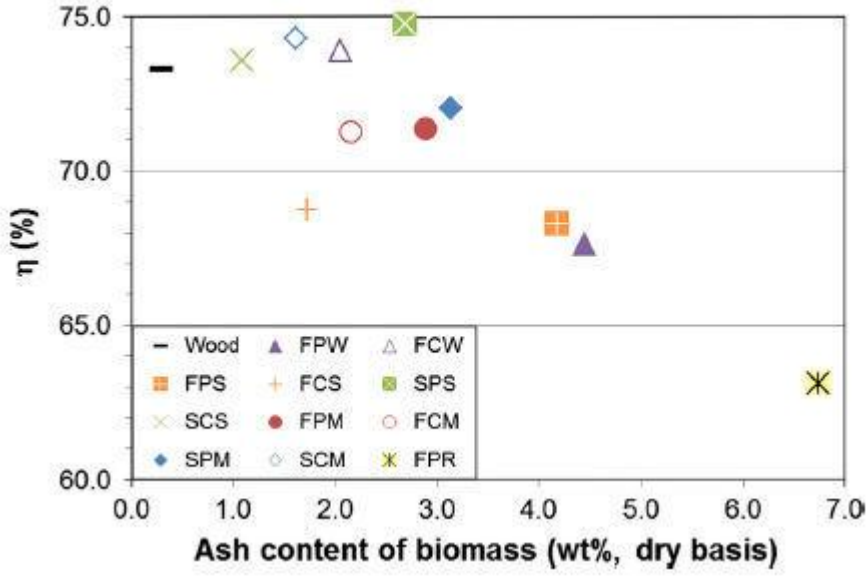

Figure 1: Thermal efficiency as a function of ash contain of biomass [2]

Co-combustion situations such as biomass mixed with fossil fuels has also resulted in reduced emissions [3]. Further, the thermal efficiency and CO emission are affected by the air flow rate in to the biomass combustion chambers [4].

In addition to the experimental approach, mathematical and empirical modelling of the biomass combustion process can help designing more efficient combustors. A collection of such models are discussed below.In [5], a mathematical model based on a single wood particle undergoing thermal degradation in the presence of diffusion, convective transport, pyrolysis reactions, shrinkage, char combustion, water evaporation and condensation is presented.When considering the numerical models, there are studies onthe combustion of densified wood under fixed-bed condition, which has been developed in to a three-dimensional (3-D) model and it has experimentally beenvalidated[6].A 3-D combustion model of thermal convection for a packed bed compaction has also been developed [5].

Recently researchers have tried to improve the biomass combustion efficiency by applying modern control techniques.It has been found that the efficiency of small scale biomass boilers can be improved by using model-based control, which can result in significant reduction of CO emission,compared to conventional controlstrategies [7].Neural network-based control has also been used in small scale biomass boilers [8]. Further, optimization methods based on Extremum-Seeking control have been

used to improve combustion efficiency of biomass boilers [9]. However, almost all of the models discussed above have justfocused on mechanised boilers with continuousbiomass fuel feeding rather than batch-fed or manuallyfuelled boiler systems.Since most of the small and medium scale biomass combustion systems in Sri Lanka are of the batch-fed type, the above studies help little in direct applications. Therefore sections below present a summary of availableresearch describing batch-fed combustorsto gain useful insights for improving combustion efficiencies of the Sri Lankan combustion systems.

Key characteristics of batch-fed biomass combustion systems

In the batch-fed combustion, fuel is fed as batches intermittently in time intervals of about tens of minutes. Usually the combustion process is interrupted in order to feed the next batch with a fresh bulk supply of the biomass.There are three fundamental stages of combustion involved: moisture evaporation, volatile matter releasing and char burning, whichoccur sequentially[5].In a given combustion chamber, the onsetand the spatial distribution of these three combustion stagescan be clearly identified. The spatial distribution of combustion processes depends on the type of the combustion bed (pack bed or grate), air flow direction and the combustion initiation point. For continuously fed systems, boundaries of three regions do not change with time. However for batch-fed systems combustion process evolves in timeandthe shapes of the boundaries of combustion stages changeover the time within each feeding cycle[10].

For each batch of biomass fed in to the combustion chamber, moisture starts evaporating instantly due to the intense heat available from the char burning occurred in the previous cycle of combustion. As the logs get heated up, at a certain temperature, volatile matter tends to get released starting from the bottom layersof the wood pile.During this process as the volatile material exit from the biomass, it gradually turns in to char.The volatile matter is easily transported by the induced or forced draft of air before getting ignited and the actual ignition location depends on many related factors. At the end, remaining char burns releasing only a little heat. Then it's the time for the next batch of biomass to be fedin order to sustain the required heat output.

In [4], there is a study supporting the combustion sequence described previously. As seen in Fig. 2the bed is heated up and moisture is evaporated within 0 -100s and then the combustion process really kicks off at around 100s. Within 100 – 1100s, volatile matter getsreleased and its combustion takes place in a strong and sustained mass reduction rate, as presented. Thus the combustion process has a prolong period of heat emission at the middle before the heat output diminishes during 1100-1500s.

It is important to note that the previously mentioned sequence of batch-fed biomass combustion processhasbothsimilarities and differences to the combustion process of packed beds. The individual processes of moisture evaporation, volatile matter releasing and char burning are common to both the types of combustions. Yet the timing overlap and special distribution of these individual processes are very different for the two types.

Packed bed combustion can be used for gasification, in which the reaction rate of gasification combustion is slower than the direct combustion. Region of the combustion is determined by the size of the fuel particles. For small particles, a clear separation among boundaries can be noticed. All the three stages; moisture evaporation, volatile releasing and char burning occurs within different parts of the chamber at same time when wood logsare used as seen in Fig 3. That is one of the key differences between packed bed combustion and batch-fed wood log combustion.

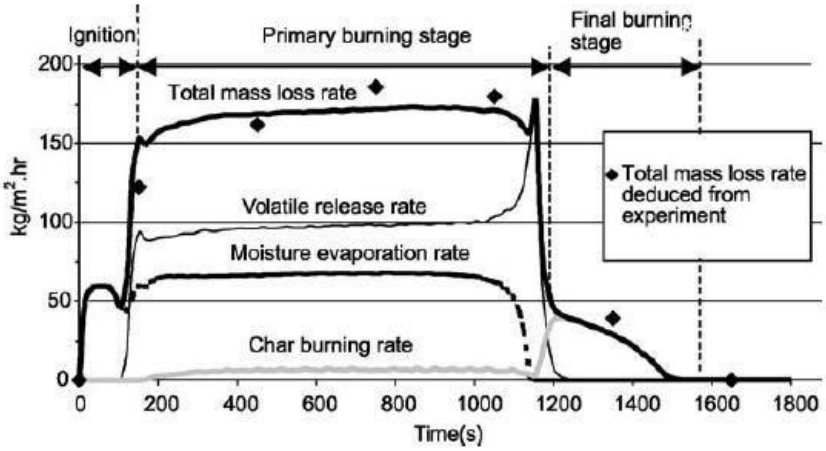

Figure2: Calculated combustion process rates versus time[4]

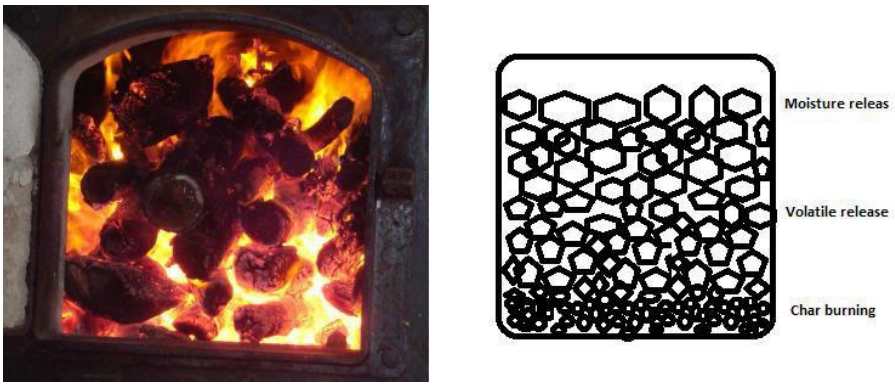

Figure 3: Pack Bed Combustion[4]

Uncertainties involve in batch-fed biomass combustion system

The process of biomass combustionhardly becomes steady at any given period or uniform between batches due to variations in the fuel properties such as bulk density and moisture content [8]. The resultreported in[4]shows that the rate of moisture evaporation, rate of volatile release and char burning significantly change according to the moisture content of the fuel evident from Figures 4-6, below. Thecomposition of biomass fuel can also play a significant role in the dynamics of the combustion process[11].

Typical Boiler Control Systems and Their Limitations

Any primitive boiler system is equipped with a pressure regulation system. Typical boiler control systems rely on pressure and temperature feedback to regulate thermal output of the system. To control combustion process, it requires some additional sensors to measure or estimate combustion chamber inputs and outputs. The inputs into the combustion chamber are the biomass quantity and airflow rate. The remaining amount of burning biomass and its combustible state would determine the state of the combustion process. The outputs of the combustion system are the flue gas rate and heat outputs. The dynamics of the combustion process are largely determined by the thermo chemical processes, which should be controlled by varying the air flow rate into the chamber in order to optimize the combustion process. For an example, air flow rate into the chamber can be varied by altering the forced draft or induced draft fans. Oxygen sensing is one of the most popular methods to determine combustion efficiency.Moreover, in modern biomass boiler, mechanised fuel feeding system is usedto improve the efficiency of operation by controlling the fuel mass flow rate as well.

In modern control applications for boilers may requiremore parameters be measured to precisely determine the state of the combustion process.[12]and [8]have used measured oxygen consumption to estimate thermal decomposition rate. In turn, combustion power can be derived from the thermal decomposition rate. Because of the uncertainties, biomasscombustion power cannot be measured by using biomass flow rate alone.

Measurement ofthe moisture content is another feedback that can potentially improve the process. Some researchershave used mass balance between inlet air and flue gas to measure the fuel moisture content. For that, advanced humidity sensors or flue gas sensors are essential. This approach deemed impractical for most of the medium of small scale applications. In-addition to high cost of these sensors, the reliability of measurements and durability of sensors can make these options not viable for small or medium scale industrial applications.

What approach might work in improving efficiency of low or medium scale industrial biomass boiler systems

To mitigate burdens of expensive unreliable sensor techniques, mathematical modelling can be used to indirectly estimate the state of the combustion process. For example, a series of thermocouples may reveal a great deal about the process if an appropriate mathematical model-based estimation is used.

Experimental studies can reveal patterns related with batch-fed biomass combustion systems that may be parameterized against some easily measurable indicators. Advanced control methods like model predictive control orartificial intelligence tools can significantly take the burden off from the measurement systems.

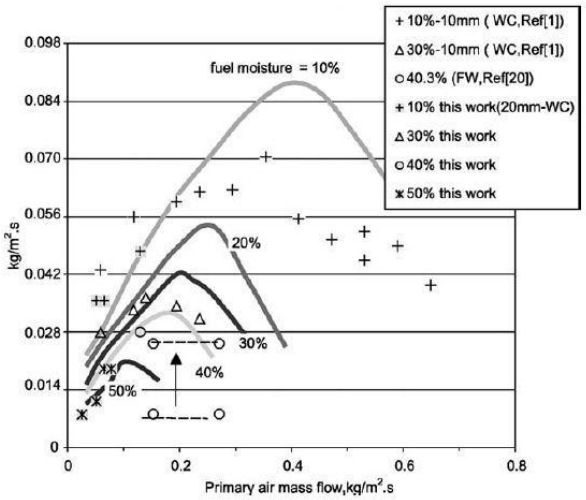

Figure4: Biomass burning rate as a function of both primary air flow rate and moisture content in the fuel[4].

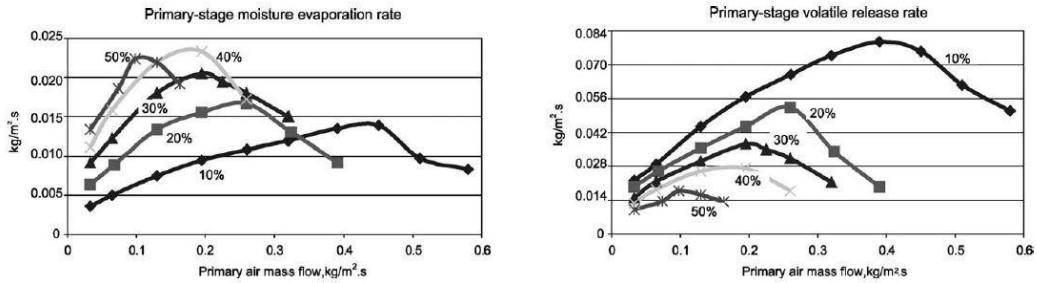

Figure5: Moisture evaporation rate of the biomass as a function of both primary air flow rate, and moisture content in the fuel; Volatile release rate as a function of both primary air flow rate and moisture content in the fuel[4].

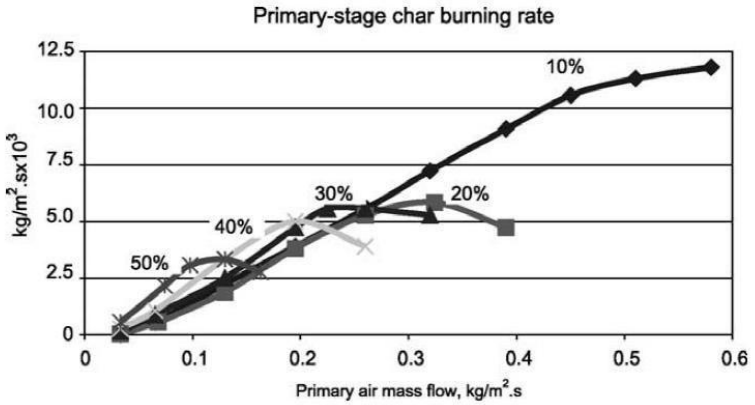

Figure 6: Calculated char burning rate of biomass as a function of both primary air flow rate and moisture content in the fuel[4].

Conclusions

Some of the key differences between the biomass combustion system popular in other countries and somesmall to medium scale Sri Lankan biomass systems we discussed leading to the identification of knowledge gaps in understanding the combustion process of batch-fed combustors, commonly available in Sri Lanka. Finally a broader conceptual framework has been proposed as a potential control strategy in order to optimise the combustion performance of a small or medium scale batch-fed biomass combustion system.

References

[1] A. Namal, "Biomass Combustion," in *Training Workshop on Biomass to Energy in industrial Application*, Thulhiriya, Sri Lanka, 2015.

[2] S. Fournel, J. H. Palacios, R. Morissette, J. Villeneuve, S. Godbout, M. Heitz*, et al.*, "Influence of biomass properties on technical and environmental performance of a multi-fuel boiler during on-farm combustion of energy crops," *Applied Energy,* vol. 141, pp. 247-259, 3/1/ 2015.

[3] F. Okasha, G. Zaater, S. El-Emam, M. Awad, and E. Zeidan, "Co-combustion of biomass and gaseous fuel in a novel configuration of fluidized bed: Combustion characteristics," *Fuel,* vol. 133, pp. 143-152, 10/1/ 2014.

[4] Y. B. Yang, V. N. Sharifi, and J. Swithenbank, "Effect of air flow rate and fuel moisture on the burning behaviours of biomass and simulated municipal solid wastes in packed beds," *Fuel,* vol. 83, pp. 1553-1562, 2004.

[5] M. A. Gómez, J. Porteiro, D. Patiño, and J. L. Míguez, "CFD modelling of thermal conversion and packed bed compaction in biomass

combustion," *Fuel,* vol. 117, Part A, pp. 716-732, 1/30/ 2014.

[6] J. Collazo, J. Porteiro, D. Patiño, and E. Granada, "Numerical modeling of the combustion of densified wood under fixed-bed conditions," *Fuel,* vol. 93, pp. 149-159, 2012.

[7] M. Gölles, S. Reiter, T. Brunner, N. Dourdoumas, and I. Obernberger, "Model based control of a small-scale biomass boiler," *Control Engineering Practice,* vol. 22, pp. 94-102, 2014.

[8] S. Vrana and B. Sulc, "Neural network inference of biomass fuel moisture during combustion process evaluating of directly unmeasurable variables," in *Control Conference (ICCC), 2014 15th International Carpathian*, 2014, pp. 671-674.

[9] C. Oswald, V. Placek, and B. Sulc, "Advanced control with economic - ecological optimization for biomass-fired boilers," in *Control Conference (ICCC), 2014 15th International Carpathian*, 2014, pp. 407-412.

[10] R. Bauer, M. Gölles, T. Brunner, N. Dourdoumas, and I. Obernberger, "Modelling of grate combustion in a medium scale biomass furnace for control purposes," *Biomass and Bioenergy,* vol. 34, pp. 417-427, 2010.

[11] C. Yin, L. A. Rosendahl, and S. K. Kær, "Grate-firing of biomass for heat and power production," *Progress in Energy and Combustion Science,* vol. 34, pp. 725-754, 2008.

[12] J. Kortela and S. L. Jämsä-Jounela, "Model predictive control utilizing fuel and moisture soft-sensors for the BioPower 5 combined heat and power (CHP) plant," *Applied Energy,* vol. 131, pp. 189-200, 10/15/ 2014.